BULLETIN OF THE EARTHQUAKE
RESEARCH INSTITUTE
UNIVERSITY OF TOKYO
Vol. 67 (1992) pp. 89 – 238

Potential and Gravity Changes Caused by Dislocations in Spherically Symmetric Earth Models

Wenke SUN*

Earthquake Research Institute, The University of Tokyo, Japan

(Received March 16, 1992)

Abstract

This thesis studied for the first time the potential and gravity changes caused by dislocations in spherically symmetric earth models.

We introduced equations of equilibrium with an arbitrary body force in a SNREI model as well as boundary conditions. Integration of the fundamental equations with the body force was divided into two parts: one to solve the basic equations of equilibrium without considering the body force; the another to consider it as initial values. We defined dislocation Love numbers to describe the elastic deformation of the earth raised by source functions. We proved that only four components of the nine-part solution are independent in a general dislocation model. We discuss the shear dislocation, tensile dislocation and explosion, which can be expressed by the four independent components corresponding (in this paper) to a vertical strike-slip, a vertical dip-slip, a dip-slip at a 45° dipping plane, and a tensile opening at the horizontal plane. Based on the above-mentioned equations of equilibrium and the dislocation models, we derived expressions of the potential and gravity changes caused by dislocations buried in a spherically symmetric earth model. We derived general formulas for practical applications.

We discussed the special case of a point source on the earth's surface. We handled particularly the case of $n = 1$ using principle of conservation of the mass center. In our integrations and summations, we used some techniques to truncate the infinite series and to accelerate the covergence, such as normalization, truncation of harmonic degree n, the disk factor, Euler transformation, interpolation, and asymptotic solutions.

We started our calculations with a homogeneous earth model by comparing the results from those obtained from flat-earth theory. We showed that they coincide very well, at least within 1°. The far-field results indicated no larger than a 10% difference within 10°. We conclude that in this case it is the same to use both the spherical and flat-earth theories in the near field, while it is reasonable to use spherical theory for a global calculation. After that, we proceeded to undertake calculations with a radially heterogeneous earth model (Model 1066A). The results are, as a whole, similar to those for a homogeneous sphere. In some cases, however, the difference between the two becomes very large. For example, the locations of the

* On leave from: Center for Analysis and Prediction of State Seismological Bureau, Beijing, People's Republic of China

nodal lines of the gravity change differ significantly between the two models. This indicates that the vertical layering can cause considerable effects on the deformation fields. As main numerical results of the study, we list the dislocation Love numbers in Appendix D and the deformations including the radial displacement, potential and gravity changes in Appendix E.

We extended the theory of the point dislocation to that of a finite fault, and used it to calculate the gravity changes caused by the 1964 Alaska earthquake. The computed results are in excellent agreement with the observed gravity changes during the earthquake. In the far field (epicentral distance $\gg$ fault dimension), we also demonstrate that the gravity change is large enough to be detected by a superconducting gravimeter.

Contents

1. Introduction

1.1 History of Dislocation Theory Applied to Geophysics

Since STEKETEE (1958) introduced dislocation theory to seismology, numerous theoretical formulations have been developed to describe the deformation of an isotropic homogeneous earth model due to a variety of dislocations.

Scientists started their study with a semi-infinite medium. As a mathematical model of faulting, STEKETEE (1958) assumed a dislocation surface, across which the displacement vector is discontinuous. He constructed Green's functions for a strike-slip fault by considering a dislocation in a semi-infinite medium. CHINNERY (1961, 1963) used Steketee's results to determine the displacement and stress fields in the vicinity of a vertical, rectangular, strike-slip fault, and obtained contour maps for some representative cases. BERRY and SALES (1962) derived the surface displacement fields due to a closure of a horizontal crack in a transversely isotropic medium. MARUYAMA (1964) gave all the sets of surface displacements due to vertical and horizontal tensile dislocations in a semi-infinite Poisson solid. He also extended CHINNERY's (1961, 1963) work to the case of a dip-slip fault.

Observations of far-field strains caused by the Alaska earthquake of 1964 (March 28) opened new avenues to studies concerning earthquake sources. This event motivated PRESS (1965) to compute the displacement, strain and tilt fields for vertical, rectangular, strike-slip and dip-slip faults in a semi-infinite medium. Press showed that the static deformation in the far field caused by earthquakes is large enough to be detected by modern instruments. More observations of strain steps associated with earthquakes have been claimed by WIDEMAN and MAJOR (1967).

YAMAZAKI (1978) treated deformation fields arising from a dilatancy source. IWASAKI and SATO (1979) studied the strain fields at a depth due to an inclined finite shear fault. DAVIS (1983) derived an expression of the vertical displacement due to an inclined tensile fault in half-space.

OKADA (1985) checked and reviewed the analytical expressions published by previous authors. He gave compact formulas to calculate the surface displacements, strains, and tilt due to an inclined finite fault in a half-space. He also gave the solutions arising from tensile dislocations.

Efforts to develop the formulations in a more realistic earth model have also been advanced through numerous studies (MCGINLEY, 1969; BEN-MENAHEM *et al.*, 1968, 1970; SMYLIE and MANSINHA, 1971). These studies have revealed that the effect of the earth curvature is negligible for shallow events at an epicentral distance of less than 20°, while the vertical layering or lateral inhomogeneity may have considerable effects on the deformation fields.

SAITO (1967) presented a theory for calculating the amplitudes of free oscillations caused by a point source in a spherically symmetric earth model. He used a variational principle and expressed his results in terms of normal mode solutions and source functions. KAGAN (1987a, 1987b) gave the source functions of elementary sources in general forms for both static and dynamic displacements.

BEN-MENAHEM and SINGH (1968) derived explicit expressions for the deformation of a uniform, non-gravitating sphere due to an internal Volterra dislocation of arbitrary orientation and depth. These results constitute the theoretical nucleus of a fundamental study by Ben-Menahem, SINGH and SOLOMON (1969) in which the displacements and strains were given everywhere on the surface of a spherical earth model. In particular, they showed that the results for a sphere are quite different from what would be expected from a half-space approximation. SINGH and BEN-MENAHEM (1969) gave formulas for calculating the deformation of a homogeneous gravitating sphere. BEN-MENAHEM and ISRAEL (1970) generalized the results of BEN-MENAHEM and SINGH (1968) by calculating the displacement field at any point of a homogeneous, isotropic, non-gravitating sphere.

1.2 Gravity Change due to Dislocations

Gravity change caused by dislocations has also been studied. HAGIWARA (1977) first investigated the elevation and gravity changes due to an explosive

source. HAGIWARA's (1977) model is sufficiently versatile for various spatial configurations of a dilatant volume which may exist in the actual earth. HAGIWARA *et al.* (1985) detected significant gravity changes due to large earthquakes: the 1978 Izu-Oshima-kinkai earthquake (M7.0) and the 1980 Izu-hanto-toho-oki earthquake (M6.7). SASAI (1986, 1988) studied the surface displacement, gravity and magnetic changes associated with multiple tensile cracks of the Gaussian distribution.

OKUBO (1991a, 1992) completely studied the problem concerning potential and gravity changes caused by point dislocations and by faulting on a finite plane in a semi-infinite medium. He derived all sets of expressions in closed forms. These expressions enable us to evaluate coseismic changes in surface gravity and geoid height. His numerical simulation shows that a great earthquake could cause a geoid height change of the order of $0.1m$. OKUBO *et al.* (1991) have detected a significant gravity change due to the 1989 earthquake swarm and the submarine eruption, off Ito. They successfully explained the gravity change by using OKUBO's (1991a) theory. The gravity change caused by the 1986 eruption of the Izu-Oshima volcano was also studied by OKUBO *et al.* (1988). OKUBO and WATANABE (1989) studied the gravity change caused by a fissure eruption. OKUBO (1989) also studied gravity change caused by fault motion on a finite rectangular plane. RUNDLE (1978) studied the relations of gravity changes and the Palmdale uplift.

1.3 Objectives of the Study

All of the above-mentioned studies, except for SAITO (1967), assumed a homogeneous semi-infinite medium or a homogeneous non-gravitating sphere. Nobody has ever succeeded in computing the displacement, strain, tilt and gravity change fields in a *spherically symmetric, self-gravitating* earth model, due to numerical difficulties.

The first objective of this research was to study global gravity changes caused by dislocations in a spherical earth. We expected a significant discrepancy between the results for a sphere and that for half-space in the far-field. We shall examine the effects of spherical curvature and radial heterogeneity by comparing the results for a flat-earth, a homogeneous sphere and a radially stratified spherical earth. We checked the consistency between OKUBO's (1991a) flat-earth theory and our spherical theory.

The second objective was to study whether a gravity step is sufficiently large in the far-field to be detected by modern instruments: a superconducting gravimeter and an absolute gravimeter. If it is the case, it will open a new research field.

We will give the formulas and numerical results of radial displacement, potential and gravity changes due to dislocations in a spherical earth model for practical applications. We calculate the gravity changes due to the 1964 Alaska earthquake and evaluate the associated geoid change.

2. Fundamental Equations

In section 2.1 we introduce equations of equilibrium with an arbitrary body force in a SNREI model. We describe the boundary conditions, initial conditions and source functions in section 2.2. In section 2.3 we present methods to integrate the inhomogeneous equations. We discuss the deformation fields of spheroidal degree $n = 0$ and 1 in section 2.4.

2.1 Equations of Equilibrium with a Point Force

We start with an earth model that is spherically symmetric, non-rotating, perfectly elastic and isotropic, i.e. the SNREI model (DAHLEN, 1968). We discuss perturbations to the density field, $\rho(r)$, the gravity field, $g(r)$, as well as the gravitational potential, $\Psi(r)$, caused by a point dislocation. In the following we assume that the disturbances to these fields are infinitesimal. For the gravitational potential we write

$$\Psi(r) + \psi(r, \theta, \phi), \tag{2.1}$$

and for the density

$$\rho(r) + \delta\rho(r, \theta, \phi), \tag{2.2}$$

where ψ and $\delta\rho$ are first-order infinitesimals.

In vector notation the linearized first-order equations of equilibrium, the stress-strain relation and Poisson's equation are as follows:

$$0 = \nabla\cdot\boldsymbol{\tau} + \rho g\mathbf{e}_r(\nabla\cdot\mathbf{u}) - \rho\nabla(\psi + gu_r) + \rho\mathbf{f}, \tag{2.3}$$

$$\boldsymbol{\tau} = \lambda\mathbf{I}\nabla\cdot\mathbf{u} + 2\mu(\nabla\mathbf{u} + (\nabla\mathbf{u})^t), \tag{2.4}$$

$$\nabla^2\psi = -4\pi G(\delta\rho) = 4\pi G\nabla\cdot(\rho\mathbf{u}) \tag{2.5}$$

(ALTERMAN *et al.*, 1959; TAKEUCHI and SAITO, 1972), where $\mathbf{u}$ is the displacement vector, $\boldsymbol{\tau}$ the stress tensor, $\mathbf{I}$ the identity tensor, λ and μ Lamé's constants, $\rho\mathbf{f}$ a point force located at a point (r_0, θ_0, ϕ_0), and the symbol 't' the operation of transpose. In Poisson's equation (2.5) the continuity equation,

$$\delta\rho = -\nabla\cdot(\rho\mathbf{u}), \tag{2.6}$$

is used. The gravity, g in (2.3), is defined as

$$g(r) = -\frac{d\Psi}{dr}. \tag{2.7}$$

The unit point force can be written as

$$\rho\mathbf{f} = \frac{\boldsymbol{\nu}}{r^2\sin\theta}\delta(r - r_0)\delta(\theta - \theta_0)\delta(\phi - \phi_0), \tag{2.8}$$

where $\boldsymbol{\nu}$ is the unit vector.

We introduce surface vector harmonics as follows:

$$\mathbf{R}_n^m(\theta, \phi) = \mathbf{e}_r Y_n^m(\theta, \phi), \tag{2.9}$$

$$\mathbf{S}_n^m(\theta, \phi) = \left[\mathbf{e}_\theta \frac{\partial}{\partial \theta} + \mathbf{e}_\phi \frac{1}{\sin\theta} \frac{\partial}{\partial \phi}\right] Y_n^m(\theta, \phi), \tag{2.10}$$

$$\mathbf{T}_n^m(\theta, \phi) = \left[\mathbf{e}_\theta \frac{1}{\sin\theta} \frac{\partial}{\partial \phi} - \mathbf{e}_\phi \frac{\partial}{\partial \theta}\right] Y_n^m(\theta, \phi), \tag{2.11}$$

where $\mathbf{e}_r$, $\mathbf{e}_\theta$, $\mathbf{e}_\phi$ are unit vectors in the spherical coordinates, and

$$Y_n^m(\theta, \phi) = P_n^m(\cos\theta) e^{im\phi} \qquad m = 0, \pm 1, \pm 2, \ldots, \pm n. \tag{2.12}$$

P_n^m is the associated Legendre's function.

Since an arbitrary vector defined on a unit sphere can be expanded in terms of the three harmonics, we may write the displacement field $\mathbf{u}$ and the potential ψ as

$$\mathbf{u} = \sum_{n,m} [y_1(r)\mathbf{R}_n^m(\theta, \phi) + y_3(r)\mathbf{S}_n^m(\theta, \phi) + y_1^{\mathrm{T}}(r)\mathbf{T}_n^m(\theta, \phi)] \tag{2.13}$$

$$\psi = \sum_{n,m} y_5(r) Y_n^m(\theta, \phi). \tag{2.14}$$

For later convenience, we define y_6 after TAKEUCHI and SAITO (1972) as

$$y_6(r) = \frac{dy_5}{dr} - 4\pi G\rho y_1 + \frac{n+1}{r} y_5. \tag{2.15}$$

Notice that the definition used here is slightly different from that of ALTERMAN *et al.* (1959).

Substituting (2.13) into the stress-strain relations (2.4) yields

$$\boldsymbol{\tau} \cdot \mathbf{e}_r = \sum_{n,m} [y_2(r)\mathbf{R}_n^m(\theta, \phi) + y_4(r)\mathbf{S}_n^m(\theta, \phi) + y_2^{\mathrm{T}}(r)\mathbf{T}_n^m(\theta, \phi)], \tag{2.16}$$

where

$$y_2 = (\lambda + 2\mu) \frac{dy_1}{dr} + \frac{\lambda}{r}[2y_1 - n(n+1)y_3], \tag{2.17}$$

$$y_4 = \frac{\mu}{r}\left(y_1 - y_3 + r\frac{dy_3}{dr}\right), \tag{2.18}$$

$$y_2^{\mathrm{T}} = \frac{dy_1^{\mathrm{T}}}{dr} - \frac{1}{r} y_1^{\mathrm{T}}. \tag{2.19}$$

The point force, $\rho\mathbf{f}$, can be described as

$$\rho\mathbf{f} = \frac{\delta(r - r_0)}{r_0^2} \sum_{n,m} [F_2(r)\mathbf{R}_n^m(\theta, \phi) + F_4(r)\mathbf{S}_n^m(\theta, \phi) + F_2^{\mathrm{T}}(r)\mathbf{T}_n^m(\theta, \phi)], \tag{2.20}$$

where

$$F_2 = \frac{2n+1}{4\pi}\frac{(n-m)!}{(n+m)!}\mathbf{R}_n^{m*}(\theta_0, \phi_0)\cdot \boldsymbol{\nu}, \tag{2.21}$$

$$F_4 = \frac{2n+1}{4\pi n(n+1)}\frac{(n-m)!}{(n+m)!}\mathbf{S}_n^{m*}(\theta_0, \phi_0)\cdot \boldsymbol{\nu}, \tag{2.22}$$

$$F_2^{\mathrm{T}} = \frac{2n+1}{4\pi n(n+1)}\frac{(n-m)!}{(n+m)!}\mathbf{T}_n^{m*}(\theta_0, \phi_0)\cdot \boldsymbol{\nu}. \tag{2.23}$$

Here, * denotes the complex conjugate.

In the above equations, y_1 and y_3 express the radial functions of the vertical and horizontal displacements, respectively. y_2 and y_4 denote the vertical and horizontal stress components, respectively. y_5 is the potential change, while y_6 concerns the derivative of y_5. y_1^{T}, y_3^{T} express the displacement and stress of the toroidal field respectively.

Since we are interested in calculating coseismic potential and gravity changes, we restrict our attention from now on to the spheroidal deformation. Then, the solutions to the equations of equilibrium and the point force reduce to:

$$\mathbf{u} = \sum_{n,m}[y_1(r)\mathbf{R}_n^m(\theta, \phi) + y_3(r)\mathbf{S}_n^m(\theta, \phi)], \tag{2.24}$$

$$\psi = \sum_{n,m} y_5(r)\mathbf{Y}_n^m(\theta, \phi), \tag{2.25}$$

$$\boldsymbol{\tau}\cdot\mathbf{e}_r = \sum_{n,m}[y_2(r)\mathbf{R}_n^m(\theta, \phi) + y_4(r)\mathbf{S}_n^m(\theta, \phi)], \tag{2.26}$$

$$\rho\mathbf{f} = \frac{\delta(r-r_0)}{r_0^2}\sum_{n,m}[F_2(r)\mathbf{R}_n^m(\theta, \phi) + F_4(r)\mathbf{S}_n^m(\theta, \phi)]. \tag{2.27}$$

Substituting equations (2.24)–(2.27) into equations (2.3)–(2.5), we obtain

$$\frac{dy_1}{dr} = \frac{1}{\lambda+2\mu}\left\{y_2 - \frac{\lambda}{r}[2y_1 - n(n+1)y_3]\right\}, \tag{2.28}$$

$$\begin{aligned}\frac{dy_2}{dr} = {} & \frac{2}{r}\left(\lambda\frac{dy_1}{dr} - y_2\right) + \frac{1}{r}\left[\frac{2(\lambda+\mu)}{r} - \rho g\right] \\ & \cdot[2y_1 - n(n+1)y_3] + \frac{n(n+1)}{r}y_4 \\ & - \rho\left(y_6 - \frac{n+1}{r}y_5 + \frac{2g}{r}y_1\right) - F_2\frac{\delta(r-r_0)}{r_0^2},\end{aligned} \tag{2.29}$$

$$\frac{dy_3}{dr} = \frac{1}{\mu}y_4 + \frac{1}{r}(y_3 - y_1), \tag{2.30}$$

$$\begin{aligned}\frac{dy_4}{dr} = {} & -\frac{\lambda}{r}\frac{dy_1}{dr} - \frac{\lambda+2\mu}{r^2}[2y_1 - n(n+1)y_3] \\ & + \frac{2\mu}{r^2}(y_1 - y_3) - \frac{3}{r}y_4 - \frac{\rho}{r}(y_5 - gy_1) - F_4\frac{\delta(r-r_0)}{r_0^2},\end{aligned} \tag{2.31}$$

$$\frac{dy_5}{dr} = y_6 + 4\pi G\rho y_1 - \frac{n+1}{r}y_5, \tag{2.32}$$

$$\frac{dy_6}{dr} = \frac{n-1}{r}(y_6 + 4\pi G\rho y_1) + \frac{4\pi G\rho}{r}[2y_1 - n(n+1)y_3]. \tag{2.33}$$

We can rewrite equations (2.28)−(2.33) in the following matrix form:

$$\frac{d\mathbf{Y}}{dr} = \mathbf{AY} - \mathbf{F}\frac{\delta(r-r_0)}{r_0^2}. \tag{2.34}$$

Here,

$$\mathbf{Y} = (y_1, \ldots, y_6)^t, \tag{2.35}$$

$$\mathbf{F} = (0, F_2, 0, F_4, 0, 0)^t, \tag{2.36}$$

where the coefficient matrix **A** depends on the radius, r, harmonics degree, n, and earth model. Notice that the solution for **Y** is redundant with respect to the harmonic order, m, since the matrix **A** is independent of m.

If the **F**-team is zero,

$$\frac{d\mathbf{Y}}{dr} = \mathbf{AY} \tag{2.37}$$

is equivalent to that used for the problems concerning free oscillation, earth tide, surface load and shear force.

When $\mu = 0$, as in the liquid core of the earth, (2.28)−(2.33) become

$$\frac{dy_1}{dr} = \frac{1}{\lambda}\left\{y_2 - \frac{\lambda}{r}[2y_1 - n(n+1)y_3]\right\}, \tag{2.38}$$

$$\frac{dy_2}{dr} = \frac{2}{r}\left(\lambda\frac{dy_1}{dr} - y_2\right) + \frac{1}{r}\left[\frac{2\lambda}{r} - \rho g\right]\cdot[2y_1 - n(n+1)y_3] - \rho\left(y_6 - \frac{n+1}{r}y_5 + \frac{2g}{r}y_1\right) - F_2\frac{\delta(r-r_0)}{r_0^2}, \tag{2.39}$$

$$y_2 = \rho(gy_1 - y_5), \tag{2.40}$$

$$\frac{dy_5}{dr} = y_6 + 4\pi G\rho y_1 - \frac{n+1}{r}y_5, \tag{2.41}$$

$$\frac{dy_6}{dr} = \frac{n-1}{r}(y_6 + 4\pi G\rho y_1) + \frac{4\pi G\rho}{r}[2y_1 - n(n+1)y_3]. \tag{2.42}$$

Notice that y_3 is indeterminate in this case. This difficulty has long been discussed by several authors (LONGMAN, 1963; JEFFEREYS and VICENTE, 1966). It had been customary to assume the neutral equilibrium (Adams-Williamson condition) that prevails in the liquid core to circumvent this difficulty (TAKEUCHI, 1950). The condition holds true only when the core is chemically homogeneous, and has an adiabatic temperature gradient. Such conditions, however, are

unlikely to be met in the actual core. SAITO (1974) solved this problem by introducing a new variable:

$$y_7(r) = y_6(r) + \frac{4\pi G\rho}{g} y_2(r)$$
$$= \frac{dy_5(r)}{dr} + \left(\frac{n+1}{r} - \frac{4\pi G\rho}{g}\right) y_5(r). \tag{2.43}$$

In terms of y_5 and y_7, he obtained the standard form of first-order differential equations:

$$\frac{dy_5}{dr} = \left(\frac{4\pi G\rho}{g} - \frac{n+1}{r}\right) y_5 + y_7 \tag{2.44}$$

$$\frac{dy_7}{dr} = \frac{2(n-1)}{r}\frac{4\pi G\rho}{g} y_5 + \left(\frac{n-1}{r} - \frac{4\pi G\rho}{g}\right) y_7. \tag{2.45}$$

Since it is impossible for an earthquake to occur in the liquid core, equations (2.44) and (2.45) are free from the point force.

We solve inhomogeneous equations (2.28)–(2.33) and (2.44)–(2.45) using appropriate boundary conditions.

2.2 Boundary Conditions

2.2.1 Source Function

The existence of a point force makes the solution vector discontinuous across $r = r_0$. We define a 'source function' as a discontinuity: that is,

$$\mathbf{S} \equiv (s_1, s_2, \ldots, s_6) = \mathbf{Y}(r_0 + 0) - \mathbf{Y}(r_0 - 0). \tag{2.46}$$

We obtain from (2.28) through (2.33)

$$s_2 = -\frac{1}{r_0^2} F_2 \tag{2.47}$$

$$s_4 = -\frac{1}{r_0^2} F_4 \tag{2.48}$$

for a single force. Notice that source functions s_5 and s_6 always vanish because the potential ψ and $(\partial\psi/\partial r - 4\pi G\rho u_r)$ must be continuous across any boundary surface. The continuity prevails even if the radial displacement, u_r, has a jump at the interface (SAITO, 1967), i.e.,

$$y_5(r_0 + 0) = y_5(r_0 - 0) \tag{2.49}$$

$$y_6(r_0 + 0) = y_6(r_0 - 0). \tag{2.50}$$

We have discussed so far only the case for a single point force. We may apply the same procedure to the deformation field excited by point dislocations. The explicit forms of s_i are given later in chapter 3.2.

2.2.2 Initial Condition at the Origin

The system of differential equations (2.37) generally has six independent solutions, of which only three are regular at $r = 0$. In order to start a numerical integration of equations (2.37) we must have initial values at some $r = r_1 \ll a$. They can be obtained by assuming a uniform sphere of radius r_1. The solution is expressed in terms of spherical Bessel functions (LOVE, 1911). Two of the three independent solutions are

$$rx_1(r) = nhj_n(kr) - fkrj_{n+1}(kr), \tag{2.51}$$

$$r^2x_2(r) = -(\lambda + 2\mu)f(kr)^2j_n(kr) + 2\mu\{n(n-1)hj_n(kr) + [2f + n(n+1)]krj_{n+1}(kr)\}, \tag{2.52}$$

$$rx_3(r) = hj_n(kr) + krj_{n+1}(kr), \tag{2.53}$$

$$r^2x_4(r) = \mu[(kr)^2j_n(kr) + 2(n-1)hj_n(kr) - 2(f+1)krj_{n+1}(kr)], \tag{2.54}$$

$$x_5(r) = 3\gamma f j_n(kr), \tag{2.55}$$

$$rx_6(r) = (2n+1)x_5(r) - 3n\gamma hj_n(kr), \tag{2.56}$$

where

$$k^2 = \frac{1}{2}\left\{\frac{4\gamma}{\alpha^2} \mp \left[\left(\frac{4\gamma}{\alpha^2}\right)^2 + \frac{4n(n+1)\gamma^2}{\alpha^2\beta^2}\right]^{\frac{1}{2}}\right\}, \tag{2.57}$$

$$\gamma = \frac{4\pi G\rho}{3}, \tag{2.58}$$

$$f = \frac{\beta^2}{\gamma}k^2, \tag{2.59}$$

$$h = f - (n+1) \tag{2.60}$$

for a static problem. α and β are the compressional and shear wave velocities. The third solution is given by

$$rx_1(r) = nr^n, \tag{2.61}$$

$$r^2x_2(r) = 2\mu n(n-1)r^n, \tag{2.62}$$

$$rx_3(r) = r^n, \tag{2.63}$$

$$r^2x_4(r) = 2\mu(n-1)r^n, \tag{2.64}$$

$$x_5(r) = n\gamma r^n, \tag{2.65}$$

$$rx_6(r) = (2n+1)x_5(r) - 3n\gamma r^n. \tag{2.66}$$

2.2.3 Inner Core–Outer Core Boundary

We have three independent solutions $\{y^s_{ij}; i = 1, 2, \ldots, 6, j = 1, 2, 3\}$ in the solid inner core, and only one $\{y^l_i\}$ in the liquid outer core. We introduce conditions at the boundary after SAITO (1974). Vanishing tangential stress at $r = c$ gives (SAITO, 1974)

$$y^s_4(c) = \sum_{j=1}^{3} Q_j y^s_{4j}(c) = 0, \tag{2.67}$$

while continuity of the radial stress means

$$\begin{aligned} y_2^s(c) &= \sum_{j=1}^{3} Q_j y_{2j}^s(c) = y_2^l(c) \\ &= \rho^l(c)[g(c)y_1^l(c) - y_5^l(c)] \\ &= \rho^l(c)\sum_{j=1}^{3} Q_j[g(c)y_{1j}^s(c) - y_{5j}^s(c)], \end{aligned} \tag{2.68}$$

where superscripts s and l refer to the values in the solid mantle and in the liquid core, respectively. The above equations determine the ratios of Q_2/Q_1 and Q_3/Q_1. All of the y_i's are thus determined at the boundary, except for a free multiplier, Q_1, which is to be determined by the surface boundary conditions.

2.2.4 Core–Mantle Boundary, $r = b$

All of the y_i's, except for y_3, should be continuous. The boundary conditions can be decomposed into three independent sets,

$$[y_{ij}^s(b)] = \begin{pmatrix} 0 & 1 & 0 \\ -\rho^l y_{51}^l(b) & \rho^l g & 0 \\ 0 & 0 & 1 \\ 0 & 0 & 0 \\ y_{51}^l(b) & 0 & 0 \\ y_{71}^l(b) + \dfrac{4\pi G\rho^l}{g} y_{51}^l(b) & -4\pi G\rho^l & 0 \end{pmatrix} \begin{pmatrix} Q_1 \\ Q_2 \\ Q_3 \end{pmatrix} \quad \begin{pmatrix} i = 1,\ldots,6 \\ j = 1, 2, 3 \end{pmatrix}, \tag{2.69}$$

where $y_{51}^l(r)$ and $y_{71}^l(r)$ are integrations of equations (2.44) and (2.45). The coefficients, Q_j, should be determined by the free boundary conditions discussed below.

2.2.5 Free Surface, $r = a$

Vanishing of the radial stress components on the free surface, $r = a$, requires that

$$y_2(a) = 0 \tag{2.70}$$

$$y_4(a) = 0. \tag{2.71}$$

The third free boundary condition can be derived as follows. Let ψ_e denote the perturbation of gravitational potential outside the earth. It must be a harmonic function since it is a solution of Laplace's equation. Thus, the solution is given by

$$\psi_e(r, \theta, \phi) = D\left(\frac{a}{r}\right)^{n+1} Y_n(\theta, \phi) \qquad \text{for } r \geq a, \tag{2.72}$$

where D is equal to $y_5(a)$, since the potential is continuous at the surface.

Substituting the above solution into the surface boundary condition,

$$\frac{\partial \psi}{\partial r} - 4\pi G\rho u_r = \frac{\partial \psi_e}{\partial r} \qquad \text{at } r = a, \tag{2.73}$$

yields

$$y_6(a) = 0. \tag{2.74}$$

Equations (2.70), (2.71) and (2.74) constitute the free boundary conditions on the surface of the earth.

2.3 Method of Integration

The basic equations (2.34) are inhomogeneous, since they include **F**-terms which represent a jump at the point source. We must solve the singular inhomogeneous equations with free boundary conditions at the earth's surface, $r = a$. SMYLIE and MANSINHA (1971) as well as TAKEUCHI and SAITO (1972) have discussed the methods for solving the problem. Hence, we solve the problem by reducing it to a boundary-value problem after TAKEUCHI and SAITO (1972).

The theory of ordinary differential equations states that the solution vector **Y** *of inhomogeneous* equations (2.34) comprises two parts,

$$\mathbf{Y} = \mathbf{X} + \mathbf{Z}, \tag{2.75}$$

where the vector **X** denotes a general solution to the *homogeneous* equations (2.37), while **Z** is a special solution to the *inhomogeneous* equations (2.34).

$$z_j(r_0) = s_j \tag{2.76}$$

$$z_j(r) = 0 \qquad \text{for } r < r_0. \tag{2.77}$$

In practice, **Z** can be obtained by integrating equations (2.37) again up to the free surface, $r = a$, with the initial values of s_j at $r = r_0$.

X is composed of

$$x_j(r) = \sum_{i=1}^{3} \beta_i x_j^i(r) \qquad (j = 1,\ldots,6), \tag{2.78}$$

where $x_j^i(r)$ are three sets of general solutions regular at the origin. β_i's are three arbitrary constants to be determined later.

The free boundary conditions ((2.70), (2.71) and (2.74)) are used to determine β_i as

$$y_2(a) = \sum_{i=1}^{3} \beta_i x_2^i(a) + z_2(a) = 0, \tag{2.79}$$

$$y_4(a) = \sum_{i=1}^{3} \beta_i x_4^i(a) + z_2(a) = 0, \tag{2.80}$$

$$y_6(a) = \sum_{i=1}^{3} \beta_i x_6^i(a) + z_6(a) = 0, \tag{2.81}$$

or equivalently as

$$\begin{pmatrix} x_2^1(a) & x_2^2(a) & x_2^3(a) \\ x_4^1(a) & x_4^2(a) & x_4^3(a) \\ x_6^1(a) & x_6^2(a) & x_6^3(a) \end{pmatrix} \begin{pmatrix} \beta_1 \\ \beta_2 \\ \beta_3 \end{pmatrix} = -\begin{pmatrix} z_2(a) \\ z_4(a) \\ z_6(a) \end{pmatrix}. \tag{2.82}$$

Once β_i is calculated, the desired solutions $(y_1(r), y_3(r), y_5(r))$ can be obtained using

$$y_1(r) = \sum_{i=1}^{3} \beta_i x_1^i(r) + z_1(r), \tag{2.83}$$

$$y_3(r) = \sum_{i=1}^{3} \beta_i x_3^i(r) + z_3(r), \tag{2.84}$$

$$y_5(r) = \sum_{i=1}^{3} \beta_i x_5^i(r) + z_5(r). \tag{2.85}$$

The inhomogeneous equations (2.34) are thus solved by integrating the homogeneous equations (2.37) two times using different initial values.

2.4 Solutions of Degrees 0 and 1

We must pay special attention to the cases $n = 0, 1$. Since a sphere of finite radius cannot remain in static equilibrium under the action of an unbalanced force system, the term of the degree-1 mode diverges.

2.4.1 Degree 0

A force proportional to $P_0(\cos\theta)$ is uniform over a spherical surface, $r =$ *constant*. It causes a radial displacement without any tangential displacement or potential perturbation. When $n = 0$ differential equations (2.34) become

$$\frac{dy_1}{dr} = \frac{-2\lambda}{\lambda + 2\mu}\frac{y_1}{r} + \frac{1}{\lambda + 2\mu} y_2, \tag{2.86}$$

$$\frac{dy_2}{dr} = \left[-4\rho g r + \frac{4\mu(3\lambda + 2\mu)}{\lambda + 2\mu}\right]\frac{y_1}{r^2} - \frac{4\mu}{\lambda + 2\mu}\frac{y_2}{r} - F_2\frac{\delta(r - r_0)}{r_0^2}, \tag{2.87}$$

$$\frac{dy_5}{dr} = 4\pi G\rho y_1, \tag{2.88}$$

$$\frac{dy_6}{dr} = 0. \tag{2.89}$$

In a liquid core ($\mu = 0$) we have

$$\frac{dy_1}{dr} = -\frac{2y_1}{r} + \frac{y_2}{\lambda}, \tag{2.90}$$

$$\frac{dy_2}{dr} = -4\rho g\frac{y_1}{r}, \tag{2.91}$$

$$\frac{dy_5}{dr} = 4\pi G\rho y_1, \tag{2.92}$$

$$\frac{dy_6}{dr} = 0. \tag{2.93}$$

We must only integrate equations (2.86) and (2.87), since (y_5, y_6) is decoupled from (y_1, y_2).

2.4.2 Degree 1

It was found by BEN-MENAHEM and SINGH (1968) that in the case of a homogeneous sphere the degree-1 term diverges. This is due to the fact that a sphere of finite radius cannot remain in static equilibrium under the action of an unbalanced force system. To find the solution corresponding to $n = 1$ for a dislocation source which is equivalent to a balanced force system, they first evaluated the displacement field in an unbounded medium due to the dislocation, and then proceeded to the case of a sphere of radius a. They used the principles of conservation of the angular momentum and the mass center, i.e.

$$\iiint r\mathbf{e}_r \times \mathbf{u}d\tau = 0 \tag{2.94}$$

and

$$\iiint \mathbf{u}d\tau = 0, \tag{2.95}$$

respectively. Here, $d\tau = r^2 \sin\theta dr d\theta d\phi$ and the integration is over the volume bounded by the sphere.

Condition (2.94), which implies the angular momentum of the sphere about its center remains zero, is used for toroidal motion. Condition (2.95), that the center of mass of the sphere is not displaced, is applied for spheroidal equilibrium. Therefore, in our present study we were only interested in (2.95).

In a load-deformation problem the degree-1 mode of deformation has a similar situation. Many authors (FARRELL, 1972; SAITO, 1974; OKUBO and ENDO, 1986) have studied the problem. They found that the degree-1 mode shifts the center of the earth, while the center of mass of the earth, plus the loading mass, should remain fixed with respect to space. The shift depends on the choice of the origin. They referred to the center of mass of the deformed earth. It is physically consistent with the above-mentioned condition (2.95).

Computationally, we proceed as follows. We choose any two of the three conventional solutions to (2.34) and propagate them from the core to the surface. At the surface the correct mix of the two solutions is found by satisfying any two of the three boundary conditions. A consistency relation,

$$y_2 + 2y_4 + \frac{g}{4\pi G}y_6 = 0, \tag{2.96}$$

assures us that the third boundary condition is automatically met.

To keep the center of mass of the earth unchanged, we add a proper amount of a rigid translation solution to solution $\mathbf{Y}^c$ calculated as described above,

$$\mathbf{Y} = \mathbf{Y}^c + \alpha\mathbf{Y}^{shift}, \tag{2.97}$$

$$\mathbf{Y}^{shift} = (1, 0, 1, 0, g, 0)^t. \tag{2.98}$$

Here, α is found by setting the center of mass of the $\mathbf{Y}$ vector equal to zero. This is equivalent to the condition that the change in potential vaishes, i.e.

$$y_5 + \alpha g = 0. \tag{2.99}$$

We then have

$$\alpha = -\frac{y_5}{g}, \tag{2.100}$$

Upon substituting (2.100) in (2.97), we obtain

$$\mathbf{Y} = \mathbf{Y}^c - \frac{y_5}{g}\mathbf{Y}^{shift}. \tag{2.101}$$

Therefore, in a practical calculation we can integrate the equations of equilibrium without considering the rigid shift solution (2.97).

3. Dislocation Models

In this chapter we discuss three kinds of excitation sources—the shear dislocation, tensile dislocation, and explosion. We show that they can be expressed by four independent components: a vertical strike-slip, a vertical dip-slip, a dip-slip at a 45° dipping plane, and a vertical tensile fracturing. In section 3.2 we describe source functions for point dislocations. We define dislocation Love numbers in section 3.4.

3.1 Geometry of a Dislocation in Spherical Coordinates

We define the geometry of an arbitrary point dislocation in terms of the conventional fault parameters (Figure 3.1). The location of an arbitrary earthquake is given by its colatitude, θ_0, longitude, ϕ_0, and radial distance, r_0 (or equivalently, its depth $d_s = a - r_0$). The fault plane is defined by its strike azimuth, α, on the earth's surface (measured here clockwise from north) and its dip angle, δ, with respect to the earth's surface. The direction of a point shear dislocation is determined by the parameter λ: the slip angle measured in the fault plane counterclockwise from the horizontal. Unit vectors $\mathbf{n}$ and $\boldsymbol{\nu}$ can be expressed in terms of strike α, dip δ, and slip λ of the fault in the following way (BEN-MENAHEM and SINGH, 1968; DAHLEN, 1971):

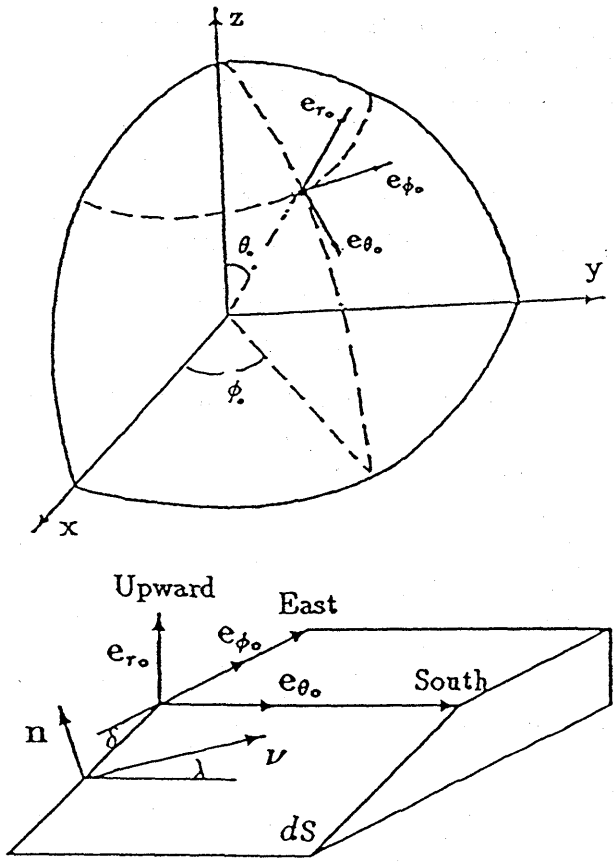

Fig. 3.1 Dislocation model. The upper figure shows the location of an earthquake within a sphere. The lower figure indicates the fault geometry in spherical coordinates.

$$\mathbf{n} = \mathbf{e}_{r_0} \cos\delta + \mathbf{e}_{\theta_0} \sin\alpha \sin\delta - \mathbf{e}_{\phi_0} \cos\alpha \sin\delta \tag{3.1}$$

$$\begin{aligned} \nu = {} & \mathbf{e}_{r_0} \sin\delta \sin\lambda + \mathbf{e}_{\theta_0}(\cos\alpha \cos\lambda - \sin\alpha \cos\delta \sin\lambda) \\ & + \mathbf{e}_{\phi_0}(\sin\alpha \cos\lambda + \cos\alpha \cos\delta \sin\lambda). \end{aligned} \tag{3.2}$$

The model discussed above is for a shear dislocation. The one used for a tensile dislocation can be easily obtained by taking $\nu = \mathbf{n}$.

3.2 Source Functions for Point Dislocations

In the following we introduce source functions (defined in chapter 2.2.1) in spherical coordinates. Without any loss of generality, we assume that

$$\theta_0 = \phi_0 = \alpha = 0 \tag{3.3}$$

in order to simplify the formulation. This is equivalent to considering an earthquake located on the polar axis, keeping the fault line along the Greenwich

meridian. The deformation field due to a source at an arbitrary position can be obtained by simply using the rotational transformation.

Then, the unit vectors $\mathbf{n}$ and ν are simplified as

$$\mathbf{n} = \mathbf{e}_{r_0} \cos\delta - \mathbf{e}_{\phi_0} \sin\delta \tag{3.4}$$

$$\nu = \mathbf{e}_{r_0} \sin\delta \sin\lambda + \mathbf{e}_{\theta_0} \cos\lambda + \mathbf{e}_{\phi_0} \cos\delta \sin\lambda. \tag{3.5}$$

We use the space-fixed bases ($\mathbf{e}_x$, $\mathbf{e}_y$, $\mathbf{e}_x$) to express the following two vectors:

$$\mathbf{n} = n_x\mathbf{e}_x + n_y\mathbf{e}_y + n_z\mathbf{e}_z \tag{3.6}$$

$$\nu = \nu_x\mathbf{e}_x + \nu_y\mathbf{e}_y + \nu_z\mathbf{e}_z. \tag{3.7}$$

We take $\mathbf{e}_x$ and $\mathbf{e}_y$ in the equatorial plane in the direction of $\phi = 0$ and $\pi/2$, respectively, and $\mathbf{e}_z$ along the polar axis. The source functions of the point dislocations can thus be expressed as (TAKEUCHI and SAITO, 1972)

$$s_1 = \frac{2n+1}{4\pi r_0^2}\left[n_z\nu_z + \frac{\lambda}{\lambda+2\mu}(n_x\nu_x + n_y\nu_y)\right]UdS; \qquad m = 0, \tag{3.8}$$

$$s_2 = -\frac{2n+1}{2\pi r_0^3}\frac{\mu(3\lambda+2\mu)}{\lambda+2\mu}(n_x\nu_x + n_y\nu_y)UdS; \qquad m = 0, \tag{3.9}$$

$$s_3 = \frac{2n+1}{4\pi n(n+1)r_0^2}\frac{1}{2}[\pm(n_z\nu_x + n_x\nu_z) - i(n_y\nu_z + n_z\nu_y)]UdS; \qquad m = \pm 1, \tag{3.10}$$

$$s_4 = \frac{2n+1}{4\pi r_0^3}\frac{\mu(3\lambda+2\mu)}{\lambda+2\mu}(n_x\nu_x + n_y\nu_y)UdS; \qquad m = 0, \tag{3.11}$$

$$= \frac{2n+1}{4\pi n(n+1)r_0^3}\frac{\mu}{2}[(-n_x\nu_x + n_y\nu_y) \pm i(n_x\nu_y + n_y\nu_x)]UdS; \qquad m = \pm 2, \tag{3.12}$$

$$s_5 = 0; \qquad m = 0, \pm 1, \pm 2, \tag{3.13}$$

$$s_6 = 0; \qquad m = 0, \pm 1, \pm 2. \tag{3.14}$$

Here, U is the dislocation on an infinitesimal fault of area dS.

3.3 Four Independent Solutions

In this section we show that the deformation caused by the above-mentioned dislocation model can be expressed by a linear combination of four independent solutions. Let $\mathbf{Y}^{ij}$ be a solution corresponding to the slip, ν_i, and normal, n_j. Then, a deformation field caused by an arbitrary dislocation is written as

$$\mathbf{Y} = \mathbf{Y}^{ij}u_i n_j dS, \tag{3.15}$$

where u_i is a dislocation on a fault plane of area dS. The general solution $\mathbf{Y}$ here includes the displacement, gravitational potential change, gravity change, and so on. If all the $\mathbf{Y}^{ij}$ are known, the deformation due to an arbitrary dislocation solution can be obtained from combinations of $\mathbf{Y}^{ij}$.

Table 3.1. 4 Types of dislocations

Type	λ	δ	ν	n	$\lvert m\rvert$	Meaning
1	0°	90°	$\mathbf{e}_{\theta_0}$	$-\mathbf{e}_{\phi_0}$	2	Vertical strike-slip
2	90°	90°	$\mathbf{e}_{r_0}$	$-\mathbf{e}_{\phi_0}$	1	Vertical dip-slip
3	90°	45°	$\frac{1}{\sqrt{2}}(\mathbf{e}_{r_0}+\mathbf{e}_{\phi_0})$	$\frac{1}{\sqrt{2}}(\mathbf{e}_{r_0}-\mathbf{e}_{\phi_0})$	0, 2	45° dip-slip
4	—	0°	$\mathbf{e}_{r_0}$	$\mathbf{e}_{r_0}$	0	Vertical tensile fracturing

Since i and j correspond to spherical basis vectors $\mathbf{e}_{\theta_0}$, $\mathbf{e}_{\phi_0}$, and $\mathbf{e}_{r_0}$, (briefly, $i, j = 1, 2, 3$), the total number of $\mathbf{Y}^{ij}$ is nine. A geophysical consideration shows that $\mathbf{Y}^{ij}$ is symmetric with respect to i and j. Hence, the number of independent $\mathbf{Y}^{ij}$ reduces to six. Furthermore, the intrinsic symmetry within the fault geometry indicates that components $\mathbf{Y}^{22}$ and $\mathbf{Y}^{13}$ can be easily calculated by applying a rotational transformation about the polar axis to $\mathbf{Y}^{11}$ and $\mathbf{Y}^{12}$, respectively. Consequently, the number of independent $\mathbf{Y}^{ij}$ is 4. In the following, we choose four such dislocations (see Table 3.1) so that they express a vertical strike-slip, a vertical dip-slip, a dip-slip on a 45° dipping plane, and a tensile faults. It is easy to verify that the four dislocations are mutually independent. Furthermore, an appropriate linear combination of the four describes a shear dislocation, a tensile dislocation and an explosion of an arbitrary geometry.

3.3.1 Shear Dislocation

If a dislocation vector $\boldsymbol{\nu}$ runs parallel to the fault plane, we have a shear dislocation problem,

$$\boldsymbol{\nu}\cdot\mathbf{n} = 0, \tag{3.16}$$

with the dyad

$$\begin{aligned}\boldsymbol{\nu}\mathbf{n} = {} & \cos\lambda[(-\mathbf{e}_{\theta_0}\mathbf{e}_{\phi_0})\sin\delta + \mathbf{e}_{\theta_0}\mathbf{e}_{r_0}\cos\delta] \\ & + \sin\lambda\left[\frac{1}{2}(\mathbf{e}_{r_0}\mathbf{e}_{r_0} - \mathbf{e}_{\phi_0}\mathbf{e}_{\phi_0})\sin 2\delta - (-\mathbf{e}_{r_0}\mathbf{e}_{\phi_0})\cos 2\delta\right].\end{aligned} \tag{3.17}$$

Let $\mathbf{Y}^{(1)}$ be the solution corresponding to $-\mathbf{e}_{\theta_0}\mathbf{e}_{\phi_0}$, $\mathbf{Y}^{(2)}$ the solution corresponding to $-\mathbf{e}_{r_0}\mathbf{e}_{\phi_0}$, and $\mathbf{Y}^{(3)}$ the solution raised by $\frac{1}{2}(\mathbf{e}_{r_0}\mathbf{e}_{r_0} - \mathbf{e}_{\phi_0}\mathbf{e}_{\phi_0})$, or,

$$\begin{aligned}\mathbf{Y}^{(1)} &: -\mathbf{e}_{\theta_0}\mathbf{e}_{\phi_0}, \\ \mathbf{Y}^{(2)} &: -\mathbf{e}_{r_0}\mathbf{e}_{\phi_0}, \\ \mathbf{Y}^{(3)} &: \frac{1}{2}(\mathbf{e}_{r_0}\mathbf{e}_{r_0} - \mathbf{e}_{\phi_0}\mathbf{e}_{\phi_0}).\end{aligned}$$

We define $\mathbf{Y}^{(2)*}$ as

$$\mathbf{Y}^{(2)*}(\phi) = \mathbf{Y}^{(2)}\left(\phi - \frac{\pi}{2}\right), \tag{3.18}$$

which corresponds to $\mathbf{e}_{\theta_0}\mathbf{e}_{r_0}$ in (3.17). It follows that the general solution $\mathbf{Y}^{(s)}$ of the shear dislocation can be written as

$$\begin{aligned}\mathbf{Y}^{(s)} = &\cos\lambda[\mathbf{Y}^{(1)}\sin\delta + \mathbf{Y}^{(2)*}\cos\delta] \\ &+ \sin\lambda[\mathbf{Y}^{(3)}\sin 2\delta - \mathbf{Y}^{(2)}\cos 2\delta].\end{aligned} \tag{3.19}$$

3.3.2 Tensile Dislocation

If $\boldsymbol{\nu}$ is perpendicular to the fault plane, we obtain a tensile dislocation problem. We have

$$\boldsymbol{\nu} = \mathbf{n} = \mathbf{e}_{r_0}\cos\delta - \mathbf{e}_{\phi_0}\sin\delta \tag{3.20}$$

and

$$\boldsymbol{\nu}\mathbf{n} = \mathbf{e}_{r_0}\mathbf{e}_{r_0} - (\mathbf{e}_{r_0}\mathbf{e}_{r_0} - \mathbf{e}_{\phi_0}\mathbf{e}_{\phi_0})\sin^2\delta - \frac{1}{2}(\mathbf{e}_{r_0}\mathbf{e}_{\phi_0} - \mathbf{e}_{\phi_0}\mathbf{e}_{r_0})\sin 2\delta. \tag{3.21}$$

A solution corresponding to $\frac{1}{2}(\mathbf{e}_{r_0}\mathbf{e}_{r_0} - \mathbf{e}_{\phi_0}\mathbf{e}_{\phi_0})$ and that corresponding to $-\mathbf{e}_{r_0}\mathbf{e}_{\phi_0}$ have been obtained in the case of a shear dislocation. We, thus, need to evaluate the contribution from $\mathbf{e}_{r_0}\mathbf{e}_{r_0}$: a vertical tensile dislocation. If we denote $\mathbf{Y}^{(4)}$ as the solution corresponding to $\mathbf{e}_{r_0}\mathbf{e}_{r_0}$, we obtain the following expression for the solution $\mathbf{Y}^{(t)}$ due to an arbitrary oriented tensile dislocation:

$$\mathbf{Y}^{(t)} = \mathbf{Y}^{(4)} - 2\mathbf{Y}^{(3)}\sin^2\delta + \mathbf{Y}^{(2)}\sin 2\delta. \tag{3.22}$$

3.3.3 Explosion

Since the dyad of an explosion is

$$\boldsymbol{\nu}\mathbf{n} = \mathbf{e}_{r_0}\mathbf{e}_{r_0} + \mathbf{e}_{\theta_0}\mathbf{e}_{\theta_0} + \mathbf{e}_{\phi_0}\mathbf{e}_{\phi_0}, \tag{3.23}$$

the corresponding solution $\mathbf{Y}^{(e)}$ is given by

$$\mathbf{Y}^{(e)} = \mathbf{Y}(\mathbf{e}_{r_0}\mathbf{e}_{r_0}) + \mathbf{Y}(\mathbf{e}_{\theta_0}\mathbf{e}_{\theta_0}) + \mathbf{Y}(\mathbf{e}_{\phi_0}\mathbf{e}_{\phi_0}), \tag{3.24}$$

where $\mathbf{Y}(\mathbf{e}_{r_0}\mathbf{e}_{r_0})$ is the solution due to $\mathbf{e}_{r_0}\mathbf{e}_{r_0}$ discussed in section 3.3.2, $\mathbf{Y}(\mathbf{e}_{\phi_0}\mathbf{e}_{\phi_0})$ the solution corresponding to $\mathbf{e}_{\phi_0}\mathbf{e}_{\phi_0}$ given by $\mathbf{Y}^{(4)} - 2\mathbf{Y}^{(3)}$, and $\mathbf{Y}(\mathbf{e}_{\theta_0}\mathbf{e}_{\theta_0})$ the solution corresponding to $\mathbf{e}_{\theta_0}\mathbf{e}_{\theta_0}$ obtained from $\mathbf{Y}^{(4)} - 2\mathbf{Y}^{(3)}$ by changing ϕ to $\phi + \pi/2$, i.e.

$$\begin{aligned}\mathbf{Y}(\mathbf{e}_{r_0}\mathbf{e}_{r_0}) &= \mathbf{Y}^{(4)}, \\ \mathbf{Y}(\mathbf{e}_{\phi_0}\mathbf{e}_{\phi_0}) &= \mathbf{Y}^{(4)} - 2\mathbf{Y}^{(3)}, \\ \mathbf{Y}(\mathbf{e}_{\theta_0}\mathbf{e}_{\theta_0}) &= \mathbf{Y}^{(4)}\left(\phi + \frac{\pi}{2}\right) - 2\mathbf{Y}^{(3)}\left(\phi + \frac{\pi}{2}\right) \\ &= \mathbf{Y}^{(4)*}(\phi) - 2\mathbf{Y}^{(3)*}(\phi).\end{aligned} \tag{3.25}$$

We thus derive the following expression for the solution due to an explosion

$$\mathbf{Y}^{(e)} = 2(\mathbf{Y}^{(4)} - \mathbf{Y}^{(3)}) + \mathbf{Y}^{(4)*} - 2\mathbf{Y}^{(3)*}. \tag{3.26}$$

3.4 Dislocation Love Numbers

Love and Shida numbers (we collectively call them Love numbers) express the elastic deformation of the earth due to external forces. For example, the tidal Love number triplet (h_n, l_n, k_n) describes the displacement and gravitational potential change at the surface of the earth. Since the surface mass load also deforms the elastic earth, one can define the load Love numbers (h'_n, l'_n, k'_n) (LONGMAN, 1962, 1963; FARRELL, 1972). SAITO (1978) defined the shear Love numbers (h''_n, l''_n, k''_n) which specify the elastic response of the earth to a shear force acting on the earth's surface.

In the same way, we define a new Love number triplet $[h_n^d(T, m), l_n^d(T, m), k_n^d(T, m)]$, so that the spheroidal deformation of the earth raised by a point dislocation of type (T, m) is described as

$$\mathbf{u}(a, \theta, \phi) = \frac{1}{a^2} \sum_{n,m} [h_n^d(T, m)\mathbf{R}_n^m(\theta, \phi) + l_n^d(T, m)\mathbf{S}_n^m(\theta, \phi)] \cdot UdS \quad (3.27)$$

$$\psi(a, \theta, \phi) = \frac{g_0}{a^2} \sum_{n,m} k_n^d(T, m) Y_n^m(\theta, \phi) \cdot UdS, \quad (3.28)$$

where 'T' indicates one of the four type dislocations chosen in Table 3.1, and 'm' is the order of the spheroidal harmonics. We call $[h_n^d(T, m), l_n^d(T, m), k_n^d(T, m)]$ dislocation Love numbers. We may derive the relation between the dislocation Love numbers and $\{y_j; j = 1, 2, \ldots, 6\}$ from equations (2.24) and (2.25) as

$$h_n^d(T, m) = y_1^{(T)} a^2, \quad (3.29)$$

$$l_n^d(T, m) = y_3^{(T)} a^2, \quad (3.30)$$

$$k_n^d(T, m) = y_5^{(T)} \frac{a^2}{g_0}. \quad (3.31)$$

We should notice that the dislocation Love numbers are independent of the magnitude of dislocation UdS. We show the relations between them in Table 3.2.

When $n = 0$, it is obvious from (2.90)−(2.93) that the dislocation Love numbers $l_0^d(T, 0)$ and $k_0^d(T, 0)$ are zero. The vanishing of $k_0^d(T, 0)$ is expected, since it is proportional to the change in the earth's mass, which should be conserved during a deformation.

For the special case $n = 1$, we have the following degree-1 dislocation Love numbers from (2.101):

$$h_1^d(T, m) = h_1^c - k_1^c, \quad (3.32)$$

$$l_1^d(T, m) = l_1^c - k_1^c, \quad (3.33)$$

$$k_1^d(T, m) = k_1^c - k_1^c. \quad (3.34)$$

They can be expressed as

$$h_1^d(T, m) = \left(y_1^{(T)}(a) - \frac{y_5^{(T)}(a)}{g_0} \right) \cdot a^2, \quad (3.35)$$

Table 3.2. Relations between the dislocation Love numbers and the source functions. $y_i^{(T)}$ in this table satisfies the source condition, $y_i^{(T)}(r_0^+) - y_i^{(T)}(r_0^-) = s_i$, and the free boundary conditions on the earth's surface

Type	Order	*Source Functions*	*Dislocation Love Numbers*		
T	m	s_i $(i = 1, 2, \cdots, 6)$	$y_1^{(T)}a^2$	$y_3^{(T)}a^2$	$y_5^{(T)}\frac{a^2}{g_0}$
1	2	$-\frac{(2n+1)\mu}{8\pi n(n+1)r_0^3}\delta_{i4}$	$h_n^d(1,2)$	$l_n^d(1,2)$	$k_n^d(1,2)$
2	1	$\frac{2n+1}{8\pi n(n+1)r_0^2}\delta_{i3}$	$h_n^d(2,1)$	$l_n^d(2,1)$	$k_n^d(2,1)$
3	0	$\frac{2n+1}{8\pi r_0^2}(1-\frac{\lambda}{\lambda+2\mu})\delta_{i1}$ $+\frac{2n+1}{4\pi r_0^3}\frac{\mu(3\lambda+2\mu)}{\lambda+2\mu}\delta_{i2}$ $-\frac{2n+1}{8\pi r_0^3}\frac{\mu(3\lambda+2\mu)}{\lambda+2\mu}\delta_{i4}$	$h_n^d(3,0)$	$l_n^d(3,0)$	$k_n^d(3,0)$
	2	$-\frac{(2n+1)\mu}{16\pi n(n+1)r_0^3}\delta_{i4}$	$-\frac{1}{2}h_n^d(1,2)$	$-\frac{1}{2}l_n^d(1,2)$	$-\frac{1}{2}k_n^d(1,2)$
4	0	$\frac{2n+1}{4\pi r_0^2}\delta_{i1}$	$h_n^d(4,0)$	$l_n^d(4,0)$	$k_n^d(4,0)$

$$l_1^d(T, m) = \left(y_3^{(T)}(a) - \frac{y_5^{(T)}(a)}{g_0}\right) \cdot a^2, \tag{3.36}$$

$$k_1^d(T, m) = (y_5^{(T)}(a) - y_5^{(T)}(a)) \cdot \frac{a^2}{g_0} = 0. \tag{3.37}$$

4. Theory of Potential and Gravity Changes

In this chapter we focus our attention on potential and gravity changes raised by dislocations buried in a radially heterogeneous earth model. We first discuss the general theory of potential and gravity changes in section 4.1. In sections 4.2–4.5, we show in detail the potential and gravity changes due to vertical strike-slip, vertical dip-slip, 45° dip-slip, and vertical tensile fracturing. In section 4.6, we discuss the special case of $d_s \to 0$, i.e. a point source approaching the earth's surface. We derive expressions for an arbitrary geometry in section 4.7 and general formulas for practical applications in section 4.8.

4.1 Potential and Gravity Changes

A dislocation within the earth causes a density change and a displacement of interfaces, perturbing the gravitational potential. Similar to the flat-earth case (OKUBO, 1991), the gravitational potential change, ψ, in a sphere may also be expressed as

$$\psi(r, \theta, \phi) = \psi^{ij}(r, \theta, \phi)u_i n_j dS, \tag{4.1}$$

where ψ^{ij} is the potential change corresponding to a dislocation, u_i, on an infinitesimal plane of area dS with a normal n_j. Expression (4.1) is a special case of equation (3.15). As discussed in chapter 3, if we obtain solutions, ψ^{ij}, of four independent dislocation models, the potential change ψ due to an arbitrary point dislocation can be easily calculated using (4.1).

We can expand ψ^{ij} in spherical harmonics as

$$\psi^{ij}(a, \theta, \phi) = \frac{g_0}{a^2} \sum_{n,m} k_n^{dij}(T, m) Y_n^m(\theta, \phi) \tag{4.2}$$

where $k_n^{dij}(T, m)$ has the same meaning as $k_n^d(T, m)$, and can be calculated using (2.34). Once all of the $k_n^{dij}(T, m)$ for different n are given, we have ψ^{ij} and ψ from (4.2) and (4.1).

The gravity change at a *space-fixed* point can be calculated from ψ as

$$\Delta g(r, \theta, \phi) = -\frac{\partial \psi}{\partial r}. \tag{4.3}$$

The gravity change at a point *fixed to the free surface* of the earth is given by

$$\delta g(a, \theta, \phi) = \Delta g(a, \theta, \phi) - \beta u_r(a, \theta, \phi), \tag{4.4}$$

where $\beta \approx 3.09 \times 10^{-6}/sec^2$ stands for the free-air gravity gradient and u_r is the radial displacement:

$$u_r(a, \theta, \phi) = u_r^{ij}(a, \theta, \phi) u_i n_j dS \tag{4.5}$$

$$u_r^{ij}(a, \theta, \phi) = \frac{1}{a^2} \sum_{n,m} h_n^{dij}(T, m) Y_n^m(\theta, \phi). \tag{4.6}$$

We must pay special attention to gravity changes on the earth's surface ($r = a$) since we must consider the surface mass distribution, $4\pi G\rho u_r$. Across this single layer, the gravity is *not* continuous. The gravity change (positive downward) just *inside* this thin layer is

$$\Delta g_- (a, \theta, \phi) = - \frac{\partial \psi(r, \theta, \phi)}{\partial r}\Big|_{r=a-0}. \tag{4.7}$$

We are mainly interested in $\Delta g_+(a, \theta, \phi)$, the gravity change just *outside* the single layer, since gravity surveying is usually carried out on the free surface. From now on, we briefly use $\Delta g(a, \theta, \phi)$ for $\Delta g_+(a + u_r, \theta, \phi)$. Figure 4.1 shows the relations between Δg_-, Δg, and $u_r(a)$.

According to potential theory, we have

$$\Delta g(a, \theta, \phi) = \Delta g_-(a, \theta, \phi) + 4\pi G\rho u_r(a, \theta, \phi). \tag{4.8}$$

Since $y_6(a) = 0$, we have from the equation (2.32)

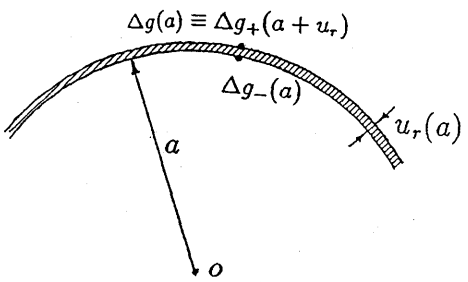

Fig. 4.1 Gravity step on the earth's surface.

$$\frac{dy_5}{dr}|_{r=a-0} = 4\pi G\rho y_1(a) - \frac{n+1}{a}y_5(a). \tag{4.9}$$

Since $\Delta g_- = -\partial\psi/\partial r$ (positive downward), Δg_- can be derived from (2.14) as

$$\begin{aligned}\Delta g_-(a, \theta, \phi) &= -\sum_{n=2}^{\infty}\frac{dy_5}{dr}|_{r=a-0}Y_n^m(\theta, \phi)\\ &= \frac{g_0}{a^3}\sum_{n=2}^{\infty}(n+1)k_n^d(T, m)Y_n^m(\theta, \phi)\\ &\quad - \frac{4\pi G\rho}{a^2}\cdot\sum_{n=2}^{\infty}h_n^d(T, m)Y_n^m(\theta, \phi)\\ &= \frac{g_0}{a^3}\sum_{n=2}^{\infty}(n+1)k_n^d(T, m)Y_n^m(\theta, \phi) - 4\pi G\rho u_r(a, \theta, \phi).\end{aligned} \tag{4.10}$$

Substituting (4.10) into (4.8), we obtain

$$\Delta g(a, \theta, \phi) = \frac{g_0}{a^3}\sum_{n=2}^{\infty}(n+1)k_n^d(T, m)Y_n^m(\theta, \phi). \tag{4.11}$$

The gravity change at a point fixed on the free surface becomes

$$\delta g(a, \theta, \phi) = \Delta g(a, \theta, \phi) - \beta u_r(a, \theta, \phi) \tag{4.12}$$

or

$$\delta g(a, \theta, \phi) = \Delta g_-(a, \theta, \phi) - (\beta - 4\pi G\rho)u_r(a, \theta, \phi), \tag{4.13}$$

where β is the free-air gravity gradient, which can be expressed as

$$\beta = \frac{dg(r)}{dr} = \frac{2g(a)}{a}. \tag{4.14}$$

4.2 Vertical Strike-Slip on the Polar Axis

From this section we derive u_r, ψ, Δg and δg for the four dislocation models assuming a dislocation magnitude of $UdS = 1$.

We begin with the vertical strike-slip model (Figure 4.2). In this case, $\lambda = 0°$, $\delta = 90°$, i.e.

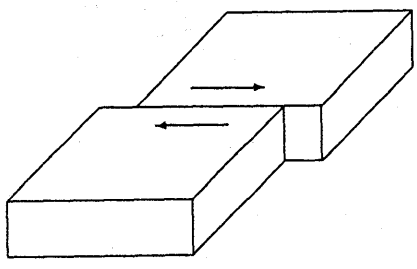

Fig. 4.2 Vertical strike-slip model.

$$\boldsymbol{\nu} = \mathbf{e}_{\theta_0} \tag{4.15}$$

$$\mathbf{n} = -\mathbf{e}_{\phi_0} \tag{4.16}$$

with the dyad

$$\boldsymbol{\nu}\mathbf{n} = -\mathbf{e}_{\theta_0}\mathbf{e}_{\phi_0}. \tag{4.17}$$

The components of the dislocation vector $\boldsymbol{\nu}$ and normal $\mathbf{n}$ are $\nu_x = 1$, $n_y = -1$, $\nu_y = \nu_z = n_x = n_z = 0$. The source functions are

$$\begin{cases} s_4^{(1)} = \mp i \dfrac{(2n+1)\mu}{8\pi n(n+1)r_0^3}; & m = \pm 2 \\ s_j^{(1)} = 0; & j = 1, 2, 3, 5, 6, \end{cases} \tag{4.18}$$

where superscript (1) denotes type 1 in Table 3.1: the vertical strike-slip model. Hence, we obtain the solution

$$\sum_n i y_j^{(1)}(r)(P_n^2(\cos\theta)e^{2i\phi} - P_n^{-2}(\cos\theta)e^{-2i\phi}) = -2\sum_n y_j^{(1)}(r)P_n^2(\cos\theta)\sin 2\phi, \tag{4.19}$$

where $y_j^{(1)}$ is the excited deformation field with

$$y_j^{(1)}(r_0^+) - y_j^{(1)}(r_0^-) = -\frac{(2n+1)\mu}{8\pi n(n+1)r_0^3}\delta_{j4}. \tag{4.20}$$

From (4.19), we obtain the radial displacement and potential due to a dislocation of magnitude $UdS = 1$ as

$$u_r^{(1)}(r, \theta, \phi) = -\hat{u}_r^{(1)}(r, \theta)\sin 2\phi \tag{4.21}$$

$$\psi^{(1)}(r, \theta, \phi) = -\hat{\psi}^{(1)}(r, \theta)\sin 2\phi, \tag{4.22}$$

where

$$\hat{u}_r^{(1)}(r, \theta) = \frac{2}{a^2}\sum_{n=2}^{\infty} h_n^d(1, 2)P_n^2(\cos\theta) \tag{4.23}$$

$$\hat{\psi}^{(1)}(r, \theta) = \frac{2g_0}{a^2}\sum_{n=2}^{\infty} k_n^d(1, 2)P_n^2(\cos\theta). \tag{4.24}$$

The displacement $u_r(a, \theta, \phi)$ at an arbitrary point (θ, ϕ) can be obtained from $\hat{u}_r(a, \theta)$ by multiplying an azimuthal factor, $-\sin 2\phi$. Therefore, we tabulate $\hat{u}_r(a, \theta)$ in the tables of Appendix E. From (4.11) and (4.12) we also have

$$\Delta\hat{g}^{(1)}(a, \theta) = \frac{2g_0}{a^3}\sum_{n=2}^{\infty}(n+1)k_n^d(1, 2)P_n^2(\cos\theta) \tag{4.25}$$

and

$$\delta\hat{g}^{(1)}(a, \theta) = \Delta\hat{g}^{(1)}(a, \theta) - \beta\hat{u}_r^{(1)}(a, \theta). \tag{4.26}$$

Formulas (4.23), (4.24), (4.25), and (4.26) are our desired results. At any point (θ, ϕ), the displacement, potential and gravity changes can be easily

calculated using the following formulas:

$$u_r^{(1)}(a, \theta, \phi) = -\hat{u}_r^{(1)}(a, \theta) \sin 2\phi, \tag{4.27}$$

$$\psi^{(1)}(a, \theta, \phi) = -\hat{\psi}^{(1)}(a, \theta) \sin 2\phi, \tag{4.28}$$

$$\Delta g^{(1)}(a, \theta, \phi) = -\Delta \hat{g}^{(1)}(a, \theta) \sin 2\phi, \tag{4.29}$$

$$\delta g^{(1)}(a, \theta, \phi) = -\delta \hat{g}^{(1)}(a, \theta) \sin 2\phi. \tag{4.30}$$

Equations (4.27)−(4.30) reveal a four-quadrant deformation pattern due to the factor $\sin 2\phi$. If u_r (or ψ, Δg, δg) is positive in quadrants 1 and 3, it becomes negative in quadrants 2 and 4.

As special cases, let us evaluate the radial displacement, potential and gravity changes for $\theta = 0$ and $\theta = \pi$. Since

$$\lim_{\theta \to 0} Y_n^m(\theta, \phi) = e^{im\phi} \delta_{0m} = \begin{cases} 1; & m = 0 \\ 0; & m \neq 0 \end{cases} \tag{4.31}$$

$$\lim_{\theta \to \pi} Y_n^m(\theta, \phi) = (-1)^n e^{im\phi} \delta_{0m} = \begin{cases} 1; & m = 0,\ n = \text{odd} \\ -1; & m = 0,\ n = \text{even} \\ 0; & m \neq 0, \end{cases} \tag{4.32}$$

it follows from (4.23), (4.24), (4.11) and (4.12) that

$$u_r^{(1)}(a, 0, \phi) = 0, \tag{4.33}$$

$$\psi^{(1)}(a, 0, \phi) = 0, \tag{4.34}$$

$$\Delta g^{(1)}(a, 0, \phi) = 0, \tag{4.35}$$

$$\delta g^{(1)}(a, 0, \phi) = 0, \tag{4.36}$$

and that

$$u_r^{(1)}(a, \pi, \phi) = 0, \tag{4.37}$$

$$\psi^{(1)}(a, \pi, \phi) = 0, \tag{4.38}$$

$$\Delta g^{(1)}(a, \pi, \phi) = 0, \tag{4.39}$$

$$\delta g^{(1)}(a, \pi, \phi) = 0. \tag{4.40}$$

4.3 Vertical Dip-Slip on the Polar Axis

In this section, we derive the potential and gravity changes caused by a vertical dip-slip model (Figure 4.3). The discussion follows exactly the same line as in section 4.2.

In this case, $\lambda = 90°$ and $\delta = 90°$, i.e.

$$\boldsymbol{\nu} = \mathbf{e}_{r_0} \tag{4.41}$$

$$\mathbf{n} = -\mathbf{e}_{\phi_0} \tag{4.42}$$

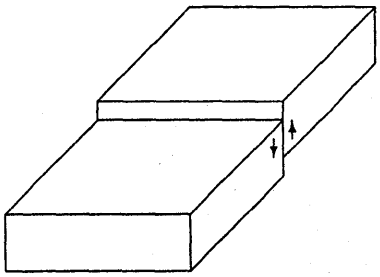

Fig. 4.3 Vertical dip-slip model.

with the dyad

$$\boldsymbol{\nu}\mathbf{n} = -\mathbf{e}_{\phi_0}\mathbf{e}_{r_0}. \tag{4.43}$$

The components of the dislocation vector $\boldsymbol{\nu}$ and the normal $\mathbf{n}$ are zero, except for $\nu_z = 1$ and $n_y = -1$. The source functions are

$$\begin{cases} s_3^{(2)} = i\dfrac{2n+1}{8\pi n(n+1)r_0^2}; & m = \pm 1 \\ s_j^{(2)} = 0; & j = 1, 2, 4, 5, 6, \end{cases} \tag{4.44}$$

where superscript (2) denotes type 2 in Table 3.1: the vertical dip-slip model. We obtain the solution

$$\sum_n iy_j^{(2)}(P_n^1(\cos\theta)e^{i\phi} + P_n^{-1}(\cos\theta)e^{-i\phi}) = -2\sum_n y_j^{(2)}P_n^1(\cos\theta)\sin\phi, \tag{4.45}$$

where $y_j^{(2)}$ is a real-valued solution defined by

$$y_j^{(2)}(r_0^+) - y_j^{(2)}(r_0^-) = -is_j^{(2)} \cdot \delta_{j4}. \tag{4.46}$$

We obtain the vertical displacement, potential and gravity changes on the earth's surface ($r = a$) due to a vertical dip-slip dislocation of unit magnitude ($UdS = 1$) as

$$u_r^{(2)}(a, \theta, \phi) = -\hat{u}_r^{(2)}(a, \theta)\sin\phi, \tag{4.47}$$

$$\psi^{(2)}(a, \theta, \phi) = -\hat{\psi}^{(2)}(a, \theta)\sin\phi, \tag{4.48}$$

$$\Delta g^{(2)}(a, \theta, \phi) = -\Delta\hat{g}^{(2)}(a, \theta)\sin\phi, \tag{4.49}$$

$$\delta g^{(2)}(a, \theta, \phi) = -\delta\hat{g}^{(2)}(a, \theta)\sin\phi. \tag{4.50}$$

Here,

$$\hat{u}_r^{(2)}(a, \theta) = \frac{2}{a^2}\sum_{n=1}^{\infty} h_n^d(2, 1)P_n^1(\cos\theta), \tag{4.51}$$

$$\hat{\psi}^{(2)}(a, \theta) = \frac{2g_0}{a^2}\sum_{n=1}^{\infty} k_n^d(2, 1)P_n^1(\cos\theta), \tag{4.52}$$

$$\Delta\hat{g}^{(2)}(a,\ \theta) = \frac{2g_0}{a^3}\sum_{n=1}^{\infty}(n+1)k_n^d(2,\ 1)P_n^1(\cos\theta), \tag{4.53}$$

$$\delta\hat{g}^{(2)}(a,\ \theta) = \Delta\hat{g}^{(2)}(a,\ \theta) - \beta\hat{u}_r^{(2)}(a,\ \theta). \tag{4.54}$$

The factor $\sin\phi$ in (4.47)–(4.50) reveals that the deformation pattern is anti-symmetric with respect to the fault line.

$\hat{u}_r^{(2)}$, $\hat{\psi}^{(2)}$, $\Delta\hat{g}^{(2)}$ and $\delta\hat{g}^{(2)}$ vanish on the two poles ($\theta = 0,\ \pi$) because P_n^1 in equations (4.51) through (4.54) is proportional to $\sin\theta$.

4.4 Dip-Slip on a Plane Dipping at 45°

We now look at the potential and gravity changes caused by a thrusting dislocation of unit magnitude ($UdS = 1$) on a plane dipping at 45° (Figure 4.4). The discussion follows exactly the same line as in the preceding section.

In this case, $\lambda = 90°$ and $\delta = 45°$, i.e.

$$\boldsymbol{\nu} = \frac{1}{\sqrt{2}}\mathbf{e}_{\phi_0} + \frac{1}{\sqrt{2}}\mathbf{e}_{r_0} \tag{4.55}$$

$$\mathbf{n} = -\frac{1}{\sqrt{2}}\mathbf{e}_{\phi_0} + \frac{1}{\sqrt{2}}\mathbf{e}_{r_0} \tag{4.56}$$

with the dyad

$$\boldsymbol{\nu}\mathbf{n} = \frac{1}{2}(\mathbf{e}_{r_0}\mathbf{e}_{r_0} - \mathbf{e}_{\phi_0}\mathbf{e}_{\phi_0}). \tag{4.57}$$

The corresponding components of the dislocation vector $\boldsymbol{\nu}$ and normal $\mathbf{n}$ are $\nu_x = 0$, $\nu_y = 1/\sqrt{2}$, $\nu_z = 1/\sqrt{2}$, $n_x = 0$, $n_y = -1/\sqrt{2}$, and $n_z = 1/\sqrt{2}$.

The source functions are non-zero only when $m = 0$ and $m = 2$. In the following we consider $m = 0$ and $|m| = 2$ separately.

When $m = 0$, the source functions are

$$\begin{cases} s_1^{(30)} = \dfrac{2n+1}{8\pi r_0^2}\left(1 - \dfrac{\lambda}{\lambda+2\mu}\right) \\ s_2^{(30)} = \dfrac{2n+1}{4\pi r_0^3}\dfrac{\mu(3\lambda+2\mu)}{\lambda+2\mu} \\ s_3^{(30)} = 0 \\ s_4^{(30)} = -\dfrac{2n+1}{8\pi r_0^3}\dfrac{\mu(3\lambda+2\mu)}{\lambda+2\mu} \\ s_5^{(30)} = 0 \\ s_6^{(30)} = 0, \end{cases} \tag{4.58}$$

where the superscript (30) denotes type 3 (45° dip-slip) with $m = 0$.

When $m = 0$, the solutions on the earth's surface are independent of the longitude, ϕ. Hence, after solving the equations of equilibrium, we obtain the corresponding solutions excited by a dislocation of unit magnitude ($UdS = 1$) as follows:

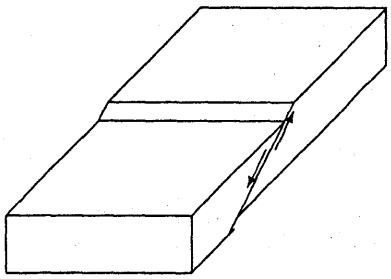

Fig. 4.4 45° Dip-slip model.

$$u_r^{(30)}(a, \theta, \phi) = \hat{u}_r^{(30)}(a, \theta) = \frac{1}{a^2}\sum_{n=0}^{\infty} h_n^d(3, 0)P_n(\cos\theta), \tag{4.59}$$

$$\psi^{(30)}(a, \theta, \phi) = \hat{\psi}^{(30)}(a, \theta) = \frac{g_0}{a^2}\sum_{n=0}^{\infty} k_n^d(3, 0)P_n(\cos\theta), \tag{4.60}$$

$$\Delta g^{(30)}(a, \theta, \phi) = \Delta\hat{g}^{(30)}(a, \theta) = \frac{g_0}{a^3}\sum_{n=0}^{\infty} (n + 1)k_n^d(3, 0)P_n(\cos\theta), \tag{4.61}$$

$$\delta g^{(30)}(a, \theta, \phi) = \delta\hat{g}^{(30)}(a, \theta) = \Delta\hat{g}^{(30)}(a, \theta) - \beta\hat{u}_r^{(30)}(a, \theta), \tag{4.62}$$

where $h_n^d(3, 0)$, $l_n^d(3, 0)$ and $k_n^d(3, 0)$ are the dislocation Love numbers corresponding to (4.58).

Since (4.59)−(4.62) are independent of the longitude, ϕ, the earth's surface deforms with the pattern of concentric circles about the north pole.

When $\theta = 0$ and π, it follows from equations (4.31), (4.32) and (4.59)−(4.62) ($m = 0$ for the dip-slip) that

$$u_r^{(30)}(a, 0, \phi) = \frac{1}{a^2}\sum_{n=0}^{\infty} h_n^d(3, 0), \tag{4.63}$$

$$\psi^{(30)}(a, 0, \phi) = \frac{g_0}{a^2}\sum_{n=0}^{\infty} k_n^d(3, 0), \tag{4.64}$$

$$\Delta g^{(30)}(a, 0, \phi) = \frac{g_0}{a^3}\sum_{n=0}^{\infty} (n + 1)k_n^d(3, 0), \tag{4.65}$$

$$\delta g^{(30)}(a, 0, \phi) = \Delta g^{(30)}(0) - \beta u_r^{(30)}(0). \tag{4.66}$$

We also have

$$u_r^{(30)}(a, \pi, \phi) = \frac{1}{a^2}\sum_{n=0}^{\infty} (-1)^n h_n^d(3, 0), \tag{4.67}$$

$$\psi^{(30)}(a, \pi, \phi) = \frac{g_0}{a^2}\sum_{n=0}^{\infty} (-1)^n k_n^d(3, 0), \tag{4.68}$$

$$\Delta g^{(30)}(a, \pi, \phi) = \frac{g_0}{a^3}\sum_{n=0}^{\infty} (-1)^n(n + 1)k_n^d(3, 0), \tag{4.69}$$

$$\delta g^{(30)}(a, \pi, \phi) = \Delta g^{(30)}(\pi) - \beta u_r^{(30)}(\pi). \tag{4.70}$$

When $|m| = 2$, the source functions are

$$\begin{cases} s_4^{(32)} = -\dfrac{(2n+1)\mu}{16\pi n(n+1)r_0^3}; & m = \pm 2 \\ s_j^{(32)} = 0; & j = 1, 2, 3, 5, 6, \end{cases} \tag{4.71}$$

where the superscript (32) denotes type 3 in Table 3.1 (the 45° dip-slip) with $|m| = 2$. Comparing them with (4.18) for the vertical strike-slip model leads to

$$s_j^{(32)} = \mp\frac{1}{2}is_j^{(1)}; \quad \text{for } m = \pm 2. \tag{4.72}$$

Equation (4.72) implies that the solution excited by the $s_j^{(32)}$ can be written in terms of $(\hat{u}_r^{(1)}, \hat{\psi}^{(1)}, \Delta\hat{g}^{(1)}, \delta\hat{g}^{(1)})$ as

$$u_r^{(32)}(a, \theta, \phi) = \frac{1}{2}\hat{u}_r^{(1)}(a, \theta)\cos 2\phi, \tag{4.73}$$

$$\psi^{(32)}(a, \theta, \phi) = \frac{1}{2}\hat{\psi}^{(1)}(a, \theta)\cos 2\phi, \tag{4.74}$$

$$\Delta g^{(32)}(a, \theta, \phi) = \frac{1}{2}\Delta\hat{g}^{(1)}(a, \theta)\cos 2\phi, \tag{4.75}$$

$$\delta g^{(32)}(a, \theta, \phi) = \frac{1}{2}\delta\hat{g}^{(1)}(a, \theta)\cos 2\phi. \tag{4.76}$$

On the two poles ($\theta = 0, \pi$), the results in (4.73)–(4.76) vanish because of (4.33)–(4.40).

4.5 Vertical Tensile Fracturing on the Polar Axis

In this case (Figure 4.5), we have

$$\boldsymbol{\nu} = \mathbf{e}_{r_0} \tag{4.77}$$

$$\mathbf{n} = \mathbf{e}_{r_0} \tag{4.78}$$

with a dyad

$$\boldsymbol{\nu}\mathbf{n} = \mathbf{e}_{r_0}\mathbf{e}_{r_0}. \tag{4.79}$$

This means that ν_j and n_j are zero, except for $\nu_z = 1$ and $n_z = 1$. The source functions are written as (TAKEUCHI and SAITO, 1972)

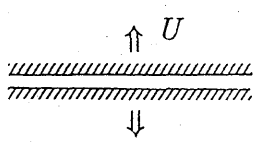

Fig. 4.5 Vertical tensile fracture model.

$$\begin{cases} s_1^{(4)} = \dfrac{2n+1}{4\pi r_0^2} \quad ; \quad m = 0 \\ s_2^{(4)} = 0 \\ s_3^{(4)} = 0 \\ s_4^{(4)} = 0 \\ s_5^{(4)} = 0 \\ s_6^{(4)} = 0, \end{cases} \tag{4.80}$$

where the superscript (4) denotes type 4 in Table 3.1: a vertical tensile dislocation.

The deformation caused by a tensile dislocation of unit magnitude ($UdS = 1$) is obtained as

$$u_r^{(4)}(a, \theta, \phi) = \hat{u}_r^{(4)}(a, \theta) = \frac{1}{a^2} \sum_{n=0}^{\infty} h_n^d(4, 0) P_n(\cos\theta), \tag{4.81}$$

$$\psi^{(4)}(a, \theta, \phi) = \hat{\psi}^{(4)}(a, \theta) = \frac{g_0}{a^2} \sum_{n=0}^{\infty} k_n^d(4, 0) P_n(\cos\theta), \tag{4.82}$$

$$\Delta g^{(4)}(a, \theta, \phi) = \Delta \hat{g}^{(4)}(a, \theta) = \frac{g_0}{a^3} \sum_{n=0}^{\infty} (n+1) k_n^d(4, 0) P_n(\cos\theta), \tag{4.83}$$

$$\delta g^{(4)}(a, \theta, \phi) = \delta \hat{g}^{(4)}(a, \theta) = \Delta \hat{g}^{(4)}(a, \theta) - \beta \hat{u}_r^{(4)}(a, \theta), \tag{4.84}$$

where $h_n^d(4, 0)$, $l_n^d(4, 0)$ and $k_n^d(4, 0)$ are the dislocation Love numbers excited by (4.80).

(4.81)−(4.84) indicated that the earth's surface deforms with the pattern of concentric circles about the north pole because they are independent of the longitude, ϕ.

Similar to the case of a 45° dip-slip with $m = 0$, we can obtain the results at two polar points by replacing the superscript (30) in equations (4.63)−(4.70) with (4).

4.6 Point Sources in the Limit of $d_s \to 0$

We must pay special attention when a point source approaches the earth's surface, i.e. $d_s \to 0$. Okada (1976) studied the problem in the case of a half space. We discuss how to obtain the corresponding solutions for a spherical earth.

4.6.1 Vertical Strike-Slip

Since the source functions for the vertical strike-slip with $d_s = 0$ have the same forms as that within the earth, the solutions can be obtained in the same way as that within the earth. We therefore do not specially discuss it here. However, the other cases show their peculiarities. We discuss them in the following separately.

4.6.2 Vertical Dip-Slip

When $d_s \to 0$ or $r_0 \to a$, the source functions become

$$\begin{cases} s_3^{(2)} = i\dfrac{2n+1}{8\pi n(n+1)a^2}; & m = \pm 1 \\ s_j^{(2)} = 0; & j = 1, 2, 4, 5, 6. \end{cases} \tag{4.85}$$

Note that all the s_j except for s_3, are zero, since the point source is located just on the earth's surface. Therefore, the solution simply becomes

$$y_j(a) = s_j(a) \qquad (j = 1, \ldots, 6). \tag{4.86}$$

Because s_j are known on the surface, they can be found without any integration,

$$\begin{cases} y_1(a) = s_1(a) = 0 \\ y_3(a) = s_3(a) = i\dfrac{2n+1}{8\pi n(n+1)a^2} \\ y_5(a) = s_5(a) = 0. \end{cases} \tag{4.87}$$

Since all y_i vanish, except for y_3, the vertical displacement, potential and gravity changes can be written as

$$u_r^{(2)}(a, \theta, \phi) = \hat{u}_r^{(2)}(a, \theta) = 0, \tag{4.88}$$

$$\psi^{(2)}(a, \theta, \phi) = \hat{\psi}^{(2)}(a, \theta) = 0, \tag{4.89}$$

$$\Delta g^{(2)}(a, \theta, \phi) = \Delta \hat{g}^{(2)}(a, \theta) = 0, \tag{4.90}$$

$$\delta g^{(2)}(a, \theta, \phi) = \delta \hat{g}^{(2)}(a, \theta) = 0. \tag{4.91}$$

4.6.3 45° Dip-Slip

In the case of a 45° dip-slip, we have only to take $m = 0, \mp 2$. For $|m| = 2$, the solution can be derived from that in the case of a strike-slip.

For $m = 0$, the source functions, or corresponding solution, are

$$\begin{cases} z_1^{(30)}(a) = s_1^{(30)}(a) = c(2n+1) \\ z_3^{(30)}(a) = s_3^{(30)}(a) = 0 \\ z_5^{(30)}(a) = s_5^{(30)}(a) = 0, \end{cases} \tag{4.92}$$

where c is a constant. The sums of the dislocation solution are given by

$$\sum_{n=0}^{\infty} z_1^{(30)}(a) = c \sum_{n=0}^{\infty} (2n+1) P_n(\cos\theta) \propto \delta(\theta), \tag{4.93}$$

$$\sum_{n=0}^{\infty} z_3^{(30)}(a) = 0, \tag{4.94}$$

$$\sum_{n=0}^{\infty} z_5^{(30)}(a) = 0, \tag{4.95}$$

in which the sum of harmonics,

$$\sum_{n=0}^{\infty} (2n+1) P_n(\cos\theta) \propto \delta(\theta), \tag{4.96}$$

is used. The sums of the dislocation solution vanish on the earth's surface, except at the singular point $\theta = 0$ where the point source is located. Therefore, the general solution needs not to include it, even though the source functions are non-zero. We therefore have

$$\sum_{n=0}^{\infty} y_j^{(30)} P_n(\cos\theta) = \sum_{n=0}^{\infty} (x_j^{(30)} + z_j^{(30)}) P_n(\cos\theta)$$
$$= \sum_{n=0}^{\infty} x_j^{(30)} P_n(\cos\theta), \tag{4.97}$$

where $x_j^{(30)}$ can be expressed by a linear combination of the press and shear solutions, which are proportional to the amplitude of the source function, $s_1^{(30)}$.

4.6.4 Vertical Tensile Fracturing

When $d_s \to 0$ the source functions for vertical tensile fracturing become

$$\begin{cases} s_1^{(4)} = \dfrac{2n+1}{4\pi a^2}; & m = \pm 0 \\ s_j^{(4)} = 0 & j = 2, 3, 4, 5, 6. \end{cases} \tag{4.98}$$

Note that all of the s_j, except for s_1 are zero, since the point source is located at the earth's surface. Therefore, as discussed in the case of a dip-slip, the solution simply becomes

$$y_j(a) = s_j(a) \qquad (j = 1, \ldots, 6). \tag{4.99}$$

Because s_j are known on the surface, they can be solved without any integration,

$$\begin{cases} y_1(a) = s_1(a) = \dfrac{2n+1}{4\pi a^2} \\ y_3(a) = s_3(a) = 0 \\ y_5(a) = s_5(a) = 0. \end{cases} \tag{4.100}$$

Since

$$\sum_{n=0}^{\infty} (2n+1) P_n(\cos\theta) = 0 \qquad \theta > 0°, \tag{4.101}$$

we have

$$u_r^{(4)}(a, \theta, \phi) = \hat{u}_r^{(4)}(a, \theta) = 0, \tag{4.102}$$
$$\psi^{(4)}(a, \theta, \phi) = \hat{\psi}^{(4)}(a, \theta) = 0, \tag{4.103}$$
$$\Delta g^{(4)}(a, \theta, \phi) = \Delta \hat{g}^{(4)}(a, \theta) = 0, \tag{4.104}$$
$$\delta g^{(4)}(a, \theta, \phi) = \delta \hat{g}^{(4)}(a, \theta) = 0. \tag{4.105}$$

When $\theta = 0$, the solutions become singular, since the point source is located there.

4.7 Formulas for an Inclined Dislocation on the Polar Axis

Using the results of the previous sections we arrive at the following expressions for the displacement, potntial and gravity changes on the free surface of a sphere. As before, we still keep the fault line along the Greenwhich meridian as well as $UdS = 1$.

Shear dislocation with arbitrary dip and slip angles δ, λ (from (3.19)):

$$\begin{aligned} u_r^{(s)}(a, \theta, \phi) = & \cos\lambda\{-\hat{u}_r^{(1)}(a, \theta)\sin\delta\sin 2\phi \\ & + \hat{u}_r^{(2)}(a, \theta)\cos\delta\cos\phi\} \\ & + \sin\lambda\left\{\sin 2\delta\left[\frac{1}{2}\hat{u}_r^{(1)}(a, \theta)\cos 2\phi + \hat{u}_r^{(30)}(a, \theta)\right]\right. \\ & \left. + \hat{u}_r^{(2)}(a, \theta)\cos 2\delta\sin\phi\right\} \end{aligned} \tag{4.106}$$

$$\begin{aligned} \psi^{(s)}(a, \theta, \phi) = & \cos\lambda\{-\hat{\psi}^{(1)}(a, \theta)\sin\delta\sin 2\phi \\ & + \hat{\psi}^{(2)}(a, \theta)\cos\delta\cos\phi\} \\ & + \sin\lambda\left\{\sin 2\delta\left[\frac{1}{2}\hat{\psi}^{(1)}(a, \theta)\cos 2\phi + \hat{\psi}^{(30)}(a, \theta)\right]\right. \\ & \left. + \hat{\psi}^{(2)}(a, \theta)\cos 2\delta\sin\phi\right\} \end{aligned} \tag{4.107}$$

$$\begin{aligned} \Delta g^{(s)}(a, \theta, \phi) = & \cos\lambda\{-\Delta\hat{g}^{(1)}(a, \theta)\sin\delta\sin 2\phi \\ & + \Delta\hat{g}^{(2)}(a, \theta)\cos\delta\cos\phi\} \\ & + \sin\lambda\left\{\sin 2\delta\left[\frac{1}{2}\Delta\hat{g}^{(1)}(a, \theta)\cos 2\phi + \Delta\hat{g}^{(30)}(a, \theta)\right]\right. \\ & \left. + \Delta\hat{g}^{(2)}(a, \theta)\cos 2\delta\sin\phi\right\} \end{aligned} \tag{4.108}$$

$$\begin{aligned} \delta g^{(s)}(a, \theta, \phi) = & \cos\lambda\{-\delta\hat{g}^{(1)}(a, \theta)\sin\delta\sin 2\phi \\ & + \delta\hat{g}^{(2)}(a, \theta)\cos\delta\cos\phi\} \\ & + \sin\lambda\left\{\sin 2\delta\left[\frac{1}{2}\delta\hat{g}^{(1)}(a, \theta)\cos 2\phi + \delta\hat{g}^{(30)}(a, \theta)\right]\right. \\ & \left. + \delta\hat{g}^{(2)}(a, \theta)\cos 2\delta\sin\phi\right\}. \end{aligned} \tag{4.109}$$

Tensile dislocation with arbitrary dip and slip angles δ, λ (from (3.22)):

$$\begin{aligned} u_r^{(t)}(a, \theta, \phi) = & \hat{u}_r^{(4)}(a, \theta) - 2\sin^2\delta\left(\hat{u}_r^{(30)}(a, \theta) + \frac{1}{2}\hat{u}_r^{(1)}(a, \theta)\cos 2\phi\right) \\ & - \hat{u}_r^{(2)}(a, \theta)\sin 2\delta\sin\phi \end{aligned} \tag{4.110}$$

$$\psi^{(t)}(a, \theta, \phi) = \hat{\psi}^{(4)}(a, \theta) - 2\sin^2\delta\left(\hat{\psi}^{(30)}(a, \theta) + \frac{1}{2}\hat{\psi}^{(1)}(a, \theta)\cos 2\phi\right) - \hat{\psi}^{(2)}(a, \theta)\sin 2\delta \sin\phi \tag{4.111}$$

$$\Delta g^{(t)}(a, \theta, \phi) = \Delta\hat{g}^{(4)}(a, \theta) - 2\sin^2\delta\left(\Delta\hat{g}^{(30)}(a, \theta) + \frac{1}{2}\Delta\hat{g}^{(1)}(a, \theta)\cos 2\phi\right) - \Delta\hat{g}^{(2)}(a, \theta)\sin 2\delta \sin\phi \tag{4.112}$$

$$\delta g^{(t)}(a, \theta, \phi) = \delta\hat{g}^{(4)}(a, \theta) - 2\sin^2\delta\left(\delta\hat{g}^{(30)}(a, \theta) + \frac{1}{2}\delta\hat{g}^{(1)}(a, \theta)\cos 2\phi\right) - \delta\hat{g}^{(2)}(a, \theta)\sin 2\delta \sin\phi. \tag{4.113}$$

Explosion (from (3.26)):

$$u_r^{(e)}(a, \theta, \phi) = 3\hat{u}_r^{(4)}(a, \theta) - 4\hat{u}_r^{(30)}(a, \theta) \tag{4.114}$$

$$\psi^{(e)}(a, \theta, \phi) = 3\hat{\psi}^{(4)}(a, \theta) - 4\hat{\psi}^{(30)}(a, \theta) \tag{4.115}$$

$$\Delta g^{(e)}(a, \theta, \phi) = 3\Delta\hat{g}^{(4)}(a, \theta) - 4\Delta\hat{g}^{(30)}(a, \theta) \tag{4.116}$$

$$\delta g^{(e)}(a, \theta, \phi) = 3\delta\hat{g}^{(4)}(a, \theta) - 4\delta\hat{g}^{(30)}(a, \theta). \tag{4.117}$$

4.8 Inclined Dislocation at an Arbitrary Point

In practice, the dislocation is not necessarily on the polar axis, nor is the fault line along the Greenwich meridian. In the following we derive formulas for an inclined dislocation at an arbitrary point.

Let the point dislocation and the observation station be at $D(\theta_1, \phi_1)$ and $P(\theta_2, \phi_2)$ (Figure 4.6). The angular distance between $D(\theta_1, \phi_1)$ and $P(\theta_2, \phi_2)$ is denoted by φ. The fault plane is defined by its strike azimuth, z_1, on the earth's surface, measured here clockwise from the north. The azimuth of the observation point with respect to point $D(\theta_1, \phi_1)$ is denoted by z_2 (clockwise from north). We define z as being the azimuth of the calculating point with respect to the fault line,

$$z = z_1 - z_2. \tag{4.118}$$

Then, φ and z_2 are derived from spherical trigonometric formulas as

$$\cos\varphi = \cos\theta_1 \cos\theta_2 + \sin\theta_1 \sin\theta_2 \cos(\phi_2 - \phi_1) \tag{4.119}$$

$$\sin z_2 = \frac{1}{\sin\varphi}\sin\theta_2 \sin(\phi_2 - \phi_1). \tag{4.120}$$

We therefore have the following:

Shear Dislocation:

$$u_r^{(s)}(a, \varphi, z) = \cos\lambda\{-\hat{u}_r^{(1)}(a, \varphi)\sin\delta \sin 2z + \hat{u}_r^{(2)}(a, \varphi)\cos\delta \cos z\} + \sin\lambda\left\{\sin 2\delta\left[\frac{1}{2}\hat{u}_r^{(1)}(a, \varphi)\cos 2z + \hat{u}_r^{(30)}(a, \varphi)\right]\right.$$

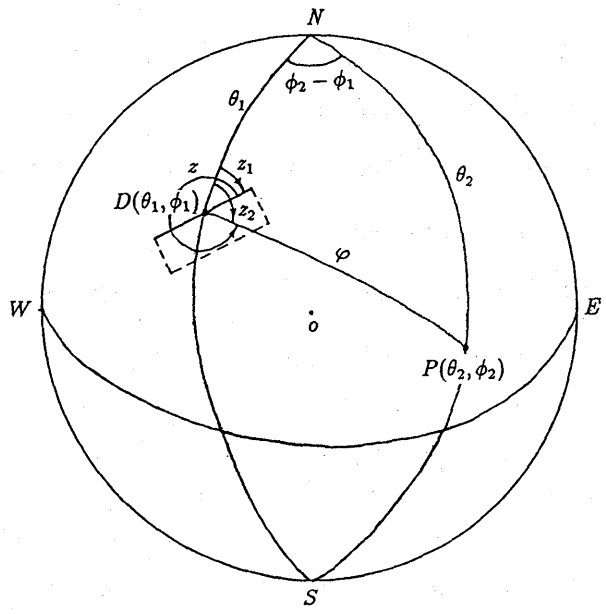

Fig. 4.6 Geometry of a dislocation D and the observation point P.

$$+ \hat{u}_r^{(2)}(a, \varphi) \cos 2\delta \sin z \Big\} \tag{4.121}$$

$$\begin{aligned}\psi^{(s)}(a, \varphi, z) = {} & \cos\lambda\{-\widehat{\psi}^{(1)}(a, \varphi) \sin\delta \sin 2z \\ & + \widehat{\psi}^{(2)}(a, \varphi) \cos\delta \cos z\} \\ & + \sin\lambda\Big\{\sin 2\delta\Big[\frac{1}{2}\widehat{\psi}^{(1)}(a, \varphi)\cos 2z + \widehat{\psi}^{(30)}(a, \varphi)\Big] \\ & + \widehat{\psi}^{(2)}(a, \varphi) \cos 2\delta \sin z\Big\}\end{aligned} \tag{4.122}$$

$$\begin{aligned}\Delta g^{(s)}(a, \varphi, z) = {} & \cos\lambda\{-\Delta\hat{g}^{(1)}(a, \varphi) \sin\delta \sin 2z \\ & + \Delta\hat{g}^{(2)}(a, \varphi) \cos\delta \cos z\} \\ & + \sin\lambda\Big\{\sin 2\delta\Big[\frac{1}{2}\Delta\hat{g}^{(1)}(a, \varphi)\cos 2z + \Delta\hat{g}^{(30)}(a, \varphi)\Big] \\ & + \Delta\hat{g}^{(2)}(a, \varphi) \cos 2\delta \sin z\Big\}\end{aligned} \tag{4.123}$$

$$\begin{aligned}\delta g^{(s)}(a, \varphi, z) = {} & \cos\lambda\{-\delta\hat{g}^{(1)}(a, \varphi) \sin\delta \sin 2z \\ & + \delta\hat{g}^{(2)}(a, \varphi) \cos\delta \cos z\} \\ & + \sin\lambda\Big\{\sin 2\delta\Big[\frac{1}{2}\delta\hat{g}^{(1)}(a, \varphi)\cos 2z + \delta\hat{g}^{(30)}(a, \varphi)\Big]\end{aligned}$$

$$+ \delta\hat{g}^{(2)}(a, \varphi) \cos 2\delta \sin z \Big\}. \tag{4.124}$$

Tensile Dislocation:

$$u_r^{(t)}(a, \varphi, z) = \hat{u}_r^{(4)}(a, \varphi) - 2\sin^2\delta\left(\hat{u}_r^{(30)}(a, \varphi) + \frac{1}{2}\hat{u}_r^{(1)}(a, \varphi) \cos 2z\right) - \hat{u}_r^{(2)}(a, \varphi) \sin 2\delta \sin z \tag{4.125}$$

$$\psi^{(t)}(a, \varphi, z) = \hat{\psi}^{(4)}(a, \varphi) - 2\sin^2\delta\left(\hat{\psi}^{(30)}(a, \varphi) + \frac{1}{2}\hat{\psi}^{(1)}(a, \varphi) \cos 2z\right) - \hat{\psi}^{(2)}(a, \varphi) \sin 2\delta \sin z \tag{4.126}$$

$$\Delta g^{(t)}(a, \varphi, z) = \Delta\hat{g}^{(4)}(a, \varphi) - 2\sin^2\delta\left(\Delta\hat{g}^{(30)}(a, \varphi) + \frac{1}{2}\Delta\hat{g}^{(1)}(a, \varphi) \cos 2z\right) - \Delta\hat{g}^{(2)}(a, \varphi) \sin 2\delta \sin z \tag{4.127}$$

$$\delta g^{(t)}(a, \varphi, z) = \delta\hat{g}^{(4)}(a, \varphi) - 2\sin^2\delta\left(\delta\hat{g}^{(30)}(a, \varphi) + \frac{1}{2}\delta\hat{g}^{(1)}(a, \varphi) \cos 2z\right) - \delta\hat{g}^{(2)}(a, \varphi) \sin 2\delta \sin z. \tag{4.128}$$

Explosion:

$$u_r^{(e)}(a, \varphi, z) = 3\hat{u}_r^{(4)}(a, \varphi) - 4\hat{u}_r^{(30)}(a, \varphi) \tag{4.129}$$

$$\psi^{(e)}(a, \varphi, z) = 3\hat{\psi}^{(4)}(a, \varphi) - 4\hat{\psi}^{(30)}(a, \varphi) \tag{4.130}$$

$$\Delta g^{(e)}(a, \varphi, z) = 3\Delta\hat{g}^{(4)}(a, \varphi) - 4\Delta\hat{g}^{(30)}(a, \varphi) \tag{4.131}$$

$$\delta g^{(e)}(a, \varphi, z) = 3\delta\hat{g}^{(4)}(a, \varphi) - 4\delta\hat{g}^{(30)}(a, \varphi). \tag{4.132}$$

We may determine the deformation on the surface by the following procedure:

(1) Compute the epicentral distance, φ, and azimuth, z, of the observation point, $P(\theta_2, \phi_2)$, from the dislocation at $D(\theta_1, \phi_1)$ after (4.119) and (4.120).

(2) Compute $\hat{u}_r^{(j)}(a, \varphi)$, $\hat{\psi}^{(j)}(a, \varphi)$, $\Delta\hat{g}^{(j)}(a, \varphi)$ and $\delta\hat{g}^{(j)}(a, \varphi)$ as described in sections 4.2–4.5.

(3) Use formulas (4.118) through (4.132) to compute $u_r^{(j)}(a, \varphi, z)$, $\psi^{(j)}(a, \varphi, z)$, $\Delta g^{(j)}(a, \varphi, z)$ and $\delta g^{(j)}(a, \varphi, z)$. These deformation fields are due to a point dislocation of unit magnitude, $UdS = 1$.

(4) Multiply the results of (3) by the magnitude of the dislocation, UdS.

5. Some Techniques

In integrating the equations of equilibrium and the summations of the harmonic solutions, many numerical problems arise, such as how to truncate the harmonic solutions, how to accelerate the convergence, and so on.

5.1 Truncation of the Infinite Series

Since it is impossible to calculate the dislocation Love numbers to infinite degrees, we must truncate the series as

$$\frac{1}{a^2}\sum_{n=0}^{\infty} h_n^d(T, m)P_n(\cos\theta) \simeq \frac{1}{a^2}\sum_{n=0}^{N} h_n^d(T, m)P_n(\cos\theta), \tag{5.1}$$

where N is the truncation order. In the following we discuss the appropriate choice of N.

OKUBO's (1988) asymptotic solutions imply that all of the Love numbers are proportional to $(r_0/a)^n$,

$$\left\{\begin{array}{c} h_n \\ l_n \\ k_n \end{array}\right\} \propto \left(\frac{r_0}{a}\right)^n, \tag{5.2}$$

where $r_0 = a - d_s$ is the radial distance of the point source. Equation (5.2) indicates that the deeper is the point source, the faster does series (5.1) converges with n.

Since

$$\left(\frac{r_0}{a}\right)^n = e^{-n\cdot\frac{d_s}{a}}\cdot\left(1 + 0\left(\frac{1}{n}\right)\right), \tag{5.3}$$

the truncated series, $\Sigma_{n=0}^{N} h_n^d P_n(\cos\theta)$, gives a sufficiently accurate result if

$$e^{-N\cdot\frac{d_s}{a}} \ll 1 \tag{5.4}$$

or

$$N \gg \frac{a}{d_s}. \tag{5.5}$$

We take

$$N \sim 10\,\frac{a}{d_s} \tag{5.6}$$

since

$$\left(\frac{r_0}{a}\right)^N \sim e^{-10} \sim 10^{-5} \tag{5.7}$$

guarantees an accuracy of 10^{-5}. Table 5.1 shows some values of the source depth, d_s, and N used in our calculation. It can be seen from the table that N becomes very large when d_s is 1 or $2\,km$.

Table 5.1. Truncation degree N

d_s(km)	$\frac{a}{d_s}$	N
637	10	100
64	100	1000
32	200	2000
20	319	3000
10	637	6000
5	1274	15000
3	2124	25000
2	3185	40000
1	6371	45000

5.2 Disk Factor

To accelerate the convergence of the infinite series as

$$\hat{u}_r^{(1)}(r, \theta) = \frac{2}{a^2} \sum_{n=2}^{\infty} h_n^d(1, 2) P_n^2(\cos\theta), \tag{5.8}$$

we multiply the summand by a disk factor, D_n,

$$D_n = -\frac{1 + \cos\alpha}{n(n+1)\sin\alpha} \frac{\partial P_n(\cos\alpha)}{\partial \alpha}. \tag{5.9}$$

Since

$$\lim_{\alpha \to 0} D_n \to \frac{2J_1(n\alpha)}{n\alpha} \to 1 \qquad \text{for } n \gg 1, \tag{5.10}$$

we may rewrite (5.8) as

$$\hat{u}_r^{(1)}(r, \theta) = \frac{2}{a^2} \lim_{\alpha \to 0} \sum_{n=2}^{\infty} h_n^d(1, 2) D_n P_n^2(\cos\theta). \tag{5.11}$$

$\hat{u}_r^{(1)}$ is accurately evaluated by $(2/a^2)\ \Sigma_{n=2}^{\infty}\ h_n^d D_n P_n^2$ when $\theta/\alpha > 10$. The disk factor has the physical meaning of a disk load (Farrell, 1972). Let γ be a unit mass distributed uniformly over a disk of radius, α, such that

$$\gamma(\theta; \alpha) = \frac{1}{\pi\alpha^2} \qquad \text{for } \theta \leq \alpha, \tag{5.12}$$

$$= 0 \qquad \text{for } \theta > \alpha. \tag{5.13}$$

Expanding γ in a Legendre series gives

$$\gamma(\theta; \alpha) = \sum_{n=0}^{\infty} \frac{2n+1}{4\pi a^2} D_n P_n(\cos\theta). \tag{5.14}$$

5.3 Euler Transformation

The Euler transformation is a method for evaluating an alternating series.

The theory of the Euler transformation states that, if an alternating series $\Sigma_{n=0}^{\infty}(-1)^n x_n$ $(x_n \geq 0)$ converges, it can be transformed as

$$\sum_{n=0}^{\infty}(-1)^n x_n = \frac{1}{2}\sum_{n=0}^{\infty}\left(-\frac{1}{2}\right)^n \Delta^n x_0, \tag{5.15}$$

where Δ^n is the nth-order difference of x_n:

$$\Delta^1 x_n = x_{n+1} - x_n, \tag{5.16}$$

$$\Delta^2 x_n = \Delta^1(\Delta^1 x_n), \tag{5.17}$$

$$\cdots$$

$$\Delta^r x_n = \Delta^{r-1} x_{n+1} - \Delta^{r-1} x_n, \tag{5.18}$$

$$\cdots$$

In calculations, it is preferable to sum the first few terms of the original series followed by applying the Euler transformation to the remainder. The Euler transformation accelerates the convergence of many series. For example, consider the following series:

$$S = \sum_{n=1}^{\infty}\frac{(-1)^{n-1}}{\sqrt{n}}$$

$$= 1 - \frac{1}{\sqrt{2}} + \frac{1}{\sqrt{3}} - \frac{1}{\sqrt{4}} + \frac{1}{\sqrt{5}} - \frac{1}{\sqrt{6}} + - \ldots. \tag{5.19}$$

Let us sum the first 5 terms, then applying the Euler transformation to the remainder. We obtain $S = 0.6049$, accurate to 10^{-4}, when we compute up to Δ^7. However, we must sum up to $n = 10^8$ in order to achieve the same accuracy without using the Euler transformation.

We must transform an original series into an alternating one in advance before applying the Euler transformation. For example, consider a radial displacement

$$u_r = \frac{1}{a^2}\sum_{n=0}^{\infty} h_n^d P_n(\cos\theta). \tag{5.20}$$

When the disk factor is included (5.20) becomes

$$u_r = \frac{1}{a^2}\sum_{n=0}^{\infty} h_n^d D_n P_n(\cos\theta). \tag{5.21}$$

The Euler transformation cannot be immediately applied to (5.21), since it is not an alternating series.

We must transform (5.21) to a partial series (see Figure 5.1),

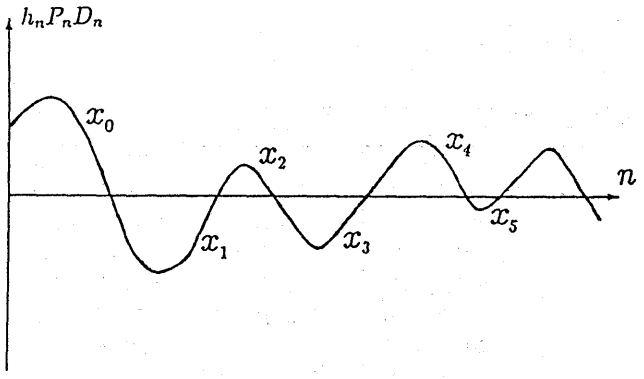

Fig. 5.1 Alternating series of x_j.

$$u_r = \frac{1}{a^2}\sum_{n=0}^{n_1-1} h_n^d D_n P_n + \frac{1}{a^2}\sum_{n=n_1}^{n_2-1} h_n^d D_n P_n + \frac{1}{a^2}\sum_{n=n_2}^{n_3-1} h_n^d D_n P_n + \cdots \qquad (5.22)$$

$x_0 > 0$ $\qquad$ $x_1 < 0$ $\qquad$ $x_2 > 0$

or

$$u_r = \sum_{j=0}^{\infty} (-1)^j |x_j|, \qquad (5.23)$$

so that the Euler transformation can be applied to (5.23).

We evaluate a series $\{h_r^K;\ k = 0, 1, 2, \ldots\}$ defined by

$$u_r^K = \sum_{k=0}^{K} (-1)^k |x_k| + \frac{1}{2}\sum_{m=K+1}^{K+19} \left(-\frac{1}{2}\right)^m \Delta^m |x_{K+1}| \qquad (5.24)$$

until we achieve a relative error of

$$\left| \frac{u_r^{K_0+1} - u_r^{K_0}}{u_r^{K_0}} \right| \leq \varepsilon = 0.0001. \qquad (5.25)$$

$u_r^{K_0}$ provides a good estimate of u_r since the accuracy is 10^{-5}.

5.4 Interpolation

The dislocation Love numbers must be known over a large range of spheroidal degree n. It is not necessary to numerically integrate the equations of equilibrium for each n if interpolation on a sparser table could give accurate dislocation Love numbers. A naive interpolation method, however, will yield large error because dislocation Love numbers vary rapidly with n (e.g. Table 5.2). For example, $l_n^d(1, 2)$ in Table 5.2 varies from 10^1 to 10^{-9}.

It is known from Okubo's asymptotic solutions that all Love numbers are appropriately scaled by a factor $(a/r_0)^n$. Hence, we multiply the dislocation Love numbers by $(a/r_0)^n$ to make them vary gently with n as

Table 5.2. Dislocation Love numbers of a homogeneous earth model. Vertical strike-slip fault. $\delta = 90°$, $\lambda = 0°$, $m = 2$. Source depth = 32 *km*

n	$h_n^d(1,2)$	$l_n^d(1,2)$	$k_n^d(1,2)$
2	.1316E − 02	.1368E − 01	.2352E − 02
3	−.2030E − 02	.5764E − 02	.6586E − 03
4	−.2270E − 02	.3228E − 02	.2876E − 03
5	−.2100E − 02	.2065E − 02	.1558E − 03
6	−.1877E − 02	.1432E − 02	.9632E − 04
8	−.1491E − 02	.8003E − 03	.4700E − 04
10	−.1207E − 02	.5071E − 03	.2808E − 04
15	−.7760E − 03	.2180E − 03	.1225E − 04
20	−.5409E − 03	.1180E − 03	.7391E − 05
30	−.2969E − 03	.4826E − 04	.3965E − 05
40	−.1747E − 03	.2487E − 04	.2648E − 05
50	−.1035E − 03	.1454E − 04	.1952E − 05
70	−.2780E − 04	.6146E − 05	.1226E − 05
100	.1915E − 04	.2230E − 05	.7278E − 06
200	.4234E − 04	.1540E − 06	.2180E − 06
300	.3185E − 04	−.7950E − 08	.8777E − 07
500	.1348E − 04	−.1403E − 07	.1924E − 07
700	.5212E − 05	−.5038E − 08	.5022E − 08
1000	.1199E − 05	−.9384E − 09	.7765E − 09
1200	.4449E − 06	−.3046E − 09	.2364E − 09
1400	.1643E − 06	−.9963E − 10	.7405E − 10
1600	.6054E − 07	−.3286E − 10	.2368E − 10
1800	.2225E − 07	−.1093E − 10	.7690E − 11
2000	.8172E − 08	−.3662E − 11	.2529E − 11

$$\bar{h}_n^d(T, m) = h_n^d(T, m) n^{m-2} \left(\frac{a}{r_0}\right)^n, \tag{5.26}$$

$$\bar{l}_n^d(T, m) = l_n^d(T, m) n^{m-1} \left(\frac{a}{r_0}\right)^n, \tag{5.27}$$

$$\bar{k}_n^d(T, m) = k_n^d(T, m) n^{m-1} \left(\frac{a}{r_0}\right)^n, \tag{5.28}$$

where $m = 2$ corresponds to the strike-slip, $m = 1$ to the dip-slip, and $m = 0$ to the 45° dip-slip dislocations and tensile fracturing. Table 5.3 shows that even a linear interpolation of the transformed Love numbers gives accurate results.

5.5 Asymptotic Solutions

We saw in section 5.1 that the truncation degree, N, becomes too large for the infinite series to be accurately evaluated when $d_s < 1\,km$ or $d_s \to 0$. We therefore introduce here the asymptotic solution technique to overcome this difficulty.

Table 5.3. Transformed dislocation Love numbers.
Homogeneous earth model with a vertical strike-slip fault.
$\delta = 90°$, $\lambda = 0°$, $m = 2$. Source depth = 32 *km*

n	$h_n^d(1,2)(\frac{a}{d_s})^n$	$l_n^d(1,2)n(\frac{a}{r_0})^n$	$k_n^d(1,2)n(\frac{a}{r_0})^n$
2	$.1329E-2$	$.2763E-1$	$.4751E-2$
3	$-.2061E-2$	$.1755E-1$	$.2006E-2$
4	$-.2316E-2$	$.1317E-1$	$.1174E-2$
5	$-.2154E-2$	$.1059E-1$	$.7990E-3$
6	$-.1935E-2$	$.8856E-2$	$.5957E-3$
8	$-.1552E-2$	$.6666E-2$	$.3915E-3$
10	$-.1270E-2$	$.5333E-2$	$.2953E-3$
15	$-.8369E-3$	$.3527E-2$	$.1982E-3$
20	$-.5982E-3$	$.2610E-2$	$.1635E-3$
30	$-.3453E-3$	$.1684E-2$	$.1384E-3$
40	$-.2137E-3$	$.1217E-2$	$.1296E-3$
50	$-.1331E-3$	$.9350E-3$	$.1255E-3$
70	$-.3955E-4$	$.6120E-3$	$.1221E-3$
100	$.3168E-4$	$.3689E-3$	$.1204E-3$
200	$.1159E-3$	$.8431E-4$	$.1194E-3$
300	$.1443E-3$	$-.1080E-4$	$.1193E-3$
500	$.1671E-3$	$-.8701E-4$	$.1193E-3$
700	$.1769E-3$	$-.1197E-3$	$.1193E-3$
1000	$.1844E-3$	$-.1443E-3$	$.1194E-3$
1200	$.1873E-3$	$-.1539E-3$	$.1194E-3$
1400	$.1894E-3$	$-.1607E-3$	$.1195E-3$
1600	$.1910E-3$	$-.1659E-3$	$.1195E-3$
1800	$.1922E-3$	$-.1699E-3$	$.1195E-3$
2000	$.1932E-3$	$-.1731E-3$	$.1196E-3$

Okubo (1988) presented six independent sets of asymptotic solutions for spheroidal deformations of the earth. Recently, he (Okubo, 1991b) also derived asymptotic expressions of dislocation solutions, (see Appendix B), expressed simply in terms of the tide, load and shear solutions. For convenience in our present study, we transform the asymptotic solutions into asymptotic dislocation Love numbers ($h_n^d(T, m)$, $l_n^d(T, m)$ and $k_n^d(T, m)$) according to definition (3.29). Using Okubo's asymptotic solutions (or asymptotic dislocation Love numbers), we may speed up the convergence of the series.

Vertical Strike-Slip:

From (4.23) we have the radial displacement,

$$\begin{aligned} a^2\hat{u}_r^{(1)}(a, \theta) &= 2\sum_{n=2}^{\infty} h_n^d(1, 2)P_n^2(\cos\theta) \\ &= 2\sum_{n=2}^{\infty} \tilde{h}_n^d(1, 2)P_n^2(\cos\theta) \\ &\quad + 2\sum_{n=2}^{\infty} (h_n^d(1, 2) - \tilde{h}_n^d(1, 2))P_n^2(\cos\theta). \end{aligned} \tag{5.29}$$

Since

$$\tilde{h}_n^d(1, 2) = \frac{3}{4\pi\rho_0\xi}\frac{\mu_s}{r_s}y_3^{Press}(r_s; n)$$
$$= \left(\frac{r_s}{a}\right)^{n-1}y_{230}^{(1)} + \frac{1}{n}\left(\frac{r_s}{a}\right)^{n-1}y_{231}^{(1)} + \frac{1}{n^2}\left(\frac{r_s}{a}\right)^{n-1}y_{232}^{(1)} \quad (5.30)$$

(Appendix B), we have

$$a^2\hat{u}_r^{(1)}(a, \theta) = 2\sum_{n=2}^{\infty}\left[y_{230}^{(1)}\left(\frac{r_s}{a}\right)^{n-1} + y_{231}^{(1)}\frac{1}{n}\left(\frac{r_s}{a}\right)^{n-1}\right.$$
$$\left. + y_{232}^{(1)}\frac{1}{n(n+1)}\left(\frac{r_s}{a}\right)^{n-1}\right]P_n^2(\cos\theta)$$
$$+ 2\sum_{n=2}^{\infty}\left[h_n^d(1, 2) - y_{230}^{(1)}\left(\frac{r_s}{a}\right)^{n-1} - y_{231}^{(1)}\frac{1}{n}\left(\frac{r_s}{a}\right)^{n-1}\right.$$
$$\left. - y_{232}^{(1)}\frac{1}{n(n+1)}\left(\frac{r_s}{a}\right)^{n-1}\right]P_n^2(\cos\theta). \quad (5.31)$$

The first series on the right-hand side is evaluated analytically by using the formulas in Appendix A and setting $t = (\frac{r_s}{a})$. It follows that

$$a^2\hat{u}_r^{(1)}(a, \theta) = 2y_{230}^{(1)}\left(\frac{r_s}{a}\right)\frac{3(\frac{r_s}{a})\sin^2\theta}{(1 - 2(\frac{r_s}{a}) + (\frac{r_s}{a})^2)^{\frac{5}{2}}}$$
$$+ 2y_{231}^{(1)}\frac{1}{(\frac{r_s}{a})}\left[\frac{2}{\sin^2\theta} - 1 - \frac{1 - (\frac{r_s}{a})\cos\theta}{(1 - 2\cos^2\theta + (\frac{r_s}{a})^2)^{\frac{3}{2}}}\right.$$
$$\left. + \frac{2\cos\theta((\frac{r_s}{a}) - \cos\theta)}{\sin^2\theta\sqrt{1 - 2\cos^2\theta + (\frac{r_s}{a})^2}}\right]$$
$$+ 2y_{232}^{(1)}\frac{1}{(\frac{r_s}{a})}\left[1 - \frac{1}{\sqrt{1 - 2(\frac{r_s}{a})\cos\theta + (\frac{r_s}{a})^2}}\right.$$
$$\left. - \frac{2\cos\theta}{(\frac{r_s}{a})\sin^2\theta}\left(1 - \left(\frac{r_s}{a}\right)\cos\theta - \sqrt{1 - 2\left(\frac{r_s}{a}\right)\cos\theta + \left(\frac{r_s}{a}\right)^2}\right)\right]$$
$$+ 2\sum_{n=2}^{\infty}\left[h_n^d(1, 2) - y_{230}^{(1)}\left(\frac{r_s}{a}\right)^{n-1} - y_{231}^{(1)}\frac{1}{n}\left(\frac{r_s}{a}\right)^{n-1}\right.$$
$$\left. - y_{232}^{(1)}\frac{1}{n(n+1)}\left(\frac{r_s}{a}\right)^{n-1}\right]P_n^2(\cos\theta). \quad (5.32)$$

It should be noted that the infinite series on the right-hand side now converges quickly because the summand is $0(1/n)\cdot(r_s/a)^n$.

Similarly, we obtain the following expressions:

$$\frac{a^2}{g_0}\hat{\psi}^{(1)}(a, \theta) = 2\sum_{n=2}^{\infty}k_n^d(1, 2)P_n^2(\cos\theta)$$
$$= 2\sum_{n=2}^{\infty}\tilde{k}_n^d(1, 2)P_n^2(\cos\theta)$$

$$
\begin{aligned}
&+ 2\sum_{n=2}^{\infty}(k_n^d(1,2) - \tilde{k}_n^d(1,2))P_n^2(\cos\theta)\\
&= 2\sum_{n=2}^{\infty}\left[y_{130}^{(1)}\frac{1}{n}\left(\frac{r_s}{a}\right)^{n-1} + y_{131}^{(1)}\frac{1}{n(n+1)}\left(\frac{r_s}{a}\right)^{n-1}\right.\\
&\left. + y_{132}^{(1)}\frac{1}{n(n^2-1)}\left(\frac{r_s}{a}\right)^{n-1}\right]P_n^2(\cos\theta)\\
&+ 2\sum_{n=2}^{\infty}\left[k_n^d(1,2) - y_{130}^{(1)}\frac{1}{n}\left(\frac{r_s}{a}\right)^{n-1} - y_{131}^{(1)}\frac{1}{n(n+1)}\left(\frac{r_s}{a}\right)^{n-1}\right.\\
&\left. - y_{132}^{(1)}\frac{1}{n(n^2-1)}\left(\frac{r_s}{a}\right)^{n-1}\right]P_n^2(\cos\theta)\\
&= 2y_{130}^{(1)}\frac{1}{(\frac{r_s}{a})}\left[\frac{2}{\sin^2\theta} - 1 - \frac{1 - (\frac{r_s}{a})\cos\theta}{(1 - 2\cos^2\theta + (\frac{r_s}{a})^2)^{\frac{3}{2}}}\right.\\
&\left. + \frac{2\cos\theta((\frac{r_s}{a}) - \cos\theta)}{\sin^2\theta\sqrt{1 - 2\cos^2\theta + (\frac{r_s}{a})^2}}\right]\\
&+ 2y_{131}^{(1)}\frac{1}{(\frac{r_s}{a})}\left[1 - \frac{1}{\sqrt{1 - 2(\frac{r_s}{a})\cos\theta + (\frac{r_s}{a})^2}}\right.\\
&\left. - \frac{2\cos\theta}{(\frac{r_s}{a})\sin^2\theta}\left(1 - \left(\frac{r_s}{a}\right)\cos\theta - \sqrt{1 - 2\left(\frac{r_s}{a}\right)\cos\theta + \left(\frac{r_s}{a}\right)^2}\right)\right]\\
&+ 2y_{132}^{(1)}\left\{\frac{1}{2}\cos\theta + \frac{\cos\theta}{(\frac{r_s}{a})^2\sin^2\theta}\left(1 - 2\left(\frac{r_s}{a}\right)\cos\theta + \left(\frac{r_s}{a}\right)^2\right)\right.\\
&- \frac{1}{(\frac{r_s}{a})^2\sin^2\theta\sqrt{1 - 2(\frac{r_s}{a})\cos\theta + (\frac{r_s}{a})^2}}\\
&\cdot\left[\cos\theta + \left(\frac{r_s}{a}\right)^3(1 - 2\cos^2\theta)\right.\\
&\left.\left. + \left(\frac{r_s}{a}\right)\left(1 - \left(\frac{r_s}{a}\right)\cos\theta\right)(1 - 4\cos^2\theta)\right]\right\}\\
&+ 2\sum_{n=2}^{\infty}\left[k_n^d(1,2) - y_{230}^{(1)}\left(\frac{r_s}{a}\right)^{n-1} - y_{231}^{(1)}\frac{1}{n}\left(\frac{r_s}{a}\right)^{n-1}\right.\\
&\left. - y_{232}^{(1)}\frac{1}{n(n+1)}\left(\frac{r_s}{a}\right)^{n-1}\right]P_n^2(\cos\theta). \qquad (5.33)
\end{aligned}
$$

$$
\begin{aligned}
\frac{a^2}{g_0}\Delta\hat{g}^{(1)}(a,\theta) &= 2\sum_{n=2}^{\infty}\frac{n+1}{a}k_n^d(1,2)P_n^2(\cos\theta)\\
&= \frac{2}{a}\sum_{n=2}^{\infty}k_n^d(1,2)P_n^2(\cos\theta) + \frac{2}{a}\sum_{n=2}^{\infty}n\tilde{k}_n^d(1,2)P_n^2(\cos\theta)\\
&\quad + \frac{2}{a}\sum_{n=2}^{\infty}n(k_n^d(1,2) - \tilde{k}_n^d(1,2))P_n^2(\cos\theta)\\
&= \frac{a}{g_0}\tilde{\psi}^{(1)}(a,\theta) + \frac{2}{a}\sum_{n=2}^{\infty}n\left[y_{130}^{(1)}\frac{1}{n}\left(\frac{r_s}{a}\right)^{n-1} + y_{131}^{(1)}\frac{1}{n(n+1)}\left(\frac{r_s}{a}\right)^{n-1}\right.
\end{aligned}
$$

$$+ y^{(1)}_{132}\frac{1}{n(n^2-1)}\left(\frac{r_s}{a}\right)^{n-1}\Big]P^2_n(\cos\theta)$$

$$+ \frac{2}{a}\sum_{n=2}^{\infty} n\Big[k^d_n(1,2) - y^{(1)}_{130}\frac{1}{n}\left(\frac{r_s}{a}\right)^{n-1} - y^{(1)}_{131}\frac{1}{n(n+1)}\left(\frac{r_s}{a}\right)^{n-1}$$

$$- y^{(1)}_{132}\frac{1}{n(n^2-1)}\left(\frac{r_s}{a}\right)^{n-1}\Big]P^2_n(\cos\theta)$$

$$= \frac{a}{g_0}\hat{\psi}^{(1)}(a,\theta) + \frac{2}{a}y^{(1)}_{130}\frac{3(\frac{r_s}{a})\sin^2\theta}{(1-2(\frac{r_s}{a})\cos\theta+(\frac{r_s}{a})^2)^{\frac{5}{2}}}$$

$$+ \frac{2}{a}y^{(1)}_{131}\Big[-\frac{2\cos\theta}{(\frac{r_s}{a})^2\sin^2\theta}\Big(-1+\frac{1-(\frac{r_s}{a})\cos\theta}{\sqrt{1-2(\frac{r_s}{a})\cos\theta+(\frac{r_s}{a})^2}}\Big)$$

$$- \frac{\cos\theta-(\frac{r_s}{a})}{(1-2\cos^2\theta+(\frac{r_s}{a})^2)^{\frac{3}{2}}}\Big]$$

$$+ \frac{2}{a}y^{(1)}_{132}\Big\{\frac{1}{2(\frac{r_s}{a})^2\sin^2\theta}\Big[2\Big(\left(\frac{r_s}{a}\right)\sin^2\theta-\cos\theta\Big)$$

$$+\left(\frac{r_s}{a}\right)^2\cos\theta(2+\sin^2\theta)\Big] - \sqrt{1-2\left(\frac{r_s}{a}\right)\cos\theta+\left(\frac{r_s}{a}\right)^2}$$

$$+ \frac{1}{(\frac{r_s}{a})^2\sin^2\theta\sqrt{1-2(\frac{r_s}{a})\cos\theta+(\frac{r_s}{a})^2}}$$

$$\cdot\Big(\cos\theta-\left(\frac{r_s}{a}\right)-\left(\frac{r_s}{a}\right)^2\cos\theta+\left(\frac{r_s}{a}\right)^3\cos^2\theta\Big)\Big\}$$

$$+ \frac{2}{a}\sum_{n=2}^{\infty} n\Big[k^d_n(1,2) - y^{(1)}_{130}\frac{1}{n}\left(\frac{r_s}{a}\right)^{n-1} - y^{(1)}_{131}\frac{1}{n(n+1)}\left(\frac{r_s}{a}\right)^{n-1}$$

$$-y^{(1)}_{132}\frac{1}{n(n^2-1)}\left(\frac{r_s}{a}\right)^{n-1}\Big]P^2_n(\cos\theta) \tag{5.34}$$

$$\delta\hat{g}^{(1)}(a,\theta) = \Delta\hat{g}^{(1)}(a,\theta) - \beta\hat{u}^{(1)}_r(a,\theta). \tag{5.35}$$

Vertical Dip-Slip:

$$a^2\hat{u}^{(2)}_r(a,\theta) = 2\sum_{n=1}^{\infty} h^d_n(2,1)P^1_n(\cos\theta)$$

$$= 2\sum_{n=1}^{\infty}\tilde{h}^d_n(2,1)P^1_n(\cos\theta)$$

$$+ 2\sum_{n=1}^{\infty}(h^d_n(2,1)-\tilde{h}^d_n(2,1))P^1_n(\cos\theta)$$

$$= 2\sum_{n=1}^{\infty}\Big[y^{(2)}_{240}n\left(\frac{r_s}{a}\right)^{n-2} + y^{(2)}_{241}\left(\frac{r_s}{a}\right)^{n-2}\Big]P^1_n(\cos\theta)$$

$$+ 2\sum_{n=1}^{\infty}\Big[h^d_n(2,1) - y^{(2)}_{240}n\left(\frac{r_s}{a}\right)^{n-2} - y^{(2)}_{241}\left(\frac{r_s}{a}\right)^{n-2}\Big]P^1_n(\cos\theta)$$

$$= 2y_{240}^{(2)}\frac{\sin\theta(1+(\frac{r_s}{a})\cos\theta-2(\frac{r_s}{a})^2)}{(\frac{r_s}{a})(1-2(\frac{r_s}{a})+(\frac{r_s}{a})^2)^{\frac{5}{2}}}$$
$$+ 2y_{241}^{(2)}\frac{\sin\theta}{(\frac{r_s}{a})(1-2(\frac{r_s}{a})+(\frac{r_s}{a})^2)^{\frac{3}{2}}}$$
$$+ 2\sum_{n=1}^{\infty}\left[h_n^d(2,1)-y_{240}^{(2)}n\left(\frac{r_s}{a}\right)^{n-2}-y_{241}^{(2)}\left(\frac{r_s}{a}\right)^{n-2}\right]P_n^1(\cos\theta). \tag{5.36}$$

$$\frac{a^2}{g_0}\widehat{\psi}^{(2)}(a,\theta) = 2\sum_{n=1}^{\infty}k_n^d(2,1)P_n^1(\cos\theta)$$
$$= 2\sum_{n=1}^{\infty}\tilde{k}_n^d(2,1)P_n^1(\cos\theta)$$
$$+ 2\sum_{n=1}^{\infty}(k_n^d(2,1)-\tilde{k}_n^d(2,1))P_n^1(\cos\theta)$$
$$= 2\sum_{n=1}^{\infty}\left[y_{140}^{(2)}\left(\frac{r_s}{a}\right)^{n-2}+y_{141}^{(2)}\frac{1}{n}\left(\frac{r_s}{a}\right)^{n-2}\right]P_n^1(\cos\theta)$$
$$+ 2\sum_{n=1}^{\infty}\left[k_n^d(2,1)-y_{140}^{(2)}\left(\frac{r_s}{a}\right)^{n-2}-y_{141}^{(2)}\frac{1}{n}\left(\frac{r_s}{a}\right)^{n-2}\right]P_n^1(\cos\theta)$$
$$= 2y_{140}^{(2)}\frac{\sin\theta}{(\frac{r_s}{a})(1-2(\frac{r_s}{a})+(\frac{r_s}{a})^2)^{\frac{3}{2}}}$$
$$+2y_{141}^{(2)}\frac{1}{(\frac{r_s}{a})}\left(\frac{\cos\theta}{\sin\theta}+\frac{(\frac{r_s}{a})-\cos\theta}{\sqrt{1-2(\frac{r_s}{a})+(\frac{r_s}{a})^2}}\right)$$
$$+ 2\sum_{n=1}^{\infty}\left[k_n^d(2,1)-y_{140}^{(2)}\left(\frac{r_s}{a}\right)^{n-2}-y_{141}^{(2)}\frac{1}{n}\left(\frac{r_s}{a}\right)^{n-2}\right]P_n^1(\cos\theta). \tag{5.37}$$

$$\frac{a^2}{g_0}\Delta\hat{g}^{(2)}(a,\theta) = 2\sum_{n=1}^{\infty}\frac{n+1}{a}k_n^d(2,1)P_n^1(\cos\theta)$$
$$= \frac{2}{a}\sum_{n=1}^{\infty}k_n^d(2,1)P_n^1(\cos\theta)+\frac{2}{a}\sum_{n=1}^{\infty}n\tilde{k}_n^d(2,1)P_n^1(\cos\theta)$$
$$+ \frac{2}{a}\sum_{n=1}^{\infty}n(k_n^d(2,1)-\tilde{k}_n^d(2,1))P_n^1(\cos\theta)$$
$$= \frac{a}{g_0}\widehat{\psi}^{(2)}(a,\theta)+\frac{2}{a}\sum_{n=1}^{\infty}n\left[y_{140}^{(2)}\left(\frac{r_s}{a}\right)^{n-2}+y_{141}^{(2)}\frac{1}{n}\left(\frac{r_s}{a}\right)^{n-2}\right]P_n^1(\cos\theta)$$
$$+ \frac{2}{a}\sum_{n=1}^{\infty}n\left[k_n^d(2,1)-y_{140}^{(2)}\left(\frac{r_s}{a}\right)^{n-2}-y_{141}^{(2)}\frac{1}{n}\left(\frac{r_s}{a}\right)^{n-2}\right]P_n^1(\cos\theta)$$
$$= \frac{a}{g_0}\widehat{\psi}^{(2)}(a,\theta)+\frac{2}{a}y_{140}^{(2)}\frac{\sin\theta(1+(\frac{r_s}{a})\cos\theta-2(\frac{r_s}{a})^2)}{(\frac{r_s}{a})(1-2(\frac{r_s}{a})+(\frac{r_s}{a})^2)^{\frac{5}{2}}}$$
$$+ \frac{2}{a}y_{141}^{(2)}\frac{\sin\theta}{(\frac{r_s}{a})(1-2(\frac{r_s}{a})+(\frac{r_s}{a})^2)^{\frac{3}{2}}}$$

$$+\frac{2}{a}\sum_{n=1}^{\infty} n\left[k_n^d(2,1) - y_{140}^{(2)}\left(\frac{r_s}{a}\right)^{n-2} - y_{141}^{(2)}\frac{1}{n}\left(\frac{r_s}{a}\right)^{n-2}\right]P_n^1(\cos\theta). \tag{5.38}$$

$$\delta\hat{g}^{(2)}(a,\theta) = \Delta\hat{g}^{(2)}(a,\theta) - \beta\hat{u}_r^{(2)}(a,\theta). \tag{5.39}$$

45° Dipping Dip-Slip:

$$\begin{aligned}
a^2\hat{u}_r^{(30)}(a,\theta) &= \sum_{n=0}^{\infty} h_n^d(3,0)P_n(\cos\theta)\\
&= \sum_{n=0}^{\infty} \tilde{h}_n^d(3,0)P_n(\cos\theta)\\
&\quad + \sum_{n=0}^{\infty}(h_n^d(3,0) - \tilde{h}_n^d(3,0))P_n(\cos\theta)\\
&= \sum_{n=0}^{\infty}\Bigg[(y_{220}^{(30)} + y_{230}^{(30)})n^2\left(\frac{r_s}{a}\right)^{n-1}\\
&\quad + (y_{210}^{(30)} + y_{221}^{(30)} + y_{230}^{(30)} + y_{231}^{(30)})n\left(\frac{r_s}{a}\right)^{n-1}\\
&\quad + (y_{211}^{(30)} + y_{222}^{(30)} + y_{231}^{(30)} + y_{232}^{(30)})\left(\frac{r_s}{a}\right)^{n-1}\\
&\quad + (y_{212}^{(30)} + y_{232}^{(30)})\frac{1}{n}\left(\frac{r_s}{a}\right)^{n-1}\Big|_{n_s=1}\Bigg]P_n(\cos\theta)\\
&\quad + \sum_{n=0}^{\infty}\Bigg[h_n^d(3,0) - (y_{220}^{(30)} + y_{230}^{(30)})n^2\left(\frac{r_s}{a}\right)^{n-1}\\
&\quad - (y_{210}^{(30)} + y_{221}^{(30)} + y_{230}^{(30)} + y_{231}^{(30)})n\left(\frac{r_s}{a}\right)^{n-1}\\
&\quad - (y_{211}^{(30)} + y_{222}^{(30)} + y_{231}^{(30)} + y_{232}^{(30)})\left(\frac{r_s}{a}\right)^{n-1}\\
&\quad - (y_{212}^{(30)} + y_{232}^{(30)})\frac{1}{n}\left(\frac{r_s}{a}\right)^{n-1}\Big|_{n_s=1}\Bigg]P_n(\cos\theta)\\
&= (y_{220}^{(30)} + y_{230}^{(30)})\frac{1}{(1 - 2(\frac{r_s}{a})\cos\theta + (\frac{r_s}{a})^2)^{\frac{5}{2}}}\Bigg[\cos\theta\left(1 - \left(\frac{r_s}{a}\right)^2\right)\\
&\quad + \left(\frac{r_s}{a}\right)\left(\cos^2\theta - 2 + \left(\frac{r_s}{a}\right)^2\right)\Bigg]\\
&\quad + (y_{210}^{(30)} + y_{221}^{(30)} + y_{230}^{(30)} + y_{231}^{(30)})\\
&\quad \cdot\frac{1}{(1 - 2(\frac{r_s}{a})\cos\theta + (\frac{r_s}{a})^2)^{\frac{3}{2}}}\left(\cos\theta - \left(\frac{r_s}{a}\right)\right)\\
&\quad + (y_{211}^{(30)} + y_{222}^{(30)} + y_{231}^{(30)} + y_{232}^{(30)})\\
&\quad \cdot\frac{1}{(\frac{r_s}{a})(1 - 2(\frac{r_s}{a})\cos\theta + (\frac{r_s}{a})^2)^{\frac{1}{2}}}
\end{aligned}$$

$$+ (y_{212}^{(30)} + y_{232}^{(30)}) \frac{1}{(\frac{r_s}{a})} \Bigg[\ln 2 - \ln\Bigg(1 - \left(\frac{r_s}{a}\right) \cos\theta + \sqrt{1 - 2\left(\frac{r_s}{a}\right) \cos\theta + \left(\frac{r_s}{a}\right)^2}\Bigg)\Bigg]$$
$$+ \sum_{n=0}^{\infty} \Bigg[h_n^d(3, 0) - (y_{220}^{(30)} + y_{230}^{(30)}) n^2 \left(\frac{r_s}{a}\right)^{n-1}$$
$$- (y_{210}^{(30)} + y_{221}^{(30)} + y_{230}^{(30)} + y_{231}^{(30)}) n \left(\frac{r_s}{a}\right)^{n-1}$$
$$- (y_{211}^{(30)} + y_{222}^{(30)} + y_{231}^{(30)} + y_{232}^{(30)}) \left(\frac{r_s}{a}\right)^{n-1}$$
$$- (y_{212}^{(30)} + y_{232}^{(30)}) \frac{1}{n} \left(\frac{r_s}{a}\right)^{n-1} \Big|_{n_s=1} \Bigg] P_n(\cos\theta). \tag{5.40}$$

If the symbol $|_{n_s=1}$ appears in the above expressions, the summation should begin from $n = 1$ as

$$\sum_{n=0}^{\infty} a_n \Big|_{n_s=1} \equiv \sum_{n=1}^{\infty} a_n. \tag{5.41}$$

$$\frac{a^2}{g_0} \widehat{\psi}^{(30)}(a, \theta) = \sum_{n=0}^{\infty} k_n^d(3, 0) P_n(\cos\theta)$$
$$= \sum_{n=0}^{\infty} \tilde{k}_n^d(3, 0) P_n(\cos\theta) + \sum_{n=0}^{\infty} (k_n^d(3, 0) - \tilde{k}_n^d(3, 0)) P_n(\cos\theta)$$
$$= \sum_{n=0}^{\infty} \Bigg[(y_{120}^{(30)} + y_{130}^{(30)}) n \left(\frac{r_s}{a}\right)^{n-1}$$
$$+ (y_{110}^{(30)} + y_{130}^{(30)} + y_{131}^{(30)}) \left(\frac{r_s}{a}\right)^{n-1}$$
$$+ (y_{111}^{(30)} + y_{131}^{(30)} + y_{132}^{(30)}) \frac{1}{n} \left(\frac{r_s}{a}\right)^{n-1} \Big|_{n_s=1}$$
$$+ (y_{112}^{(30)} + y_{132}^{(30)}) \frac{1}{n(n+1)} \left(\frac{r_s}{a}\right)^{n-1} \Big|_{n_s=1} \Bigg] P_n(\cos\theta)$$
$$+ \sum_{n=0}^{\infty} \Bigg[k_n^d(3, 0) - (y_{120}^{(30)} + y_{130}^{(30)}) n \left(\frac{r_s}{a}\right)^{n-1}$$
$$- (y_{110}^{(30)} + y_{130}^{(30)} + y_{131}^{(30)}) \left(\frac{r_s}{a}\right)^{n-1}$$
$$- (y_{111}^{(30)} + y_{131}^{(30)} + y_{132}^{(30)}) \frac{1}{n} \left(\frac{r_s}{a}\right)^{n-1} \Big|_{n_s=1}$$
$$- (y_{112}^{(30)} + y_{132}^{(30)}) \frac{1}{n(n+1)} \left(\frac{r_s}{a}\right)^{n-1} \Big|_{n_s=1} \Bigg] P_n(\cos\theta)$$
$$= (y_{120}^{(30)} + y_{130}^{(30)}) \frac{1}{(1 - 2(\frac{r_s}{a}) \cos\theta + (\frac{r_s}{a})^2)^{\frac{3}{2}}} \left(\cos\theta - \left(\frac{r_s}{a}\right)\right)$$
$$+ (y_{110}^{(30)} + y_{130}^{(30)} + y_{131}^{(30)}) \frac{1}{(\frac{r_s}{a})(1 - 2(\frac{r_s}{a}) \cos\theta + (\frac{r_s}{a})^2)^{\frac{1}{2}}}$$

$$
\begin{aligned}
&+ (y_{111}^{(30)} + y_{131}^{(30)} + y_{132}^{(30)}) \\
&\cdot \frac{1}{(\frac{r_s}{a})}\left[\ln 2 - \ln\left(1 - \left(\frac{r_s}{a}\right)\cos\theta + \sqrt{1 - 2\left(\frac{r_s}{a}\right)\cos\theta + \left(\frac{r_s}{a}\right)^2}\right)\right] \\
&+ (y_{112}^{(30)} + y_{132}^{(30)}) \\
&\cdot \frac{1}{(\frac{r_s}{a})}\left[-\left(\frac{r_s}{a}\right)\ln\left(1 - \left(\frac{r_s}{a}\right)\cos\theta + \sqrt{1 - 2\left(\frac{r_s}{a}\right)\cos\theta + \left(\frac{r_s}{a}\right)^2}\right)\right. \\
&- \ln\left(\frac{r_s}{a} - \cos\theta + \sqrt{1 - 2\left(\frac{r_s}{a}\right)\cos\theta + \left(\frac{r_s}{a}\right)^2}\right) \\
&\left.+ \ln(1 - \cos\theta) + \left(\frac{r_s}{a}\right)\ln 2\right] \\
&+ \sum_{n=0}^{\infty}\left[k_n^d(3, 0) - (y_{120}^{(30)} + y_{130}^{(30)})n\left(\frac{r_s}{a}\right)^{n-1}\right. \\
&- (y_{110}^{(30)} + y_{130}^{(30)} + y_{131}^{(30)})\left(\frac{r_s}{a}\right)^{n-1} \\
&- (y_{111}^{(30)} + y_{131}^{(30)} + y_{132}^{(30)})\frac{1}{n}\left(\frac{r_s}{a}\right)^{n-1}\Big|_{n_s=1} \\
&\left.- (y_{112}^{(30)} + y_{132}^{(30)})\frac{1}{n(n+1)}\left(\frac{r_s}{a}\right)^{n-1}\Big|_{n_s=1}\right]P_n(\cos\theta). \qquad (5.42)
\end{aligned}
$$

$$
\begin{aligned}
\frac{a^2}{g_0}\Delta\hat{g}^{(30)}(a, \theta) &= \sum_{n=0}^{\infty}\frac{n+1}{a}k_n^d(3, 0)P_n(\cos\theta) \\
&= \frac{1}{a}\sum_{n=0}^{\infty}k_n^d(3, 0)P_n(\cos\theta) + \frac{1}{a}\sum_{n=0}^{\infty}n\tilde{k}_n^d(3, 0)P_n(\cos\theta) \\
&\quad + \frac{1}{a}\sum_{n=0}^{\infty}n[k_n^d(3, 0) - \tilde{k}_n^d(3, 0)]P_n(\cos\theta) \\
&= \frac{1}{a}\sum_{n=0}^{\infty}k_n^d(3, 0)P_n(\cos\theta) + \frac{1}{a}\sum_{n=0}^{\infty}n\left[(y_{120}^{(30)} + y_{130}^{(30)})n\left(\frac{r_s}{a}\right)^{n-1}\right. \\
&\quad + (y_{110}^{(30)} + y_{130}^{(30)} + y_{131}^{(30)})\left(\frac{r_s}{a}\right)^{n-1} \\
&\quad + (y_{111}^{(30)} + y_{131}^{(30)} + y_{132}^{(30)})\frac{1}{n}\left(\frac{r_s}{a}\right)^{n-1} \\
&\quad \left.+ (y_{112}^{(30)} + y_{132}^{(30)})\frac{1}{n^2}\left(\frac{r_s}{a}\right)^{n-1}\Big|_{n_s=1}\right]P_n(\cos\theta) \\
&\quad + \frac{1}{a}\sum_{n=0}^{\infty}n\left[k_n^d(3, 0) - (y_{120}^{(30)} + y_{130}^{(30)})n\left(\frac{r_s}{a}\right)^{n-1}\right. \\
&\quad - (y_{110}^{(30)} + y_{130}^{(30)} + y_{131}^{(30)})\left(\frac{r_s}{a}\right)^{n-1} \\
&\quad \left.- (y_{111}^{(30)} + y_{131}^{(30)} + y_{132}^{(30)})\frac{1}{n}\left(\frac{r_s}{a}\right)^{n-1}\right.
\end{aligned}
$$

$$
\begin{aligned}
&- (y_{112}^{(30)} + y_{132}^{(30)})\frac{1}{n^2}\left(\frac{r_s}{a}\right)^{n-1}\Big|_{n_s=1}\Big]P_n(\cos\theta)\\
&= \frac{a}{g_0}\hat{\psi}^{(30)}(a,\theta) + \frac{1}{a}\Big\{(y_{120}^{(30)} + y_{130}^{(30)})\cdot\\
&\frac{1}{(1 - 2(\frac{r_s}{a})\cos\theta + (\frac{r_s}{a})^2)^{\frac{5}{2}}}\Big[\cos\theta\left(1 - \left(\frac{r_s}{a}\right)^2\right)\\
&+ \left(\frac{r_s}{a}\right)\left(\cos^2\theta - 2 + \left(\frac{r_s}{a}\right)^2\right)\Big]\\
&+ (y_{110}^{(30)} + y_{130}^{(30)} + y_{131}^{(30)})\\
&\cdot\frac{1}{(1 - 2(\frac{r_s}{a})\cos\theta + (\frac{r_s}{a})^2)^{\frac{3}{2}}}\left(\cos\theta - \left(\frac{r_s}{a}\right)\right)\\
&+ (y_{111}^{(30)} + y_{131}^{(30)} + y_{132}^{(30)})\\
&\cdot\frac{1}{(\frac{r_s}{a})(1 - 2(\frac{r_s}{a})\cos\theta + (\frac{r_s}{a})^2)^{\frac{1}{2}}}\\
&+ (y_{112}^{(30)} + y_{132}^{(30)})\frac{1}{(\frac{r_s}{a})}\Big[\ln 2 - \ln\Big(1 - \left(\frac{r_s}{a}\right)\cos\theta\\
&+ \sqrt{1 - 2\left(\frac{r_s}{a}\right)\cos\theta + \left(\frac{r_s}{a}\right)^2}\Big)\Big]\Big\}\\
&+ \frac{1}{a}\sum_{n=0}^{\infty} n\Big[k_n^d(3,0) - (y_{120}^{(30)} + y_{130}^{(30)})n\left(\frac{r_s}{a}\right)^{n-1}\\
&- (y_{110}^{(30)} + y_{130}^{(30)} + y_{131}^{(30)})\left(\frac{r_s}{a}\right)^{n-1}\\
&- (y_{111}^{(30)} + y_{131}^{(30)} + y_{132}^{(30)})\frac{1}{n}\left(\frac{r_s}{a}\right)^{n-1}\\
&- (y_{112}^{(30)} + y_{132}^{(30)})\frac{1}{n^2}\left(\frac{r_s}{a}\right)^{n-1}\Big|_{n_s=1}\Big]P_n(\cos\theta). \qquad (5.43)
\end{aligned}
$$

$$
\delta\hat{g}^{(30)}(a,\theta) = \Delta\hat{g}^{(30)}(a,\theta) - \beta\hat{u}_r^{(30)}(a,\theta). \qquad (5.44)
$$

Vertical Tensile Fracturing:

$$
\begin{aligned}
a^2\hat{u}_r^{(4)}(a,\theta) &= \sum_{n=0}^{\infty} h_n^d(4,0)P_n(\cos\theta)\\
&= \sum_{n=0}^{\infty} \tilde{h}_n^d(4,0)P_n(\cos\theta)\\
&\quad + \sum_{n=0}^{\infty}(h_n^d(4,0) - \tilde{h}_n^d(4,0))P_n(\cos\theta)\\
&= \sum_{n=0}^{\infty}\Big[y_{220}^{(4)}n^2\left(\frac{r_s}{a}\right)^{n-2}
\end{aligned}
$$

$$+ y_{221}^{(4)} n \left(\frac{r_s}{a}\right)^{n-2} + y_{222}^{(4)} \left(\frac{r_s}{a}\right)^{n-2} \Big] P_n(\cos\theta)$$

$$+ \sum_{n=0}^{\infty} \Big(h_n^d(4, 0) - y_{220}^{(4)} n^2 \left(\frac{r_s}{a}\right)^{n-2}$$

$$- y_{221}^{(4)} n \left(\frac{r_s}{a}\right)^{n-2} - y_{222}^{(4)} \left(\frac{r_s}{a}\right)^{n-2} \Big] P_n(\cos\theta)$$

$$= y_{220}^{(4)} \frac{1}{(\frac{r_s}{a})(1 - 2(\frac{r_s}{a})\cos\theta + (\frac{r_s}{a})^2)^{\frac{5}{2}}} \Big[\cos\theta \Big(1 - \left(\frac{r_s}{a}\right)^2 \Big)$$

$$+ \left(\frac{r_s}{a}\right) \Big(\cos^2\theta - 2 + \left(\frac{r_s}{a}\right)^2 \Big) \Big]$$

$$+ y_{221}^{(4)} \frac{1}{(\frac{r_s}{a})(1 - 2(\frac{r_s}{a})\cos\theta + (\frac{r_s}{a})^2)^{\frac{3}{2}}} \Big(\cos\theta - \left(\frac{r_s}{a}\right) \Big)$$

$$+ y_{222}^{(4)} \frac{1}{(\frac{r_s}{a})(1 - 2(\frac{r_s}{a})\cos\theta + (\frac{r_s}{a})^2)^{\frac{1}{2}}}$$

$$+ \sum_{n=0}^{\infty} \Big[h_n^d(4, 0) - y_{220}^{(4)} n^2 \left(\frac{r_s}{a}\right)^{n-2}$$

$$- y_{221}^{(4)} n \left(\frac{r_s}{a}\right)^{n-2} - y_{222}^{(4)} \left(\frac{r_s}{a}\right)^{n-2} \Big] P_n(\cos\theta). \tag{5.45}$$

$$\frac{a^2}{g_0} \hat{\psi}^{(4)}(a, \theta) = \sum_{n=0}^{\infty} k_n^d(4, 0) P_n(\cos\theta)$$

$$= \sum_{n=0}^{\infty} \tilde{k}_n^d(4, 0) P_n(\cos\theta)$$

$$+ \sum_{n=0}^{\infty} (k_n^d(4, 0) - \tilde{k}_n^d(4, 0)) P_n(\cos\theta)$$

$$= \sum_{n=0}^{\infty} y_{120}^{(4)} n \left(\frac{r_s}{a}\right)^{n-2} P_n(\cos\theta)$$

$$+ \sum_{n=0}^{\infty} \Big[k_n^d(4, 0) - y_{120}^{(4)} n \left(\frac{r_s}{a}\right)^{n-2} \Big] P_n(\cos\theta)$$

$$= y_{120}^{(4)} \frac{1}{(\frac{r_s}{a})(1 - 2(\frac{r_s}{a})\cos\theta + (\frac{r_s}{a})^2)^{\frac{3}{2}}} \Big(\cos\theta - \left(\frac{r_s}{a}\right) \Big)$$

$$+ \sum_{n=0}^{\infty} \Big[k_n^d(4, 0) - y_{120}^{(4)} n \left(\frac{r_s}{a}\right)^{n-2} \Big] P_n(\cos\theta). \tag{5.46}$$

$$\frac{a^2}{g_0} \Delta\hat{g}^{(4)}(a, \theta) = \sum_{n=0}^{\infty} \frac{n+1}{a} k_n^d(4, 0) P_n(\cos\theta)$$

$$= \frac{1}{a} \sum_{n=0}^{\infty} k_n^d(4, 0) P_n(\cos\theta) + \frac{1}{a} \sum_{n=0}^{\infty} n \tilde{k}_n^d(4, 0) P_n(\cos\theta)$$

$$+ \frac{1}{a} \sum_{n=0}^{\infty} n (k_n^d(4, 0) - \tilde{k}_n^d(4, 0)) P_n(\cos\theta)$$

$$= \frac{a}{g_0}\hat{\psi}^{(4)}(a, \theta) + \frac{1}{a}\sum_{n=0}^{\infty} y_{120}^{(4)} n^2 \left(\frac{r_s}{a}\right)^{n-2} P_n(\cos\theta)$$
$$+ \frac{1}{a}\sum_{n=0}^{\infty} n\left[k_n^d(4, 0) - y_{120}^{(4)} n\left(\frac{r_s}{a}\right)^{n-2}\right] P_n(\cos\theta)$$
$$= \frac{a}{g_0}\hat{\psi}^{(4)}(a, \theta)$$
$$+ \frac{1}{a} y_{120}^{(4)} \frac{1}{(\frac{r_s}{a})(1 - 2(\frac{r_s}{a})\cos\theta + (\frac{r_s}{a})^2)^{\frac{5}{2}}}\left[\cos\theta\left(1 - \left(\frac{r_s}{a}\right)^2\right)\right.$$
$$\left. - \left(\frac{r_s}{a}\right)^2\left(\cos^2\theta - 2 + \left(\frac{r_s}{a}\right)^2\right)\right]$$
$$+ \frac{1}{a}\sum_{n=0}^{\infty} n\left[k_n^d(4, 0) - y_{120}^{(4)} n\left(\frac{r_s}{a}\right)^{n-2}\right] P_n(\cos\theta). \tag{5.47}$$

$$\delta\hat{g}^{(4)}(a, \theta) = \Delta\hat{g}^{(4)}(a, \theta) - \beta\hat{u}_r^{(4)}(a, \theta). \tag{5.48}$$

In the following, we discuss the special case of $d_s = 0$. In the case of a strike-slip, the radial displacement at colatitude θ at sin $2\phi = 1$ is written from (4.23) as

$$a^2\hat{u}_r^{(1)}(a, \theta) = 2\sum_{n=2}^{\infty} h_n^d(1, 2) P_n^2(\cos\theta). \tag{5.49}$$

The summand in (5.49) is of order $0(n)$ since

$$P_n^2(\cos\theta) = 0(n^2) \tag{5.50}$$

$$h_n^d(1, 2) = 0\left(\frac{1}{n}\right). \tag{5.51}$$

This raises a serious problem concerning the naive numerical approach.

The summation can be performed with the aid of the asymptotic solutions. Since

$$y_1^{Shear}(a; n) = \frac{1}{n} y_{310} + \frac{1}{n^2} y_{311} + 0(n^{-3}) \tag{5.52}$$

(Appendix B), (5.49) can be rewritten as

$$2\sum_{n=2}^{\infty} h_n^d(1, 2) P_n^2(\cos\theta) = 2\sum_{n=2}^{\infty}\left[\frac{y_{310}}{n} + \frac{y_{311}}{n(n+1)}\right] P_n^2(\cos\theta)$$
$$+ 2\sum_{n=2}^{\infty}\left[h_n^d(1, 2) - \frac{y_{310}}{n} - \frac{y_{311}}{n(n+1)}\right] P_n^2(\cos\theta). \tag{5.53}$$

We should notice that there exists a scaling factor between $h_n^d(1, 2)$ and $y_1^{Shear}(a; n)$ which should taken into accunt in a practical calculation. The second series on the right-hand side (RHS) of (5.53) quickly converges because its summand is of order $0(1/n)$. On the other hand, the first series of RHS of (5.53) can be analytically evaluated by using the following formulas:

$$\sum_{n=2}^{\infty}\frac{1}{n}P_n^2(\cos\theta) = \frac{(1-\sin\frac{\theta}{2})(4\sin^2\frac{\theta}{2}+5\sin\frac{\theta}{2}+2)}{4\sin^2\frac{\theta}{2}(1+\sin\frac{\theta}{2})} \tag{5.54}$$

$$\sum_{n=2}^{\infty}\frac{1}{n(n+1)}P_n^2(\cos\theta) = \frac{(1-\sin\frac{\theta}{2})(1+2\sin\frac{\theta}{2})}{2\sin\frac{\theta}{2}(1+\sin\frac{\theta}{2})}. \tag{5.55}$$

Substituting (5.54) and (5.55) into (5.53), we obtain

$$\begin{aligned} a^2\hat{u}_r^{(1)}(a,\theta) = {} & \frac{1-\sin\frac{\theta}{2}}{2\sin^2\frac{\theta}{2}(1+\sin\frac{\theta}{2})}\left[y_{310}\left(4\sin^2\frac{\theta}{2}+5\sin\frac{\theta}{2}+2\right)\right. \\ & \left.+2y_{311}\sin\frac{\theta}{2}\left(1+2\sin\frac{\theta}{2}\right)\right] \\ & +2\sum_{n=2}^{\infty}\left(h_n^d(1,2)-\frac{y_{310}}{n}-\frac{y_{311}}{n(n+1)}\right)P_n^2(\cos\theta). \end{aligned} \tag{5.56}$$

Similarly, we obtain the potential and gravity changes as

$$\begin{aligned} \frac{a^2}{g_0}\hat{\psi}^{(1)}(a,\theta) &= 2\sum_{n=2}^{\infty}k_n^d(1,2)P_n^2(\cos\theta) \\ &= 2\sum_{n=2}^{\infty}\frac{y_{351}}{n(n^2-1)}P_n^2(\cos\theta) \\ &\quad +2\sum_{n=2}^{\infty}\left[k_n^d(1,2)-\frac{y_{351}}{n(n^2-1)}\right]P_n^2(\cos\theta) \\ &= 2y_{351}\left\{-\cot\theta\left[-\cos\frac{\theta}{2}+\frac{\cos\frac{\theta}{2}(1+\sin^2\frac{\theta}{2})}{1+\sin\frac{\theta}{2}}\right.\right. \\ &\quad \left.+2\sin\frac{\theta}{2}\cos\frac{\theta}{2}\ln\left(\sin\frac{\theta}{2}+\sin^2\frac{\theta}{2}\right)\right] \\ &\quad \left.-\left[-2\sin\frac{\theta}{2}+1-\cos\theta-\cos\theta\ln\left(\sin\frac{\theta}{2}+\sin^2\frac{\theta}{2}\right)\right]\right\} \\ &\quad +2\sum_{n=2}^{\infty}\left[k_n^d(1,2)-\frac{y_{351}}{n(n^2-1)}\right]P_n^2(\cos\theta). \end{aligned} \tag{5.57}$$

$$\begin{aligned} \frac{a^2}{g_0}\Delta\hat{g}^{(1)}(a,\theta) &= 2\sum_{n=2}^{\infty}\frac{n+1}{a}k_n^d(1,2)P_n^2(\cos\theta) \\ &= \frac{2}{a}\sum_{n=2}^{\infty}k_n^d(1,2)P_n^2(\cos\theta)+\frac{2}{a}\sum_{n=2}^{\infty}\frac{y_{351}}{n(n+1)}P_n^2(\cos\theta) \\ &\quad +\frac{2}{a}\sum_{n=2}^{\infty}\left[nk_n^d(1,2)-\frac{y_{351}}{n(n+1)}\right]P_n^2(\cos\theta) \\ &= \frac{a}{g_0}\hat{\psi}^{(1)}(a,\theta)+\frac{2}{a}y_{351}\frac{(1-\sin\frac{\theta}{2})(1+2\sin^2\frac{\theta}{2})}{2\sin\frac{\theta}{2}(1+\sin\frac{\theta}{2})} \\ &\quad +\frac{2}{a}\sum_{n=2}^{\infty}\left[nk_n^d(1,2)-\frac{y_{351}}{n(n+1)}\right]P_n^2(\cos\theta). \end{aligned} \tag{5.58}$$

The above discussions have demonstrated the importance of the asymptotic solutions in numerical calculations.

6. Computational Results

We compute the gravity and potential changes due to dislocations in the homogeneous and radially heterogeneous earth models discussed in this chapter. Since we have assumed simplified source functions and normalized all of the variables (see Appendix C), we must now reverse them back in order to obtain appropriate dimensions. The procedure for this unnormalization is discussed in section 6.1. We present the results for a homogeneous earth model in section 6.2. The results agree well with those calculated from half-space theory in the near field (OKUBO, 1991a). The agreement confirms that our spherical theory is consistent with Okubo's half-space theory. The difference between the two becomes evident as the epicentral distance increases because of the curvature of the earth. In section 6.3 we proceed to calculations for a radially heterogeneous earth model 1066A (GILBERT and DZIEWONSKI, 1975). The dislocation Love numbers are tabulated in Appendix D. The radial displacement, potential and gravity changes are given in Appendix E, which can be used for practical applications.

6.1 Remark Concerning the Units

Since we have made some simplification and normalizations before, we must now reverse them back in order to obtain their actual units. For example, an actual displacement should be written as

$$u_r^{Actual}(a, \theta) = u_r^{Table}(\theta) \cdot a \cdot \frac{UdS}{a^3}, \tag{6.1}$$

where the superscript '*Table*' indicates our tabulated results; the 'a' in the middle of the right-hand side (RHS) comes from the normalization $y_1 = a\bar{y}_1$, and the last term of RHS is due to the simplification for source functions $UdS/a^3 = 1$. (6.1) is rewritten as

$$u_r^{Actual}(a, \theta) = u_r^{Table}(\theta) \frac{UdS}{a^2}. \tag{6.2}$$

Similarly, we have

$$\psi^{Actual}(a, \theta) = \psi^{Table}(\theta) \frac{g_0 UdS}{a^2} \tag{6.3}$$

$$\Delta g^{Actual}(a, \theta) = \Delta g^{Table}(\theta) \frac{g_0 UdS}{a^3}, \tag{6.4}$$

and

$$\begin{aligned} \delta g^{Actual}(a, \theta) &= \Delta g^{Actual}(a, \theta) - \beta u_r^{Actual}(a, \theta) \\ &= (\Delta g^{Table}(a, \theta) - 2u_r^{Table}(a, \theta)) \frac{g_0 UdS}{a^3} \end{aligned}$$

$$= \delta g^{Table}(\theta)\frac{g_0 UdS}{a^3}. \tag{6.5}$$

In our calculations, we take

$$g_0 = 982gal$$
$$a = 6.371 \times 10^8 cm.$$

6.2 Results for a Homogeneous Earth Model

We present our results for a homogenous earth model, assuming that

$$\rho_0 = 2.183 g/cm^3,$$
$$\mu = 1.45 \times 10^{11} dyn/cm^2,$$
$$\lambda = 1.90 \times 10^{11} dyn/cm^2.$$

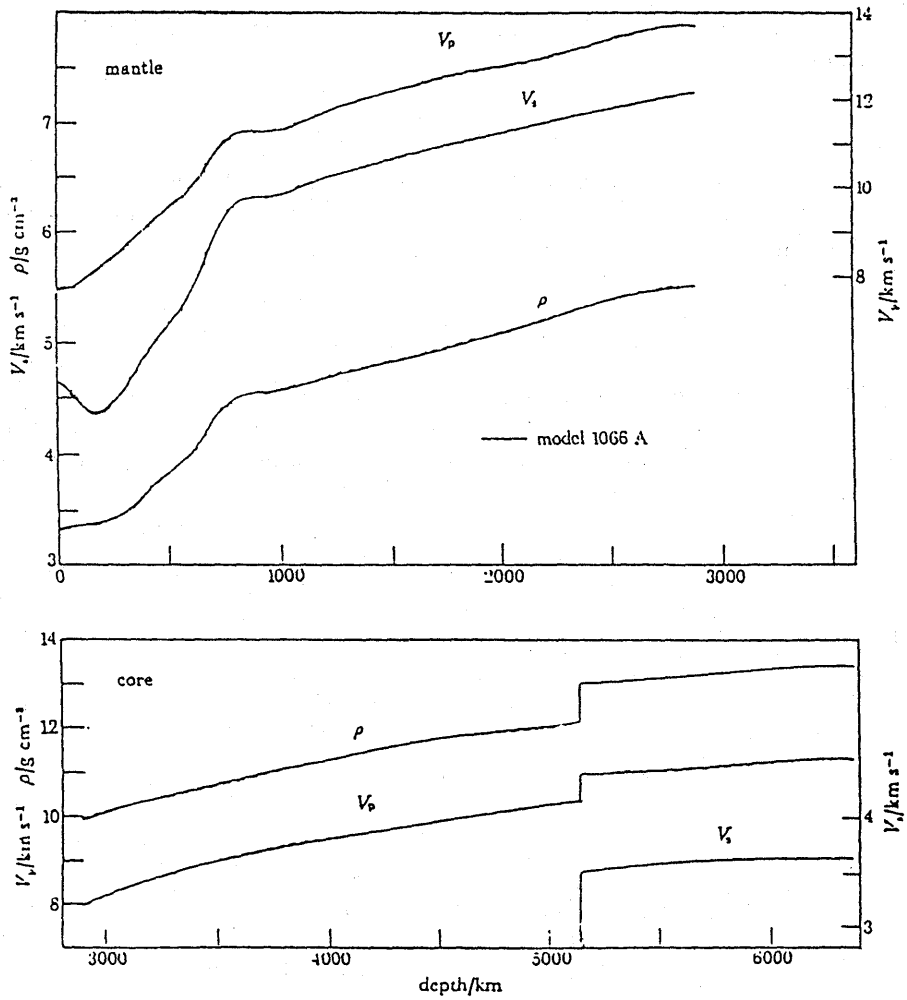

Fig. 6.1 1066A Earth model (after Gilbert and Dziewonski, 1975).

These parameters are taken from the top layer of the 1066A (GILBERT and DZIEONSKI, 1975) earth model (see Figure 6.1). For Newton's gravitational constant we take $G = 6.67 \times 10^{-8} cm^3/gs^2$.

We have considered the following source depths: 0, 2, 5, 10, 20, 32, 64, 100, 200, 300, 400 and 637 km.

Numerical integrations were carried out to obtain the dislocation Love numbers by using the Runge-Kutta method. Tables 6.1–6.4 give the dislocation Love numbers for the four types of dislocations.

From the dislocation Love numbers, we have calculated the corresponding deformation fields. Figures 6.2(a) and 6.2(b) show the global gravity change on the free surface caused by a vertical strike-slip dislocation at a depth of 32 km.

In these figures we take the seismic moment, M_0, to be $3.61 \times 10^{30} dyn \cdot cm$. The point sources are located on the polar axis. Fiture 6.2(a) illustrates the result on the upper hemisphere, including the source, while Figure 6.2(b) shows the result on the lower hemisphere. In these figures, the upper hemisphere is mapped onto a tangent plane at the epicenter. Each point on the hemisphere is moved to the tangent plane in such a way that the epicenter distance is preserved. The lower hemishere is similarly mapped on the same

Table 6.1. Dislocation Love numbers of a homogeneous earth model (1). Vertical strike-slip fault. $\delta = 90°$, $\lambda = 0°$, $m = 2$. Source depth = 2 km

n	$\bar{h}_n^d(1,2)$	$\bar{l}_n^d(1,2)$	$\bar{k}_n^d(1,2)$
2	.1009$E-2$	.2768$E-1$	.4613$E-2$
3	−.2309$E-2$	.1767$E-1$	.1890$E-2$
4	−.2541$E-2$	.1331$E-1$	.1064$E-2$
5	−.2367$E-2$	.1074$E-1$	.6910$E-3$
6	−.2142$E-2$	.9011$E-2$	.4886$E-3$
8	−.1752$E-2$	.6830$E-2$	.2848$E-3$
10	−.1466$E-2$	.5502$E-2$	.1884$E-3$
20	−.7894$E-3$	.2789$E-2$	.5506$E-4$
30	−.5354$E-3$	.1866$E-2$	.2903$E-4$
50	−.3225$E-3$	.1120$E-2$	.1532$E-4$
70	−.2287$E-3$	.7979$E-3$	.1146$E-4$
100	−.1574$E-3$	.5557$E-3$	.9396$E-5$
300	−.4465$E-4$	.1774$E-3$	.7625$E-5$
500	−.2185$E-4$	.1015$E-3$	.7487$E-5$
700	−.1206$E-4$	.6892$E-4$	.7450$E-5$
1000	−.4701$E-5$	.4451$E-4$	.7431$E-5$
1200	−.1838$E-5$	.3501$E-4$	.7426$E-5$
1400	.2077$E-6$	.2822$E-4$	.7423$E-5$
1600	.1742$E-5$	.2314$E-4$	.7421$E-5$
1800	.2936$E-5$	.1918$E-4$	.7419$E-5$
2000	.3892$E-5$	.1601$E-4$	.7419$E-5$
3000	.6759$E-5$	.6509$E-5$	.7417$E-5$
4000	.8193$E-5$	.1758$E-5$	.7416$E-5$
5000	.9053$E-5$	−.1092$E-5$	.7416$E-5$
7000	.1004$E-4$	−.4351$E-5$	.7416$E-5$
10000	.1077$E-4$	−.6794$E-5$	.7416$E-5$
20000	.1164$E-4$	−.9645$E-5$	.7416$E-5$
30000	.1192$E-4$	−.1059$E-4$	.7416$E-5$

Table 6.2. Dislocation Love numbers of a homogeneous earth model (2). Vertical dip-slip fault. $\delta = 90°$, $\lambda = 90°$, $m = 1$. Source depth $= 20\,km$

n	$\bar{h}_n^d(2,1)$	$\bar{l}_n^d(2,1)$	$\bar{k}_n^d(2,1)$
1	$-.3210E-4$	$.5966E-1$	$.0000E+0$
2	$.2334E-3$	$.3310E-1$	$.1012E-3$
3	$.2454E-3$	$.2308E-1$	$.1122E-3$
4	$.2485E-3$	$.1774E-1$	$.1187E-3$
5	$.2494E-3$	$.1440E-1$	$.1231E-3$
6	$.2497E-3$	$.1212E-1$	$.1262E-3$
8	$.2498E-3$	$.9186E-2$	$.1306E-3$
10	$.2497E-3$	$.7379E-2$	$.1335E-3$
20	$.2497E-3$	$.3650E-2$	$.1401E-3$
30	$.2499E-3$	$.2370E-2$	$.1427E-3$
40	$.2500E-3$	$.1723E-2$	$.1441E-3$
50	$.2501E-3$	$.1332E-2$	$.1449E-3$
80	$.2502E-3$	$.7424E-3$	$.1462E-3$
100	$.2503E-3$	$.5448E-3$	$.1467E-3$
200	$.2506E-3$	$.1481E-3$	$.1477E-3$
300	$.2508E-3$	$.1541E-4$	$.1481E-3$
400	$.2510E-3$	$-.5113E-4$	$.1484E-3$
500	$.2512E-3$	$-.9114E-4$	$.1486E-3$
600	$.2513E-3$	$-.1178E-3$	$.1487E-3$
800	$.2517E-3$	$-.1514E-3$	$.1490E-3$
1000	$.2520E-3$	$-.1717E-3$	$.1492E-3$
1400	$.2526E-3$	$-.1951E-3$	$.1497E-3$
1800	$.2533E-3$	$-.2084E-3$	$.1501E-3$
2000	$.2536E-3$	$-.2132E-3$	$.1503E-3$
2200	$.2539E-3$	$-.2171E-3$	$.1505E-3$
2400	$.2542E-3$	$-.2205E-3$	$.1507E-3$
2600	$.2546E-3$	$-.2233E-3$	$.1509E-3$
2800	$.2549E-3$	$-.2259E-3$	$.1511E-3$
3000	$.2552E-3$	$-.2281E-3$	$.1513E-3$
3500	$.2560E-3$	$-.2327E-3$	$.1518E-3$

plane.

Note that the angle ϕ runs in a counter-clockwise direction on both the upper and lower hemisphere maps. This means that in both cases we are looking at the sphere from a point above the upper hemisphere.

The contour maps show the magnitude of the gravity change field. The solid line indicates the gravity increase, while the broken line indicates the decrease. No gravity change occurs on the cross line and the circle marked zero.

We can see from Figure 6.2(a) that the gravity change shows a four-quadrant pattern. Since the earth's surface in quadrants 1 and 3 rises, the gravity should decrease. On the contrary, since the earth's surface in quadrants 2 and 4 becomes lower, the gravity should increase.

It is of special interest to compare our results with the half-space solution. We compare the gravity change with that of Okubo's (1991a) half-space solution. The distance x on the free surface of the half-space is related to its image on

Table 6.3. Dislocation Love numbers of a homogeneous earth model (3). 45° dip-slip fault. $\delta = 45°$, $\lambda = 90°$, $m = 0$. Source depth = 64 km

n	$\bar{h}_n^d(3,0)$	$\bar{l}_n^d(3,0)$	$\bar{k}_n^d(3,0)$
0	$-.3330E-1$	$.0000E+0$	$.0000E+0$
1	$-.6711E-1$	$.1919E+0$	$.0000E+0$
2	$-.2434E-1$	$.7209E-1$	$-.4886E-2$
3	$-.9098E-2$	$.4423E-1$	$-.2401E-2$
4	$-.3776E-2$	$.3124E-1$	$-.1285E-2$
5	$-.1398E-2$	$.2386E-1$	$-.6865E-3$
6	$-.1731E-3$	$.1915E-1$	$-.3265E-3$
8	$.9352E-3$	$.1353E-1$	$.6845E-4$
10	$.1366E-2$	$.1031E-1$	$.2705E-3$
15	$.1657E-2$	$.6220E-2$	$.4911E-3$
20	$.1678E-2$	$.4265E-2$	$.5773E-3$
30	$.1612E-2$	$.2373E-2$	$.6455E-3$
40	$.1547E-2$	$.1451E-2$	$.6723E-3$
50	$.1498E-2$	$.9062E-3$	$.6860E-3$
60	$.1460E-2$	$.5459E-3$	$.6941E-3$
80	$.1409E-2$	$.9914E-4$	$.7032E-3$
100	$.1375E-2$	$-.1673E-3$	$.7082E-3$
120	$.1352E-2$	$-.3443E-3$	$.7114E-3$
140	$.1336E-2$	$-.4706E-3$	$.7137E-3$
160	$.1323E-2$	$-.5653E-3$	$.7155E-3$
180	$.1313E-2$	$-.6391E-3$	$.7169E-3$
200	$.1306E-2$	$-.6982E-3$	$.7182E-3$
300	$.1284E-2$	$-.8769E-3$	$.7229E-3$
400	$.1275E-2$	$-.9683E-3$	$.7266E-3$
500	$.1271E-2$	$-.1025E-2$	$.7299E-3$
600	$.1270E-2$	$-.1064E-2$	$.7331E-3$
800	$.1273E-2$	$-.1117E-2$	$.7391E-3$
1000	$.1278E-2$	$-.1153E-2$	$.7451E-3$

the sphere through the relation

$$x = a\theta. \tag{6.6}$$

We first compare the gravity changes in the near field caused by the same source as that in Figure 6.2(a). Figure 6.2(c) gives contour maps of our result in the near field of 1° and Figure 6.3(a) gives that from Okubo's theory. We see that the two results agree very well with each other within the epicentral distance $\theta < 1°$ or 111km. It simultaneously verifies that our theory is consistent with Okubo's flat-earth theory.

The gravity change caused by the same dislocation in the flat-earth is shown in Figure 6.3(b). The discrepancy between Figures 6.3(b) and 6.2(a) is no larger than 10% within an epicentral distance of $\theta = 10°$. The difference becomes larger when $\theta > 10°$. This is a natural effect of the curvature of the sphere.

To make a more quantitative comparison, we consider their ratio,

$$R_g(\theta) = \frac{\delta g^{Sphere}(\theta, \phi)}{\delta g^{F.E.}(\theta, \phi)},$$

Table 6.4. Dislocation Love numbers of a homogeneous earth model (4). Vertical tensile fault ($m = 0$). Source depth = 637 km

n	$\bar{h}_n^d(4,0)$	$\bar{l}_n^d(4,0)$	$\bar{k}_n^d(4,0)$
0	$.1142E+0$	$.0000E+0$	$.0000E+0$
1	$.3007E+0$	$-.7702E-1$	$.0000E+0$
2	$.1450E+0$	$-.2706E-1$	$.1171E-1$
3	$.9563E-1$	$-.2315E-1$	$.1115E-1$
4	$.7366E-1$	$-.2156E-1$	$.1093E-1$
5	$.6136E-1$	$-.2075E-1$	$.1083E-1$
6	$.5352E-1$	$-.2027E-1$	$.1078E-1$
8	$.4414E-1$	$-.1975E-1$	$.1074E-1$
10	$.3874E-1$	$-.1948E-1$	$.1073E-1$
15	$.3180E-1$	$-.1919E-1$	$.1074E-1$
20	$.2846E-1$	$-.1907E-1$	$.1076E-1$
25	$.2650E-1$	$-.1902E-1$	$.1079E-1$
30	$.2522E-1$	$-.1900E-1$	$.1081E-1$
35	$.2432E-1$	$-.1900E-1$	$.1083E-1$
40	$.2365E-1$	$-.1900E-1$	$.1085E-1$
45	$.2314E-1$	$-.1901E-1$	$.1087E-1$
50	$.2274E-1$	$-.1902E-1$	$.1089E-1$
60	$.2216E-1$	$-.1905E-1$	$.1092E-1$
70	$.2176E-1$	$-.1909E-1$	$.1096E-1$
80	$.2146E-1$	$-.1911E-1$	$.1098E-1$
90	$.2121E-1$	$-.1906E-1$	$.1097E-1$
100	$.2112E-1$	$-.1924E-1$	$.1106E-1$

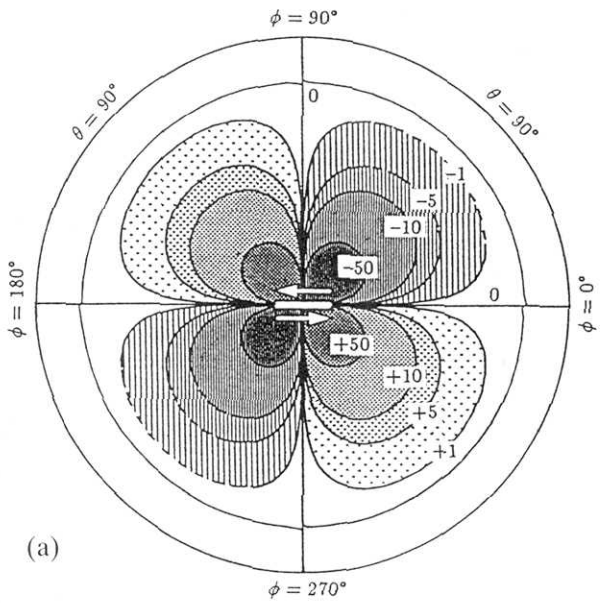

(a)

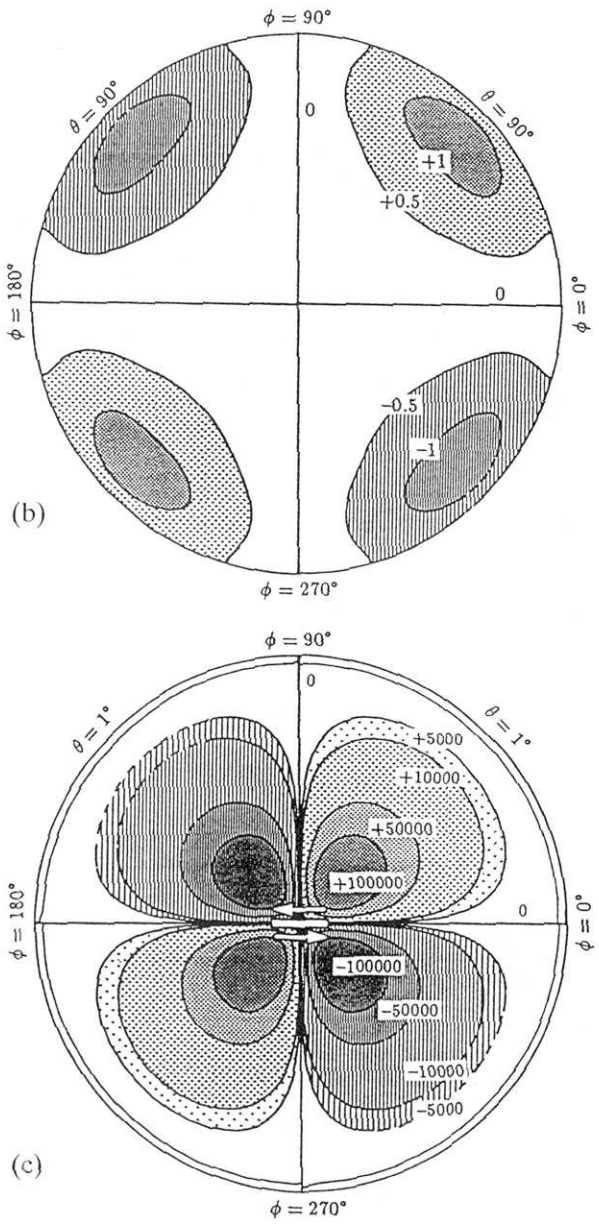

Fig. 6.2 Gravity changes due to a strike-slip dislocation in a homogeneous earth model. The epicentral distance is proportional to the radial distance. The depth of the dislocation is $32\,km$. The seismic moment is $M_{12} = 3.61 \times 10^{30}\,dyn{\cdot}cm$, or $UdS = 2.49 \times 10^{19}\,cm^3$. The units are '$\mu gal$'. (a) The upper hemisphere ($0° < \theta < 90°$). We find the positive gravity change in $90° < \phi < 180°$ and $270° < \phi < 360°$. A negative gravity change arises in $0° < \phi < 90°$ and $180° < \phi < 270°$. (b) The lower hemisphere ($90° < \theta < 180°$) with positive gravity change in $0° < \phi < 90°$ and $180° < \phi < 270°$, and negative gravity change in $90° < \phi < 180°$ and $270° < \phi < 360°$. (c) The near field ($0° < \theta < 1°$). It shows a positive gravity change in $0° < \phi < 90°$ and $180° < \phi < 270°$. A negative gravity change arises in $90° < \phi < 180°$ and $270° < \phi < 360°$.

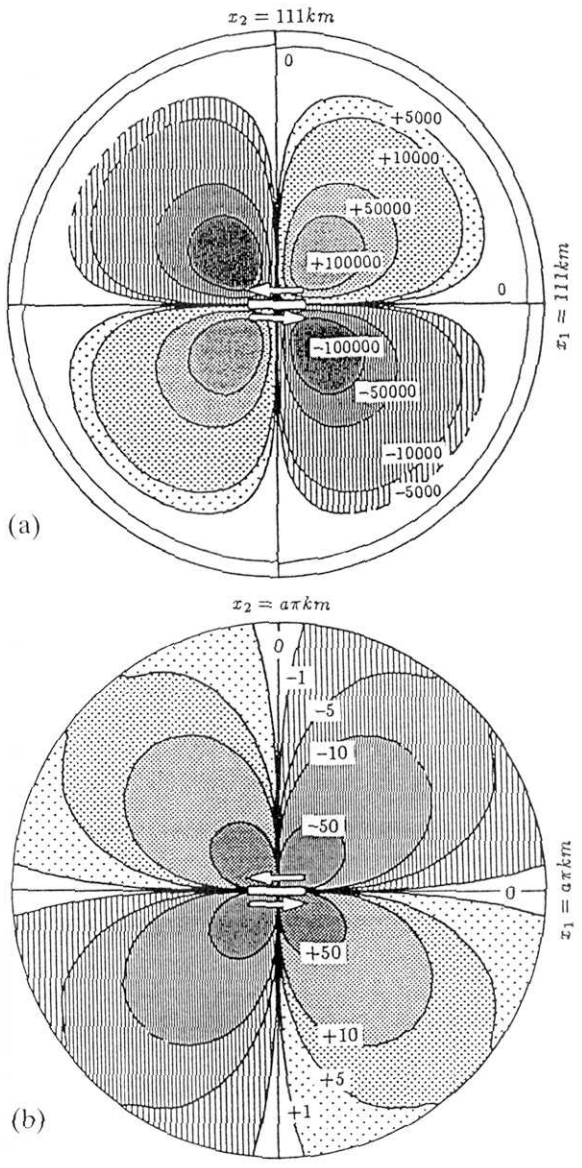

Fig. 6.3 Gravity changes obtained from Okubo's (1991a) theory due to a strike-slip dislocation in a flat-earth model. The depth of the dislocation is $32\,km$. The dislocation is $UdS = 2.49 \times 10^{19}\,cm^3$. The units are '$\mu gal$'. (a) $x < 111\,km$. (b) $x < a\pi\,km$.

where δg^{Sphere} and $\delta g^{F.E.}$ represent gravity changes on the homogeneous sphere and the flat-earth, respectively. If δg^{Sphere} agrees with $\delta g^{F.E.}$ well, R_g should be close to 1. We can see from Figure 6.4 that $0.9 < R_g < 1.1$ when the epicentral distance $< 1°$. This means that the difference between the two results is less than 10%. Because of the curvature of the earth, the difference becomes more evident in remote areas. It is reasonable to use spherical theory

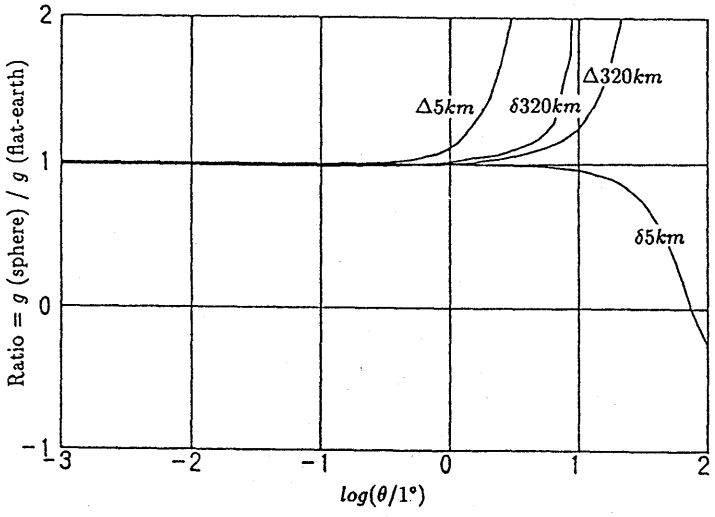

Fig. 6.4 Ratio, R_g, of gravity changes for a sphere to that of a flat-earth. Δ indicates a gravity change on the earth's surface without a free-air correction. δ denotes a gravity change on the earth's surface with the free-air correction. The number following Δ or δ indicates the depth of the point source.

for a global calculation.

In Figure 6.5(a) we present the gravity change caused by a dip-slip dislocation. It shows a different pattern from that of a strike-slip. The outer circle in Figure 6.5(a) is the line of epicentral distance 10°. The gravity increases in the upper-half part of the figure and decreases in the lower half.

We show a contour map of the gravity change, which is increased by a 45° dip-slip dislocation in Figure 6.5(b). The depth of the source is 32km. The solid line denotes the positive gravity change, while the broken line denotes the negative gravity change.

6.3 Results for a Radially Heterogeneous Earth Model

Our final purpose is to obtain results for a radially heterogeneous earth model. We use the 1066A SNREI model (GILBERT and DZIEWONSKI, 1975). Using the above theory, we calculate the deformation fields caused by dislocations.

As in section 6.2, we first calculate the dislocation Love numbers. The results are given in Appendix D.

Then, by using the dislocation Love numbers, we obtain the displacement, potential and gravity changes. In Appendix E we tabulate the numerical results of the radial displacement, potential and gravity change without any free-air correction or gravity change with the free-air correction caused by the four types of dislocations.

We show some contour maps of the gravity changes.

Figures 6.6(a) and 6.6(b) give the global gravity changes caused by a

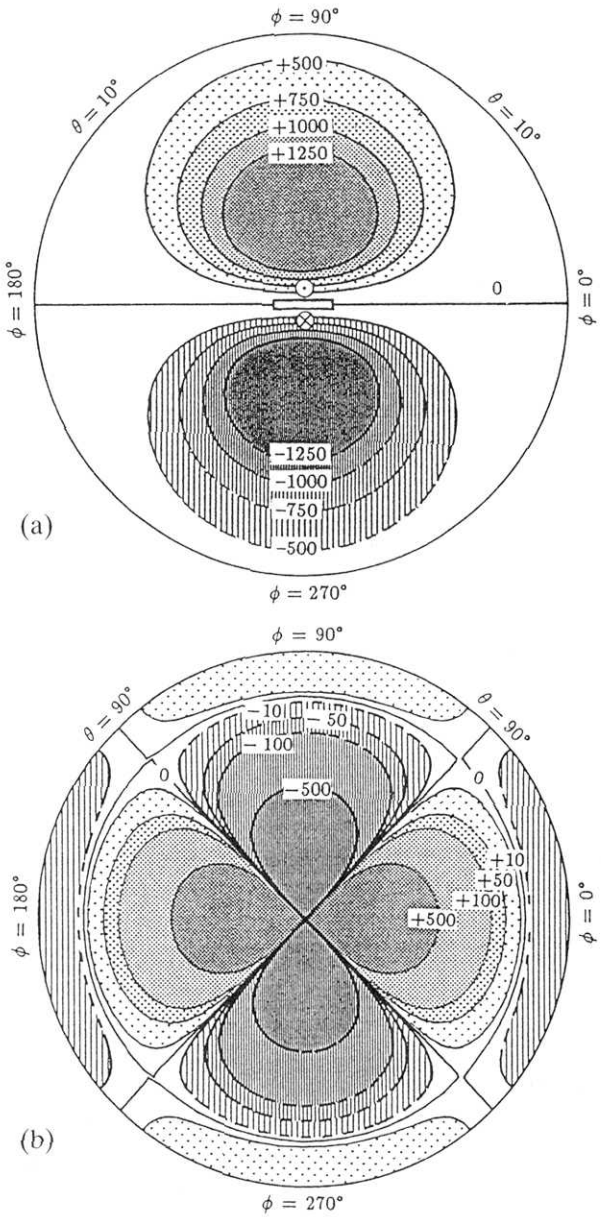

Fig. 6.5 Gravity changes caused by a dislocation in a homogeneous earth model. The epicentral distance is proportional to the radial distance. The solid line (with point shadow) denotes the positive gravity change, and the broken line (with line shadow) denotes the negative gravity change. The seismic moment is $M_{13} = 3.61 \times 10^{30}\, dyn{\cdot}cm$, or $UdS = 2.49 \times 10^{19}\, cm^3$. The units are '$\mu gal$'. (a) A dip-slip dislocation, $0° < \theta < 10°$. The depth of the dislocation is $637\, km$. (b) A 45° dip-slip dislocation, $0° < \theta < 90°$. The depth of the dislocation is $32\, km$.

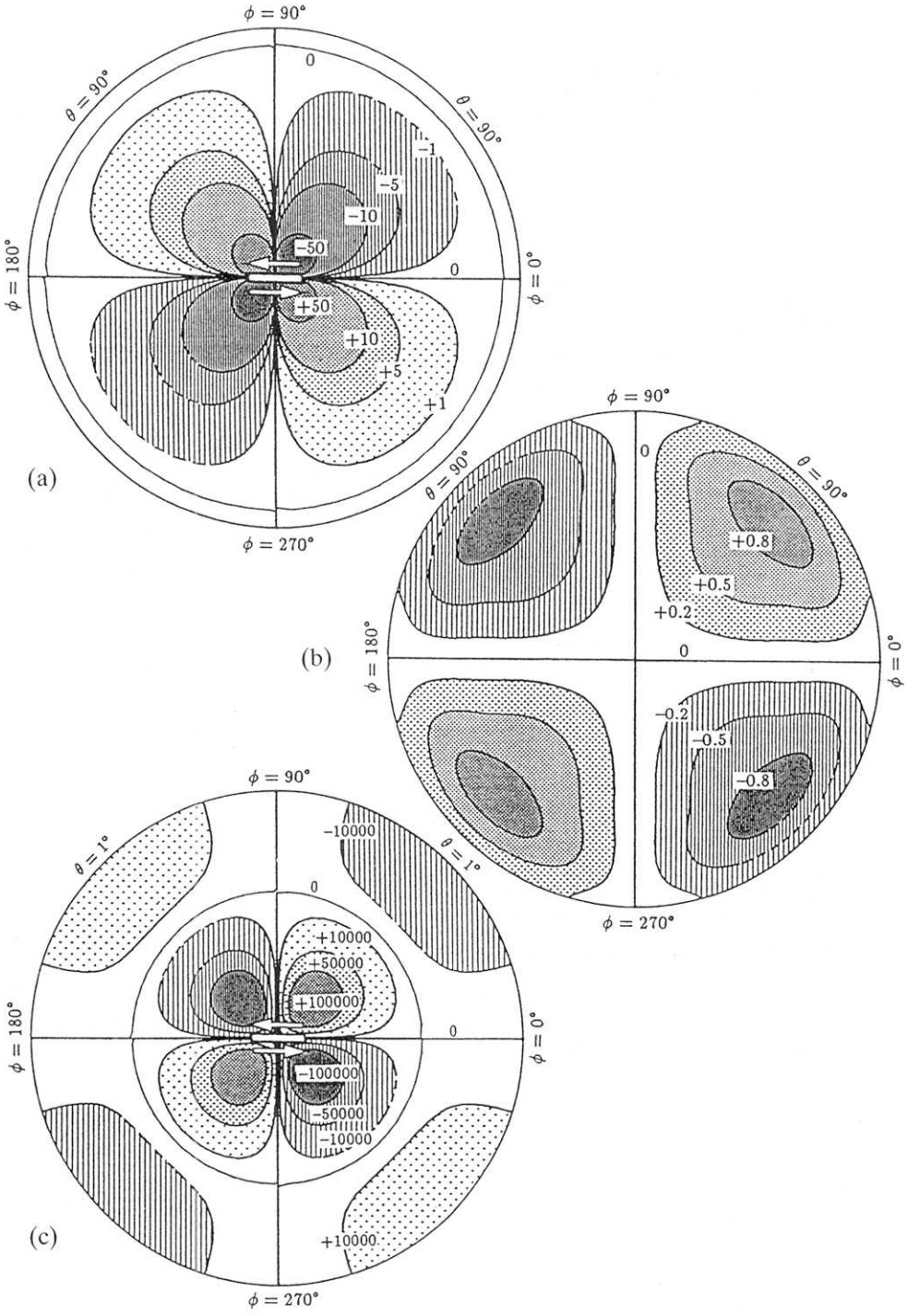

Fig.6.6 Gravity changes caused by a strike-slip dislocation in the 1066A earth model. The depth of the dislocation is 32 km. The solid line (with dotted shadow) denotes the positive change, and the broken line (with line shadow) the negative gravity change. The dislocation is $u_1 n_2 dS = 2.49 \times 10^{19}\, cm^3$. The units are '$\mu gal$'. (a) The upper hemisphere ($0° < \theta < 90°$). (b) The lower hemisphere ($90° < \theta < 180°$). (c) The near field ($0° < \theta < 1°$).

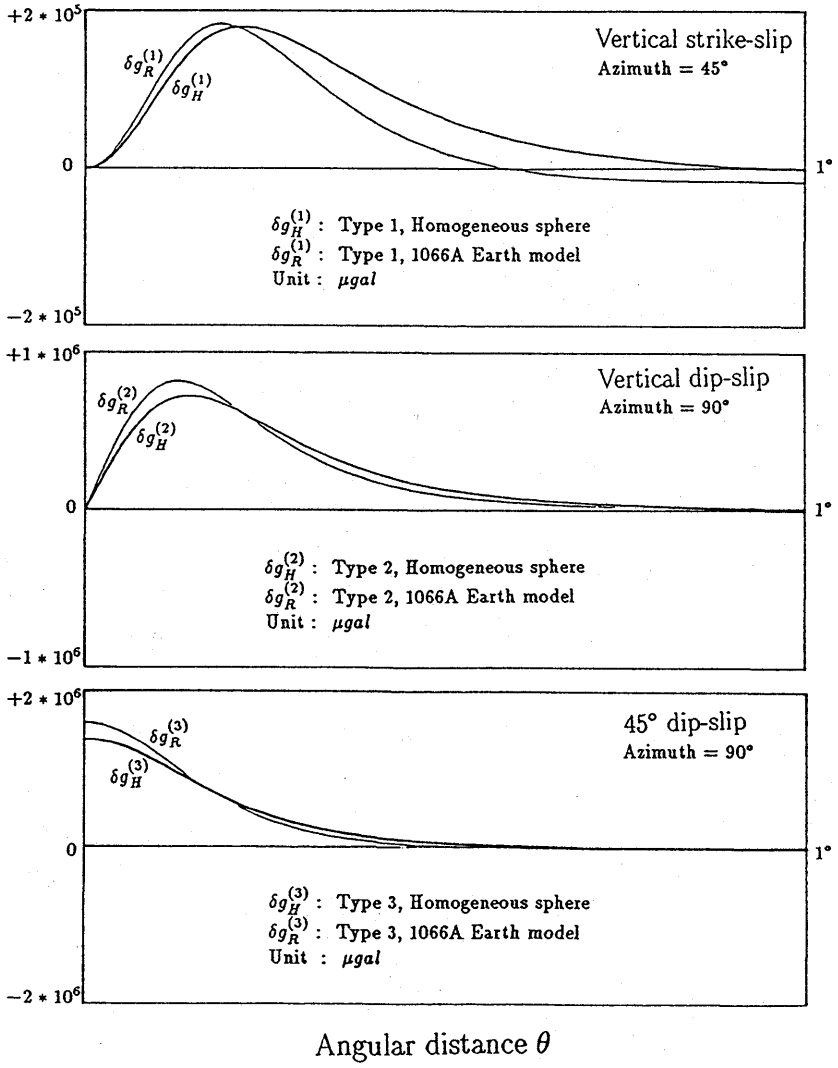

Fig. 6.7 Comparison of gravity changes of the homogeneous and 1066A models

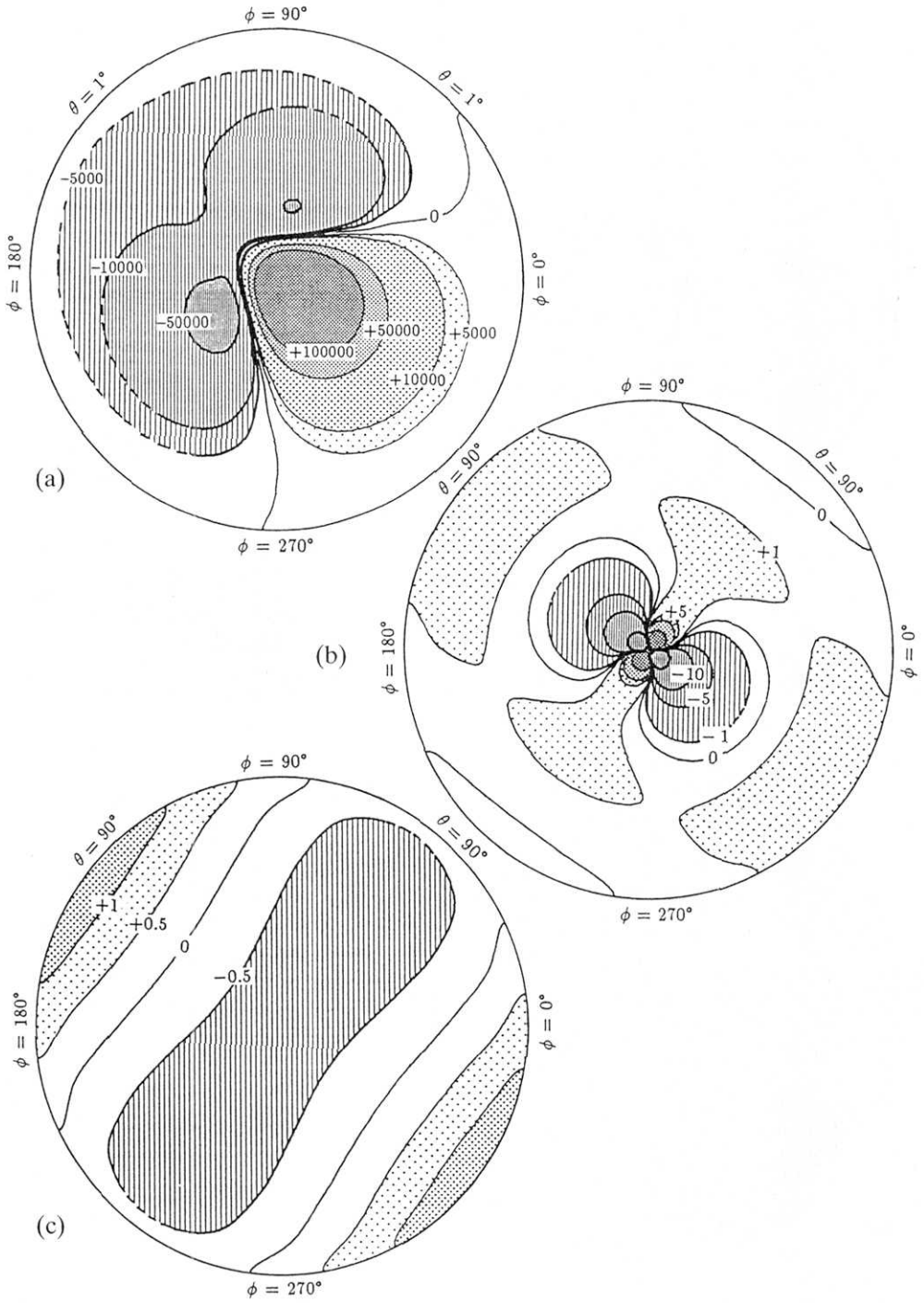

Fig. 6.8 Radial displacements, u_r, caused by a shear dislocation ($\delta = 60°$, $\lambda = 30°$, $d_s = 32\,km$) in the 1066A earth model. The dislocation is located at the center of the map. The epicentral distance is proportional to the radial distance. The solid line (with dotted shadow) denotes the uplift, and the broken line (with line shadow) the subsidence. The dislocation is $UdS = 2.49 \times 10^{19}\,cm^3$. The units are '$cm$'. (a) The near field ($0° < \theta < 1°$). (b) The upper hemisphere ($0° < \theta < 90°$). (c) The lower hemisphere ($90° < \theta < 180°$).

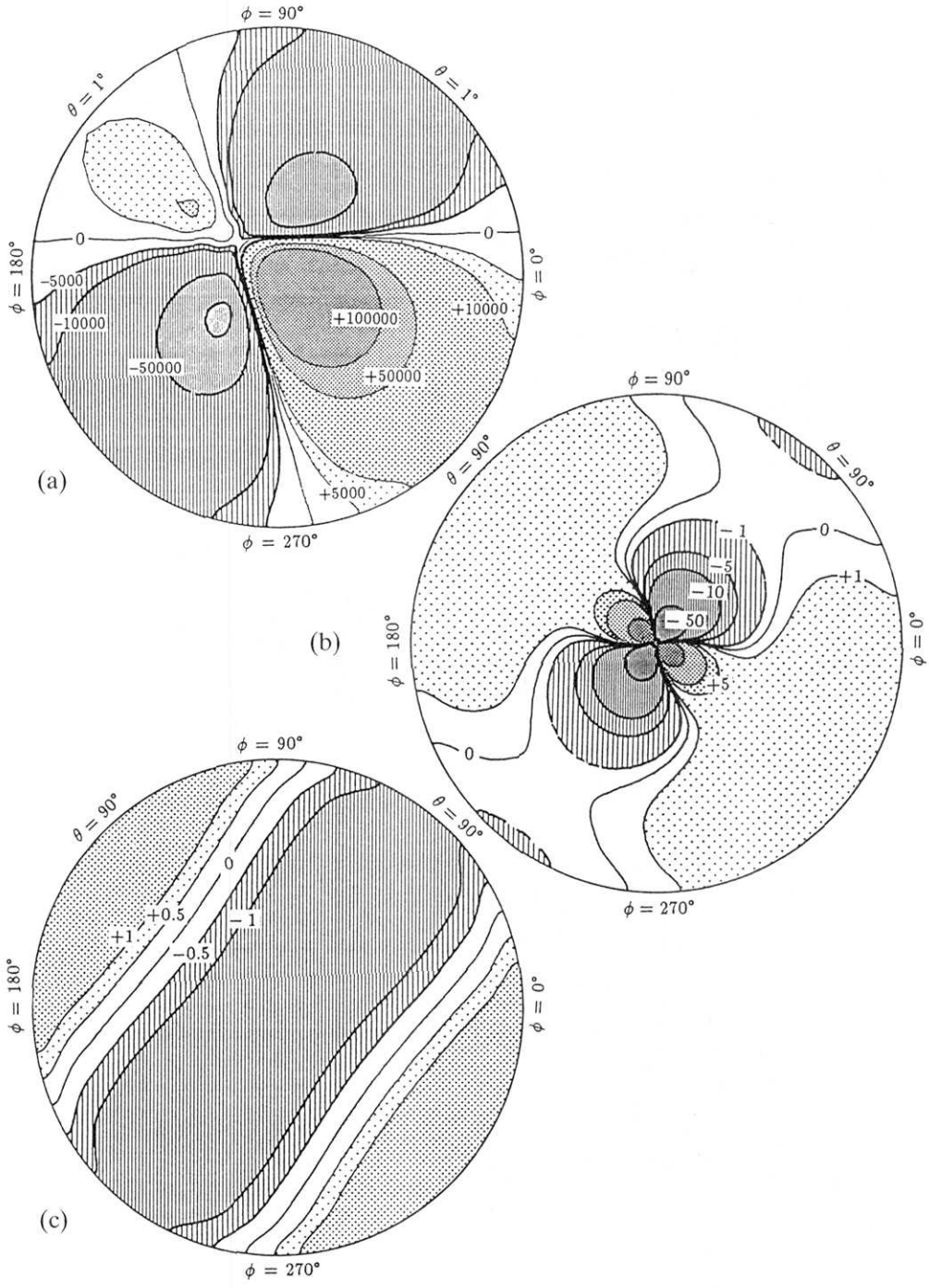

Fig. 6.9 Gravity changes Δg (without the free-air correction) caused by a shear dislocation ($\delta = 60°$, $\lambda = 30°$, $d_s = 32km$) in the 1066A earth model. The dislocation is located at the center of the map. The epicentral distance is proportional to the radial distance. The solid line (with dotted shadow) denotes the positive gravity change, and the broken line (with line shadow) the negative gravity change. The dislocation is $UdS = 2.49 \times 10^{19} cm^3$. The units are '$\mu gal$'. (a) The near field ($0° < \theta < 1°$). (b) The upper hemisphere ($0° < \theta < 90°$). (c) The lower hemisphere ($90° < \theta < 180°$).

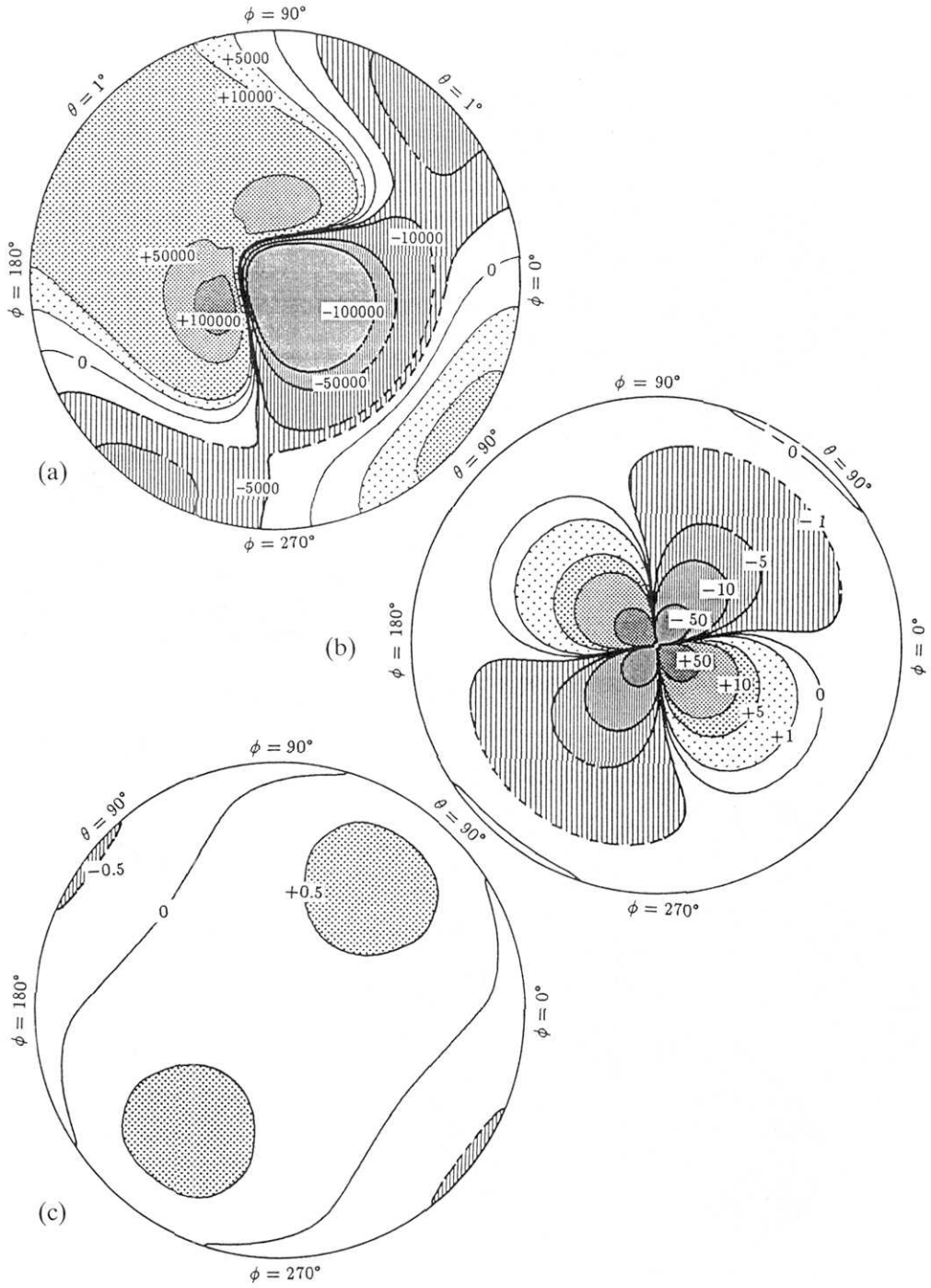

Fig. 6.10 Gravity changes δg (with the free air correction) caused by a shear dislocation ($\delta = 60°$, $\lambda = 30°$, $d_s = 32\,km$) in the 1066A earth model. The dislocation is located at the center of the map. The epicentral distance is proportional to the radial distance. The dislocation is $UdS = 2.49 \times 10^{19}\,cm^3$. The units are '$\mu gal$'. (a) The near field ($0° < \theta < 1°$). (b) The upper hemisphere ($0° < \theta < 90°$). (c) The lower hemisphere ($90° < \theta < 180°$).

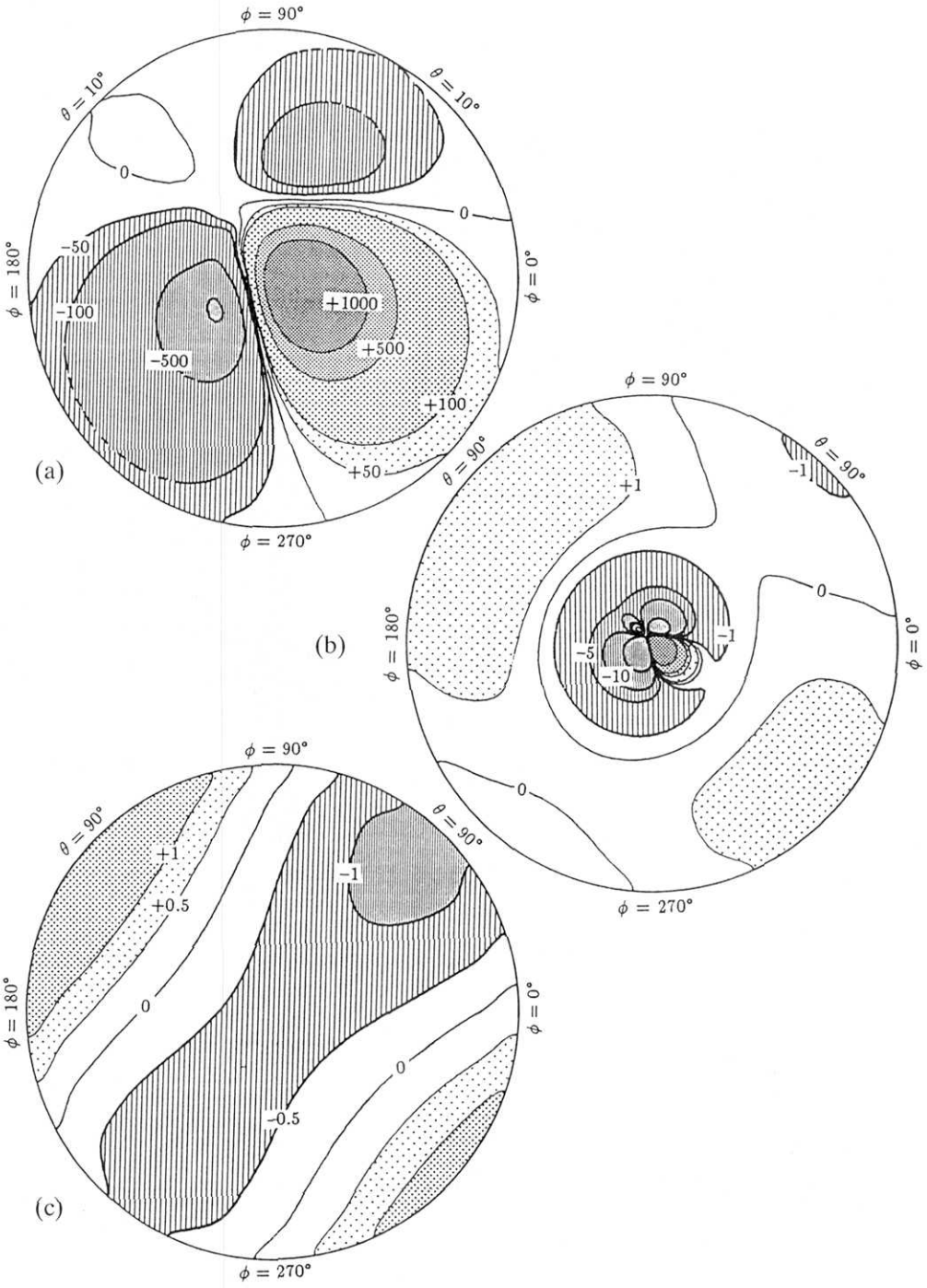

Fig. 6.11 Radial displacements u_r caused by a shear dislocation ($\delta = 50°$, $\lambda = 20°$, $d_s = 400\,km$) in the 1066A earth model. The dislocation is located at the center of the map. The epicentral distance is proportional to the radial distance. The dislocation is $UdS = 2.49 \times 10^{19}\,cm^3$. The units are '*cm*'. (a) The near field ($0° < \theta < 10°$). (b) The upper hemisphere ($0° < \theta < 90°$). (c) The lower hemisphere ($90° \theta < 180°$).

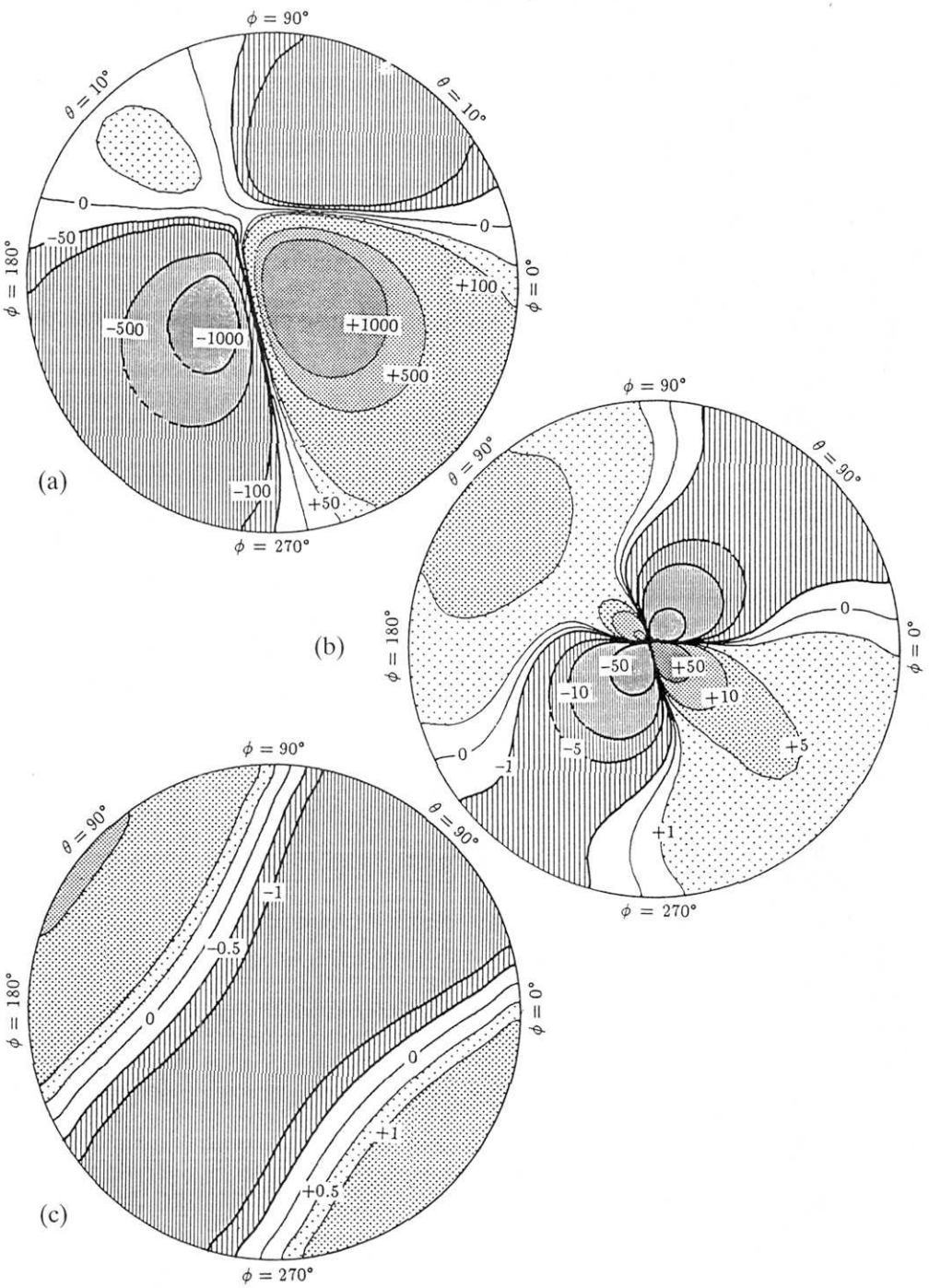

Fig. 6.12 Gravity changes Δg (without the free air correction) caused by a shear dislocation ($\delta = 50°$, $\lambda = 20°$, $d_s = 400\,km$) in the 1066A earth model. The dislocation is located at the center of the map. The epicentral distance is proportional to the radial distance. The dislocation is $UdS = 2.49 \times 10^{19}\,cm^3$. The units are '$\mu gal$'. (a) The near field ($0° < \theta < 10°$). (b) The upper hemisphere ($0° < \theta < 90°$). (c) The lower hemisphere ($90° < \theta < 180°$).

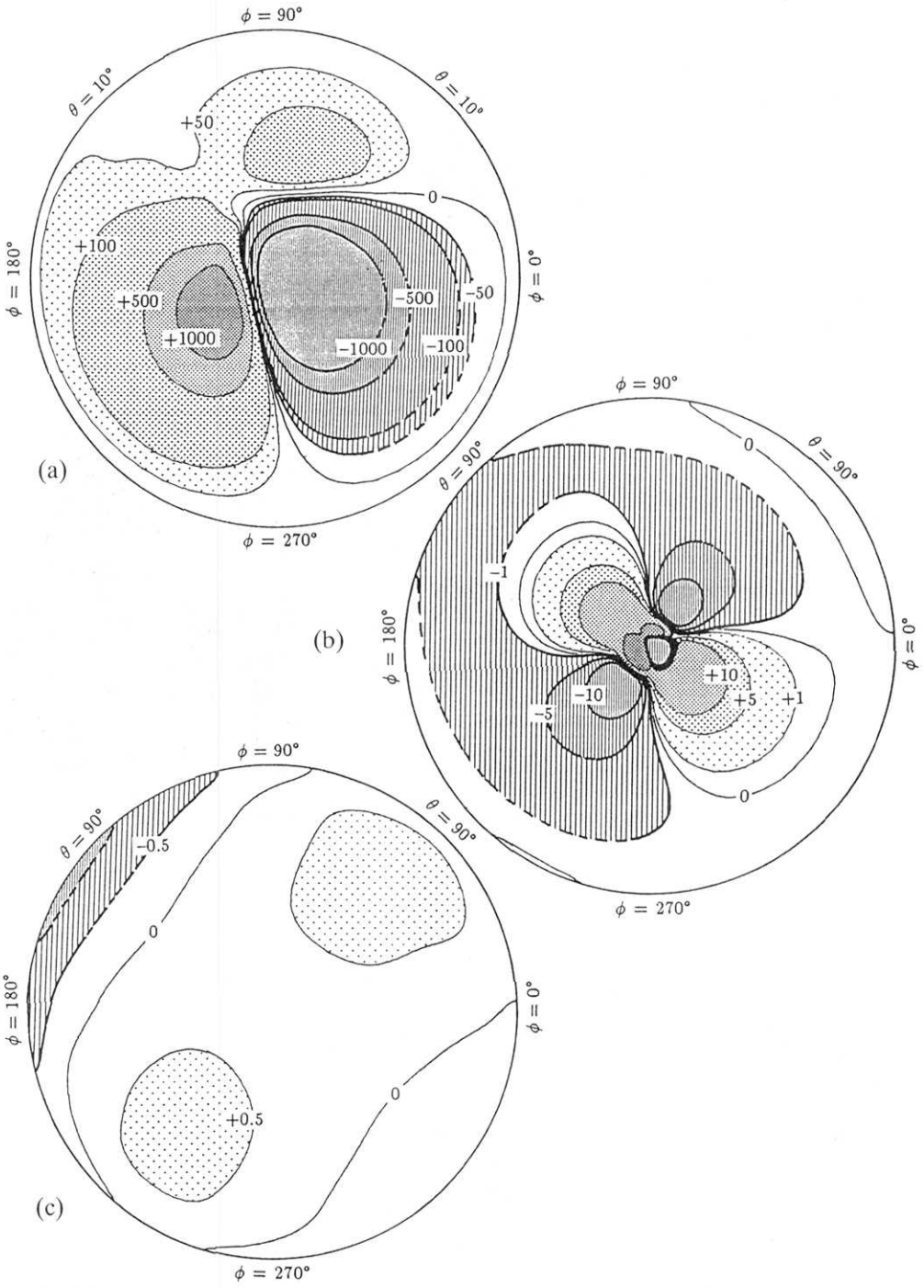

Fig. 6.13 Gravity changes δg (with the free air correction) caused by a shear dislocation ($\delta = 50°$, $\lambda = 20°$, $d_s = 400km$) in the 1066A earth model. The dislocation is located at the center of the map. The epicentral distance is proportional to the radial distance. The dislocation is $UdS = 2.49 \times 10^{19} cm^3$. The units are '$\mu gal$'. (a) The near field ($0° < \theta < 10°$). (b) The upper hemisphere ($0° < \theta < 90°$). (c) The lower hemisphere ($90° < \theta < 180°$).

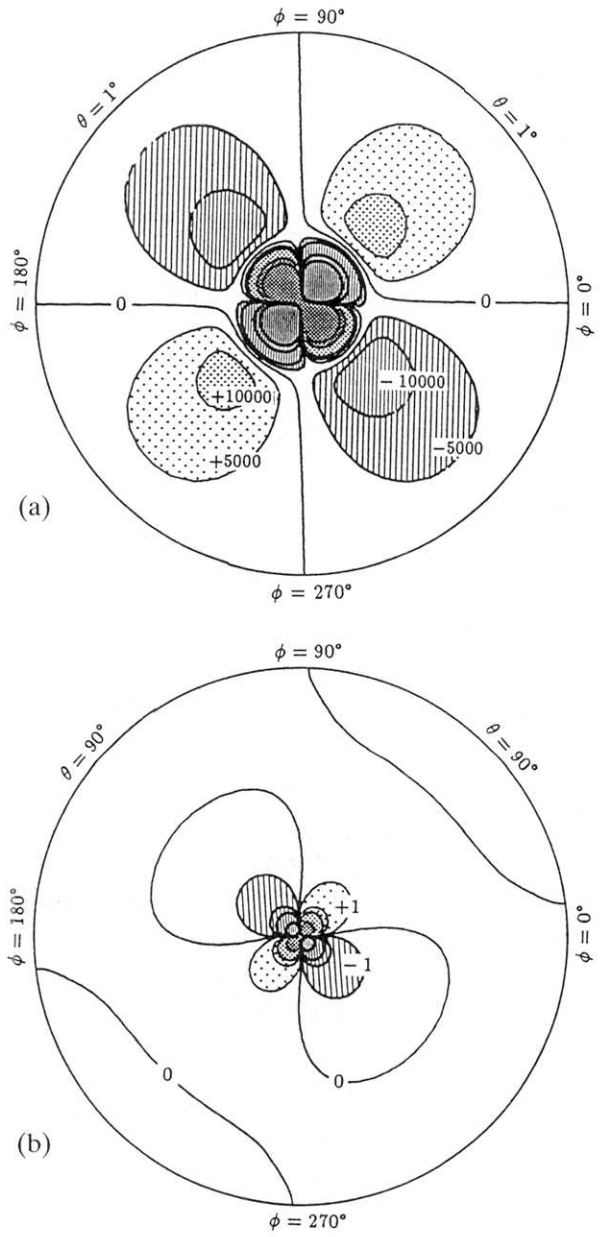

Fig. 6.14 Radial displacements u_r caused by a shear dislocation ($\delta = 75°$, $\lambda = 15°$, $d_s = 5\,km$) in the 1066A earth model. The dislocation is located at the center of the map. The epicentral distance is proportional to the radial distance. The dislocation is $UdS = 2.49 \times 10^{19}\,cm^3$. The units are '*cm*'. (a) The near field ($0° < \theta < 1°$). (b) The upper hemisphere ($0° < \theta < 90°$).

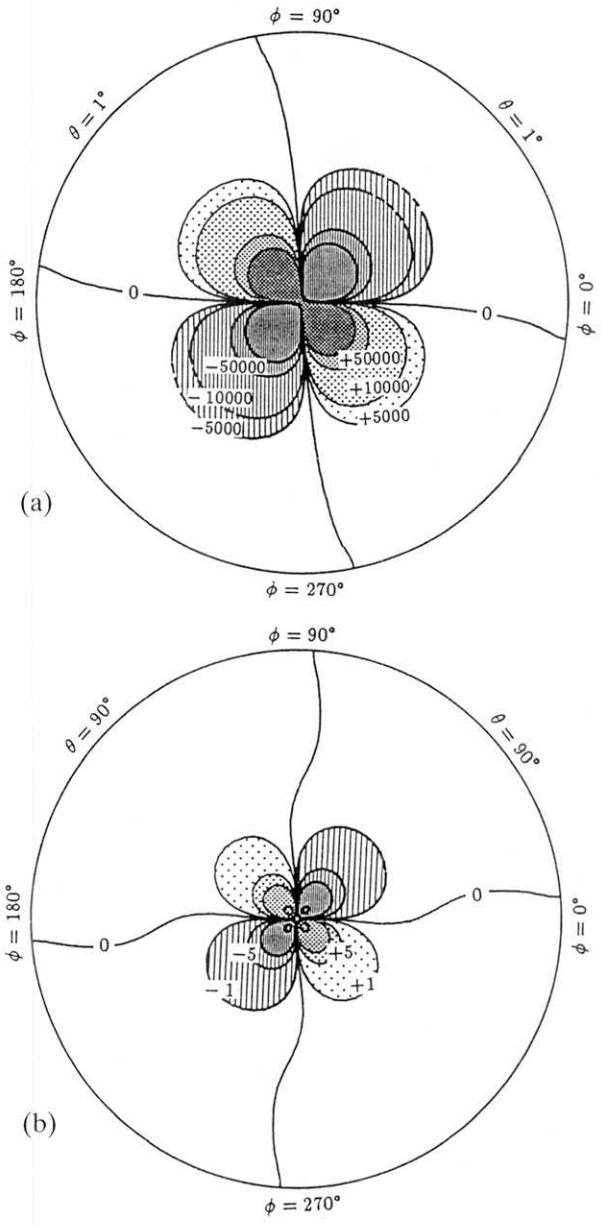

Fig. 6.15 Gravity changes Δg (without the free air correction) caused by a shear dislocation ($\delta = 75°$, $\lambda = 15°$, $d_s = 5\,km$) in the 1066A earth model. The dislocation is located at the center of the map. The epicentral distance is proportional to the radial distance. The dislocation is $UdS = 2.49 \times 10^{19}\,cm^3$. The units are '$\mu gal$'. (a) The near field ($0° < \theta < 1°$). (b) The upper hemisphere ($0° < \theta < 90°$).

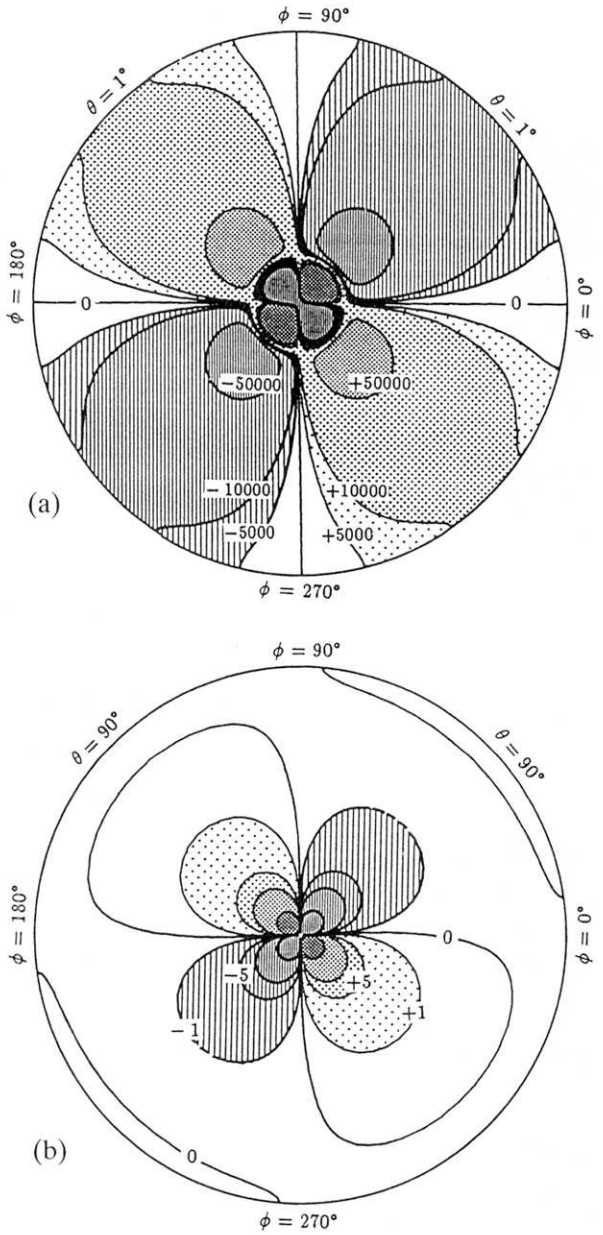

Fig. 6.16 Gravity changes δg (with the free air correction) caused by a shear dislocation ($\delta = 75°$, $\lambda = 15°$, $d_s = 5\,km$) in the 1066A earth model. The dislocation is located at the center of the map. The epicentral distance is proportional to the radial distance. The dislocation is $UdS = 2.49 \times 10^{19}\,cm^3$. The units are '$\mu gal$'. (a) The near field ($0° < \theta < 1°$). (b) The upper hemisphere ($0° < \theta < 90°$).

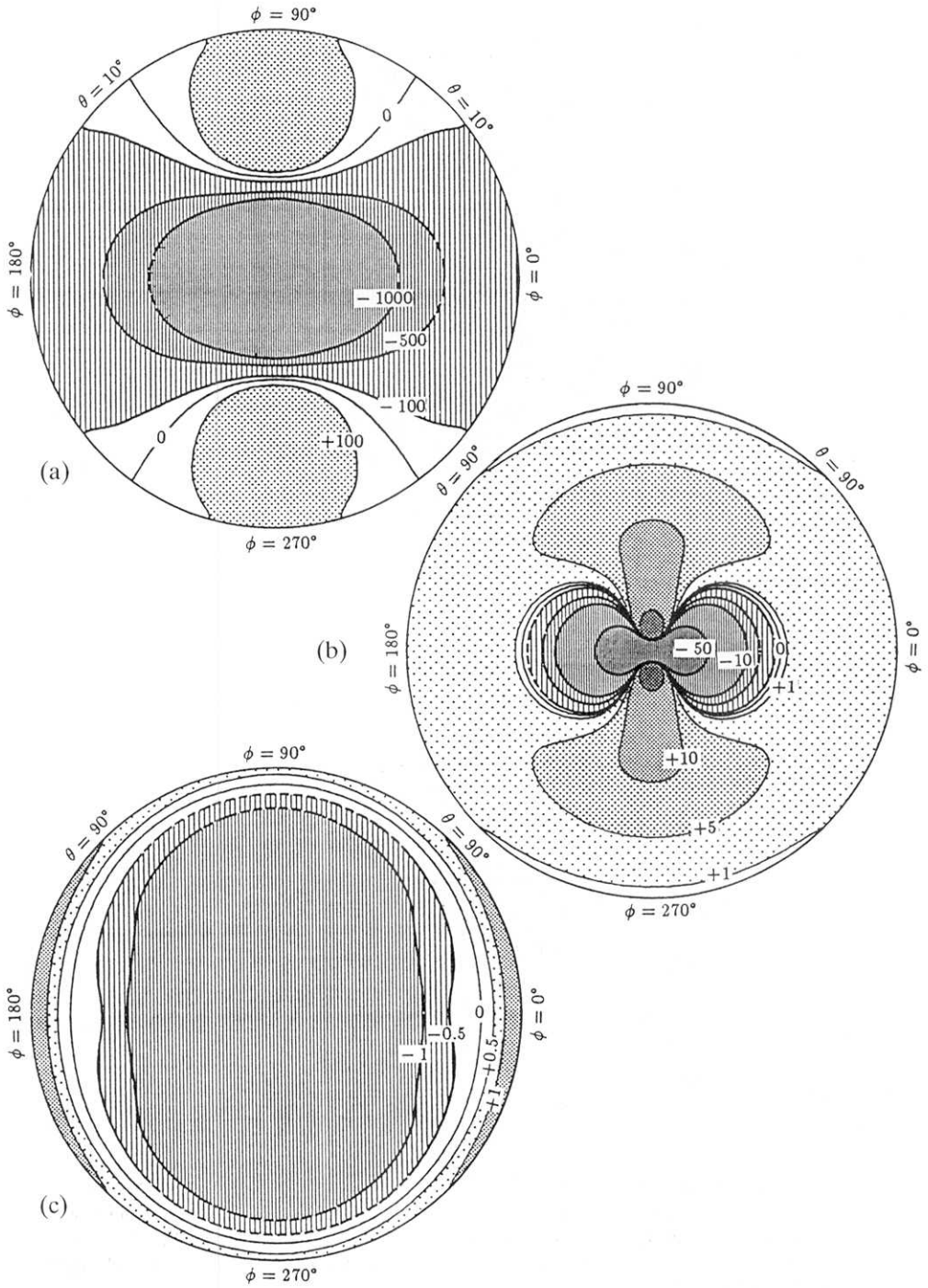

Fig. 6.17 Gravity changes δg (with the free air correction) caused by a tensile dislocation ($\delta = 90°$, $d_s = 100\,km$) in the 1066A earth model. The dislocation is located at the center of the map. The epicentral distance is proportional to the radial distance. The dislocation is $UdS = 2.49 \times 10^{19}\,cm^3$. The units are '$\mu gal$'. (a) The near field ($0° < \theta < 10°$). (b) The upper hemisphere ($0° < \theta < 90°$). (c) The lower hemisphere ($90° < \theta < 180°$).

strike-slip dislocation at a depth of $32\,km$. We observe a slight difference between these results and those for the homogeneous earth model (Figure 6.2(a)), although the distribution patterns and numerical order are essentially the same.

Figure 6.6(c) shows the gravity changes in the near field caused by the same dislocation. Comparing Figures 6.6(c) with 6.2(c), we find that the results for the 1066A model are, as a whole, similar to those for a homogeneous sphere. In some cases, however, the difference between the two becomes very large. For example, the locations of the nodal lines of the gravity change significantly differ between the two models. For a more detailed comparison, we show both results for the homogeneous and 1066A models in Figure 6.7. We know from Fgure 6.7 that the difference between the two models depends on both the epicentral distance and the dislocation types. The above discussions indicate that vertical layering can cause considerable effects on the deformation fields. The distribution pattern and numerical order are basically the same within $0° < \theta < 0.5°$.

We give some results concerning inclined dislocations in Figure 6.8–6.17.

7. Applications and Discussions

In this chapter we extend the theory of point dislocations to that of a finite fault. We then apply it to calculate the gravity changes caused by the 1964 Alaska earthquake ($m_w = 9.2$) and compare the results with the observed gravity changes. Both the calculations and observations show that the gravity changes can reach some hundreds of μgals, which can be easily detected by any modern gravimeter.

We compute the gravity change due to the 1964 Alaska earthquake in the far field. The result indicates that it can cause a significant gravity change, $|\delta g| > 10\mu gal$, within the epicentral distance of $\theta < 6°$, $|\delta g| > 1\mu gal$ within $\theta < 16°$, $|\delta g| > 0.1\mu gal$ within $\theta < 40°$, and $|\delta g| > 0.01\mu gal$ globally. Finally, we calculate and discuss the geoid change caused by the dislocations.

7.1 Calculations for a Finite Fault

When the epicentral distance is much larger than the geometrical size of an earthquake, the point-dislocation theory of the present study can be used immediately. In the case of the near field, however, we may no longer regard the source as being a point dislocation. We must take the distribution of dislocations on a finite fault into account. In the following we discuss how to derive the deformation in the near field from the results concerning point dislocations.

Figure 7.1 shows a seismic fault located at a point $(\theta_1, \lambda_1, d_s)$, with length L, width W, dip angle δ and strike angle z_1. Notice that we take here the upper-left corner of the fault as being the origin for computational convenience.

Theoretically, we may use the following formulas:

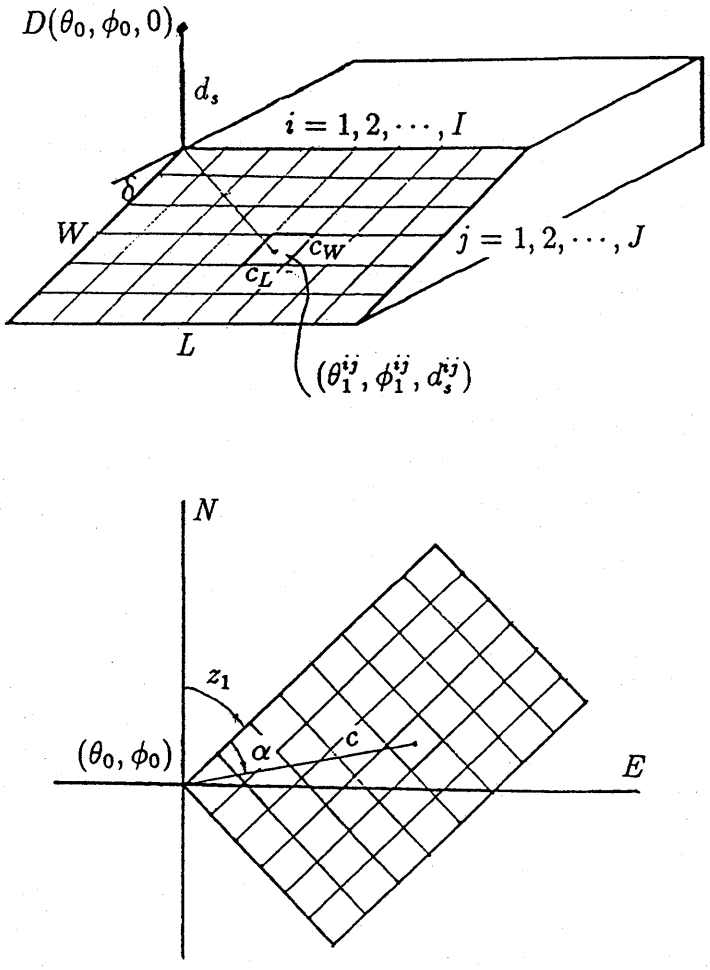

Fig. 7.1 Finite fault model.

$$u_r(a, \theta, \lambda) = \int_S u_r^{ij}(a, \Theta, \Xi; D_s)u_i(r_1, \theta_1, \lambda_1)n_j dS(r_1, \theta_1, \lambda_1), \tag{7.1}$$

$$\psi(a, \theta, \lambda) = \int_S \psi^{ij}(a, \Theta, \Xi; D_s)u_i(r_1, \theta_1, \lambda_1)n_j dS(r_1, \theta_1, \lambda_1), \tag{7.2}$$

$$\Delta g(a, \theta, \lambda) = \int_S \Delta g^{ij}(a, \Theta, \Xi; D_s)u_i(r_1, \theta_1, \lambda_1)n_j dS(r_1, \theta_1, \lambda_1), \tag{7.3}$$

$$\delta g(a, \theta, \lambda) = \int_S \delta g^{ij}(a, \Theta, \Xi; D_s)u_i(r_1, \theta_1, \lambda_1)n_j dS(r_1, \theta_1, \lambda_1), \tag{7.4}$$

where S denotes the fault area, Θ the angular distance between the surface element dS at $(r_1, \theta_1, \lambda_1)$ and the observation station, Ξ the azimuth of the observation point with respect to the fault line, and $D_s = a - r_1$ the source depth of $dS(r_1, \theta_1, \lambda_1)$. The $3 \times 3 = 9$ components of the integral kernels (u_r^{ij},

ψ^{ij}, Δg^{ij} and δg^{ij}) are expressed in terms of the linear combinations of (u_r^T, ψ^T, Δg^T and δg^T) discussed in chapter 4.

Since there are no analytical forms of u_r^{ij}, ψ^{ij}, Δg^{ij} and δg^{ij}, we must perform numerical integration to evaluate (7.1)–(7.4). To do that, we may divide the fault plane into $I \times J$ finite elements with

$$I = \frac{L}{q/k} \tag{7.5}$$

$$J = \frac{W}{q/k}, \tag{7.6}$$

where q is the nearest distance from the calculating point to the fault plane. (7.5) and (7.6) imply that the small elments have a dimension of (q/k); k should be taken larger than 10 in order that the dislocation on a small element can be regarded as being a point source. The side lengths of each elements are

$$C_L = \frac{L}{\mathrm{I}} \tag{7.7}$$

$$C_W = \frac{W}{J}. \tag{7.8}$$

We can obtain the spherical coordinate (θ_1^{ij}, ϕ_1^{ij}, d_s^{ij}) of the center of each element,

$$\theta_1^{ij} = \theta_0 - \frac{c}{a}\cos(z_1 + \alpha), \tag{7.9}$$

$$\phi_1^{ij} = \phi_0 + \frac{c}{a \sin\theta_1^{ij}}\sin(z_1 + \alpha), \tag{7.10}$$

$$D_s^{ij} = d_s + \left(j - \frac{1}{2}\right)C_W \sin\delta \tag{7.11}$$

with

$$c = \left\{\left[\left(i - \frac{1}{2}\right)C_W \cos\delta\right]^2 + \left[\left(j - \frac{1}{2}\right)C_L\right]^2\right\}^{\frac{1}{2}} \tag{7.12}$$

$$\alpha = \tan^{-1}\frac{(i - \frac{1}{2})C_W \cos\delta}{(j - \frac{1}{2})C_L}, \tag{7.13}$$

where $i = 1, 2, \ldots, I$ and $j = 1, 2, \ldots, J$. The angular distance, Θ^{ij}, between the center of dS and the observation point (θ_2, ϕ_2), and the azimuth, z_2^{ij}, of the line connecting the two points with respect to the fault line are given as

$$\cos\Theta^{ij} = \cos\theta_1^{ij}\cos\theta_2 + \sin\theta_1^{ij}\sin\theta_2\cos(\phi_2 - \phi_1^{ij}), \tag{7.14}$$

$$\sin z_2^{ij} = \frac{1}{\sin\varphi^{ij}}\sin\theta_2 \sin(\phi_2 - \phi_1^{ij}), \tag{7.15}$$

and

$$\Xi^{ij} = z_1 - z_2^{ij}. \tag{7.16}$$

Now that we have the arguments (Θ, Ξ, D_s) of each element dS at $(\theta^{ij}, \phi^{ij}, d_s^{ij})$, the integral kernels $(u_r^{ij}, \psi^{ij}, \Delta g^{ij}, \delta g^{ij})$ are derived from the numerical tables (Appendix E) by interpolations. Numerical integrations can be performed to evaluated (7.1)−(7.4).

7.2 Gravity Changes Caused by Alaska Earthquake (1964)

We apply our theory to explain the gravity changes caused by the Alaska earthquake (1964, $m_W = 9.2$). The fault parameters of the earthquake given by SAVAGE and HASTIE (1966) are listed in Table 7.1.

Before and after the earthquake, gravity surveys were made at some stations covering both the uplifted and subsided areas (Figure 7.2). The gravity changes at these stations are also given in Figure 7.2 with contour lines. The gravity changes versus the elevation changes obtained from leveling or shoreline studies near these stations are shown in Figure 7.3 (BARNES, 1966).

Using the fault model given in Table 7.1 we calculated the gravity changes at the 10 stations. The results are shown in both Figure 7.4 and Figure 7.5. We can see that the computed gravity changes are in excellent agreement with the observed ones.

We also considered the far-field gravity change (Figure 7.6). Figure 7.6 shows that $|\delta g| > 10 \mu gal$ within the epicentral distance $\theta < 6°$, $|\delta g| > 1 \mu gal$ within $\theta < 16°$, $|\delta g| > 0.1 \mu gal$ within $\theta < 40°$, and $|\delta g| > 0.01 \mu gal$ globally. This observation is encouraging to detect a gravity step by an absolute gravimeter and a superconducting gravimeter, especially when $\theta < 40°$.

7.3 Geoid Height Change

As an application of the potential change, we estimate the geoid height change due to a large earthquake in this section. We assume a rectangular fault with a barrier buried in the 1066A earth model at a depth of $2\,km$ (see Figure 7.7). The fault has the same size as that of the 1964 Alaska earthquake

Table 7.1. Fault parameters of the 1964 Alaska earthquake (1964, $m_w = 9.2$)

L	Length	$600km$
W	Width	$200km$
d_s	Depth	$20km$
δ	Dip-angle	$9°$
z_1	Strike	$N35°E$
U	Dislocation	$10m$
M_o	Moment	$0.82 \times 10^{30} dyn \cdot cm$

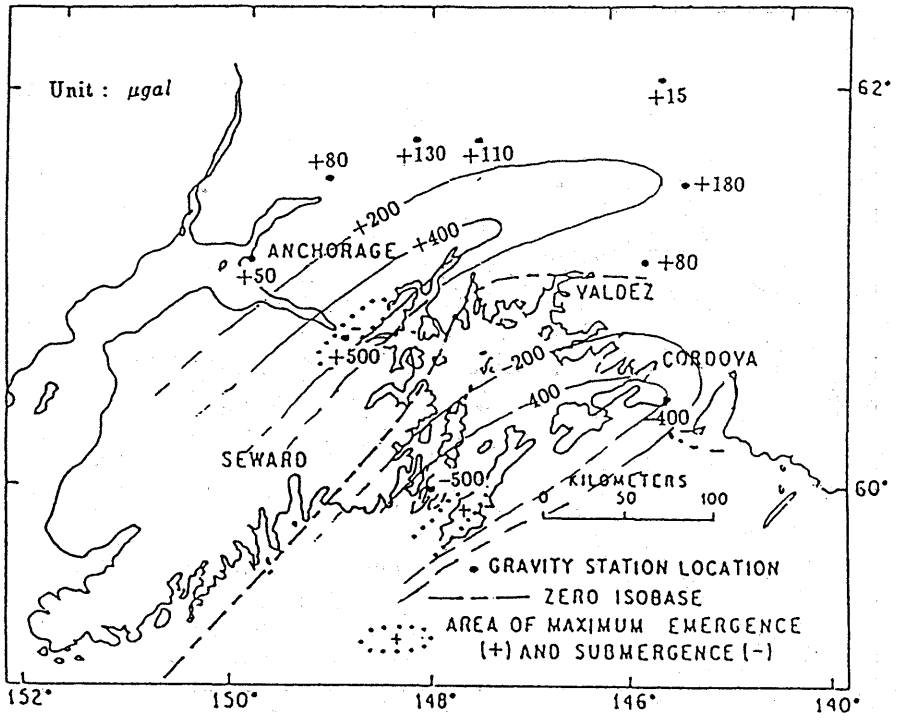

Fig. 7.2 Location of stations and observed gravity changes (after Barnes, 1966)

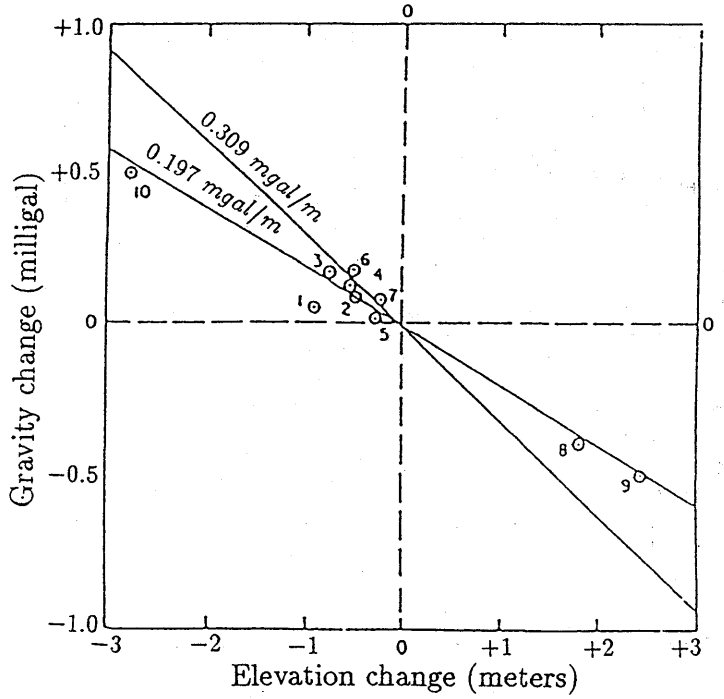

Fig. 7.3 Observed gravity changes versus elevation changes (after Barnes, 1966)

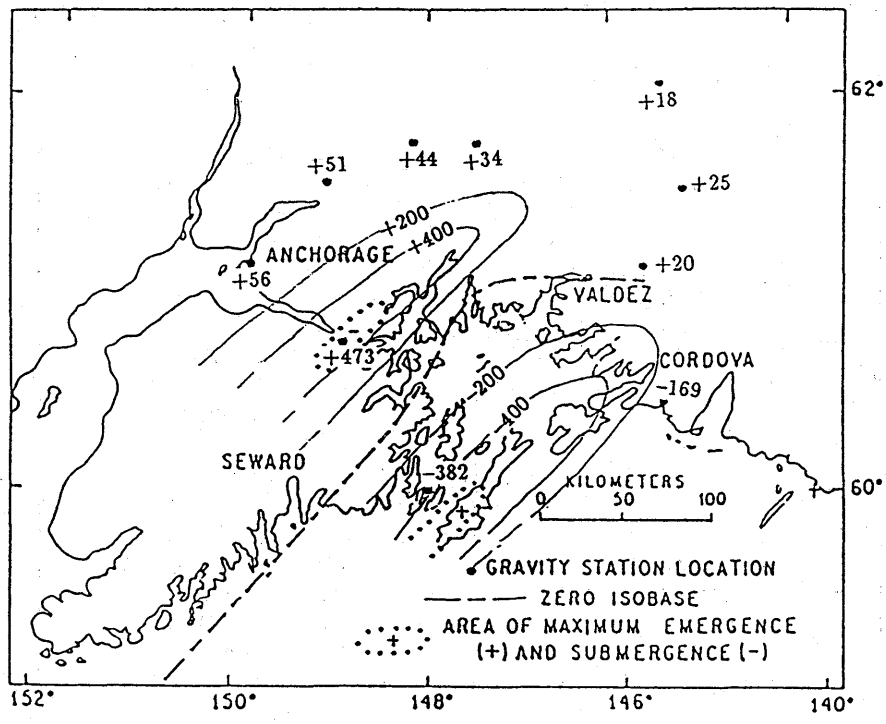

Fig. 7.4 Calculated gravity changes.

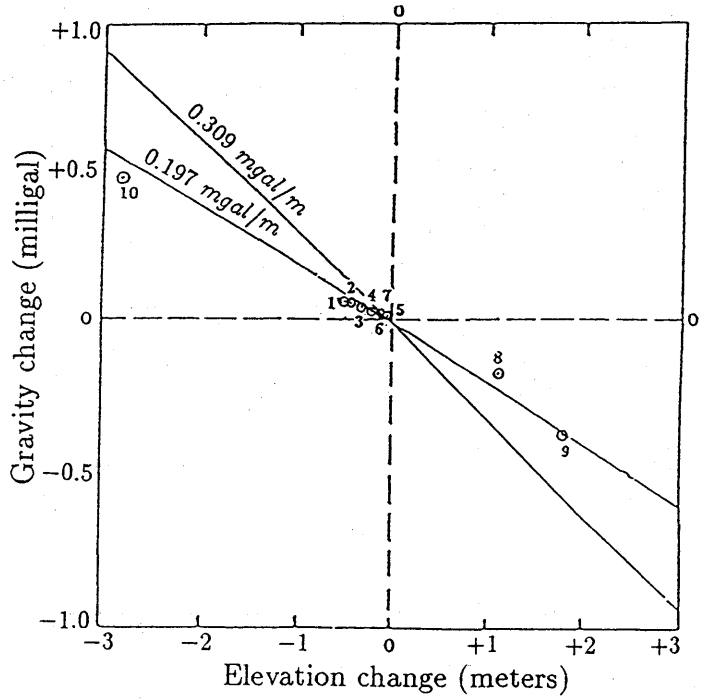

Fig. 7.5 Calculated gravity changes versus elevation changes.

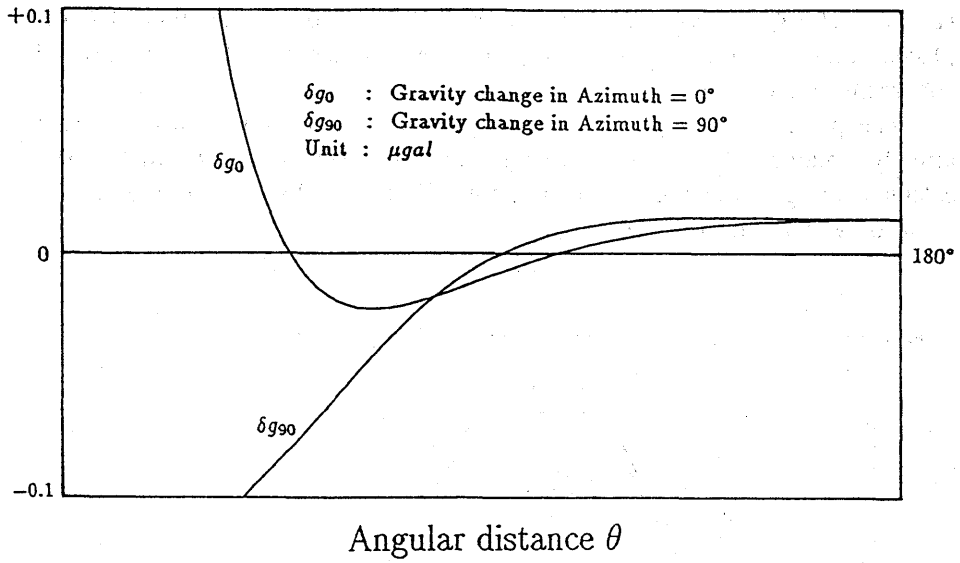

Fig. 7.6 Far-field gravity changes due to the 1964 Alaska earthquake.

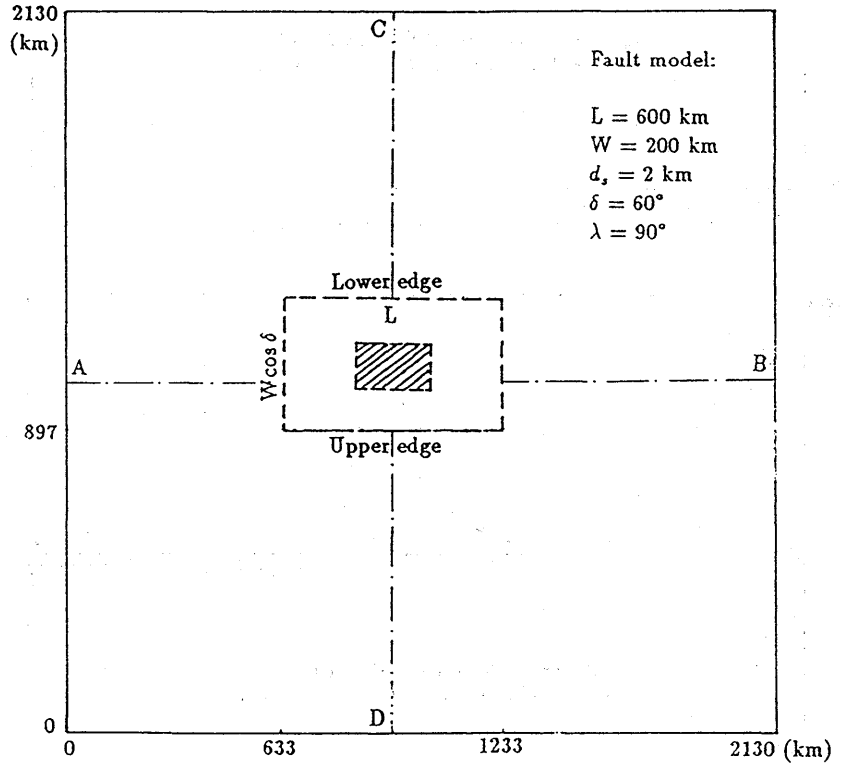

Fig. 7.7 Fault model with a barrier.

($L \times W = 600 \times 200\,km$) with a dislocation of $10\,m$. A barrier of $200 \times 50\,km$ is placed in the center of the fault. The dip angle, δ, and slip angle, λ, are 60° and 90°, respectively.

The principle of the geoid height change is very simple. Since we have already obtained the potential changes due to dislocations, we may easily calculate the geoid change from the potential changes by dividing the gravity value on earth's surface, i.e.

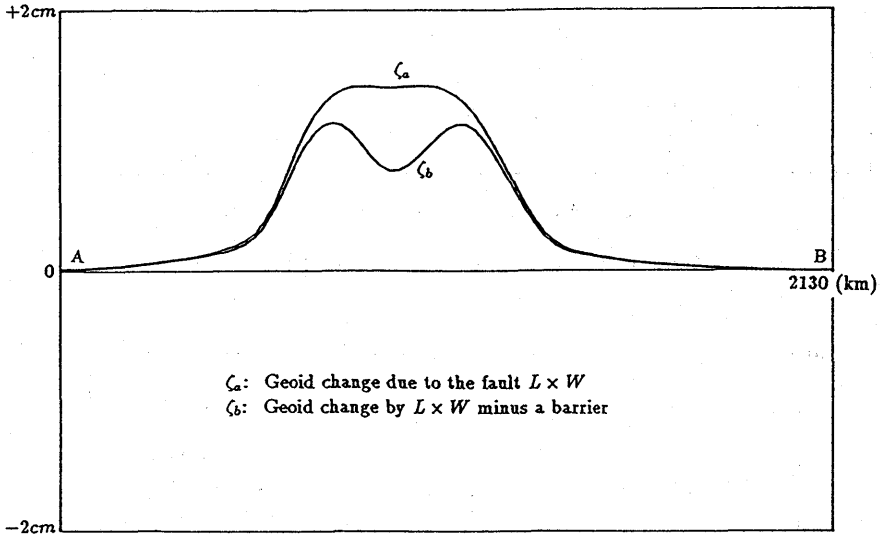

Fig. 7.8 Geoid changes of section A-B.

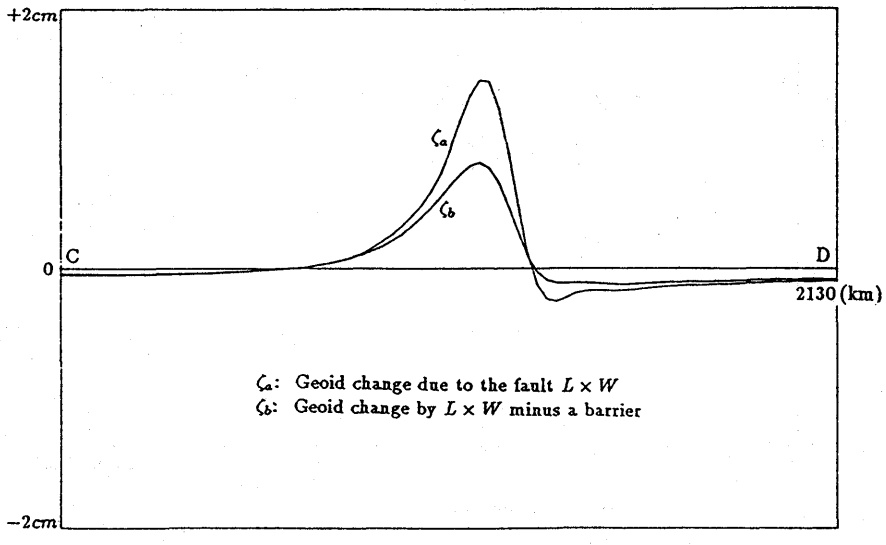

Fig. 7.9 Geoid changes of section C-D.

$$\zeta = \frac{\psi}{g_0}. \tag{7.17}$$

We first estimate the geoid height changes by considering two cases: a change ζ_b caused by the fault with the barrier, and a change ζ_a due to the fault without the barrier. We can then observe the difference between the two.

We calculate ζ_a and ζ_b along two profiles: A−B and C−D (see Figure 7.7). We show the results of ζ_a and ζ_b along the profile A−B in Figure 7.8, and that along C−D in Figure 7.9.

The results show that the geoid height change due to a large earthquake can reach 1.5 *cm*. The barrier in the fault has an evident effect on the geoid height change. We expect to detect such a geoid height change because the precision of satellite altimetry reaches 1 *cm*.

8. Conclusions

This thesis studied the potential and gravity changes caused by dislocations in spherically symmetric earth models. We derived expressions for potential and gravity changes caused by dislocations buried in a spherically symmetric earth model.

We defined dislocation Love numbers to describe the elastic deformation of the earth caused by source functions. We discussed three kinds of typical problems—shear dislocation, tensile dislocation and explosion—which can be expressed by four independent components: a vertical strike-slip, a vertical dip-slip, a dip-slip at a 45° dipping plane, and a vertical tensile opening.

Since a sphere of finite radius cannot remain in static equilibrium under the action of an unbalanced force system, the term of degree 1 requires special treatment. We dealt with this problem by urging that the center of mass of the deformed earth should remain fixed to the space (BEN-MENAHEM and SINGN, 1968; FARRELL, 1972; SAITO, 1974; MERRIAM, 1985 and OKUBO and ENDO, 1986).

Although our formulation is rather simple, we had to overcome several difficulties shown below to obtain numerical results:

1. For computational convenience we normalized all of the equations, boundary conditions, and source functions to dimensionless forms.
2. We showed that truncation of the finite series by $N = 10a/d_s$, gives results that are sufficiently accurate for the present purpose.
3. To accelerate the convergence of series (1) and (2), we multiplied the summand by a disk factor.
4. We transformed the original series into new partial sums so that they alternate in sign. We applied the Euler transformation to the transformed series in order to achieve accelerated convergence.
5. The dislocation Love numbers must be known over a large number of Legendre degree n. The values of the Love numbers, however, vary rapidly with n. In order for the interpolation to work well, we transformed

them into a gently varying series by multiplying a factor proportional to $(a/r_0)^n$.

6. When $d_s < 1km$ or $d_s \to 0$, the truncation degree, N, becomes too large for the truncated series to be calculated in practice. We therefore introduced Okubo's (1988, 1991b) asymptotic solutions in order to overcome this difficulty.

When a point source approaches the earth's surface, the problem apparently becomes singular. We discussed how to obtain the corresponding solutions and how to speed up the summations of harmonic solutions. We found that the source functions and solutions for a vertical strike-slip at the earth's surface have the same forms as that within the earth; the solutions can obtained in the same way as that of the latter. In the case of a dip-slip, we found that its solution can be simply obtained by summing the source functions without any integration. While the solution in this case makes no contribution to the vertical displacement, the potential and gravity changes, except for the tangential displacement. For a 45° dip-slip we proved that the general solution needs not include the part of the source functions, since the sum of the source functions vanishes on the earth's surface.

We carried out calculations for both homogeneous and radially heterogeneous earth models. We started our calculations with a homogeneous earth model corresponding to the top values of the 1066A earth model. Numerical integrations were carried out by using the Runge-Kutta method. For depths of 0, 2, 5, 10, 20, 32, 64, 100, 200, 300, 400, 637 km, we obtained the dislocation Love numbers. We then use the dislocation Love numbers to calculate the corresponding deformation fields. The calculated gravity changes agree well with the previous results derived based on the assumption of a homogeneous flat earth, particularly in the near field within 1°, or 111 km. The agreement confirms that our theory is consistent with the flat-earth theory (OKUBO, 1991). The discrepancy between the two theories was found to be no larger than 10% within the epicentral distance $\theta \approx 10°$. The difference becomes larger in the area $\theta > 10°$, where the effect of the curvature becomes evident.

We proceeded to calculations of the radially heterogeneous 1066A earth model. The results are, as a whole, similar to those for a homogeneous sphere. In some cases, however, the difference between the two becomes very large. For example, the locations of the nodal lines of the gravity change significantly differ between the two models, indicating that the vertical layering has considerable effects on the deformation fields.

The most important results of this study are the radial displacement, potential and gravity changes tabulated in Appendix E. These results enable us to compute the potential and gravity changes at any place on the surface due to an arbitrary point dislocation in an SNREI earth.

If we integrate the contributions from point dislocations distributed over a finite plane, we can more accurately estimate the gravity change caused by an earthquake. This was done by the following procedure: (1) divide the finite

fault into small elements; (2) evaluate the contribution of each element by referring to the numerical tables (Appendix E); and (3) add all of the contributions over the finite plane.

We used this scheme to estimate the gravity changes caused by the 1964 Alaska earthquake ($m_W = 9.2$), taking the finiteness of the fault area into account. We obtained good agreement between the observed gravity change around the fault and the computed one. We also computed the gravity change in the far field. The result is surprising in that the 1964 Alaska earthquake could cause a significant gravity change $|\delta g| > 10 \mu gal$ within the epicentral distance $\theta < 6°$, $|\delta g| > 1 \mu gal$ within $\theta < 16°$, $|\delta g| > 0.1 \mu gal$ within $\theta < 40°$, and $|\delta g| > 0.001 \mu gal$ globally.

The following are the conclusions of this thesis:

1. We successded in calculating the potential and gravity changes due to dislocations in the SNREI earth model.
2. The gravity change reveals a spatial pattern characteristic of the dislocation types. For example, the gravity change for a vertical strike-slip dislocation shows a four-quadrant pattern.
3. The result of a homogeneous sphere agrees well with that of a flat earth. The difference between the two is smaller than 10% within an epicentral distance of 10°.
4. The results for the radially heterogeneous 1066A model are, as a whole, similar to those for a homogeneous sphere. The difference, however, between the two indicates that the vertical layering can cause considerable effects on the deformation fields.
5. We show that the present theory can be applied to explain the observed coseismic gravity changes which took place during the 1964 Alaska earthquake.
6. The gravity change caused by a large earthquake is sufficiently large, even in the far field, to be detected by using appropriate instruments, such as a superconducting gravimeter.

This paper is a thesis submitted to the Faculty of the Graduate School of the University of Tokyo in partial fulfillment of the requirements for the degree of Doctor of Science.

Acknowledgements

I gratefully acknowledge the help and guidance of a number of people who contributed to this work. First and foremost are my former and present supervisors: Professor Emeritus Y. Hagiwara and Professor I. Murata, whose advice and support throughout really made this thesis possible. I thank them for giving me a great opportunity to study at the University of Tokyo and for their continuous encouragement, valuable suggestions and critical review throughout my work on this thesis.

I also wish to specially thank Dr. S. Okubo for many intellectual and invaluable suggestions and discussions which significantly helped me to improve the content and orientation of this work. His help and encouragement has left me greatly in his debt. Without his support, this thesis might not have been possible.

I also benefited from discussions with Dr. K. Nagasawa and Dr. M. Yanagisawa over the years. I thank them for their continuous encouragement and comments concerning this thesis and their help in many aspects. A critical review by Professor K. Abe was quite helpful. Many thanks are also given to the referees for their valuable comments concerning this thesis.

I used the HITAC M-680H computer system at the Earthquake Research Institute of the University of Tokyo. This research was partially supported by a Japanese Government Scholarship.

Finally, I thank my parents and my wife. My parents have been supported by my daughter for us during these many years. My wife, Shi Ping, helped me greatly in both my studies and life, even though she has been studying for her Master degree.

Appendix A
Infinite Sums of Legendre Functions

We begin with the generating function of Legendre's polynomials,

$$F(r,\ \theta) \equiv \sum_{n=0}^{\infty} r^n P_n(\cos\theta) = \frac{1}{\sqrt{1 - 2r\cos\theta + r^2}}. \qquad (A.1)$$

Integrating $(A.1)$ with respect to r gives the following desired formulas:

$$\int_0^t \frac{F(r,\ \theta) - 1}{r} dr = \sum_{n=1}^{\infty} \frac{1}{n} t^n P_n(\cos\theta)$$
$$= -\ln(1 - t\cos\theta + \sqrt{1 - 2t\cos\theta + t^2}) + \ln 2, \qquad (A.2)$$

$$\int_0^t ds \int_0^s \frac{F(r,\ \theta) - 1}{r} dr = \sum_{n=1}^{\infty} \frac{1}{n(n+1)} t^{n+1} P_n(\cos\theta)$$
$$= -t\ln(1 - t\cos\theta + \sqrt{1 - 2t\cos\theta + t^2})$$
$$- \ln(t - \cos\theta + \sqrt{1 - 2t\cos\theta + t^2})$$
$$+ \ln(1 - \cos\theta) + t\ln 2, \qquad (A.3)$$

$$\int_0^t ds \int_0^s dx \int_0^x \frac{F(r,\ \theta) - r\cos\theta - 1}{r^2} dr$$
$$= \sum_{n=2}^{\infty} \frac{1}{n(n^2 - 1)} t^{n+1} P_n(\cos\theta)$$
$$= \left(1 - \frac{1}{2}t\cos\theta\right) t\ln(1 - t\cos\theta$$
$$+ \sqrt{1 - 2t\cos\theta + t^2})$$
$$- t + \frac{1}{2}\ln(t - \cos\theta + \sqrt{1 - 2t\cos\theta + t^2})$$
$$- \frac{1}{2}\ln(1 - \cos\theta) + t(1 - \ln 2) + \frac{1}{2}t^2\cos\theta\ln 2$$
$$- \frac{1}{2}t\sqrt{1 - 2t\cos\theta + t^2} + \frac{1}{4}t^2\cos\theta. \qquad (A.4)$$

Differentiations of $(A.1)$ gives

$$\sum_{n=0}^{\infty} n t^{n-1} P_n(\cos\theta) = \frac{1}{(1 - 2t\cos\theta + t^2)^{\frac{3}{2}}}(\cos\theta - t). \qquad (A.5)$$

In the same way, we obtain the following formulas after some manipulations:

$$\sum_{n=0}^{\infty} n^2 t^{n-1} P_n(\cos\theta) = \frac{1}{(1 - 2t\cos\theta + t^2)^{\frac{5}{2}}}[(1 - t^2)\cos\theta$$
$$+ t(\cos^2\theta - 2 + t^2)], \qquad (A.6)$$

$$\sum_{n=0}^{\infty} n^3 t^{n-1} P_n(\cos\theta) = \frac{1}{(1 - 2t\cos\theta + t^2)^{\frac{7}{2}}}[-t^5 - t^4\cos\theta + t^3(10 - 2\cos^2\theta + t^2\cos\theta(\cos^2\theta - 9) + t(5\cos^2\theta - 4) + \cos\theta], \quad \text{(A.7)}$$

$$\sum_{n=0}^{\infty} n^4 t^{n-1} P_n(\cos\theta) = \frac{1}{(1 - 2t\cos\theta + t^2)^{\frac{9}{2}}}[t^7 + 7t^6\cos\theta + t^5(9\cos^2\theta - 36) + t^4\cos\theta(21 - 2\cos^2\theta) + t^3(\cos^4\theta - 42\cos^2\theta + 60) + t^2\cos\theta(18\cos^2\theta - 45) + t(15\cos^2\theta - 8) + \cos\theta], \quad \text{(A.8)}$$

$$\sum_{n=0}^{\infty} (n + 1) t^{n-1} P_n(\cos\theta) = \frac{1 - t\cos\theta}{t(1 - 2t\cos\theta + t^2)^{\frac{3}{2}}}, \quad \text{(A.9)}$$

$$\sum_{n=0}^{\infty} n(n + 1) t^{n-1} P_n(\cos\theta) = \frac{1}{(1 - 2t\cos\theta + t^2)^{\frac{5}{2}}}[2\cos\theta - t(3 + \cos^2\theta - 2t\cos\theta], \quad \text{(A.10)}$$

$$\sum_{n=0}^{\infty} \frac{1}{n - 1} t^{n-1} P_n(\cos\theta) = \frac{1}{t}\sqrt{1 - 2t\cos\theta + t^2} - \cos\theta \ln(1 - t\cos\theta + \sqrt{1 - 2t\cos\theta + t^2}) - \cos\theta(1 - \ln 2), \quad \text{(A.11)}$$

$$\sum_{n=0}^{\infty} \frac{1}{n + 1} t^{n+1} P_n(\cos\theta) = \ln(t - \cos\theta + \sqrt{1 - 2t\cos\theta + t^2}) - \ln(1 - \cos\theta), \quad \text{(A.12)}$$

$$\sum_{n=2}^{\infty} \frac{n}{n - 1} t^{n-1} P_n(\cos\theta) = -\frac{1}{t} - \cos\theta[2 - \ln 2 + \ln(1 - t\cos\theta + \sqrt{1 - 2t\cos\theta + t^2})] + \frac{2 + t(t - 2\cos\theta)}{t\sqrt{1 - 2t\cos\theta + t^2}}, \quad \text{(A.13)}$$

$$\sum_{n=0}^{\infty} t^n \frac{\partial P_n(\cos\theta)}{\partial\theta} = -\frac{t\sin\theta}{(1 - 2t\cos\theta + t^2)^{\frac{3}{2}}}, \quad \text{(A.14)}$$

$$\sum_{n=0}^{\infty} n t^{n-1} \frac{\partial P_n(\cos\theta)}{\partial\theta} = -\frac{\sin\theta(1 + t\cos\theta - 2t^2)}{(1 - 2t\cos\theta + t^2)^{\frac{5}{2}}}, \quad \text{(A.15)}$$

$$\sum_{n=0}^{\infty} n^2 t^{n-1} \frac{\partial P_n(\cos\theta)}{\partial\theta} = -\frac{\sin\theta}{(1 - 2t\cos\theta + t^2)^{\frac{7}{2}}}[1 + 5t\cos\theta + t^2(\cos^2\theta - 10) - t^3\cos\theta + 4t^4], \quad \text{(A.16)}$$

$$\sum_{n=1}^{\infty} \frac{1}{n} t^n \frac{\partial P_n(\cos\theta)}{\partial\theta} = -\frac{\cos\theta}{\sin\theta} - \frac{t - \cos\theta}{\sin\theta\sqrt{1 - 2t\cos\theta + t^2}}, \quad \text{(A.17)}$$

$$\sum_{n=1}^{\infty}\frac{1}{n(n+1)}t^{n+1}\frac{\partial P_n(\cos\theta)}{\partial\theta}=\frac{1}{\sin\theta}(1-t\cos\theta-\sqrt{1-2t\cos\theta+t^2}),\tag{A.18}$$

$$\sum_{n=2}^{\infty}\frac{1}{n(n^2-1)}t^{n+1}\frac{\partial P_n(\cos\theta)}{\partial\theta}=\frac{1}{2\sin\theta}[t\cos\theta(2-t\cos\theta)-1]+\frac{1}{2\sin\theta\sqrt{1-2t\cos\theta+t^2}}[1+2t^2+t\cos\theta(t\cos\theta-3-t^2)]+\frac{1}{2}t^2\sin\theta\cdot\left[\ln\frac{1}{2}\left(1-t\cos\theta+\sqrt{1-2t\cos\theta+t^2}\right)-\frac{1}{\sqrt{1-2t\cos\theta+t^2}}-\frac{1}{2}\right],\tag{A.19}$$

$$\sum_{n=2}^{\infty}\frac{1}{n-1}t^{n-1}\frac{\partial P_n(\cos\theta)}{\partial\theta}=\frac{1-t\cos\theta}{\sin\theta\sqrt{1-2t\cos\theta+t^2}}+\sin\theta\ln(1-t\cos\theta+\sqrt{1-2t\cos\theta+t^2})-\frac{\cos^2\theta}{\sin\theta}+\sin\theta(1-\ln 2),\tag{A.20}$$

$$\sum_{n=0}^{\infty}\frac{1}{n+1}t^{n+1}\frac{\partial P_n(\cos\theta)}{\partial\theta}=-\frac{1}{\sin\theta}+\frac{1-t\cos\theta}{\sin\theta\sqrt{1-2t\cos\theta+t^2}},\tag{A.21}$$

$$\sum_{n=2}^{\infty}t^{n-1}P_n^2(\cos\theta)=\frac{3t\sin^2\theta}{(1-2t\cos\theta+t^2)^{\frac{5}{2}}},\tag{A.22}$$

$$\sum_{n=2}^{\infty}\frac{1}{n}t^{n-1}P_n^2(\cos\theta)=\frac{1}{t}\left[\frac{2}{\sin^2\theta}-1-\frac{1-t\cos\theta}{(1-2\cos^2\theta+t^2)^{\frac{3}{2}}}+\frac{2\cos\theta(t-\cos\theta)}{\sin^2\theta\sqrt{1-2\cos^2\theta+t^2}}\right],\tag{A.23}$$

$$\sum_{n=2}^{\infty}\frac{1}{n(n+1)}t^{n-1}P_n^2(\cos\theta)=\frac{1}{t}\left[1-\frac{1}{\sqrt{1-2t\cos\theta+t^2}}-\frac{2\cos\theta}{t\sin^2\theta}(1-t\cos\theta-\sqrt{1-2t\cos\theta+t^2})\right],\tag{A.24}$$

$$\sum_{n=2}^{\infty}\frac{1}{n(n^2-1)}t^{n-1}P_n^2(\cos\theta)=\frac{1}{2}\cos\theta+\frac{\cos\theta}{t^2\sin^2\theta}(1-2t\cos\theta+t^2)-\frac{1}{t^2\sin^2\theta\sqrt{1-2t\cos\theta+t^2}}\cdot[\cos\theta+t^3(1-2\cos^2\theta)+t(1-t\cos\theta)(1-4\cos^2\theta)],\tag{A.25}$$

$$\sum_{n=2}^{\infty}\frac{1}{n+1}t^{n-1}P_n^2(\cos\theta) = -\frac{2\cos\theta}{t^2\sin^2\theta}\left(-1+\frac{1-t\cos\theta}{\sqrt{1-2t\cos\theta+t^2}}\right) - \frac{\cos\theta - t}{(1-2\cos^2\theta+t^2)^{\frac{3}{2}}}, \tag{A.26}$$

$$\sum_{n=2}^{\infty}\frac{1}{n-1}t^{n-1}P_n^2(\cos\theta) = \cos\theta\left(1+\frac{2}{\sin^2\theta}\right) + \frac{2}{t}(1-\sqrt{1-2t\cos\theta+t^2}) + \frac{t-\cos\theta}{(1-2\cos^2\theta+t^2)^{\frac{3}{2}}} - \frac{2}{\sqrt{1-2\cos^2\theta+t^2}} \cdot\left[\frac{1}{t}+\frac{\cos\theta}{\sin^2\theta}(1-t\cos\theta)\right], \tag{A.27}$$

$$\sum_{n=2}^{\infty}\frac{1}{n^2-1}t^{n-1}P_n^2(\cos\theta) = \frac{1}{2t^2\sin^2\theta}[2(t\sin^2\theta-\cos\theta) + t^2\cos\theta(2+\sin^2\theta)] - \sqrt{1-2t\cos\theta+t^2} + \frac{1}{t^2\sin^2\theta\sqrt{1-2t\cos\theta+t^2}} \cdot(\cos\theta - t - t^2\cos\theta + t^3\cos^2\theta). \tag{A.28}$$

When $t \to 1$, we obtain the following useful formulas, i.e. sums of certain series of spherical functions:

$$\sum_{n=0}^{\infty}P_n(\cos\theta) = \frac{1}{2\sin\frac{\theta}{2}}, \tag{A.29}$$

$$\sum_{n=0}^{\infty}nP_n(\cos\theta) = -\frac{1}{4\sin\frac{\theta}{2}}, \tag{A.30}$$

$$\sum_{n=0}^{\infty}\frac{1}{n}P_n(\cos\theta) = -\ln\left(\sin\frac{\theta}{2}+\sin^2\frac{\theta}{2}\right), \tag{A.31}$$

$$\sum_{n=1}^{\infty}\frac{1}{n+1}P_n(\cos\theta) = -1+\ln\frac{1+\sin\frac{\theta}{2}}{\sin\frac{\theta}{2}}, \tag{A.32}$$

$$\sum_{n=1}^{\infty}\frac{1}{n(n+1)}P_n(\cos\theta) = 1-2\ln\left(1+\sin\frac{\theta}{2}\right), \tag{A.33}$$

$$\sum_{n=1}^{\infty}\frac{\partial P_n(\cos\theta)}{\partial\theta} = -\frac{\cos\frac{\theta}{2}}{4\sin^2\frac{\theta}{2}}, \tag{A.34}$$

$$\sum_{n=1}^{\infty}\frac{1}{n}\frac{\partial P_n(\cos\theta)}{\partial\theta} = -\frac{\cos\frac{\theta}{2}(1+2\sin\frac{\theta}{2})}{2\sin\frac{\theta}{2}(1+\sin\frac{\theta}{2})}, \tag{A.35}$$

$$\sum_{n=1}^{\infty}\frac{1}{n(n+1)}\frac{\partial P_n(\cos\theta)}{\partial\theta} = -\frac{\cos\frac{\theta}{2}}{1+\sin\frac{\theta}{2}}, \tag{A.36}$$

$$\sum_{n=1}^{\infty}\frac{2n+1}{n(n+1)}P_n^1(\cos\theta)=\frac{\cos\frac{\theta}{2}}{\sin\frac{\theta}{2}}, \tag{A.37}$$

$$\sum_{n=1}^{\infty}\frac{2n+1}{n(n+1)}\frac{\partial P_n^1(\cos\theta)}{\partial\theta}=-\frac{1+\sin\frac{\theta}{2}+\sin^2\frac{\theta}{2}}{2\sin^2\frac{\theta}{2}(1+\sin\frac{\theta}{2})}, \tag{A.38}$$

$$\sum_{n=2}^{\infty}\frac{1}{n}P_n^2(\cos\theta)=\frac{(1-\sin\frac{\theta}{2})(4\sin^2\frac{\theta}{2}+5\sin\frac{\theta}{2}+2)}{4\sin^2\frac{\theta}{2}(1+\sin\frac{\theta}{2})}, \tag{A.39}$$

$$\sum_{n=2}^{\infty}\frac{1}{n(n+1)}P_n^2(\cos\theta)=\frac{(1-\sin\frac{\theta}{2})(1+2\sin\frac{\theta}{2})}{2\sin\frac{\theta}{2}(1+\sin\frac{\theta}{2})}, \tag{A.40}$$

$$\begin{aligned}\sum_{n=2}^{\infty}\frac{1}{n(n^2-1)}P_n^2(\cos\theta)=&-\cot\theta\Big[-\cos\frac{\theta}{2}+\frac{\cos\frac{\theta}{2}(1+\sin^2\frac{\theta}{2})}{1+\sin\frac{\theta}{2}}\\&+2\sin\frac{\theta}{2}\cos\frac{\theta}{2}\ln\Big(\sin\frac{\theta}{2}+\sin^2\frac{\theta}{2}\Big)\Big]\\&-\Big[-2\sin\frac{\theta}{2}+1-\cos\theta\\&-\cos\theta\ln\Big(\sin\frac{\theta}{2}+\sin^2\frac{\theta}{2}\Big)\Big],\end{aligned} \tag{A.41}$$

$$\sum_{n=2}^{\infty}\frac{1}{n(n+1)}\frac{\partial P_n^2(\cos\theta)}{\partial\theta}=-\frac{\cos\frac{\theta}{2}(3\sin^2\frac{\theta}{2}+2\sin\frac{\theta}{2}+1)}{4\sin\frac{\theta}{2}(1+\sin^2\frac{\theta}{2})}, \tag{A.42}$$

$$\begin{aligned}\sum_{n=2}^{\infty}\frac{1}{n(n^2-1)}\frac{\partial P_n^2(\cos\theta)}{\partial\theta}=&\frac{\cos\frac{\theta}{2}\sin\frac{\theta}{2}}{\sin^2\theta}\Big[-\frac{1-\sin\frac{\theta}{2}}{1+\sin\frac{\theta}{2}}\\&+2\ln\Big(\sin\frac{\theta}{2}+\sin^2\frac{\theta}{2}\Big)\Big]\\&-\cot\theta\Big[\frac{1}{(1+\sin^2\frac{\theta}{2})}\Big(\sin^2\frac{\theta}{2}\Big(1-\sin^2\frac{\theta}{2}\Big)\\&+2\cos^2\frac{\theta}{2}\Big(1+\sin\frac{\theta}{2}\Big)\Big(1+3\sin\frac{\theta}{2}\Big)\\&-\cos^2\frac{\theta}{2}\Big(1+\sin^2\frac{\theta}{2}\Big)\Big)\\&+\Big(\cos^2\frac{\theta}{2}-\sin^2\frac{\theta}{2}\Big)\ln\Big(\sin\frac{\theta}{2}+\sin^2\frac{\theta}{2}\Big)\Big]\\&+\cos\frac{\theta}{2}-\sin\theta\Big(1+\ln\Big(\sin\frac{\theta}{2}+\sin^2\frac{\theta}{2}\Big)\Big)\\&+\frac{\cos\theta\cos\frac{\theta}{2}(1+2\sin\frac{\theta}{2})}{2\sin\frac{\theta}{2}(1+\sin\frac{\theta}{2})}.\end{aligned} \tag{A.43}$$

Appendix B
Asymptotic Solutions

OKUBO (1988) proposed asymptotic solutions for all six sets of independent solutions of the spheroidal deformations of the earth. Recently, he (OKUBO, 1991b) found that the deformation on the surface ($r = a$) caused by dislocations can be simply expressed by the tide, load and shear solutions at the source depth, d_s. The following are Okubo's asymptotic solutions. For convenience in our present study, we transformed the asymptotic solutions into asymptotic dislocation Love numbers. Below, $h_n^d(T, m)$, $l_n^d(T, m)$, and $k_n^d(T, \mathrm{m})$ denote the four types of asymptotic dislocation Love numbers on the surface of the earth, corresponding to a vertical strike-slip, a vertical dip-slip, a 45° dipping dip-slip, and tensile, respectively. Superscripts *'Tide'*, *'Press'*, and *'Shear'* indicate the tide, press, and shear asymptotic solutions at the point source.

Vertical strike-slip:

$$h_n^d(1, 2) = -\frac{3}{8\pi\rho_0\xi}\frac{\mu_s}{r_s}y_3^{Press}(r_s; n)$$
$$= \left(\frac{r_s}{a}\right)^{n-1} y_{230}^{(1)} + \frac{1}{n}\left(\frac{r_s}{a}\right)^{n-1} y_{231}^{(1)} + \frac{1}{n^2}\left(\frac{r_s}{a}\right)^{n-1} y_{232}^{(1)} \qquad \text{(B.1)}$$

$$l_n^d(1, 2) = \frac{3}{8\pi\rho_0\xi}\frac{\mu_s}{r_s}y_3^{Shear}(r_s; n)$$
$$= \frac{1}{n}\left(\frac{r_s}{a}\right)^{n-1} y_{330}^{(1)} + \frac{1}{n^2}\left(\frac{r_s}{a}\right)^{n-1} y_{331}^{(1)} + \frac{1}{n^3}\left(\frac{r_s}{a}\right)^{n-1} y_{332}^{(1)} \qquad \text{(B.2)}$$

$$k_n^d(1, 2) = \frac{Ga\mu_s}{2r_s}y_3^{Tide}(r_s; n)$$
$$= \frac{1}{n}\left(\frac{r_s}{a}\right)^{n-1} y_{130}^{(1)} + \frac{1}{n^2}\left(\frac{r_s}{a}\right)^{n-1} y_{131}^{(1)} + \frac{1}{n^3}\left(\frac{r_s}{a}\right)^{n-1} y_{132}^{(1)}. \qquad \text{(B.3)}$$

Vertical dip-slip:

$$h_n^d(2, 1) = -\frac{3}{8\pi\rho_0\xi}y_4^{Press}(r_s; n)$$
$$= n\left(\frac{r_s}{a}\right)^{n-2} y_{240}^{(2)} + \left(\frac{r_s}{a}\right)^{n-2} y_{241}^{(2)} \qquad \text{(B.4)}$$

$$l_n^d(2, 1) = \frac{3}{8\pi\rho_0\xi}y_4^{Shear}(r_s; n)$$
$$= \left(\frac{r_s}{a}\right)^{n-2} y_{340}^{(2)} + \frac{1}{n}\left(\frac{r_s}{a}\right)^{n-2} y_{341}^{(2)} + \frac{1}{n^2}\left(\frac{r_s}{a}\right)^{n-2} y_{342}^{(2)} \qquad \text{(B.5)}$$

$$k_n^d(2, 1) = \frac{Ga}{2}y_4^{Tide}(r_s; n)$$
$$= \left(\frac{r_s}{a}\right)^{n-2} y_{140}^{(2)} + \frac{1}{n}\left(\frac{r_s}{a}\right)^{n-2} y_{141}^{(2)}. \qquad \text{(B.6)}$$

45° Dipping dip-slip with $m = 0$:

$$h_n^d(3, 0) = \frac{3}{8\pi\rho_0\xi}\left\{\left(\frac{\lambda_s}{\sigma_s} - 1\right)y_2^{Press}(r_s; n) + \frac{3k_s}{\sigma_s}\frac{\mu_s}{r_s}[2y_1^{Press}(r_s; n) - n(n+1)y_3^{Press}(r_s; n)]\right\}$$
$$= n^2\left(\frac{r_s}{a}\right)^{n-1}(y_{220}^{(30)} + y_{230}^{(30)}) + n\left(\frac{r_s}{a}\right)^{n-1}(y_{210}^{(30)} + y_{221}^{(30)} + y_{230}^{(30)} + y_{231}^{(30)}) + \left(\frac{r_s}{a}\right)^{n-1}(y_{211}^{(30)} + y_{222}^{(30)} + y_{231}^{(30)} + y_{232}^{(30)}) \quad \text{(B.7)}$$

$$l_n^d(3, 0) = -\frac{3}{8\pi\rho_0\xi}\left\{\left(\frac{\lambda_s}{\sigma_s} - 1\right)y_2^{Shear}(r_s; n) + \frac{3k_s}{\sigma_s}\frac{\mu_s}{r_s}[2y_1^{Shear}(r_s; n) - n(n+1)y_3^{Shear}(r_s; n)]\right\}$$
$$= n\left(\frac{r_s}{a}\right)^{n-1}(y_{320}^{(30)} + y_{330}^{(30)}) + \left(\frac{r_s}{a}\right)^{n-1}(y_{310}^{(30)} + y_{321}^{(30)} + y_{330}^{(30)} + y_{331}^{(30)}) + \frac{1}{n}\left(\frac{r_s}{a}\right)^{n-1}(y_{311}^{(30)} + y_{331}^{(30)} + y_{332}^{(30)}) \quad \text{(B.8)}$$

$$k_n^d(3, 0) = -\frac{Ga}{2}\left\{\left(\frac{\lambda_s}{\sigma_s} - 1\right)y_2^{Tide}(r_s; n) + \frac{3k_s}{\sigma_s}\frac{\mu_s}{r_s}[2y_1^{Tide}(r_s; n) - n(n+1)y_3^{Tide}(r_s; n)]\right\}$$
$$= n\left(\frac{r_s}{a}\right)^{n-1}(y_{120}^{(30)} + y_{130}^{(30)}) + \left(\frac{r_s}{a}\right)^{n-1}(y_{110}^{(30)} + y_{130}^{(30)} + y_{131}^{(30)}) + \frac{1}{n}\left(\frac{r_s}{a}\right)^{n-1}(y_{111}^{(30)} + y_{131}^{(30)} + y_{132}^{(30)}). \quad \text{(B.9)}$$

Vertical Tensile Fracturing:

$$h_n^d(4, 0) = -\frac{3}{4\pi\rho_0\xi}y_2^{Press}(r_s; n)$$
$$= n^2\left(\frac{r_s}{a}\right)^{n-2}y_{220}^{(4)} + n\left(\frac{r_s}{a}\right)^{n-2}y_{221}^{(4)} + \left(\frac{r_s}{a}\right)^{n-2}y_{222}^{(4)} \quad \text{(B.10)}$$

$$l_n^d(4, 0) = \frac{3}{4\pi\rho_0\xi}y_2^{Shear}(r_s; n)$$

$$= n\left(\frac{r_s}{a}\right)^{n-2} y_{320}^{(4)} + \left(\frac{r_s}{a}\right)^{n-2} y_{321}^{(4)} \tag{B.11}$$

$$k_n^d(4, 0) = Gay_2^{Tide}(r_s; n)$$
$$= n\left(\frac{r_s}{a}\right)^{n-2} y_{120}^{(4)}. \tag{B.12}$$

with constants:

$$y_{230}^{(1)} = -\frac{1}{16\pi\rho_0\beta^2}\frac{\mu_s d_s}{r_s}\left[-2 + \frac{d_s}{a}(P - Q)\right] \tag{B.13}$$

$$y_{231}^{(1)} = -\frac{a}{16\pi\rho_0\beta^2}\frac{\mu_s}{r_s}\left[2M + \frac{d_s}{a}\left(2\frac{\alpha t}{\beta} - 3\Lambda - 2\Delta\mu\right)\right] \tag{B.14}$$

$$y_{232}^{(1)} = -\frac{a}{16\pi\rho_0\beta^2}\frac{\mu_s}{r_s}\left[1 + \frac{1}{N}(2T + S - 6) + \Delta\mu\right] \tag{B.15}$$

$$y_{330}^{(1)} = \frac{1}{16\pi\rho_0\beta^2}\frac{\mu_s d_s}{r_s}\left[-2 + \frac{d_s}{a}(P - Q)\right] \tag{B.16}$$

$$y_{331}^{(1)} = \frac{a}{16\pi\rho_0\beta^2}\frac{\mu_s}{r_s}\left[\frac{2}{N} - \frac{d_s}{a}(1 + 6M)\right] \tag{B.17}$$

$$y_{332}^{(1)} = \frac{a}{16\pi\rho_0\beta^2}\frac{\mu_s}{r_s}\left[-4\Lambda + \frac{2T + S}{N} + \Delta\mu\right] \tag{B.18}$$

$$y_{130}^{(1)} = \frac{Ga}{4\beta^2}\frac{\mu_s d_s}{r_s}\left(1 - \frac{d_s}{2a}P\right) \tag{B.19}$$

$$y_{131}^{(1)} = \frac{Ga}{4\beta^2}\frac{\mu_s d_s}{r_s}\left(1 - \frac{\alpha t}{\beta} + \Delta v\right) \tag{B.20}$$

$$y_{132}^{(1)} = \frac{Ga^2}{8\beta^2}\frac{\mu_s}{r_s}(4 - T - \Delta v) \tag{B.21}$$

$$y_{240}^{(2)} = -\frac{1}{8\pi a}d_s\left[-2 + \frac{d_s}{a}(P - Q + 2\Delta\mu)\right] \tag{B.22}$$

$$y_{241}^{(2)} = -\frac{1}{8\pi a}d_s\left[1 - 2(P - Q + M + 2\Delta\mu) + \frac{2\alpha t}{\beta}(1 - M)\right] \tag{B.23}$$

$$y_{340}^{(2)} = \frac{1}{8\pi a}d_s\left[-2 + \frac{d_s}{a}(P - Q + 2\Delta\mu)\right] \tag{B.24}$$

$$y_{341}^{(2)} = \frac{1}{8\pi}\left[2 + \frac{d_s}{a}(3 - 2T - 2S - 2N\Delta\mu)\right] \tag{B.25}$$

$$y_{342}^{(2)} = -\frac{1}{8\pi} \tag{B.26}$$

$$y_{140}^{(2)} = \frac{1}{2}G\rho_0 d_s\left[1 - \frac{d_s}{2a}(P + 2\Delta\mu)\right] \tag{B.27}$$

$$y_{141}^{(2)} = \frac{G\rho_0 N}{4} d_s \left(\Delta v - \frac{2\alpha t}{\beta} \right) \tag{B.28}$$

$$y_{210}^{(30)} = \frac{3}{8\pi\rho_0\beta^2} \frac{k_s\mu_s d_s}{\sigma_s r_s} \left[-2 + \frac{d_s}{a}(P - Q) \right] \tag{B.29}$$

$$y_{211}^{(30)} = \frac{3a}{8\pi\rho_0\beta^2} \frac{k_s\mu_s}{\sigma_s r_s} \left[-\frac{2}{N} + \frac{2\alpha t}{\beta}\frac{d_s}{a}(2 - \Lambda) + \frac{d_s}{a}(\Lambda - S - 2\Delta\mu(N + 1)) \right] \tag{B.30}$$

$$y_{212}^{(30)} = \frac{3a}{8\pi\rho_0\beta^2} \frac{k_s\mu_s}{\sigma_s r_s} \left[-\frac{S}{N} - 3\Delta\mu + \frac{2\alpha t}{\beta N}(2 - \Lambda) + 2M^2\left(\frac{\alpha t}{\beta} - 1 \right) \right] \tag{B.31}$$

$$y_{220}^{(30)} = \left(\frac{\lambda_s}{\sigma_s} - 1 \right) \frac{d_s}{8\pi r_s} \left[-2 + \frac{d_s}{a}(P - Q + 2\Delta\mu) \right] \tag{B.32}$$

$$y_{221}^{(30)} = \left(\frac{\lambda_s}{\sigma_s} - 1 \right) \frac{a}{8\pi r_s} \left[-2 + \frac{d_s}{a}(5 - 2T) \right] \tag{B.33}$$

$$y_{222}^{(30)} = -\left(\frac{\lambda_s}{\sigma_s} - 1 \right) \frac{a}{8\pi r_s} \tag{B.34}$$

$$y_{230}^{(30)} = -\frac{3}{16\pi\rho_0\beta^2} \frac{k_s\mu_s d_s}{\sigma_s r_s} \left[-2 + \frac{d_s}{a}(P - Q) \right] \tag{B.35}$$

$$y_{231}^{(30)} = -\frac{3a}{16\pi\rho_0\beta^2} \frac{k_s\mu_s}{\sigma_s r_s} \left[2M + \frac{d_s}{a}\left(\frac{2\alpha t}{\beta} - 3\Lambda - 2\Delta\mu \right) \right] \tag{B.36}$$

$$y_{232}^{(30)} = -\frac{3a}{16\pi\rho_0\beta^2} \frac{k_s\mu_s}{\sigma_s r_s} \left[1 + \Delta\mu + \frac{1}{N}(2T + S - 6) \right] \tag{B.37}$$

$$y_{310}^{(30)} = -\frac{3a}{8\pi\rho_0\beta^2} \frac{k_s\mu_s d_s}{\sigma_s r_s} \left[-2 + \frac{d_s}{a}(P - Q) \right] \tag{B.38}$$

$$y_{311}^{(30)} = -\frac{3a^2}{8\pi\rho_0\beta^2} \frac{k_s\mu_s}{\sigma_s r_s} \left[-2M + \frac{d_s}{a}\left(1 + \frac{6}{N} \right) - \frac{2d_s}{a}(P - Q - 1 + 2T + 2\Delta\mu) \right] \tag{B.39}$$

$$y_{312}^{(30)} = -\frac{3a^2}{8\pi\rho_0\beta^2} \frac{k_s\mu_s}{\sigma_s r_s} \left[-1 + \frac{6}{N} - \frac{1}{N}(P - Q - 1 + 2T + 2\Delta\mu) \right] \tag{B.40}$$

$$y_{320}^{(30)} = -\left(\frac{\lambda_s}{\sigma_s} - 1 \right) \frac{d_s}{8\pi r_s} \left[-2 + \frac{d_s}{a}(P - Q + 2\Delta\mu) \right] \tag{B.41}$$

$$y_{321}^{(30)} = -\left(\frac{\lambda_s}{\sigma_s} - 1 \right) \frac{d_s}{8\pi r_s} \left[5 - 2M - \frac{2\alpha t}{\beta N} \right] \tag{B.42}$$

$$y_{330}^{(30)} = \frac{3}{16\pi\rho_0\beta^2}\frac{k_s\mu_s d_s}{\sigma_s r_s}\left[-2 + \frac{d_s}{a}(P - Q)\right] \tag{B.43}$$

$$y_{331}^{(30)} = \frac{3a}{16\pi\rho_0\beta^2}\frac{k_s\mu_s}{\sigma_s r_s}\left[\frac{2}{N} - \frac{d_s}{a}(1 + 6M)\right] \tag{B.44}$$

$$y_{332}^{(30)} = \frac{3a}{16\pi\rho_0\beta^2}\frac{k_s\mu_s}{\sigma_s r_s}\left[-4\Lambda + \frac{2T + S}{N} + \Delta\mu\right] \tag{B.45}$$

$$y_{110}^{(30)} = -\frac{3G}{4\beta^2}\frac{k_s\mu_s d_s}{\sigma_s r_s}(2a - d_s P) \tag{B.46}$$

$$y_{111}^{(30)} = -\frac{3Ga}{4\beta^2}\frac{k_s\mu_s}{\sigma_s r_s}\left[2a + d_s\left(2P - 4 - \frac{2\alpha t}{\beta} + 6\nu\right)\right] \tag{B.47}$$

$$y_{112}^{(30)} = -\frac{3Ga^2}{4\beta^2}\frac{k_s\mu_s}{\sigma_s r_s}\left[-2 + T - \frac{2\alpha t}{\beta} + 3\nu\right] \tag{B.48}$$

$$y_{120}^{(30)} = -\left(\frac{\lambda_s}{\sigma_s} - 1\right)\frac{G\rho_0 d_s}{2}\left[1 - \frac{d_s}{2a}(P + 2\Delta\mu)\right] \tag{B.49}$$

$$y_{130}^{(30)} = \frac{3Ga}{4\beta^2}\frac{k_s\mu_s d_s}{\sigma_s r_s}\left(1 - \frac{d_s}{2a}P\right) \tag{B.50}$$

$$y_{131}^{(30)} = \frac{3Ga}{4\beta^2}\frac{k_s\mu_s d_s}{\sigma_s r_s}\left(1 - \frac{\alpha t}{\beta} + \Delta\nu\right) \tag{B.51}$$

$$y_{132}^{(30)} = \frac{3Ga^2}{8\beta^2}\frac{k_s\mu_s}{\sigma_s r_s}(4 - T - \Delta\nu) \tag{B.52}$$

$$y_{220}^{(4)} = -\frac{1}{4\pi a}d_s\left[-2 + \frac{d_s}{a}(P - Q + 2\Delta\mu)\right] \tag{B.53}$$

$$y_{221}^{(4)} = -\frac{1}{4\pi}\left[-2 + \frac{d_s}{a}(5 - 2T)\right] \tag{B.54}$$

$$y_{222}^{(4)} = \frac{1}{4\pi} \tag{B.55}$$

$$y_{320}^{(4)} = \frac{1}{4\pi a}d_s\left[-2 + \frac{d_s}{a}(P - Q + 2\Delta\mu)\right] \tag{B.56}$$

$$y_{321}^{(4)} = \frac{1}{4\pi a}d_s\left(5 - 2M - \frac{2\alpha t}{\beta N}\right) \tag{B.57}$$

$$y_{120}^{(4)} = G\rho_0 d_s\left[1 - \frac{d_s}{2a}(P + 2\Delta\mu)\right] \tag{B.58}$$

where

$\alpha = P$ – wave velocity

$\beta = S$ – wave velocity

ρ_0 = density

λ_s, μ_s = Lamè's constants at the source

d_s = source depth

G = Newton's gravitational constant

$$N = 1 - \frac{\beta^2}{\alpha^2}$$

$$M = \frac{\beta^2}{\alpha^2 - \beta^2}$$

$$\Lambda = \frac{\alpha^2 + \beta^2}{\alpha^2 - \beta^2}$$

$$\gamma = \frac{4}{3}\pi G\rho_0$$

$$t = \frac{g_0 a}{2\alpha\beta}$$

$$T = \frac{1 + \frac{\beta t}{\alpha}}{1 - \frac{\beta^2}{\alpha^2}}$$

$$\Delta\mu = \frac{a}{\mu}\frac{d\mu}{dr}\bigg|_{r=a}$$

$$\Delta\rho_0 = \frac{a}{\rho_0}\frac{d\rho_0}{dr}\bigg|_{r=a}$$

$$\Delta v = \Delta\mu - \frac{\Delta\rho_0}{2}$$

$$P = 1 + \frac{\beta t}{\alpha} - \left(1 + \frac{\beta^2}{\alpha^2}\right)\Delta v$$

$$S = \frac{\beta^2}{\alpha^2}\frac{a}{\lambda + \mu}\frac{d(\lambda + \mu)}{dr}\bigg|_{r=a}$$

$$Q = \frac{\beta t}{\alpha} - S + \left(1 + \frac{\beta^2}{\alpha^2}\right)\frac{\Delta\rho_0}{2}$$

$$\xi = \frac{g_0}{\gamma a}$$

$$\sigma = \lambda + 2\mu$$

$$k = \lambda + \frac{2}{3}\mu.$$

For the special case of $r = a$, we list Okubo's (1988) asymptotic solutions of the tidal, loading and shear forces. Since 'load solution = press force solution + tidal solution', we use here the press solution instead of the load solution. We also transform the asymptotic solutions by separating them into n factors and constants. The following are the transformed Okubo's asymptotic solutions at $r = a$:

Tide:

$$y_1^{Tide}(a;\, n) = \frac{1}{n} y_{110} + \frac{1}{n^2} y_{111} + 0(n^{-3}) \tag{B.59}$$

$$y_3^{Tide}(a;\, n) = \frac{1}{n^3} y_{131} + 0(n^{-4}) \tag{B.60}$$

$$y_5^{Tide}(a;\, n) = 1 + \frac{1}{n^2} y_{151} + \frac{1}{n^3} y_{152} + 0(n^{-4}). \tag{B.61}$$

Press:

$$y_1^{Press}(a;\, n) = y_{210} + \frac{1}{n} y_{211} + 0(n^{-2}) \tag{B.62}$$

$$y_3^{Press}(a;\, n) = \frac{1}{n} y_{230} + \frac{1}{n^2} y_{231} + 0(n^{-3}) \tag{B.63}$$

$$y_5^{Press}(a;\, n) = \frac{1}{n} y_{250} + \frac{1}{n^2} y_{251} + 0(n^{-3}). \tag{B.64}$$

Shear:

$$y_1^{Shear}(a;\, n) = \frac{1}{n} y_{310} + \frac{1}{n^2} y_{311} + 0(n^{-3}) \tag{B.65}$$

$$y_3^{Shear}(a;\, n) = \frac{1}{n^2} y_{330} + \frac{1}{n^3} y_{331} + 0(n^{-4}) \tag{B.66}$$

$$y_5^{Shear}(a;\, n) = \frac{1}{n^3} y_{351} + 0(n^{-4}) \tag{B.67}$$

with constants

$$y_{110} = \frac{a}{2\beta^2} \tag{B.68}$$

$$y_{111} = \frac{a}{4\beta^2}\left(T - 2 - \frac{2\alpha t}{\beta} - 3\Delta v\right) \tag{B.69}$$

$$y_{131} = \frac{a}{4\beta^2}(4 - T - \Delta v) \tag{B.70}$$

$$y_{151} = \frac{3\gamma a^2}{4\beta^2} \tag{B.71}$$

$$y_{152} = \frac{3\gamma a^2}{4\beta^2}\left(-1 - \frac{\alpha t}{\beta} + \frac{3}{2}\Delta v\right) \tag{B.72}$$

$$y_{210} = -\frac{\xi a}{3\beta^2 N} \tag{B.73}$$

$$y_{211} = \frac{\xi a}{6\beta^2}\left(\frac{2\alpha t}{\beta N}(2 - \Lambda) + 2M^2\left(-1 + \frac{\alpha t}{\beta}\right) - \frac{S}{N} - 3\Delta\mu\right) \tag{B.74}$$

$$y_{230} = \frac{\xi a}{3\beta^2} M \tag{B.75}$$

$$y_{231} = \frac{\xi a}{6\beta^2}\left(1 + \frac{1}{N}(2T - 6 + S) + \Delta\mu\right) \tag{B.76}$$

$$y_{250} = -\frac{g_0 a}{2\beta^2} \tag{B.77}$$

$$y_{251} = \frac{g_0 a}{2\beta^2}\left(1 + \frac{3}{2}\frac{\alpha t}{\beta} - \frac{1}{2N} - \frac{\alpha t}{2\beta N} - \frac{3}{2}\Delta v\right) \tag{B.78}$$

$$y_{310} = -\frac{\xi a}{3\beta^2} M \tag{B.79}$$

$$y_{311} = \frac{\xi a}{6\beta^2 N}(-P + Q + 7 - 2T - N - 2\Delta\mu) \tag{B.80}$$

$$y_{330} = \frac{\xi a}{3\beta^2 N} \tag{B.81}$$

$$y_{331} = \frac{\xi a}{6\beta^2}\left(-4\Lambda + \frac{2T + S}{N} + \Delta\mu\right) \tag{B.82}$$

$$y_{351} = \frac{g_0 a}{2\beta^2}\left(2 - \frac{T}{2} - \frac{\Delta v}{2}\right). \tag{B.83}$$

Appendix C
Solving Normalized Differential Equations

For computational convenience we reduced our problem to a dimensionless form in order to solve differential equations (2.28)−(2.33). We now denote λ^* and ρ^* as the values of λ and ρ at the center of the earth, g_0 the gravity value on the surface of the earth, and a the radius of the earth. We introduce dimensionless parameters $\bar{\lambda}$, $\bar{\mu}$, $\bar{\rho}$, $\bar{g}$ and dimensionless variables $\bar{y}_i$, $i = 1,2, \ldots, 7$, and s in accordance with the following scheme

$$\begin{cases} r = as, & y_2 = \bar{y}_2\lambda^* \\ \lambda = \bar{\lambda}\lambda^*, & y_3 = \bar{y}_3 a \\ \mu = \bar{\mu}\lambda^*, & y_4 = \bar{y}_4\lambda^* \\ \rho = \bar{\rho}\rho^* & y_5 = \bar{y}_5 a g_0 \\ g = \bar{g}g_0. & y_6 = \bar{y}_6 g_0 \\ y_1 = \bar{y}_1 a, & y_7 = \bar{y}_7 g_0. \end{cases} \tag{C.1}$$

We also define three dimensionless constants

$$\begin{cases} A = \dfrac{[g_0(a)]^2}{4\pi G\lambda^*} \\ B = \dfrac{4\pi G\rho^* a}{g_0(a)} \\ C = \dfrac{\rho^* g_0(a) a}{\lambda^*}. \end{cases} \tag{C.2}$$

We summarize below the dimensionless equations.

(a) Mantle and Solid Inner Core for $n > 0$

$$\frac{d\bar{y}_1}{ds} = \frac{-2\bar{\lambda}}{\bar{\lambda} + 2\bar{\mu}}\frac{\bar{y}_1}{s} + \frac{\bar{y}_2}{\bar{\lambda} + 2\bar{\mu}} + n(n+1)\frac{\bar{\lambda}}{\bar{\lambda} + 2\bar{\mu}}\frac{\bar{y}_3}{s} \tag{C.3}$$

$$\begin{aligned} \frac{d\bar{y}_2}{ds} = {} & \left[-4C\bar{\rho}\bar{g}s + \frac{4\bar{\mu}(3\bar{\lambda} + 2\bar{\mu})}{\bar{\lambda} + 2\bar{\mu}}\right]\frac{\bar{y}_1}{s^2} - \frac{4\bar{\mu}}{\bar{\lambda} + 2\bar{\mu}}\frac{\bar{y}_2}{s} \\ & + n(n+1)\left[C\bar{\rho}\bar{g}s - \frac{2\bar{\mu}(3\bar{\lambda} + 2\bar{\mu})}{\bar{\lambda} + 2\bar{\mu}}\right]\frac{\bar{y}_3}{s^2} \\ & + n(n+1)\frac{\bar{y}_4}{s} + C\bar{\rho}\frac{n+1}{s}\bar{y}_5 - C\bar{\rho}\bar{y}_6 - \bar{F}_2\frac{\delta(s - s_0)}{s_0^2} \end{aligned} \tag{C.4}$$

$$\frac{d\bar{y}_3}{ds} = -\frac{\bar{y}_1}{s} + \frac{\bar{y}_3}{s} + \frac{\bar{y}_4}{\bar{\mu}} \tag{C.5}$$

$$\begin{aligned} \frac{d\bar{y}_4}{ds} = {} & \left[4C\bar{\rho}\bar{g}s - \frac{2\bar{\mu}(3\bar{\lambda} + 2\bar{\mu})}{\bar{\lambda} + 2\bar{\mu}}\right]\frac{\bar{y}_1}{s^2} - \frac{\bar{\lambda}}{\bar{\lambda} + 2\bar{\mu}}\frac{\bar{y}_2}{s} \\ & + \left\{\frac{2\bar{\mu}}{\bar{\lambda} + 2\bar{\mu}}\left[\bar{\lambda}(2n^2 + 2n - 1) + 2\bar{\mu}(n^2 + n - 1)\right]\right\}\frac{\bar{y}_3}{s^2} \\ & - \frac{3\bar{y}_4}{s} - C\bar{\rho}\frac{\bar{y}_5}{s} - \bar{F}_4\frac{\delta(s - s_0)}{s_0^2} \end{aligned} \tag{C.6}$$

$$\frac{d\bar{y}_5}{ds} = B\bar{\rho}\bar{y}_1 - \frac{n+1}{s}\bar{y}_5 + \bar{y}_6 \tag{C.7}$$

$$\frac{d\bar{y}_6}{ds} = \frac{B(n+1)\bar{\rho}}{s}\bar{y}_1 - n(n+1)B\bar{\rho}\frac{\bar{y}_3}{s} + \frac{n-1}{s}\bar{y}_6. \tag{C.8}$$

(b) Liquid Core for $n > 0$

$$\frac{d\bar{y}_5}{ds} = \left(\frac{B\bar{\rho}}{\bar{g}} - \frac{n+1}{s}\right)\bar{y}_5 + \bar{y}_7 \tag{C.9}$$

$$\frac{d\bar{y}_7}{ds} = \frac{2(n-1)}{s}\frac{B\bar{\rho}}{\bar{g}}\bar{y}_5 + \left(\frac{n-1}{s} - \frac{B\bar{\rho}}{\bar{g}}\right)\bar{y}_7 \tag{C.10}$$

with

$$\bar{y}_7 = \bar{y}_6 + \frac{1}{A\bar{g}}\bar{y}_2. \tag{C.11}$$

(c) Mantle and Inner Core for $n = 0$

$$\frac{d\bar{y}_1}{ds} = \frac{-2\bar{\lambda}}{\bar{\lambda} + 2\bar{\mu}} \frac{\bar{y}_1}{s} + \frac{\bar{y}_2}{\bar{\lambda} + 2\bar{\mu}} \tag{C.12}$$

$$\frac{d\bar{y}_2}{ds} = \left[-4C\bar{\rho}\bar{g}s + \frac{4\bar{\mu}(3\bar{\lambda} + 2\bar{\mu})}{\bar{\lambda} + 2\bar{\mu}} \right] \frac{\bar{y}_1}{s^2} - \frac{4\bar{\mu}}{\bar{\lambda} + 2\bar{\mu}} \frac{\bar{y}_2}{s} \tag{C.13}$$

$$\frac{d\bar{y}_5}{ds} = B\bar{\rho}\bar{y}_1 \tag{C.14}$$

$$\frac{d\bar{y}_6}{ds} = 0. \tag{C.15}$$

(d) Liquid Core for $n = 0$

$$\frac{d\bar{y}_1}{ds} = -\frac{2\bar{y}_1}{s} + \frac{\bar{y}_2}{\bar{\lambda}} \tag{C.16}$$

$$\frac{d\bar{y}_2}{ds} = -4C\bar{\rho}\bar{g}\frac{\bar{y}_1}{s} \tag{C.17}$$

$$\frac{d\bar{y}_5}{ds} = B\bar{\rho}\bar{y}_1 \tag{C.18}$$

$$\frac{d\bar{y}_6}{ds} = 0. \tag{C.19}$$

(e) Core-Mantle Boundary Conditions

$$\bar{y}_{ij}^{s}(\bar{b}) = \begin{pmatrix} 0 & 1 & 0 \\ -C\bar{\rho}^{l}\bar{y}_{51}^{l}(\bar{b}) & C\bar{\rho}^{l}\bar{g} & 0 \\ 0 & 0 & 1 \\ 0 & 0 & 0 \\ \bar{y}_{51}^{l}(\bar{b}) & 0 & 0 \\ \bar{y}_{71}^{l}(\bar{b}) + \dfrac{B\bar{\rho}^{l}}{\bar{g}}\bar{y}_{51}^{l}(\bar{b}) & -B\bar{\rho}^{l} & 0 \end{pmatrix} \begin{pmatrix} Q_1 \\ Q_2 \\ Q_3 \end{pmatrix}; \quad \begin{pmatrix} i = 1,\ldots,6 \\ j = 1,2,3 \end{pmatrix} \tag{C.20}$$

where $\bar{b} = b/a$.

(f) Free Boundary Conditions

$$\bar{y}_2(1) = 0 \tag{C.21}$$

$$\bar{y}_4(1) = 0 \tag{C.22}$$

$$\bar{y}_6(1) = 0. \tag{C.23}$$

(g) Source Functions

Similarly, we normalize the source functions as

$$\begin{cases} s_1 = \bar{s}_1 a, & s_4 = \bar{s}_4 \lambda^* \\ s_2 = \bar{s}_2 \lambda^*, & s_5 = \bar{s}_5 a g_0 \\ s_3 = \bar{s}_3 a, & s_6 = \bar{s}_6 g_0. \end{cases} \tag{C.24}$$

Then, for s_1, as an example, we have

$$\bar{s}_1 = \frac{2n+1}{4\pi s_0^2}\left[n_z v_z + \frac{\bar{\lambda}}{\bar{\lambda} + 2\bar{\mu}}(n_x v_x + n_y v_y) \right] \cdot \frac{1}{a^3}. \tag{C.25}$$

We obtained the source functions based on the assumption that $UdS = 1$, which is normalized as

$$UdS = [\overline{UdS}]a^3. \tag{C.26}$$

Therefore, (C.25) becomes

$$\bar{s}_1 = \frac{2n+1}{4\pi s_0^2}\left[n_z v_z + \frac{\bar{\lambda}}{\bar{\lambda} + 2\bar{\mu}}(n_x v_x + n_y v_y) \right] \tag{C.27}$$

with $[\overline{UdS}] = 1$. We should keep in mind that the normalization factor, $[\overline{UdS}] = UdS/a^3 (= 1)$, must be considered in the final results. We thus obtain the normalized source functions as follows:

$$\bar{s}_1 = \frac{2n+1}{4\pi s_0^2}\left[n_z v_z + \frac{\bar{\lambda}}{\bar{\lambda} + 2\bar{\mu}}(n_x v_x + n_y v_y) \right], \qquad m = 0, \tag{C.28}$$

$$\bar{s}_2 = -\frac{2n+1}{2\pi s_0^3}\frac{\bar{\mu}(3\bar{\lambda} + 2\bar{\mu})}{\bar{\lambda} + 2\bar{\mu}}(n_x v_x + n_y v_y), \qquad m = 0, \tag{C.29}$$

$$\bar{s}_3 = \frac{2n+1}{8\pi s_0^2 n(n+1)}[\pm (n_z v_x + n_x v_z) - i(n_y v_z + n_z v_y)], \qquad m = \pm 1, \tag{C.30}$$

$$\bar{s}_4 = \frac{2n+1}{4\pi s_0^3}\frac{\bar{\mu}(3\bar{\lambda} + 2\bar{\mu})}{\bar{\lambda} + 2\bar{\mu}}(n_x v_x + n_y v_y) \qquad m = 0 \tag{C.31}$$

$$= \frac{(2n+1)\bar{\mu}}{8\pi s_0^3 n(n+1)}[(-n_x v_x + n_y v_y) \pm i(n_x v_y + n_y v_y)], \qquad m = \pm 2, \tag{C.32}$$

$$\bar{s}_5 = 0, \tag{C.33}$$

$$\bar{s}_6 = 0. \tag{C.34}$$

(h) Dislocation Love Numbers

The dislocation Love numbers become

$$h_n^d(T, m) = \bar{y}_1^T(a), \tag{C.35}$$

$$l_n^d(T, m) = \bar{y}_3^T(a), \tag{C.36}$$

$$k_n^d(T, m) = \bar{y}_5^T(a). \tag{C.37}$$

Appendix D
Dislocation Love Numbers

We list the dislocation Love numbers for earth model 1066A with 4 types of dislocations, which are transformed as follows:

$$\bar{h}_n^d(T,\ m) = h_n^d(T,\ m)n^{m-2}\left(\frac{a}{r_0}\right)^n,$$

$$\bar{l}_n^d(T,\ m) = l_n^d(T,\ m)n^{m-1}\left(\frac{a}{r_0}\right)^n,$$

$$\bar{k}_n^d(T,\ m) = k_n^d(T,\ m)n^{m-1}\left(\frac{a}{r_0}\right)^n.$$

Table D.1. Dislocation Love numbers of a vertical strike-slip faulting at depth of $2\,km$

n	$\bar{h}_n^d(1,2)$	$\bar{l}_n^d(1,2)$	$\bar{k}_n^d(1,2)$
2	$.3071E-3$	$.3228E-2$	$.8550E-3$
3	$-.2822E-3$	$.2555E-2$	$.2283E-3$
4	$-.2489E-3$	$.2157E-2$	$.2107E-3$
5	$-.1942E-3$	$.1857E-2$	$.2182E-3$
6	$-.1642E-3$	$.1636E-2$	$.2102E-3$
8	$-.1408E-3$	$.1335E-2$	$.1785E-3$
10	$-.1323E-3$	$.1135E-2$	$.1486E-3$
15	$-.1242E-3$	$.8380E-3$	$.9494E-4$
20	$-.1204E-3$	$.6766E-3$	$.6087E-4$
30	$-.1106E-3$	$.5071E-3$	$.2541E-4$
40	$-.9828E-4$	$.4176E-3$	$.1106E-4$
50	$-.8642E-4$	$.3612E-3$	$.5206E-5$
70	$-.6741E-4$	$.2931E-3$	$.2278E-5$
100	$-.4879E-4$	$.2378E-3$	$.3329E-5$
200	$-.2196E-4$	$.1613E-3$	$.8800E-5$
300	$-.1142E-4$	$.1254E-3$	$.1180E-4$
500	$-.2867E-5$	$.8372E-4$	$.1334E-4$
800	$.6922E-6$	$.5197E-4$	$.1177E-4$
1000	$.1478E-5$	$.4028E-4$	$.1046E-4$
1200	$.2033E-5$	$.3231E-4$	$.9429E-5$
1400	$.2586E-5$	$.2652E-4$	$.8693E-5$
1600	$.3180E-5$	$.2207E-4$	$.8205E-5$
1800	$.3794E-5$	$.1852E-4$	$.7893E-5$
2000	$.4397E-5$	$.1561E-4$	$.7700E-5$
2200	$.4968E-5$	$.1317E-4$	$.7583E-5$
2400	$.5494E-5$	$.1111E-4$	$.7512E-5$
2600	$.5971E-5$	$.9345E-5$	$.7470E-5$
2800	$.6400E-5$	$.7814E-5$	$.7445E-5$
3000	$.6784E-5$	$.6478E-5$	$.7430E-5$
3500	$.7577E-5$	$.3786E-5$	$.7414E-5$
4000	$.8186E-5$	$.1756E-5$	$.7410E-5$
4500	$.8663E-5$	$.1737E-6$	$.7410E-5$
5000	$.9046E-5$	$-.1093E-5$	$.7410E-5$
7000	$.1003E-4$	$-.4351E-5$	$.7411E-5$
10000	$.1077E-4$	$-.6795E-5$	$.7412E-5$
15000	$.1134E-4$	$-.8696E-5$	$.7413E-5$
20000	$.1163E-4$	$-.9647E-5$	$.7414E-5$
25000	$.1180E-4$	$-.1021E-4$	$.7414E-5$
30000	$.1192E-4$	$-.1059E-4$	$.7414E-5$
35000	$.1201E-4$	$-.1088E-4$	$.7420E-5$

Table D.2. Dislocation Love numbers of a vertical strike-slip faulting at depth of $20\,km$

n	$\bar{h}_n^d(1,2)$	$\bar{l}_n^d(1,2)$	$\bar{k}_n^d(1,2)$
2	$.1641E-2$	$.1551E-1$	$.4341E-2$
3	$-.1314E-2$	$.1215E-1$	$.1200E-2$
4	$-.1160E-2$	$.1017E-1$	$.1103E-2$
5	$-.8906E-3$	$.8688E-2$	$.1140E-2$
6	$-.7400E-3$	$.7591E-2$	$.1102E-2$
8	$-.6183E-3$	$.6097E-2$	$.9512E-3$
10	$-.5701E-3$	$.5104E-2$	$.8084E-3$
15	$-.5178E-3$	$.3624E-2$	$.5529E-3$
20	$-.4910E-3$	$.2818E-2$	$.3907E-3$
30	$-.4342E-3$	$.1968E-2$	$.2208E-3$
40	$-.3706E-3$	$.1519E-2$	$.1503E-3$
50	$-.3120E-3$	$.1237E-2$	$.1196E-3$
70	$-.2207E-3$	$.8981E-3$	$.9955E-4$
100	$-.1340E-3$	$.6275E-3$	$.9549E-4$
200	$-.1493E-4$	$.2806E-3$	$.9811E-4$
300	$.3015E-4$	$.1472E-3$	$.9832E-4$
500	$.7299E-4$	$.2559E-4$	$.9720E-4$
800	$.1093E-4$	$-.5221E-4$	$.9959E-3$
1000	$.1278E-3$	$-.8172E-4$	$.1034E-3$
1200	$.1432E-3$	$-.1034E-3$	$.1077E-3$
1400	$.1556E-3$	$-.1201E-3$	$.1116E-3$
1600	$.1653E-3$	$-.1331E-3$	$.1148E-3$
1800	$.1727E-3$	$-.1433E-3$	$.1173E-3$
2000	$.1783E-3$	$-.1514E-3$	$.1191E-3$
2200	$.1826E-3$	$-.1578E-3$	$.1204E-3$
2400	$.1860E-3$	$-.1630E-3$	$.1214E-3$
2600	$.1886E-3$	$-.1673E-3$	$.1222E-3$
2800	$.1908E-3$	$-.1709E-3$	$.1227E-3$
3000	$.1926E-3$	$-.1740E-3$	$.1232E-3$
3500	$.1955E-3$	$-.1795E-3$	$.1237E-3$

where $m = 2, 1, 0$, correspond to the strike-slip, dip-slip, and 45° dip-slip dislocations (or tensile), respectively. All of the dislocation Love numbers ($h_n^d(T, m)$, $l_n^d(T, m)$ and $k_n^d(T, m)$) are obtained using the definitions of $(C.37)-(C.39)$.

Table D.3. Dislocation Love numbers of a vertical strike-slip faulting at depth of 200 *km*

n	$\bar{h}_n^d(1,2)$	$\bar{l}_n^d(1,2)$	$\bar{k}_n^d(1,2)$
2	.2648E − 2	.1309E − 1	.4998E − 2
3	−.4494E − 3	.9859E − 2	.1729E − 2
4	−.4214E − 3	.8088E − 2	.1530E − 2
5	−.1914E − 3	.6771E − 2	.1547E − 2
6	−.3806E − 4	.5800E − 2	.1527E − 2
8	.1288E − 3	.4477E − 2	.1437E − 2
10	.2338E − 3	.3593E − 2	.1359E − 2
15	.4208E − 3	.2244E − 2	.1244E − 2
20	.5551E − 3	.1475E − 2	.1188E − 2
25	.6615E − 3	.9750E − 3	.1161E − 2
30	.7497E − 3	.6185E − 3	.1150E − 2
35	.8239E − 3	.3491E − 3	.1146E − 2
40	.8867E − 3	.1369E − 3	.1147E − 2
45	.9400E − 3	−.3545E − 4	.1149E − 2
50	.9855E − 3	−.1788E − 3	.1151E − 2
60	.1058E − 2	−.4052E − 3	.1155E − 2
70	.1113E − 2	−.5773E − 3	.1157E − 2
80	.1156E − 2	−.7141E − 3	.1157E − 2
90	.1190E − 2	−.8266E − 3	.1156E − 2
100	.1219E − 2	−.9218E − 3	.1155E − 2
110	.1244E − 2	−.1004E − 2	.1153E − 2
120	.1265E − 2	−.1076E − 2	.1150E − 2
130	.1285E − 2	−.1140E − 2	.1148E − 2
140	.1302E − 2	−.1198E − 2	.1145E − 2
150	.1318E − 2	−.1251E − 2	.1142E − 2
160	.1333E − 2	−.1299E − 2	.1139E − 2
170	.1347E − 2	−.1344E − 2	.1137E − 2
180	.1360E − 2	−.1385E − 2	.1134E − 2
200	.1385E − 2	−.1460E − 2	.1129E − 2
300	.1489E − 2	−.1721E − 2	.1111E − 2

Table D.4. Dislocation Love numbers of a vertical strike-slip faulting at depth of 400 *km*

n	$\bar{h}_n^d(1,2)$	$\bar{l}_n^d(1,2)$	$\bar{k}_n^d(1,2)$
2	.5328E − 2	.1568E − 1	.8270E − 2
3	.4902E − 3	.1107E − 1	.3193E − 2
4	.2809E − 3	.8762E − 2	.2686E − 2
5	.5148E − 3	.7069E − 2	.2636E − 2
6	.7074E − 3	.5828E − 2	.2591E − 2
8	.9573E − 3	.4152E − 2	.2486E − 2
10	.1143E − 2	.3043E − 2	.2415E − 2
15	.1530E − 2	.1340E − 2	.2370E − 2
20	.1840E − 2	.3373E − 3	.2400E − 2
25	.2088E − 2	−.3383E − 3	.2449E − 2
30	.2285E − 2	−.8307E − 3	.2497E − 2
35	.2444E − 2	−.1208E − 2	.2538E − 2
40	.2572E − 2	−.1510E − 2	.2573E − 2
45	.2678E − 2	−.1757E − 2	.2600E − 2
50	.2765E − 2	−.1966E − 2	.2622E − 2
60	.2902E − 2	−.2303E − 2	.2653E − 2
70	.3005E − 2	−.2566E − 2	.2672E − 2
80	.3086E − 2	−.2782E − 2	.2683E − 2
90	.3152E − 2	−.2966E − 2	.2689E − 2
100	.3208E − 2	−.3125E − 2	.2692E − 2
110	.3256E − 2	−.3268E − 2	.2693E − 2
120	.3302E − 2	−.3401E − 2	.2693E − 2
130	.3346E − 2	−.3532E − 2	.2695E − 2
140	.3396E − 2	−.3680E − 2	.2701E − 2
150	.3468E − 2	−.3882E − 2	.2722E − 2
160	.3574E − 2	−.3952E − 2	.2786E − 2

Table D.5. Dislocation Love numbers of a vertical dip-slip faulting at depth of $2\,km$

n	$\tilde{h}^d_n(2,1)$	$\tilde{l}^d_n(2,1)$	$\tilde{k}^d_n(2,1)$
1	$-.2066E-5$	$.5973E-1$	$.0000E+0$
2	$.8763E-5$	$.3320E-1$	$.1172E-4$
3	$.9760E-5$	$.2324E-1$	$.1279E-4$
4	$.9983E-5$	$.1793E-1$	$.1295E-4$
5	$.1001E-4$	$.1461E-1$	$.1289E-4$
6	$.1004E-4$	$.1234E-1$	$.1284E-4$
8	$.1019E-4$	$.9416E-2$	$.1281E-4$
10	$.1040E-4$	$.7616E-2$	$.1284E-4$
15	$.1096E-4$	$.5156E-2$	$.1304E-4$
20	$.1152E-4$	$.3899E-2$	$.1332E-4$
30	$.1248E-4$	$.2623E-2$	$.1389E-4$
40	$.1314E-4$	$.1976E-2$	$.1429E-4$
50	$.1360E-4$	$.1585E-2$	$.1455E-4$
70	$.1413E-4$	$.1135E-2$	$.1479E-4$
100	$.1450E-4$	$.7955E-3$	$.1482E-4$
200	$.1474E-4$	$.3919E-3$	$.1404E-4$
300	$.1460E-4$	$.2541E-3$	$.1291E-4$
500	$.1453E-4$	$.1426E-3$	$.1115E-4$
800	$.1600E-4$	$.8031E-4$	$.1059E-4$
1000	$.1766E-4$	$.5934E-4$	$.1110E-4$
1200	$.1939E-4$	$.4506E-4$	$.1185E-4$
1400	$.2093E-4$	$.3465E-4$	$.1262E-4$
1600	$.2217E-4$	$.2674E-4$	$.1326E-4$
1800	$.2310E-4$	$.2059E-4$	$.1376E-4$
2000	$.2375E-4$	$.1571E-4$	$.1412E-4$
2200	$.2419E-4$	$.1177E-4$	$.1437E-4$
2400	$.2448E-4$	$.8548E-5$	$.1453E-4$
2600	$.2467E-4$	$.5856E-5$	$.1464E-4$
2800	$.2478E-4$	$.3578E-5$	$.1470E-4$
3000	$.2486E-4$	$.1625E-5$	$.1475E-4$
3500	$.2494E-4$	$-.2229E-5$	$.1479E-4$
4000	$.2497E-4$	$-.5091E-5$	$.1481E-4$
4500	$.2497E-4$	$-.7307E-5$	$.1481E-4$
5000	$.2498E-4$	$-.9077E-5$	$.1482E-4$
7000	$.2498E-4$	$-.1362E-4$	$.1482E-4$
10000	$.2499E-4$	$-.1703E-4$	$.1482E-4$
15000	$.2499E-4$	$-.1969E-4$	$.1482E-4$
20000	$.2499E-4$	$-.2101E-4$	$.1482E-4$
25000	$.2499E-4$	$-.2181E-4$	$.1482E-4$
30000	$.2499E-4$	$-.2234E-4$	$.1482E-4$
35000	$.2498E-4$	$-.2270E-4$	$.1482E-4$

Table D.6. Dislocation Love numbers of a vertical dip-slip faulting at depth of $20\,km$

n	$\tilde{h}^d_n(2,1)$	$\tilde{l}^d_n(2,1)$	$\tilde{k}^d_n(2,1)$
1	$-.5345E-4$	$.6014E-1$	$.0000E+0$
2	$.1097E-3$	$.3350E-1$	$.1621E-3$
3	$.1224E-3$	$.2344E-1$	$.1695E-3$
4	$.1186E-3$	$.1807E-1$	$.1617E-3$
5	$.1146E-3$	$.1472E-1$	$.1547E-3$
6	$.1131E-3$	$.1242E-1$	$.1505E-3$
8	$.1146E-3$	$.9470E-2$	$.1469E-3$
10	$.1182E-3$	$.7649E-2$	$.1460E-3$
15	$.1295E-3$	$.5161E-2$	$.1486E-3$
20	$.1417E-3$	$.3887E-2$	$.1542E-3$
30	$.1626E-3$	$.2588E-2$	$.1661E-3$
40	$.1772E-3$	$.1926E-2$	$.1750E-3$
50	$.1871E-3$	$.1523E-2$	$.1809E-3$
70	$.1992E-3$	$.1055E-2$	$.1873E-3$
100	$.2087E-3$	$.6942E-3$	$.1910E-3$
200	$.2257E-3$	$.2395E-3$	$.1924E-3$
300	$.2387E-3$	$.6409E-4$	$.1911E-3$
400	$.2510E-3$	$-.3349E-4$	$.1903E-3$
500	$.2636E-3$	$-.9637E-4$	$.1909E-3$
800	$.3036E-3$	$-.2017E-3$	$.2006E-3$
1000	$.3295E-3$	$-.2440E-3$	$.2106E-3$
1200	$.3522E-3$	$-.2762E-3$	$.2206E-3$
1400	$.3705E-3$	$-.3014E-3$	$.2292E-3$
1600	$.3843E-3$	$-.3210E-3$	$.2358E-3$
1800	$.3943E-3$	$-.3361E-3$	$.2407E-3$
2000	$.4013E-3$	$-.3477E-3$	$.2441E-3$
2200	$.4063E-3$	$-.3568E-3$	$.2464E-3$
2400	$.4098E-3$	$-.3640E-3$	$.2481E-3$
2600	$.4124E-3$	$-.3698E-3$	$.2492E-3$
2800	$.4143E-3$	$-.3746E-3$	$.2500E-3$
3000	$.4159E-3$	$-.3787E-3$	$.2507E-3$
3500	$.4198E-3$	$-.3877E-3$	$.2525E-3$

Table D.7. Dislocation Love numbers of a vertical dip-slip faulting at depth of 200 km

n	$\bar{h}_n^d(2,1)$	$\bar{l}_n^d(2,1)$	$\bar{k}_n^d(2,1)$
1	$-.6435E-3$	$.6327E-1$	$.0000E+0$
2	$.1718E-2$	$.3576E-1$	$.2307E-2$
3	$.1871E-2$	$.2437E-1$	$.2364E-2$
4	$.1753E-2$	$.1832E-1$	$.2182E-2$
5	$.1653E-2$	$.1455E-1$	$.2038E-2$
6	$.1607E-2$	$.1196E-1$	$.1952E-2$
8	$.1605E-2$	$.8589E-2$	$.1876E-2$
10	$.1643E-2$	$.6486E-2$	$.1847E-2$
15	$.1776E-2$	$.3591E-2$	$.1845E-2$
20	$.1924E-2$	$.2081E-2$	$.1895E-2$
25	$.2066E-2$	$.1134E-2$	$.1961E-2$
30	$.2189E-2$	$.4756E-3$	$.2024E-2$
35	$.2291E-2$	$-.1284E-5$	$.2078E-2$
40	$.2374E-2$	$-.3915E-3$	$.2122E-2$
45	$.2443E-2$	$-.6951E-3$	$.2157E-2$
50	$.2499E-2$	$-.9450E-3$	$.2185E-2$
60	$.2584E-2$	$-.1335E-2$	$.2224E-2$
70	$.2646E-2$	$-.1629E-2$	$.2247E-2$
80	$.2693E-2$	$-.1863E-2$	$.2261E-2$
90	$.2730E-2$	$-.2055E-2$	$.2268E-2$
100	$.2760E-2$	$-.2217E-2$	$.2272E-2$
110	$.2786E-2$	$-.2358E-2$	$.2272E-2$
120	$.2810E-2$	$-.2482E-2$	$.2271E-2$
130	$.2831E-2$	$-.2593E-2$	$.2269E-2$
140	$.2850E-2$	$-.2693E-2$	$.2266E-2$
150	$.2869E-2$	$-.2785E-2$	$.2263E-2$
160	$.2887E-2$	$-.2869E-2$	$.2259E-2$
170	$.2904E-2$	$-.2947E-2$	$.2255E-2$
180	$.2921E-2$	$-.3019E-2$	$.2251E-2$
200	$.2953E-2$	$-.3150E-2$	$.2243E-2$
300	$.3117E-2$	$-.3619E-2$	$.2216E-2$

Table D.8. Dislocation Love numbers of a vertical dip-slip faulting at depth of 400 km

n	$\bar{h}_n^d(2,1)$	$\bar{l}_n^d(2,1)$	$\bar{k}_n^d(2,1)$
1	$-.9257E-3$	$.6683E-1$	$.0000E+0$
2	$.4399E-2$	$.3850E-1$	$.5281E-2$
3	$.4769E-2$	$.2544E-1$	$.5460E-2$
4	$.4502E-2$	$.1852E-1$	$.5066E-2$
5	$.4274E-2$	$.1425E-1$	$.4752E-2$
6	$.4176E-2$	$.1129E-1$	$.4577E-2$
8	$.4197E-2$	$.7361E-2$	$.4447E-2$
10	$.4312E-2$	$.4855E-2$	$.4420E-2$
15	$.4649E-2$	$.1331E-2$	$.4467E-2$
20	$.4990E-2$	$-.5612E-3$	$.4590E-2$
25	$.5307E-2$	$-.1791E-2$	$.4738E-2$
30	$.5584E-2$	$-.2680E-2$	$.4881E-2$
35	$.5818E-2$	$-.3362E-2$	$.5006E-2$
40	$.6011E-2$	$-.3908E-2$	$.5108E-2$
45	$.6171E-2$	$-.4357E-2$	$.5190E-2$
50	$.6302E-2$	$-.4735E-2$	$.5255E-2$
60	$.6501E-2$	$-.5341E-2$	$.5343E-2$
70	$.6643E-2$	$-.5811E-2$	$.5394E-2$
80	$.6750E-2$	$-.6194E-2$	$.5421E-2$
90	$.6834E-2$	$-.6518E-2$	$.5435E-2$
100	$.6906E-2$	$-.6799E-2$	$.5440E-2$
110	$.6968E-2$	$-.7049E-2$	$.5439E-2$
120	$.7022E-2$	$-.7265E-2$	$.5434E-2$
130	$.7068E-2$	$-.7447E-2$	$.5425E-2$
140	$.7097E-2$	$-.7564E-2$	$.5406E-2$
150	$.7090E-2$	$-.7564E-2$	$.5367E-2$
160	$.7219E-2$	$-.8019E-2$	$.5402E-2$

Table D.9. Dislocation Love numbers at a 45° dip-slip faulting at depth of 2 *km*

n	$\bar{h}_n^d(3,0)$	$\bar{l}_n^d(3,0)$	$\bar{k}_n^d(3,0)$
0	$.2162E-1$	$.0000E+0$	$.0000E+0$
1	$.6499E-1$	$.1683E-1$	$.0000E+0$
2	$.2361E-1$	$.8112E-2$	$-.3175E-2$
3	$.1531E-1$	$.6426E-2$	$-.1194E-2$
4	$.1156E-1$	$.5039E-2$	$-.3173E-3$
5	$.9280E-2$	$.4117E-2$	$.7296E-5$
6	$.7712E-2$	$.3503E-2$	$.1224E-3$
8	$.5720E-2$	$.2739E-2$	$.1708E-3$
10	$.4524E-2$	$.2270E-2$	$.1624E-3$
15	$.2941E-2$	$.1616E-2$	$.1144E-3$
20	$.2157E-2$	$.1279E-2$	$.7410E-4$
30	$.1390E-2$	$.9371E-3$	$.2998E-4$
40	$.1021E-2$	$.7607E-3$	$.1339E-4$
50	$.8078E-3$	$.6514E-3$	$.7899E-5$
70	$.5731E-3$	$.5210E-3$	$.7558E-5$
100	$.4041E-3$	$.4169E-3$	$.1226E-4$
200	$.2149E-3$	$.2755E-3$	$.2412E-4$
300	$.1544E-3$	$.2101E-3$	$.2989E-4$
400	$.1245E-3$	$.1666E-3$	$.3237E-4$
500	$.1062E-3$	$.1348E-3$	$.3294E-4$
800	$.7696E-4$	$.7770E-4$	$.3033E-4$
1000	$.6641E-4$	$.5670E-4$	$.2804E-4$
1200	$.5937E-4$	$.4242E-4$	$.2617E-4$
1400	$.5456E-4$	$.3207E-4$	$.2481E-4$
1600	$.5122E-4$	$.2416E-4$	$.2388E-4$
1800	$.4888E-4$	$.1786E-4$	$.2327E-4$
2000	$.4721E-4$	$.1271E-4$	$.2287E-4$
2200	$.4598E-4$	$.8400E-5$	$.2262E-4$
2400	$.4505E-4$	$.4741E-5$	$.2247E-4$
2600	$.4433E-4$	$.1599E-5$	$.2237E-4$
2800	$.4375E-4$	$-.1124E-5$	$.2231E-4$
3000	$.4328E-4$	$-.3505E-5$	$.2227E-4$
3500	$.4240E-4$	$-.8314E-5$	$.2224E-4$
4000	$.4177E-4$	$-.1194E-4$	$.2223E-4$
4500	$.4129E-4$	$-.1478E-4$	$.2223E-4$
5000	$.4091E-4$	$-.1705E-4$	$.2223E-4$
7000	$.3993E-4$	$-.2289E-4$	$.2223E-4$
10000	$.3920E-4$	$-.2727E-4$	$.2223E-4$
15000	$.3863E-4$	$-.3068E-4$	$.2224E-4$
20000	$.3835E-4$	$-.3238E-4$	$.2224E-4$
25000	$.3817E-4$	$-.3340E-4$	$.2224E-4$
30000	$.3806E-4$	$-.3408E-4$	$.2224E-4$
35000	$.3800E-4$	$-.3460E-4$	$.2225E-4$

Table D.10. Dislocation Love numbers of a 45° dip-slip faulting at depth of 20 *km*

n	$\bar{h}_n^d(3,0)$	$\bar{l}_n^d(3,0)$	$\bar{k}_n^d(3,0)$
0	$.1886E-1$	$.0000E+0$	$.0000E+0$
1	$.5716E-1$	$.7072E-1$	$.0000E+0$
2	$.9103E-2$	$.3362E-1$	$-.1348E-1$
3	$.8390E-2$	$.2647E-1$	$-.4975E-2$
4	$.8252E-2$	$.2056E-1$	$-.1197E-2$
5	$.7494E-2$	$.1663E-1$	$.2054E-3$
6	$.6606E-2$	$.1401E-1$	$.7073E-3$
8	$.5133E-2$	$.1076E-1$	$.9265E-3$
10	$.4124E-2$	$.8757E-2$	$.8997E-3$
15	$.2692E-2$	$.5959E-2$	$.7104E-3$
20	$.1951E-2$	$.4512E-2$	$.5472E-3$
30	$.1241E-2$	$.3034E-2$	$.3668E-3$
40	$.9326E-3$	$.2269E-2$	$.2968E-3$
50	$.7746E-3$	$.1795E-2$	$.2709E-3$
70	$.6258E-3$	$.1231E-2$	$.2610E-3$
100	$.5373E-3$	$.7838E-3$	$.2669E-3$
200	$.4580E-3$	$.2091E-3$	$.2790E-3$
300	$.4431E-3$	$-.1358E-5$	$.2805E-3$
400	$.4442E-3$	$-.1370E-3$	$.2812E-3$
500	$.4527E-3$	$-.2163E-3$	$.2835E-3$
800	$.4974E-3$	$-.3505E-3$	$.3013E-3$
1000	$.5310E-3$	$-.4059E-3$	$.3177E-3$
1200	$.5611E-3$	$-.4488E-3$	$.3335E-3$
1400	$.5853E-3$	$-.4826E-3$	$.3467E-3$
1600	$.6032E-3$	$-.5087E-3$	$.3568E-3$
1800	$.6158E-3$	$-.5288E-3$	$.3641E-3$
2000	$.6243E-3$	$-.5440E-3$	$.3691E-3$
2200	$.6299E-3$	$-.5558E-3$	$.3724E-3$
2400	$.6337E-3$	$-.5649E-3$	$.3747E-3$
2600	$.6362E-3$	$-.5723E-3$	$.3763E-3$
2800	$.6379E-3$	$-.5783E-3$	$.3774E-3$
3000	$.6392E-3$	$-.5834E-3$	$.3783E-3$
3500	$.6404E-3$	$-.5924E-3$	$.3792E-3$

Table D.11. Dislocation Love numbers of a 45° dip-slip faulting at depth of 200 *km*

n	$\bar{h}_n^d(3,0)$	$\bar{l}_n^d(3,0)$	$\bar{k}_n^d(3,0)$
0	$.1402E-1$	$.0000E+0$	$.0000E+0$
1	$.4337E-1$	$.7094E-1$	$.0000E+0$
2	$.3742E-2$	$.3234E-1$	$-.1309E-1$
3	$.6107E-2$	$.2487E-1$	$-.3694E-2$
4	$.7489E-2$	$.1861E-1$	$.5597E-3$
5	$.7582E-2$	$.1443E-1$	$.2200E-2$
6	$.7231E-2$	$.1166E-1$	$.2836E-2$
8	$.6422E-2$	$.8222E-2$	$.3220E-2$
10	$.5837E-2$	$.6093E-2$	$.3315E-2$
15	$.5070E-2$	$.3044E-2$	$.3367E-2$
20	$.4736E-2$	$.1389E-2$	$.3381E-2$
25	$.4574E-2$	$.3325E-3$	$.3397E-2$
30	$.4493E-2$	$-.4116E-3$	$.3416E-2$
35	$.4451E-2$	$-.9707E-3$	$.3435E-2$
40	$.4430E-2$	$-.1410E-2$	$.3452E-2$
45	$.4419E-2$	$-.1767E-2$	$.3465E-2$
50	$.4413E-2$	$-.2064E-2$	$.3475E-2$
60	$.4410E-2$	$-.2534E-2$	$.3486E-2$
70	$.4410E-2$	$-.2895E-2$	$.3488E-2$
80	$.4412E-2$	$-.3185E-2$	$.3484E-2$
90	$.4416E-2$	$-.3427E-2$	$.3477E-2$
100	$.4423E-2$	$-.3634E-2$	$.3468E-2$
110	$.4430E-2$	$-.3815E-2$	$.3458E-2$
120	$.4440E-2$	$-.3977E-2$	$.3448E-2$
130	$.4451E-2$	$-.4123E-2$	$.3438E-2$
140	$.4463E-2$	$-.4257E-2$	$.3429E-2$
150	$.4476E-2$	$-.4379E-2$	$.3419E-2$
160	$.4490E-2$	$-.4493E-2$	$.3410E-2$
170	$.4505E-2$	$-.4599E-2$	$.3401E-2$
180	$.4521E-2$	$-.4697E-2$	$.3393E-2$
200	$.4554E-2$	$-.4877E-2$	$.3377E-2$
300	$.4741E-2$	$-.5513E-2$	$.3317E-2$

Table D.12. Dislocation Love numbers of a 45° dip-slip faulting at depth of 400 *km*

n	$\bar{h}_n^d(3,0)$	$\bar{l}_n^d(3,0)$	$\bar{k}_n^d(3,0)$
0	$.1260E-1$	$.0000E+0$	$.0000E+0$
1	$.4036E-1$	$.8839E-1$	$.0000E+0$
2	$-.9849E-3$	$.3769E-1$	$-.1631E-1$
3	$.5241E-2$	$.2799E-1$	$-.3525E-2$
4	$.8634E-2$	$.1975E-1$	$.2375E-2$
5	$.9701E-2$	$.1425E-1$	$.4725E-2$
6	$.9863E-2$	$.1061E-1$	$.5686E-2$
8	$.9590E-2$	$.6150E-2$	$.6355E-2$
10	$.9338E-2$	$.3413E-2$	$.6614E-2$
15	$.9196E-2$	$-.5595E-3$	$.7010E-2$
20	$.9340E-2$	$-.2813E-2$	$.7313E-2$
25	$.9540E-2$	$-.4310E-2$	$.7552E-2$
30	$.9727E-2$	$-.5393E-2$	$.7735E-2$
35	$.9884E-2$	$-.6222E-2$	$.7871E-2$
40	$.1001E-1$	$-.6883E-2$	$.7972E-2$
45	$.1011E-1$	$-.7428E-2$	$.8047E-2$
50	$.1020E-1$	$-.7890E-2$	$.8101E-2$
60	$.1034E-1$	$-.8641E-2$	$.8170E-2$
70	$.1044E-1$	$-.9239E-2$	$.8203E-2$
80	$.1052E-1$	$-.9738E-2$	$.8217E-2$
90	$.1060E-1$	$-.1016E-1$	$.8218E-2$
100	$.1066E-1$	$-.1055E-1$	$.8212E-2$
110	$.1072E-1$	$-.1089E-1$	$.8202E-2$
120	$.1078E-1$	$-.1122E-1$	$.8192E-2$
130	$.1085E-1$	$-.1155E-1$	$.8184E-2$
140	$.1094E-1$	$-.1193E-1$	$.8187E-2$
150	$.1108E-1$	$-.1244E-1$	$.8216E-2$
160	$.1099E-1$	$-.1222E-1$	$.8121E-2$

Table D.13. Dislocation Love numbers of a tensile faulting at depth of $2\,km$

n	$\bar{h}_n^d(4,0)$	$\bar{l}_n^d(4,0)$	$\bar{k}_n^d(4,0)$
0	$.7962E-1$	$.0000E+0$	$.0000E+0$
1	$.2389E+0$	$-.1455E-3$	$.0000E+0$
2	$.9959E-1$	$-.8120E-4$	$.4088E-4$
3	$.6198E-1$	$-.7333E-4$	$.3421E-4$
4	$.4484E-1$	$-.6783E-4$	$.3140E-4$
5	$.3508E-1$	$-.6435E-4$	$.3034E-4$
6	$.2880E-1$	$-.6206E-4$	$.2991E-4$
8	$.2120E-1$	$-.5927E-4$	$.2964E-4$
10	$.1677E-1$	$-.5761E-4$	$.2958E-4$
15	$.1102E-1$	$-.5538E-4$	$.2958E-4$
20	$.8212E-2$	$-.5428E-4$	$.2962E-4$
30	$.5447E-2$	$-.5322E-4$	$.2967E-4$
40	$.4081E-2$	$-.5273E-4$	$.2969E-4$
50	$.3267E-2$	$-.5246E-4$	$.2969E-4$
70	$.2341E-2$	$-.5220E-4$	$.2967E-4$
100	$.1650E-2$	$-.5207E-4$	$.2966E-4$
200	$.8489E-3$	$-.5201E-4$	$.2969E-4$
300	$.5827E-3$	$-.5193E-4$	$.2982E-4$
400	$.4500E-3$	$-.5184E-4$	$.3002E-4$
500	$.3705E-3$	$-.5179E-4$	$.3025E-4$
800	$.2516E-3$	$-.5183E-4$	$.3079E-4$
1000	$.2118E-3$	$-.5183E-4$	$.3092E-4$
1200	$.1850E-3$	$-.5173E-4$	$.3087E-4$
1400	$.1657E-3$	$-.5152E-4$	$.3072E-4$
1600	$.1511E-3$	$-.5125E-4$	$.3052E-4$
1800	$.1396E-3$	$-.5099E-4$	$.3031E-4$
2000	$.1305E-3$	$-.5076E-4$	$.3014E-4$
2200	$.1230E-3$	$-.5056E-4$	$.3000E-4$
2400	$.1167E-3$	$-.5041E-4$	$.2989E-4$
2600	$.1115E-3$	$-.5030E-4$	$.2982E-4$
2800	$.1070E-3$	$-.5022E-4$	$.2976E-4$
3000	$.1032E-3$	$-.5017E-4$	$.2973E-4$
3500	$.9555E-4$	$-.5009E-4$	$.2968E-4$
4000	$.8983E-4$	$-.5006E-4$	$.2966E-4$
4500	$.8540E-4$	$-.5004E-4$	$.2966E-4$
5000	$.8185E-4$	$-.5004E-4$	$.2966E-4$
7000	$.7275E-4$	$-.5002E-4$	$.2966E-4$
10000	$.6592E-4$	$-.5001E-4$	$.2966E-4$
15000	$.6061E-4$	$-.5000E-4$	$.2966E-4$
20000	$.5795E-4$	$-.5000E-4$	$.2966E-4$
25000	$.5636E-4$	$-.5000E-4$	$.2966E-4$
30000	$.5530E-4$	$-.5000E-4$	$.2966E-4$
35000	$.5456E-4$	$-.5000E-4$	$.2966E-4$

Table D.14. Dislocation Love numbers of a tensile faulting at depth of $20\,km$

n	$\bar{h}_n^d(4,0)$	$\bar{l}_n^d(4,0)$	$\bar{k}_n^d(4,0)$
0	$.8002E-1$	$.0000E+0$	$.0000E+0$
1	$.2403E+0$	$-.1365E-2$	$.0000E+0$
2	$.1007E+0$	$-.7351E-3$	$.4574E-3$
3	$.6283E-1$	$-.6746E-3$	$.4055E-3$
4	$.4557E-1$	$-.6339E-3$	$.3844E-3$
5	$.3575E-1$	$-.6089E-3$	$.3763E-3$
6	$.2942E-1$	$-.5930E-3$	$.3729E-3$
8	$.2178E-1$	$-.5744E-3$	$.3705E-3$
10	$.1732E-1$	$-.5642E-3$	$.3697E-3$
15	$.1154E-1$	$-.5529E-3$	$.3693E-3$
20	$.8719E-2$	$-.5496E-3$	$.3693E-3$
30	$.5941E-2$	$-.5508E-3$	$.3690E-3$
40	$.4569E-2$	$-.5556E-3$	$.3685E-3$
50	$.3753E-2$	$-.5616E-3$	$.3678E-3$
70	$.2826E-2$	$-.5748E-3$	$.3665E-3$
100	$.2137E-2$	$-.5948E-3$	$.3647E-3$
200	$.1352E-2$	$-.6484E-3$	$.3598E-3$
300	$.1106E-2$	$-.6811E-3$	$.3581E-3$
400	$.9971E-3$	$-.7004E-3$	$.3610E-3$
500	$.9433E-3$	$-.7133E-3$	$.3683E-3$
800	$.9087E-3$	$-.7476E-3$	$.4065E-3$
1000	$.9214E-3$	$-.7734E-3$	$.4351E-3$
1200	$.9381E-3$	$-.7984E-3$	$.4603E-3$
1400	$.9513E-3$	$-.8197E-3$	$.4799E-3$
1600	$.9591E-3$	$-.8359E-3$	$.4939E-3$
1800	$.9620E-3$	$-.8473E-3$	$.5033E-3$
2000	$.9612E-3$	$-.8549E-3$	$.5092E-3$
2200	$.9581E-3$	$-.8597E-3$	$.5127E-3$
2400	$.9540E-3$	$-.8626E-3$	$.5148E-3$
2600	$.9494E-3$	$-.8643E-3$	$.5159E-3$
2800	$.9448E-3$	$-.8654E-3$	$.5166E-3$
3000	$.9406E-3$	$-.8662E-3$	$.5170E-3$
3500	$.9313E-3$	$-.8672E-3$	$.5173E-3$

Table D.15. Dislocation Love numbers of a tensile faulting at depth of 200 *km*

n	$\bar{h}_n^d(4,0)$	$\bar{l}_n^d(4,0)$	$\bar{k}_n^d(4,0)$
0	$.8397E-1$	$.0000E+0$	$.0000E+0$
1	$.2543E+0$	$-.1309E-1$	$.0000E+0$
2	$.1116E+0$	$-.6914E-2$	$.5194E-2$
3	$.7137E-1$	$-.6511E-2$	$.4865E-2$
4	$.5309E-1$	$-.6274E-2$	$.4772E-2$
5	$.4274E-1$	$-.6149E-2$	$.4757E-2$
6	$.3609E-1$	$-.6080E-2$	$.4763E-2$
8	$.2809E-1$	$-.6013E-2$	$.4792E-2$
10	$.2345E-1$	$-.5992E-2$	$.4827E-2$
15	$.1750E-1$	$-.6022E-2$	$.4915E-2$
20	$.1462E-1$	$-.6091E-2$	$.4978E-2$
25	$.1292E-1$	$-.6163E-2$	$.5011E-2$
30	$.1179E-1$	$-.6229E-2$	$.5022E-2$
35	$.1098E-1$	$-.6290E-2$	$.5019E-2$
40	$.1036E-1$	$-.6346E-2$	$.5006E-2$
45	$.9883E-1$	$-.6398E-2$	$.4988E-2$
50	$.9494E-2$	$-.6448E-2$	$.4966E-2$
60	$.8902E-2$	$-.6542E-2$	$.4917E-2$
70	$.8476E-2$	$-.6630E-2$	$.4869E-2$
80	$.8156E-2$	$-.6717E-2$	$.4823E-2$
90	$.7910E-2$	$-.6802E-2$	$.4781E-2$
100	$.7717E-2$	$-.6886E-2$	$.4744E-2$
110	$.7563E-2$	$-.6970E-2$	$.4711E-2$
120	$.7439E-2$	$-.7053E-2$	$.4681E-2$
130	$.7339E-2$	$-.7135E-2$	$.4655E-2$
140	$.7257E-2$	$-.7214E-2$	$.4630E-2$
150	$.7190E-2$	$-.7293E-2$	$.4608E-2$
160	$.7135E-2$	$-.7369E-2$	$.4588E-2$
170	$.7090E-2$	$-.7442E-2$	$.4570E-2$
180	$.7054E-2$	$-.7514E-2$	$.4553E-2$
200	$.7001E-2$	$-.7650E-2$	$.4523E-2$
300	$.6954E-2$	$-.8159E-2$	$.4415E-2$

Table D.16. Dislocation Love numbers of a tensile faulting at depth of 400 *km*

n	$\bar{h}_n^d(4,0)$	$\bar{l}_n^d(4,0)$	$\bar{k}_n^d(4,0)$
0	$.8791E-1$	$.0000E+0$	$.0000E+0$
1	$.2689E+0$	$-.2612E-1$	$.0000E+0$
2	$.1235E+0$	$-.1438E-1$	$.1045E-1$
3	$.8104E-1$	$-.1373E-1$	$.9993E-2$
4	$.6190E-1$	$-.1344E-1$	$.9975E-2$
5	$.5115E-1$	$-.1335E-1$	$.1006E-1$
6	$.4430E-1$	$-.1333E-1$	$.1015E-1$
8	$.3611E-1$	$-.1336E-1$	$.1032E-1$
10	$.3145E-1$	$-.1343E-1$	$.1049E-1$
15	$.2569E-1$	$-.1374E-1$	$.1093E-1$
20	$.2307E-1$	$-.1410E-1$	$.1129E-1$
25	$.2158E-1$	$-.1443E-1$	$.1153E-1$
30	$.2059E-1$	$-.1472E-1$	$.1168E-1$
35	$.1987E-1$	$-.1495E-1$	$.1176E-1$
40	$.1931E-1$	$-.1516E-1$	$.1179E-1$
45	$.1886E-1$	$-.1535E-1$	$.1180E-1$
50	$.1850E-1$	$-.1552E-1$	$.1179E-1$
60	$.1793E-1$	$-.1584E-1$	$.1174E-1$
70	$.1752E-1$	$-.1614E-1$	$.1167E-1$
80	$.1721E-1$	$-.1641E-1$	$.1160E-1$
90	$.1697E-1$	$-.1668E-1$	$.1152E-1$
100	$.1679E-1$	$-.1694E-1$	$.1146E-1$
110	$.1665E-1$	$-.1719E-1$	$.1139E-1$
120	$.1655E-1$	$-.1745E-1$	$.1133E-1$
130	$.1648E-1$	$-.1772E-1$	$.1128E-1$
140	$.1645E-1$	$-.1806E-1$	$.1124E-1$
150	$.1643E-1$	$-.1852E-1$	$.1119E-1$
160	$.1598E-1$	$-.1791E-1$	$.1087E-1$

Appendix E
Tables of Deformations Raised by Dislocations

In this Appendix we give the numerical results of the study, i.e. the radial displacement ($\hat{u}_r^{(i)}(a, \theta)$), the potential change ($\widehat{\psi}^{(i)}(a, \theta)$), the gravity change ($\Delta\hat{g}^{(i)}(a, \theta)$) at a space-fixed point, and the gravity change ($\delta\hat{g}^{(i)}(a, \theta)$) at the free surface of the earth, where superscript i indicates the four types of dislocations: vertical strike-slip, vertical dip-slip, 45° dip-slip, and vertical tensile fracturing.

Again, we introduce practical formulas (4.118)−(4.132) for convenient applications.

Let the point dislocation be at $D(\theta_1, \phi_1)$ and the observation point be at $P(\theta_2, \phi_2)$ in Figure 4.6. The angular distance between $D(\theta_1, \phi_1)$ and $P(\theta_2, \phi_2)$ is denoted by φ. The fault plane is defined by its strike azimuth, z_1, on the earth's surface, measured here clockwise from north. The azimuth of the calculating point, with respect to point $D(\theta_1, \phi_1)$, is denoted as z_2, measured

clockwise from the north. The azimuth z of P with respect to the fault line is

$$z = z_1 - z_2. \tag{E.1}$$

We can obtain φ and the z_2 from following formulas:

$$\cos\varphi = \cos\theta_1 \cos\theta_2 + \sin\theta_1 \sin\theta_2 \cos(\phi_2 - \phi_1) \tag{E.2}$$

$$\sin z_2 = \frac{1}{\sin\varphi}\sin\theta_1 \sin(\phi_2 - \phi_1). \tag{E.3}$$

We therefore have the following:

Shear Dislocation:

$$\begin{aligned} u_r^{(s)}(a, \varphi, z) = {} & \cos\lambda\{-\hat{u}_r^{(1)}(a, \varphi) \sin\delta \sin 2z \\ & + \hat{u}_r^{(2)}(a, \varphi) \cos\delta \cos z\} \\ & + \sin\lambda\left\{\sin 2\delta\left[\frac{1}{2}\hat{u}_r^{(1)}(a, \varphi) \cos 2z + \hat{u}_r^{(30)}(a, \varphi)\right]\right. \\ & \left. + \hat{u}_r^{(2)}(a, \varphi) \cos 2\delta \sin z\right\} \end{aligned} \tag{E.4}$$

$$\begin{aligned} \psi^{(s)}(a, \varphi, z) = {} & \cos\lambda\{-\widehat{\psi}^{(1)}(a, \varphi) \sin\delta \sin 2z \\ & + \widehat{\psi}^{(2)}(a, \varphi) \cos\delta \cos z\} \\ & + \sin\lambda\left\{\sin 2\delta\left[\frac{1}{2}\widehat{\psi}^{(1)}(a, \varphi) \cos 2z + \widehat{\psi}^{(30)}(a, \varphi)\right]\right. \\ & \left. + \widehat{\psi}^{(2)}(a, \varphi) \cos 2\delta \sin z\right\} \end{aligned} \tag{E.5}$$

$$\begin{aligned} \Delta g^{(s)}(a, \varphi, z) = {} & \cos\lambda\{-\Delta\hat{g}^{(1)}(a, \varphi) \sin\delta \sin 2z \\ & + \Delta\hat{g}^{(2)}(a, \varphi) \cos\delta \cos z\} \\ & + \sin\lambda\left\{\sin 2\delta\left[\frac{1}{2}\Delta\hat{g}^{(1)}(a, \varphi) \cos 2z + \Delta\hat{g}^{(30)}(a, \varphi)\right]\right. \\ & \left. + \Delta\hat{g}^{(2)}(a, \varphi) \cos 2\delta \sin z\right\} \end{aligned} \tag{E.6}$$

$$\begin{aligned} \delta g^{(s)}(a, \varphi, z) = {} & \cos\lambda\{-\delta\hat{g}^{(1)}(a, \varphi) \sin\delta \sin 2z \\ & + \delta\hat{g}^{(2)}(a, \varphi) \cos\delta \cos z\} \\ & + \sin\lambda\left\{\sin 2\delta\left[\frac{1}{2}\delta\hat{g}^{(1)}(a, \varphi) \cos 2z + \delta\hat{g}^{(30)}(a, \varphi)\right]\right. \\ & \left. + \delta\hat{g}^{(2)}(a, \varphi) \cos 2\delta \sin z\right\}. \end{aligned} \tag{E.7}$$

Tensile Dislocation:

$$\begin{aligned} u_r^{(t)}(a, \varphi, z) = {} & \hat{u}_r^{(4)}(a, \varphi) - 2\sin^2\delta\left(\hat{u}_r^{(30)}(a, \varphi) + \frac{1}{2}\hat{u}_r^{(1)}(a, \varphi)\cos 2z\right) \\ & -\hat{u}_r^{(2)}(a, \varphi) \sin 2\delta \sin z \end{aligned} \tag{E.8}$$

$$\psi^{(t)}(a, \varphi, z) = \widehat{\psi}^{(4)}(a, \varphi) - 2\sin^2\delta\left(\widehat{\psi}^{(30)}(a, \varphi) + \frac{1}{2}\widehat{\psi}^{(1)}(a, \varphi)\cos 2z\right) - \widehat{\psi}^{(2)}(a, \varphi)\sin 2\delta \sin z \tag{E.9}$$

$$\Delta g^{(t)}(a, \varphi, z) = \Delta\hat{g}^{(4)}(a, \varphi) - 2\sin^2\delta\left(\Delta\hat{g}^{(30)}(a, \varphi) + \frac{1}{2}\Delta\hat{g}^{(1)}(a, \varphi)\cos 2z\right) - \Delta\hat{g}^{(2)}(a, \varphi)\sin 2\delta \sin z \tag{E.10}$$

$$\delta g^{(t)}(a, \varphi, z) = \delta\hat{g}^{(4)}(a, \varphi) - 2\sin^2\delta\left(\delta\hat{g}^{(30)}(a, \varphi) + \frac{1}{2}\delta\hat{g}^{(1)}(a, \varphi)\cos 2z\right) - \delta\hat{g}^{(2)}(a, \varphi)\sin 2\delta \sin z. \tag{E.11}$$

Explosion:

$$u_r^{(e)}(a, \varphi, z) = 3\hat{u}_r^{(4)}(a, \varphi) - 4\hat{u}_r^{(30)}(a, \varphi) \tag{E.12}$$

$$\psi^{(e)}(a, \varphi, z) = 3\widehat{\psi}^{(4)}(a, \varphi) - 4\widehat{\psi}^{(30)}(a, \varphi) \tag{E.13}$$

$$\Delta g^{(e)}(a, \varphi, z) = 3\Delta\hat{g}^{(4)}(a, \varphi) - 4\Delta\hat{g}^{(30)}(a, \varphi) \tag{E.14}$$

$$\delta g^{(e)}(a, \varphi, z) = 3\delta\hat{g}^{(4)}(a, \varphi) - 4\delta\hat{g}^{(30)}(a, \varphi). \tag{E.15}$$

Notice that φ in $(E.4)-(E.15)$ corresponds θ in following tables for practical applications. On the other hand, the results listed in the tables of this appendix are dimensionless. The final results should be obtained as follows:

$$\hat{u}_r^{Actual}(a, \theta) = \hat{u}_r^{Table}(a, \theta)\frac{UdS}{a^2},$$

$$\widehat{\psi}^{Actual}(a, \theta) = \widehat{\psi}^{\text{Table}}(a, \theta)\frac{g_0 UdS}{a^2},$$

$$\Delta\hat{g}^{Actual}(a, \theta) = \Delta\hat{g}^{\text{Table}}(a, \theta)\frac{g_0 UdS}{a^3},$$

$$\delta\hat{g}^{Actual}(a, \theta) = \delta\hat{g}^{\text{Table}}(a, \theta)\frac{g_0 UdS}{a^3},$$

where a is the radius of the earth, g_0 the gravity on the earth's surface, and U the amplitude of an actual dislocation on the fault plane area, d_s.

Table E.1. Radial displacement $\hat{u}_r^{(1)}(a, \theta)$ caused by a vertical strike-slip faulting

$\theta(\circ)$	$d_s = 0km$	$d_s = 2km$	$d_s = 5km$	$d_s = 10km$	$d_s = 20km$	$d_s = 32km$
.0000	—	$.000E+0$	$.000E+0$	$.000E+0$	$.000E+0$	$.000E+0$
.0001	$-.226E$ 11	$.660E+2$	$.171E+1$	$.898E-1$	$.919E-2$	$.130E-2$
.0010	$-.226E+9$	$.655E+4$	$.171E+3$	$.898E+1$	$.919E+0$	$.130E+0$
.0100	$-.226E+7$	$.331E+6$	$.151E+5$	$.869E+3$	$.912E+2$	$.130E+2$
.0200	$-.563E+6$	$.318E+6$	$.430E+5$	$.315E+4$	$.356E+3$	$.514E+2$
.0300	$-.250E+6$	$.168E+6$	$.599E+5$	$.603E+4$	$.770E+3$	$.114E+3$
.0400	$-.141E+6$	$.809E+5$	$.598E+5$	$.862E+4$	$.130E+4$	$.198E+3$
.0600	$-.581E+5$	$.182E+5$	$.418E+5$	$.112E+5$	$.249E+4$	$.419E+3$
.0800	$-.311E+5$	$.339E+4$	$.249E+5$	$.993E+4$	$.358E+4$	$.684E+3$
.1000	$-.155E+5$	$-.151E+3$	$.144E+5$	$.753E+4$	$.431E+4$	$.959E+3$
.1600	$-.333E+4$	$-.472E+3$	$.275E+4$	$.200E+4$	$.415E+4$	$.157E+4$
.2000	$-.129E+4$	$-.274E+3$	$.813E+3$	$.628E+3$	$.319E+4$	$.172E+4$
.2500	$-.155E+3$	$-.269E+3$	$.403E+2$	$.500E+2$	$.204E+4$	$.158E+4$
.3000	$-.428E+3$	$-.305E+3$	$-.167E+3$	$-.105E+3$	$.118E+4$	$.134E+4$
.4000	$-.310E+3$	$-.292E+3$	$-.220E+3$	$-.144E+3$	$.344E+3$	$.841E+3$
.5000	$-.271E+3$	$-.231E+3$	$-.186E+3$	$-.128E+3$	$.280E+2$	$.474E+3$
.6000	$-.199E+3$	$-.176E+3$	$-.147E+3$	$-.105E+3$	$-.861E+2$	$.261E+3$
.8000	$-.115E+3$	$-.105E+3$	$-.916E+2$	$-.703E+2$	$-.142E+3$	$.534E+2$
1.0000	$-.717E+2$	$-.672E+2$	$-.602E+2$	$-.486E+2$	$-.131E+3$	$-.144E+2$
1.2000	$-.492E+2$	$-.460E+2$	$-.419E+2$	$-.351E+2$	$-.109E+3$	$-.358E+2$
1.6000	$-.262E+2$	$-.249E+2$	$-.232E+2$	$-.203E+2$	$-.727E+2$	$-.392E+2$
2.0000	$-.158E+2$	$-.152E+2$	$-.143E+2$	$-.128E+2$	$-.495E+2$	$-.321E+2$
2.5000	$-.931E+1$	$-.903E+1$	$-.860E+1$	$-.788E+1$	$-.320E+2$	$-.231E+2$
3.0000	$-.597E+1$	$-.578E+1$	$-.554E+1$	$-.514E+1$	$-.216E+2$	$-.166E+2$
4.0000	$-.276E+1$	$-.270E+1$	$-.261E+1$	$-.246E+1$	$-.107E+2$	$-.883E+1$
5.0000	$-.143E+1$	$-.141E+1$	$-.137E+1$	$-.131E+1$	$-.584E+1$	$-.498E+1$
6.0000	$-.815E+0$	$-.804E+0$	$-.784E+0$	$-.752E+0$	$-.341E+1$	$-.298E+1$
7.0000	$-.498E+0$	$-.488E+0$	$-.478E+0$	$-.460E+0$	$-.211E+1$	$-.187E+1$
8.0000	$-.321E+0$	$-.314E+0$	$-.308E+0$	$-.298E+0$	$-.137E+1$	$-.123E+1$
9.0000	$-.216E+0$	$-.213E+0$	$-.209E+0$	$-.203E+0$	$-.940E+0$	$-.852E+0$
10.0000	$-.153E+0$	$-.152E+0$	$-.149E+0$	$-.145E+0$	$-.675E+0$	$-.616E+0$
12.0000	$-.880E-1$	$-.874E-1$	$-.861E-1$	$-.839E-1$	$-.394E+0$	$-.364E+0$
16.0000	$-.424E-1$	$-.421E-1$	$-.416E-1$	$-.408E-1$	$-.194E+0$	$-.182E+0$
20.0000	$-.263E-1$	$-.261E-1$	$-.258E-1$	$-.254E-1$	$-.121E+0$	$-.115E+0$
25.0000	$-.167E-1$	$-.165E-1$	$-.164E-1$	$-.162E-1$	$-.777E-1$	$-.742E-1$
30.0000	$-.117E-1$	$-.115E-1$	$-.114E-1$	$-.112E-1$	$-.541E-1$	$-.518E-1$
40.0000	$-.613E-2$	$-.604E-2$	$-.599E-2$	$-.590E-2$	$-.284E-1$	$-.271E-1$
50.0000	$-.263E-2$	$-.254E-2$	$-.251E-2$	$-.245E-2$	$-.116E-1$	$-.108E-1$
60.0000	$.682E-4$	$.146E-3$	$.170E-3$	$.209E-3$	$.142E-2$	$.190E-2$
70.0000	$.208E-2$	$.208E-2$	$.209E-2$	$.212E-2$	$.108E-1$	$.110E-1$
80.0000	$.317E-2$	$.322E-2$	$.323E-2$	$.325E-2$	$.163E-1$	$.163E-1$
90.0000	$.362E-2$	$.365E-2$	$.366E-2$	$.367E-2$	$.183E-1$	$.183E-1$
100.0000	$.356E-2$	$.357E-2$	$.358E-2$	$.359E-2$	$.178E-1$	$.178E-1$
110.0000	$.314E-2$	$.317E-2$	$.317E-2$	$.318E-2$	$.158E-1$	$.157E-1$
120.0000	$.256E-2$	$.257E-2$	$.257E-2$	$.258E-2$	$.128E-1$	$.127E-1$
130.0000	$.192E-2$	$.191E-2$	$.191E-2$	$.191E-2$	$.950E-2$	$.944E-2$
140.0000	$.131E-2$	$.129E-2$	$.129E-2$	$.129E-2$	$.642E-2$	$.638E-2$
150.0000	$.717E-3$	$.754E-3$	$.754E-3$	$.755E-3$	$.374E-2$	$.372E-2$
160.0000	$.278E-3$	$.333E-3$	$.333E-3$	$.333E-3$	$.165E-2$	$.164E-2$
170.0000	$.608E-4$	$.794E-4$	$.795E-4$	$.796E-4$	$.395E-3$	$.393E-3$
180.0000	$.000E+0$	$.000E+0$	$.000E+0$	$.000E+0$	$.000E+0$	$.000E+0$

(to be continued)

(continued)

$\theta(\circ)$	$d_s = 64km$	$d_s = 100km$	$d_s = 200km$	$d_s = 300km$	$d_s = 400km$	$d_s = 637km$
.0000	$.000E+0$	$.000E+0$	$.000E+0$	$.000E+0$	$.000E+0$	$.000E+0$
.0001	$.735E-4$	$.117E-4$	$.707E-6$	$.142E-6$	$.473E-7$	$.776E-8$
.0010	$.735E-2$	$.117E-2$	$.707E-4$	$.142E-4$	$.473E-5$	$.776E-6$
.0100	$.734E+0$	$.117E+0$	$.707E-2$	$.142E-2$	$.473E-3$	$.776E-4$
.0200	$.293E+1$	$.468E+0$	$.283E-1$	$.566E-2$	$.189E-2$	$.310E-3$
.0300	$.657E+1$	$.105E+1$	$.636E-1$	$.127E-1$	$.425E-2$	$.698E-3$
.0400	$.116E+2$	$.187E+1$	$.113E+0$	$.226E-1$	$.756E-2$	$.124E-2$
.0600	$.257E+2$	$.418E+1$	$.254E+0$	$.509E-1$	$.170E-1$	$.279E-2$
.0800	$.448E+2$	$.736E+1$	$.450E+0$	$.904E-1$	$.302E-1$	$.496E-2$
.1000	$.681E+2$	$.114E+2$	$.702E+0$	$.141E+0$	$.472E-1$	$.775E-2$
.1600	$.155E+3$	$.278E+2$	$.178E+1$	$.360E+0$	$.120E+0$	$.198E-1$
.2000	$.219E+3$	$.416E+2$	$.275E+1$	$.559E+0$	$.188E+0$	$.309E-1$
.2500	$.291E+3$	$.609E+2$	$.422E+1$	$.868E+0$	$.292E+0$	$.483E-1$
.3000	$.347E+3$	$.810E+2$	$.597E+1$	$.124E+1$	$.419E+0$	$.694E-1$
.4000	$.404E+3$	$.118E+3$	$.101E+2$	$.215E+1$	$.735E+0$	$.123E+0$
.5000	$.382E+3$	$.146E+3$	$.148E+2$	$.327E+1$	$.113E+1$	$.191E+0$
.6000	$.336E+3$	$.161E+3$	$.198E+2$	$.455E+1$	$.160E+1$	$.272E+0$
.8000	$.225E+3$	$.156E+3$	$.291E+2$	$.743E+1$	$.270E+1$	$.475E+0$
1.0000	$.136E+3$	$.132E+3$	$.362E+2$	$.104E+2$	$.397E+1$	$.723E+0$
1.2000	$.812E+2$	$.104E+3$	$.405E+2$	$.132E+2$	$.530E+1$	$.101E+1$
1.6000	$.253E+2$	$.577E+2$	$.401E+2$	$.172E+2$	$.783E+1$	$.166E+1$
2.0000	$.555E+1$	$.308E+2$	$.346E+2$	$.190E+2$	$.975E+1$	$.236E+1$
2.5000	$-.242E+1$	$.139E+2$	$.259E+2$	$.179E+2$	$.111E+2$	$.318E+1$
3.0000	$-.438E+1$	$.635E+1$	$.182E+2$	$.157E+2$	$.115E+2$	$.385E+1$
4.0000	$-.399E+1$	$.828E+0$	$.869E+1$	$.103E+2$	$.929E+1$	$.460E+1$
5.0000	$-.275E+1$	$-.429E+0$	$.420E+1$	$.633E+1$	$.686E+1$	$.449E+1$
6.0000	$-.183E+1$	$-.609E+0$	$.214E+1$	$.380E+1$	$.473E+1$	$.401E+1$
7.0000	$-.123E+1$	$-.545E+0$	$.111E+1$	$.233E+1$	$.323E+1$	$.337E+1$
8.0000	$-.855E+0$	$-.442E+0$	$.590E+0$	$.144E+1$	$.217E+1$	$.274E+1$
9.0000	$-.614E+0$	$-.352E+0$	$.317E+0$	$.922E+0$	$.149E+1$	$.216E+1$
10.0000	$-.457E+0$	$-.283E+0$	$.162E+0$	$.591E+0$	$.102E+1$	$.171E+1$
12.0000	$-.283E+0$	$-.195E+0$	$.295E-1$	$.258E+0$	$.516E+0$	$.108E+1$
16.0000	$-.150E+0$	$-.117E+0$	$-.340E-1$	$.477E-1$	$.152E+0$	$.466E+0$
20.0000	$-.982E-1$	$-.806E-1$	$-.384E-1$	$.162E-2$	$.539E-1$	$.238E+0$
25.0000	$-.646E-1$	$-.547E-1$	$-.315E-1$	$-.104E-1$	$.166E-1$	$.124E+0$
30.0000	$-.454E-1$	$-.390E-1$	$-.240E-1$	$-.106E-1$	$.631E-2$	$.759E-1$
40.0000	$-.236E-1$	$-.200E-1$	$-.117E-1$	$-.402E-2$	$.600E-2$	$.478E-1$
50.0000	$-.873E-2$	$-.653E-2$	$-.104E-2$	$.487E-2$	$.133E-1$	$.464E-1$
60.0000	$.308E-2$	$.434E-2$	$.801E-2$	$.132E-1$	$.211E-1$	$.504E-1$
70.0000	$.115E-1$	$.121E-1$	$.145E-1$	$.191E-1$	$.267E-1$	$.532E-1$
80.0000	$.164E-1$	$.165E-1$	$.180E-1$	$.220E-1$	$.291E-1$	$.525E-1$
90.0000	$.181E-1$	$.180E-1$	$.188E-1$	$.223E-1$	$.286E-1$	$.487E-1$
100.0000	$.175E-1$	$.173E-1$	$.177E-1$	$.206E-1$	$.259E-1$	$.426E-1$
110.0000	$.154E-1$	$.151E-1$	$.153E-1$	$.176E-1$	$.219E-1$	$.351E-1$
120.0000	$.124E-1$	$.122E-1$	$.123E-1$	$.140E-1$	$.173E-1$	$.273E-1$
130.0000	$.924E-2$	$.904E-2$	$.906E-2$	$.103E-1$	$.127E-1$	$.197E-1$
140.0000	$.620E-2$	$.606E-2$	$.605E-2$	$.685E-2$	$.840E-2$	$.130E-1$
150.0000	$.360E-2$	$.352E-2$	$.351E-2$	$.396E-2$	$.485E-2$	$.747E-2$
160.0000	$.164E-2$	$.160E-2$	$.159E-2$	$.179E-2$	$.219E-2$	$.336E-2$
170.0000	$.414E-3$	$.404E-3$	$.401E-3$	$.452E-3$	$.553E-3$	$.845E-3$
180.0000	$.000E+0$	$.000E+0$	$.000E+0$	$.000E+0$	$.000E+0$	$.000E+0$

Table E.2. Radial displacement $\hat{u}_r^{(2)}(a, \theta)$ caused by a vertical dip-slip faulting

$\theta(^\circ)$	$d_s = 0km$	$d_s = 2km$	$d_s = 5km$	$d_s = 10km$	$d_s = 20km$	$d_s = 32km$
.0000	$.000E+0$	$.000E+0$	$.000E+0$	$.000E+0$	$.000E+0$	$.000E+0$
.0001	$.000E+0$	$.268E+5$	$.168E+4$	$.207E+3$	$.377E+2$	$.843E+1$
.0010	$.000E+0$	$.266E+6$	$.168E+5$	$.207E+4$	$.377E+3$	$.843E+2$
.0100	$.000E+0$	$.139E+7$	$.149E+6$	$.201E+5$	$.374E+4$	$.840E+3$
.0200	$.000E+0$	$.718E+6$	$.213E+6$	$.368E+5$	$.730E+4$	$.166E+4$
.0300	$.000E+0$	$.286E+6$	$.197E+6$	$.478E+5$	$.105E+5$	$.246E+4$
.0400	$.000E+0$	$.119E+6$	$.149E+6$	$.529E+5$	$.132E+5$	$.320E+4$
.0600	$.000E+0$	$.239E+5$	$.674E+5$	$.490E+5$	$.169E+5$	$.451E+4$
.0800	$.000E+0$	$.359E+4$	$.270E+5$	$.375E+5$	$.183E+5$	$.552E+4$
.1000	$.000E+0$	$-.148E+4$	$.102E+5$	$.260E+5$	$.179E+5$	$.618E+4$
.1600	$.000E+0$	$-.124E+4$	$.588E+3$	$.715E+4$	$.112E+5$	$.648E+4$
.2000	$.000E+0$	$-.307E+3$	$.437E+3$	$.312E+4$	$.728E+4$	$.591E+4$
.2500	$.000E+0$	$.836E+2$	$.437E+3$	$.132E+4$	$.409E+4$	$.434E+4$
.3000	$.000E+0$	$.115E+3$	$.319E+3$	$.675E+3$	$.241E+4$	$.323E+4$
.4000	$.000E+0$	$.451E+2$	$.116E+3$	$.227E+3$	$.952E+3$	$.170E+4$
.5000	$.000E+0$	$.142E+2$	$.389E+2$	$.813E+2$	$.433E+3$	$.933E+3$
.6000	$.000E+0$	$.428E+1$	$.129E+2$	$.304E+2$	$.215E+3$	$.524E+3$
.8000	$.000E+0$	$-.626E-1$	$.761E+0$	$.419E+1$	$.710E+2$	$.194E+3$
1.0000	$.000E+0$	$-.430E+0$	$-.655E+0$	$.174E-1$	$.265E+2$	$.829E+2$
1.2000	$.000E+0$	$-.360E+0$	$-.686E+0$	$-.683E+0$	$.999E+1$	$.392E+2$
1.6000	$.000E+0$	$-.216E+0$	$-.470E+0$	$-.707E+0$	$.148E+1$	$.102E+2$
2.0000	$.000E+0$	$-.144E+0$	$-.330E+0$	$-.557E+0$	$-.433E+0$	$.200E+1$
2.5000	$.000E+0$	$-.947E-1$	$-.224E+0$	$-.403E+0$	$-.890E+0$	$-.545E+0$
3.0000	$.000E+0$	$-.653E-1$	$-.157E+0$	$-.291E+0$	$-.839E+0$	$-.107E+1$
4.0000	$.000E+0$	$-.331E-1$	$-.806E-1$	$-.154E+0$	$-.533E+0$	$-.880E+0$
5.0000	$.000E+0$	$-.177E-1$	$-.433E-1$	$-.835E-1$	$-.310E+0$	$-.551E+0$
6.0000	$.000E+0$	$-.982E-2$	$-.242E-1$	$-.470E-1$	$-.178E+0$	$-.327E+0$
7.0000	$.000E+0$	$-.567E-2$	$-.140E-1$	$-.273E-1$	$-.104E+0$	$-.193E+0$
8.0000	$.000E+0$	$-.338E-2$	$-.836E-2$	$-.164E-1$	$-.610E-1$	$-.114E+0$
9.0000	$.000E+0$	$-.208E-2$	$-.514E-2$	$-.101E-1$	$-.362E-1$	$-.676E-1$
10.0000	$.000E+0$	$-.131E-2$	$-.325E-2$	$-.638E-2$	$-.216E-1$	$-.398E-1$
12.0000	$.000E+0$	$-.571E-3$	$-.142E-2$	$-.279E-2$	$-.764E-2$	$-.132E-1$
16.0000	$.000E+0$	$-.175E-3$	$-.435E-3$	$-.859E-3$	$-.927E-3$	$-.716E-3$
20.0000	$.000E+0$	$-.956E-4$	$-.238E-3$	$-.473E-3$	$-.128E-3$	$.495E-3$
25.0000	$.000E+0$	$-.634E-4$	$-.158E-3$	$-.315E-3$	$-.802E-5$	$.496E-3$
30.0000	$.000E+0$	$-.494E-4$	$-.124E-3$	$-.246E-3$	$-.188E-4$	$.350E-3$
40.0000	$.000E+0$	$-.408E-4$	$-.102E-3$	$-.204E-3$	$-.199E-3$	$-.163E-3$
50.0000	$.000E+0$	$-.390E-4$	$-.976E-4$	$-.195E-3$	$-.398E-3$	$-.655E-3$
60.0000	$.000E+0$	$-.366E-4$	$-.916E-4$	$-.183E-3$	$-.497E-3$	$-.914E-3$
70.0000	$.000E+0$	$-.332E-4$	$-.830E-4$	$-.165E-3$	$-.511E-3$	$-.975E-3$
80.0000	$.000E+0$	$-.294E-4$	$-.729E-4$	$-.145E-3$	$-.469E-3$	$-.906E-3$
90.0000	$.000E+0$	$-.254E-4$	$-.635E-4$	$-.127E-3$	$-.407E-3$	$-.786E-3$
100.0000	$.000E+0$	$-.223E-4$	$-.557E-4$	$-.111E-3$	$-.348E-3$	$-.668E-3$
110.0000	$.000E+0$	$-.193E-4$	$-.486E-4$	$-.968E-4$	$-.291E-3$	$-.551E-3$
120.0000	$.000E+0$	$-.167E-4$	$-.419E-4$	$-.835E-4$	$-.239E-3$	$-.447E-3$
130.0000	$.000E+0$	$-.142E-4$	$-.357E-4$	$-.712E-4$	$-.195E-3$	$-.361E-3$
140.0000	$.000E+0$	$-.117E-4$	$-.291E-4$	$-.584E-4$	$-.154E-3$	$-.283E-3$
150.0000	$.000E+0$	$-.888E-5$	$-.222E-4$	$-.443E-4$	$-.113E-3$	$-.203E-3$
160.0000	$.000E+0$	$-.589E-5$	$-.151E-4$	$-.302E-4$	$-.757E-4$	$-.136E-3$
170.0000	$.000E+0$	$-.303E-5$	$-.780E-5$	$-.157E-4$	$-.406E-4$	$-.738E-4$
180.0000	$.000E+0$	$.000E+0$	$.000E+0$	$.000E+0$	$.000E+0$	$.000E+0$

(to be continued)

(continued)

θ(°)	$d_s = 64km$	$d_s = 100km$	$d_s = 200km$	$d_s = 300km$	$d_s = 400km$	$d_s = 637km$
.0000	$.000E+0$	$.000E+0$	$.000E+0$	$.000E+0$	$.000E+0$	$.000E+0$
.0001	$.951E+0$	$.235E+0$	$.283E-1$	$.847E-2$	$.379E-2$	$.103E-2$
.0010	$.951E+1$	$.235E+1$	$.283E+0$	$.847E-1$	$.379E-1$	$.103E-1$
.0100	$.950E+2$	$.235E+2$	$.283E+1$	$.847E+0$	$.379E+0$	$.103E+0$
.0200	$.190E+3$	$.469E+2$	$.566E+1$	$.169E+1$	$.758E+0$	$.205E+0$
.0300	$.283E+3$	$.703E+2$	$.849E+1$	$.254E+1$	$.114E+1$	$.308E+0$
.0400	$.376E+3$	$.935E+2$	$.113E+2$	$.339E+1$	$.151E+1$	$.410E+0$
.0600	$.555E+3$	$.139E+3$	$.169E+2$	$.508E+1$	$.227E+1$	$.616E+0$
.0800	$.724E+3$	$.184E+3$	$.225E+2$	$.676E+1$	$.303E+1$	$.821E+0$
.1000	$.881E+3$	$.228E+3$	$.281E+2$	$.844E+1$	$.378E+1$	$.103E+1$
.1600	$.125E+4$	$.348E+3$	$.444E+2$	$.134E+2$	$.603E+1$	$.164E+1$
.2000	$.141E+4$	$.416E+3$	$.550E+2$	$.167E+2$	$.752E+1$	$.205E+1$
.2500	$.151E+4$	$.487E+3$	$.676E+2$	$.207E+2$	$.936E+1$	$.255E+1$
.3000	$.152E+4$	$.540E+3$	$.794E+2$	$.247E+2$	$.112E+2$	$.306E+1$
.4000	$.139E+4$	$.593E+3$	$.101E+3$	$.322E+2$	$.147E+2$	$.406E+1$
.5000	$.106E+4$	$.594E+3$	$.118E+3$	$.390E+2$	$.181E+2$	$.504E+1$
.6000	$.806E+3$	$.563E+3$	$.131E+3$	$.452E+2$	$.213E+2$	$.601E+1$
.8000	$.438E+3$	$.412E+3$	$.144E+3$	$.552E+2$	$.270E+2$	$.785E+1$
1.0000	$.241E+3$	$.289E+3$	$.144E+3$	$.617E+2$	$.316E+2$	$.957E+1$
1.2000	$.134E+3$	$.194E+3$	$.137E+3$	$.650E+2$	$.351E+2$	$.111E+2$
1.6000	$.465E+2$	$.882E+2$	$.999E+2$	$.645E+2$	$.387E+2$	$.138E+2$
2.0000	$.176E+2$	$.406E+2$	$.692E+2$	$.553E+2$	$.388E+2$	$.156E+2$
2.5000	$.522E+1$	$.159E+2$	$.409E+2$	$.427E+2$	$.360E+2$	$.169E+2$
3.0000	$.771E+0$	$.611E+1$	$.239E+2$	$.311E+2$	$.289E+2$	$.171E+2$
4.0000	$-.895E+0$	$.570E+0$	$.810E+1$	$.151E+2$	$.181E+2$	$.152E+2$
5.0000	$-.808E+0$	$-.440E+0$	$.276E+1$	$.729E+1$	$.105E+2$	$.121E+2$
6.0000	$-.546E+0$	$-.505E+0$	$.917E+0$	$.351E+1$	$.601E+1$	$.910E+1$
7.0000	$-.343E+0$	$-.366E+0$	$.282E+0$	$.175E+1$	$.354E+1$	$.662E+1$
8.0000	$-.209E+0$	$-.239E+0$	$.122E+0$	$.966E+0$	$.210E+1$	$.472E+1$
9.0000	$-.125E+0$	$-.147E+0$	$.521E-1$	$.546E+0$	$.133E+1$	$.336E+1$
10.0000	$-.737E-1$	$-.866E-1$	$.341E-1$	$.364E+0$	$.863E+0$	$.242E+1$
12.0000	$-.229E-1$	$-.243E-1$	$.284E-1$	$.189E+0$	$.421E+0$	$.130E+1$
16.0000	$.865E-3$	$.449E-2$	$.274E-1$	$.739E-1$	$.154E+0$	$.458E+0$
20.0000	$.249E-2$	$.537E-2$	$.178E-1$	$.389E-1$	$.742E-1$	$.212E+0$
25.0000	$.192E-2$	$.382E-2$	$.107E-1$	$.213E-1$	$.371E-1$	$.103E+0$
30.0000	$.135E-2$	$.261E-2$	$.687E-2$	$.131E-1$	$.223E-1$	$.612E-1$
40.0000	$-.852E-4$	$.771E-4$	$.765E-3$	$.213E-2$	$.434E-2$	$.157E-1$
50.0000	$-.132E-2$	$-.205E-2$	$-.400E-2$	$-.583E-2$	$-.734E-2$	$-.974E-2$
60.0000	$-.199E-2$	$-.321E-2$	$-.657E-2$	$-.101E-1$	$-.137E-1$	$-.235E-1$
70.0000	$-.218E-2$	$-.354E-2$	$-.735E-2$	$-.115E-1$	$-.159E-1$	$-.282E-1$
80.0000	$-.204E-2$	$-.333E-2$	$-.698E-2$	$-.109E-1$	$-.152E-1$	$-.275E-1$
90.0000	$-.177E-2$	$-.290E-2$	$-.612E-2$	$-.967E-2$	$-.134E-1$	$-.244E-1$
100.0000	$-.150E-2$	$-.246E-2$	$-.520E-2$	$-.819E-2$	$-.115E-1$	$-.208E-1$
110.0000	$-.123E-2$	$-.202E-2$	$-.429E-2$	$-.677E-2$	$-.946E-2$	$-.171E-1$
120.0000	$-.983E-3$	$-.163E-2$	$-.343E-2$	$-.551E-2$	$-.757E-2$	$-.137E-1$
130.0000	$-.795E-3$	$-.130E-2$	$-.277E-2$	$-.437E-2$	$-.611E-2$	$-.109E-1$
140.0000	$-.618E-3$	$-.101E-2$	$-.215E-2$	$-.338E-2$	$-.475E-2$	$-.842E-2$
150.0000	$-.441E-3$	$-.721E-3$	$-.154E-2$	$-.248E-2$	$-.339E-2$	$-.593E-2$
160.0000	$-.295E-3$	$-.480E-3$	$-.103E-2$	$-.163E-2$	$-.226E-2$	$-.396E-2$
170.0000	$-.161E-3$	$-.262E-3$	$-.555E-3$	$-.808E-3$	$-.122E-2$	$-.215E-2$
180.0000	$.000E+0$	$.000E+0$	$.000E+0$	$.000E+0$	$.000E+0$	$.000E+0$

Table E.3. Radial displacement $\hat{u}_r^{(30)}(a, \theta)$ caused by a 45° dip-slip faulting

θ(°)	$d_s = 0km$	$d_s = 2km$	$d_s = 5km$	$d_s = 10km$	$d_s = 20km$	$d_s = 32km$
.0000	—	$.261E+7$	$.427E+6$	$.105E+6$	$.341E+5$	$.123E+5$
.0001	$-.171E+6$	$.261E+7$	$.427E+6$	$.105E+6$	$.341E+5$	$.123E+5$
.0010	$-.357E+5$	$.258E+7$	$.426E+6$	$.105E+6$	$.341E+5$	$.123E+5$
.0100	$.593E+4$	$.117E+7$	$.372E+6$	$.101E+6$	$.338E+5$	$.123E+5$
.0200	$.186E+5$	$.188E+6$	$.262E+6$	$.901E+5$	$.328E+5$	$.122E+5$
.0300	$.238E+5$	$.106E+4$	$.145E+6$	$.756E+5$	$.311E+5$	$.119E+5$
.0400	$.197E+5$	$-.189E+5$	$.743E+5$	$.610E+5$	$.290E+5$	$.116E+5$
.0600	$.108E+5$	$-.892E+4$	$.142E+5$	$.308E+5$	$.239E+5$	$.107E+5$
.0800	$.986E+4$	$-.296E+4$	$-.633E+3$	$.135E+5$	$.189E+5$	$.966E+4$
.1000	$.608E+4$	$-.104E+4$	$-.369E+4$	$.474E+4$	$.129E+5$	$.851E+4$
.1600	$.812E+3$	$-.510E+3$	$-.225E+4$	$-.796E+3$	$.340E+4$	$.488E+4$
.2000	$-.128E+3$	$-.500E+3$	$-.114E+4$	$-.608E+3$	$.101E+4$	$.308E+4$
.2500	$-.288E+3$	$-.363E+3$	$-.488E+3$	$-.264E+3$	$-.137E+3$	$.161E+4$
.3000	$-.203E+3$	$-.225E+3$	$-.238E+3$	$-.125E+3$	$-.356E+3$	$.772E+3$
.4000	$-.624E+2$	$-.755E+2$	$-.809E+2$	$-.524E+2$	$-.329E+3$	$.627E+2$
.5000	$-.143E+2$	$-.238E+2$	$-.317E+2$	$-.317E+2$	$-.230E+3$	$-.942E+2$
.6000	$-.326E+0$	$-.593E+1$	$-.126E+2$	$-.185E+2$	$-.156E+3$	$-.125E+3$
.8000	$.525E+1$	$.258E+1$	$-.118E+1$	$-.656E+1$	$-.742E+2$	$-.883E+2$
1.0000	$.475E+1$	$.336E+1$	$.124E+1$	$-.212E+1$	$-.369E+2$	$-.530E+2$
1.2000	$.399E+1$	$.312E+1$	$.183E+1$	$-.257E+0$	$-.178E+2$	$-.313E+2$
1.6000	$.286E+1$	$.247E+1$	$.190E+1$	$.951E+0$	$-.360E+1$	$-.118E+2$
2.0000	$.215E+1$	$.194E+1$	$.164E+1$	$.113E+1$	$.687E+0$	$-.409E+1$
2.5000	$.153E+1$	$.143E+1$	$.127E+1$	$.996E+0$	$.206E+1$	$-.601E+0$
3.0000	$.110E+1$	$.104E+1$	$.943E+0$	$.787E+0$	$.208E+1$	$.486E+0$
4.0000	$.559E+0$	$.534E+0$	$.497E+0$	$.434E+0$	$.134E+1$	$.682E+0$
5.0000	$.272E+0$	$.261E+0$	$.244E+0$	$.216E+0$	$.688E+0$	$.377E+0$
6.0000	$.119E+0$	$.114E+0$	$.106E+0$	$.911E-1$	$.271E+0$	$.114E+0$
7.0000	$.370E-1$	$.341E-1$	$.296E-1$	$.219E-1$	$.295E-1$	$-.556E-1$
8.0000	$-.716E-2$	$-.882E-2$	$-.114E-1$	$-.156E-1$	$-.104E+0$	$-.153E+0$
9.0000	$-.303E-1$	$-.312E-1$	$-.327E-1$	$-.353E-1$	$-.174E+0$	$-.203E+0$
10.0000	$-.415E-1$	$-.421E-1$	$-.431E-1$	$-.446E-1$	$-.206E+0$	$-.225E+0$
12.0000	$-.469E-1$	$-.472E-1$	$-.476E-1$	$-.482E-1$	$-.214E+0$	$-.223E+0$
16.0000	$-.378E-1$	$-.380E-1$	$-.381E-1$	$-.383E-1$	$-.167E+0$	$-.170E+0$
20.0000	$-.272E-1$	$-.272E-1$	$-.273E-1$	$-.274E-1$	$-.119E+0$	$-.120E+0$
25.0000	$-.169E-1$	$-.169E-1$	$-.169E-1$	$-.170E-1$	$-.735E-1$	$-.743E-1$
30.0000	$-.902E-2$	$-.903E-2$	$-.906E-2$	$-.909E-2$	$-.394E-1$	$-.399E-1$
40.0000	$.167E-2$	$.166E-2$	$.163E-2$	$.159E-2$	$.659E-2$	$.623E-2$
50.0000	$.705E-2$	$.703E-2$	$.700E-2$	$.695E-2$	$.297E-1$	$.294E-1$
60.0000	$.866E-2$	$.865E-2$	$.863E-2$	$.859E-2$	$.368E-1$	$.366E-1$
70.0000	$.802E-2$	$.801E-2$	$.800E-2$	$.796E-2$	$.341E-1$	$.340E-1$
80.0000	$.626E-2$	$.624E-2$	$.623E-2$	$.621E-2$	$.266E-1$	$.266E-1$
90.0000	$.410E-2$	$.410E-2$	$.410E-2$	$.408E-2$	$.175E-1$	$.175E-1$
100.0000	$.194E-2$	$.195E-2$	$.195E-2$	$.195E-2$	$.838E-2$	$.840E-2$
110.0000	$-.133E-4$	$-.362E-4$	$-.795E-5$	$.118E-5$	$.807E-6$	$.566E-4$
120.0000	$-.169E-2$	$-.169E-2$	$-.168E-2$	$-.166E-2$	$-.714E-2$	$-.705E-2$
130.0000	$-.308E-2$	$-.307E-2$	$-.305E-2$	$-.302E-2$	$-.130E-1$	$-.129E-1$
140.0000	$-.418E-2$	$-.417E-2$	$-.416E-2$	$-.412E-2$	$-.177E-1$	$-.176E-1$
150.0000	$-.501E-2$	$-.500E-2$	$-.498E-2$	$-.495E-2$	$-.213E-1$	$-.211E-1$
160.0000	$-.559E-2$	$-.557E-2$	$-.554E-2$	$-.550E-2$	$-.237E-1$	$-.235E-1$
170.0000	$-.593E-2$	$-.593E-2$	$-.590E-2$	$-.586E-2$	$-.252E-1$	$-.250E-1$
180.0000	$-.604E-2$	$-.605E-2$	$-.602E-2$	$-.598E-2$	$-.257E-1$	$-.256E-1$

(to be continued)

(continued)

$\theta(^\circ)$	$d_s = 64km$	$d_s = 100km$	$d_s = 200km$	$d_s = 300km$	$d_s = 400km$	$d_s = 637km$
.0000	$.286E+4$	$.113E+4$	$.277E+3$	$.124E+3$	$.735E+2$	$.300E+2$
.0001	$.286E+4$	$.113E+4$	$.277E+3$	$.124E+3$	$.735E+2$	$.300E+2$
.0010	$.286E+4$	$.113E+4$	$.277E+3$	$.124E+3$	$.735E+2$	$.300E+2$
.0100	$.286E+4$	$.113E+4$	$.277E+3$	$.124E+3$	$.735E+2$	$.300E+2$
.0200	$.285E+4$	$.113E+4$	$.277E+3$	$.124E+3$	$.735E+2$	$.300E+2$
.0300	$.284E+4$	$.112E+4$	$.277E+3$	$.124E+3$	$.735E+2$	$.300E+2$
.0400	$.282E+4$	$.112E+4$	$.277E+3$	$.124E+3$	$.735E+2$	$.300E+2$
.0600	$.277E+4$	$.111E+4$	$.276E+3$	$.124E+3$	$.735E+2$	$.300E+2$
.0800	$.270E+4$	$.110E+4$	$.276E+3$	$.124E+3$	$.734E+2$	$.300E+2$
.1000	$.261E+4$	$.109E+4$	$.275E+3$	$.124E+3$	$.733E+2$	$.300E+2$
.1600	$.227E+4$	$.103E+4$	$.271E+3$	$.123E+3$	$.731E+2$	$.299E+2$
.2000	$.201E+4$	$.975E+3$	$.267E+3$	$.122E+3$	$.728E+2$	$.299E+2$
.2500	$.170E+4$	$.901E+3$	$.262E+3$	$.121E+3$	$.725E+2$	$.298E+2$
.3000	$.143E+4$	$.823E+3$	$.256E+3$	$.120E+3$	$.720E+2$	$.298E+2$
.4000	$.785E+3$	$.670E+3$	$.241E+3$	$.117E+3$	$.709E+2$	$.296E+2$
.5000	$.433E+3$	$.487E+3$	$.223E+3$	$.113E+3$	$.695E+2$	$.293E+2$
.6000	$.223E+3$	$.353E+3$	$.203E+3$	$.108E+3$	$.678E+2$	$.290E+2$
.8000	$.318E+2$	$.168E+3$	$.166E+3$	$.970E+2$	$.636E+2$	$.283E+2$
1.0000	$-.163E+2$	$.718E+2$	$.121E+3$	$.854E+2$	$.588E+2$	$.274E+2$
1.2000	$-.269E+2$	$.219E+2$	$.875E+2$	$.742E+2$	$.536E+2$	$.263E+2$
1.6000	$-.196E+2$	$-.687E+1$	$.410E+2$	$.486E+2$	$.434E+2$	$.237E+2$
2.0000	$-.115E+2$	$-.106E+2$	$.165E+2$	$.304E+2$	$.313E+2$	$.210E+2$
2.5000	$-.615E+1$	$-.816E+1$	$.219E+1$	$.151E+2$	$.202E+2$	$.176E+2$
3.0000	$-.301E+1$	$-.552E+1$	$-.242E+1$	$.639E+1$	$.121E+2$	$.146E+2$
4.0000	$-.977E+0$	$-.256E+1$	$-.363E+1$	$-.821E+0$	$.309E+1$	$.758E+1$
5.0000	$-.439E+0$	$-.135E+1$	$-.267E+1$	$-.220E+1$	$-.477E+0$	$.361E+1$
6.0000	$-.314E+0$	$-.805E+0$	$-.182E+1$	$-.201E+1$	$-.143E+1$	$.128E+1$
7.0000	$-.293E+0$	$-.577E+0$	$-.126E+1$	$-.163E+1$	$-.158E+1$	$-.221E-1$
8.0000	$-.291E+0$	$-.462E+0$	$-.924E+0$	$-.124E+1$	$-.137E+1$	$-.582E+0$
9.0000	$-.287E+0$	$-.394E+0$	$-.710E+0$	$-.975E+0$	$-.117E+1$	$-.807E+0$
10.0000	$-.278E+0$	$-.348E+0$	$-.566E+0$	$-.783E+0$	$-.947E+0$	$-.858E+0$
12.0000	$-.247E+0$	$-.280E+0$	$-.387E+0$	$-.519E+0$	$-.652E+0$	$-.785E+0$
16.0000	$-.178E+0$	$-.189E+0$	$-.228E+0$	$-.282E+0$	$-.363E+0$	$-.525E+0$
20.0000	$-.124E+0$	$-.130E+0$	$-.150E+0$	$-.183E+0$	$-.225E+0$	$-.352E+0$
25.0000	$-.765E-1$	$-.798E-1$	$-.912E-1$	$-.110E+0$	$-.138E+0$	$-.224E+0$
30.0000	$-.414E-1$	$-.435E-1$	$-.505E-1$	$-.620E-1$	$-.787E-1$	$-.132E+0$
40.0000	$.530E-2$	$.435E-2$	$.175E-2$	$-.119E-2$	$-.488E-2$	$-.187E-1$
50.0000	$.288E-1$	$.283E-1$	$.278E-1$	$.289E-1$	$.315E-1$	$.357E-1$
60.0000	$.361E-1$	$.360E-1$	$.364E-1$	$.392E-1$	$.442E-1$	$.559E-1$
70.0000	$.337E-1$	$.337E-1$	$.346E-1$	$.377E-1$	$.429E-1$	$.560E-1$
80.0000	$.264E-1$	$.265E-1$	$.274E-1$	$.302E-1$	$.346E-1$	$.459E-1$
90.0000	$.175E-1$	$.176E-1$	$.184E-1$	$.204E-1$	$.236E-1$	$.319E-1$
100.0000	$.847E-2$	$.862E-2$	$.919E-2$	$.103E-1$	$.121E-1$	$.169E-1$
110.0000	$.197E-3$	$.342E-3$	$.689E-3$	$.108E-2$	$.148E-2$	$.268E-2$
120.0000	$-.685E-2$	$-.673E-2$	$-.657E-2$	$-.693E-2$	$-.766E-2$	$-.967E-2$
130.0000	$-.127E-1$	$-.125E-1$	$-.126E-1$	$-.135E-1$	$-.153E-1$	$-.199E-1$
140.0000	$-.173E-1$	$-.172E-1$	$-.174E-1$	$-.188E-1$	$-.214E-1$	$-.283E-1$
150.0000	$-.208E-1$	$-.207E-1$	$-.210E-1$	$-.228E-1$	$-.260E-1$	$-.346E-1$
160.0000	$-.232E-1$	$-.231E-1$	$-.235E-1$	$-.256E-1$	$-.292E-1$	$-.388E-1$
170.0000	$-.247E-1$	$-.246E-1$	$-.250E-1$	$-.272E-1$	$-.311E-1$	$-.416E-1$
180.0000	$-.252E-1$	$-.251E-1$	$-.256E-1$	$-.277E-1$	$-.318E-1$	$-.426E-1$

Table E.4. Radial displacement $\hat{u}_r^{(4)}(a, \theta)$ caused by a tensile faulting

$\theta(\circ)$	$d_s = 0km$	$d_s = 2km$	$d_s = 5km$	$d_s = 10km$	$d_s = 20km$	$d_s = 32km$
.0000	$.000E+0$	$.484E+7$	$.794E+6$	$.245E+6$	$.626E+5$	$.229E+5$
.0001	$.000E+0$	$.484E+7$	$.794E+6$	$.245E+6$	$.626E+5$	$.229E+5$
.0010	$.000E+0$	$.481E+7$	$.793E+6$	$.245E+6$	$.626E+5$	$.229E+5$
.0100	$.000E+0$	$.247E+7$	$.707E+6$	$.237E+6$	$.621E+5$	$.228E+5$
.0200	$.000E+0$	$.660E+6$	$.523E+6$	$.216E+6$	$.605E+5$	$.226E+5$
.0300	$.000E+0$	$.180E+6$	$.324E+6$	$.187E+6$	$.579E+5$	$.222E+5$
.0400	$.000E+0$	$.597E+5$	$.194E+6$	$.156E+6$	$.545E+5$	$.217E+5$
.0600	$.000E+0$	$.111E+5$	$.670E+5$	$.912E+5$	$.464E+5$	$.203E+5$
.0800	$.000E+0$	$.289E+4$	$.240E+5$	$.491E+5$	$.381E+5$	$.185E+5$
.1000	$.000E+0$	$.598E+3$	$.851E+4$	$.249E+5$	$.283E+5$	$.166E+5$
.1600	$.000E+0$	$-.286E+3$	$-.489E+3$	$.244E+4$	$.109E+5$	$.105E+5$
.2000	$.000E+0$	$-.148E+3$	$-.435E+3$	$.529E+3$	$.568E+4$	$.734E+4$
.2500	$.000E+0$	$-.322E+2$	$-.103E+3$	$.245E+3$	$.253E+4$	$.458E+4$
.3000	$.000E+0$	$.952E+0$	$.215E+2$	$.199E+3$	$.130E+4$	$.286E+4$
.4000	$.000E+0$	$.383E+1$	$.229E+2$	$.873E+2$	$.426E+3$	$.114E+4$
.5000	$.000E+0$	$.126E+1$	$.784E+1$	$.255E+2$	$.166E+3$	$.517E+3$
.6000	$.000E+0$	$.404E+0$	$.279E+1$	$.113E+2$	$.707E+2$	$.243E+3$
.8000	$.000E+0$	$.568E-1$	$.304E+0$	$.166E+1$	$.139E+2$	$.687E+2$
1.0000	$.000E+0$	$-.296E-2$	$.268E-1$	$.257E+0$	$.263E+1$	$.247E+2$
1.2000	$.000E+0$	$-.498E-2$	$-.993E-2$	$.312E-1$	$.150E+1$	$.109E+2$
1.6000	$.000E+0$	$-.484E-2$	$-.126E-1$	$-.181E-1$	$.311E+0$	$.218E+1$
2.0000	$.000E+0$	$-.333E-2$	$-.584E-2$	$-.150E-1$	$.830E-1$	$.681E+0$
2.5000	$.000E+0$	$-.222E-2$	$-.633E-2$	$-.126E-1$	$.955E-2$	$.175E+0$
3.0000	$.000E+0$	$-.150E-2$	$-.414E-2$	$-.116E-1$	$-.122E-1$	$.323E-1$
4.0000	$.000E+0$	$-.649E-3$	$-.204E-2$	$-.440E-2$	$-.100E-1$	$-.208E-1$
5.0000	$.000E+0$	$-.233E-3$	$-.821E-3$	$-.211E-2$	$-.556E-2$	$-.189E-1$
6.0000	$.000E+0$	$.181E-5$	$-.119E-3$	$-.524E-3$	$-.287E-2$	$-.106E-1$
7.0000	$.000E+0$	$.114E-3$	$.231E-3$	$.320E-3$	$-.398E-3$	$-.477E-2$
8.0000	$.000E+0$	$.177E-3$	$.403E-3$	$.618E-3$	$.713E-3$	$-.185E-2$
9.0000	$.000E+0$	$.192E-3$	$.469E-3$	$.894E-3$	$.114E-2$	$-.221E-3$
10.0000	$.000E+0$	$.195E-3$	$.479E-3$	$.891E-3$	$.124E-2$	$.553E-3$
12.0000	$.000E+0$	$.176E-3$	$.434E-3$	$.851E-3$	$.126E-2$	$.138E-2$
16.0000	$.000E+0$	$.121E-3$	$.303E-3$	$.604E-3$	$.869E-3$	$.115E-2$
20.0000	$.000E+0$	$.781E-4$	$.196E-3$	$.390E-3$	$.535E-3$	$.695E-3$
25.0000	$.000E+0$	$.405E-4$	$.101E-3$	$.203E-3$	$.238E-3$	$.255E-3$
30.0000	$.000E+0$	$.138E-4$	$.345E-4$	$.689E-4$	$.299E-4$	$-.248E-4$
40.0000	$.000E+0$	$-.200E-4$	$-.499E-4$	$-.998E-4$	$-.222E-3$	$-.364E-3$
50.0000	$.000E+0$	$-.352E-4$	$-.879E-4$	$-.175E-3$	$-.324E-3$	$-.497E-3$
60.0000	$.000E+0$	$-.378E-4$	$-.944E-4$	$-.188E-3$	$-.332E-3$	$-.497E-3$
70.0000	$.000E+0$	$-.326E-4$	$-.813E-4$	$-.162E-3$	$-.278E-3$	$-.410E-3$
80.0000	$.000E+0$	$-.227E-4$	$-.576E-4$	$-.115E-3$	$-.188E-3$	$-.271E-3$
90.0000	$.000E+0$	$-.117E-4$	$-.293E-4$	$-.585E-4$	$-.814E-4$	$-.104E-3$
100.0000	$.000E+0$	$.224E-7$	$.569E-7$	$.781E-7$	$.303E-4$	$.706E-4$
110.0000	$.000E+0$	$.112E-4$	$.282E-4$	$.562E-4$	$.139E-3$	$.242E-3$
120.0000	$.000E+0$	$.213E-4$	$.538E-4$	$.107E-3$	$.239E-3$	$.400E-3$
130.0000	$.000E+0$	$.306E-4$	$.762E-4$	$.152E-3$	$.329E-3$	$.546E-3$
140.0000	$.000E+0$	$.376E-4$	$.949E-4$	$.190E-3$	$.405E-3$	$.668E-3$
150.0000	$.000E+0$	$.439E-4$	$.110E-3$	$.219E-3$	$.465E-3$	$.765E-3$
160.0000	$.000E+0$	$.481E-4$	$.120E-3$	$.240E-3$	$.509E-3$	$.836E-3$
170.0000	$.000E+0$	$.509E-4$	$.127E-3$	$.253E-3$	$.535E-3$	$.879E-3$
180.0000	$.000E+0$	$.515E-4$	$.129E-3$	$.257E-3$	$.544E-3$	$.894E-3$

(to be continued)

(continued)

$\theta(°)$	$d_s = 64km$	$d_s = 100km$	$d_s = 200km$	$d_s = 300km$	$d_s = 400km$	$d_s = 637km$
.0000	$.530E+4$	$.211E+4$	$.545E+3$	$.254E+3$	$.151E+3$	$.638E+2$
.0001	$.530E+4$	$.211E+4$	$.545E+3$	$.254E+3$	$.151E+3$	$.638E+2$
.0010	$.530E+4$	$.211E+4$	$.545E+3$	$.254E+3$	$.151E+3$	$.638E+2$
.0100	$.530E+4$	$.211E+4$	$.545E+3$	$.254E+3$	$.151E+3$	$.638E+2$
.0200	$.529E+4$	$.211E+4$	$.545E+3$	$.254E+3$	$.151E+3$	$.638E+2$
.0300	$.527E+4$	$.211E+4$	$.544E+3$	$.254E+3$	$.151E+3$	$.638E+2$
.0400	$.524E+4$	$.210E+4$	$.544E+3$	$.254E+3$	$.151E+3$	$.638E+2$
.0600	$.515E+4$	$.209E+4$	$.543E+3$	$.254E+3$	$.151E+3$	$.638E+2$
.0800	$.504E+4$	$.207E+4$	$.542E+3$	$.254E+3$	$.151E+3$	$.638E+2$
.1000	$.490E+4$	$.205E+4$	$.541E+3$	$.253E+3$	$.151E+3$	$.638E+2$
.1600	$.435E+4$	$.195E+4$	$.534E+3$	$.252E+3$	$.150E+3$	$.637E+2$
.2000	$.392E+4$	$.187E+4$	$.528E+3$	$.251E+3$	$.150E+3$	$.636E+2$
.2500	$.341E+4$	$.174E+4$	$.520E+3$	$.249E+3$	$.149E+3$	$.635E+2$
.3000	$.294E+4$	$.161E+4$	$.509E+3$	$.247E+3$	$.149E+3$	$.634E+2$
.4000	$.184E+4$	$.136E+4$	$.483E+3$	$.241E+3$	$.147E+3$	$.631E+2$
.5000	$.118E+4$	$.105E+4$	$.453E+3$	$.234E+3$	$.144E+3$	$.626E+2$
.6000	$.756E+3$	$.814E+3$	$.420E+3$	$.226E+3$	$.141E+3$	$.621E+2$
.8000	$.311E+3$	$.471E+3$	$.355E+3$	$.207E+3$	$.134E+3$	$.608E+2$
1.0000	$.141E+3$	$.270E+3$	$.277E+3$	$.186E+3$	$.126E+3$	$.591E+2$
1.2000	$.671E+2$	$.153E+3$	$.216E+3$	$.166E+3$	$.116E+3$	$.572E+2$
1.6000	$.196E+2$	$.563E+2$	$.126E+3$	$.120E+3$	$.979E+2$	$.527E+2$
2.0000	$.714E+1$	$.224E+2$	$.719E+2$	$.845E+2$	$.762E+2$	$.477E+2$
2.5000	$.187E+1$	$.810E+1$	$.350E+2$	$.528E+2$	$.550E+2$	$.414E+2$
3.0000	$.846E+0$	$.317E+1$	$.177E+2$	$.325E+2$	$.386E+2$	$.357E+2$
4.0000	$.259E-1$	$.419E+0$	$.470E+1$	$.118E+2$	$.181E+2$	$.223E+2$
5.0000	$-.532E-1$	$-.595E-1$	$.127E+1$	$.433E+1$	$.814E+1$	$.139E+2$
6.0000	$-.449E-1$	$-.717E-1$	$.310E+0$	$.166E+1$	$.373E+1$	$.846E+1$
7.0000	$-.287E-1$	$-.594E-1$	$.319E-1$	$.592E+0$	$.166E+1$	$.500E+1$
8.0000	$-.168E-1$	$-.398E-1$	$-.441E-1$	$.237E+0$	$.797E+0$	$.303E+1$
9.0000	$-.907E-2$	$-.242E-1$	$-.536E-1$	$.742E-1$	$.350E+0$	$.186E+1$
10.0000	$-.415E-2$	$-.137E-1$	$-.426E-1$	$.498E-2$	$.194E+0$	$.118E+1$
12.0000	$.429E-4$	$-.274E-2$	$-.110E-1$	$-.963E-3$	$.656E-1$	$.491E+0$
16.0000	$.167E-2$	$.207E-2$	$.326E-2$	$.121E-1$	$.170E-1$	$.124E+0$
20.0000	$.107E-2$	$.149E-2$	$.280E-2$	$.490E-2$	$.145E-1$	$.398E-1$
25.0000	$.334E-3$	$.383E-3$	$.576E-3$	$.798E-3$	$.107E-2$	$.188E-2$
30.0000	$-.177E-3$	$-.334E-3$	$-.726E-3$	$-.107E-2$	$-.144E-2$	$-.287E-2$
40.0000	$-.737E-3$	$-.109E-2$	$-.190E-2$	$-.246E-2$	$-.264E-2$	$-.152E-2$
50.0000	$-.938E-3$	$-.140E-2$	$-.246E-2$	$-.311E-2$	$-.332E-2$	$-.128E-2$
60.0000	$-.921E-3$	$-.138E-2$	$-.246E-2$	$-.323E-2$	$-.349E-2$	$-.190E-2$
70.0000	$-.752E-3$	$-.113E-2$	$-.203E-2$	$-.272E-2$	$-.310E-2$	$-.208E-2$
80.0000	$-.488E-3$	$-.721E-3$	$-.133E-2$	$-.177E-2$	$-.202E-2$	$-.140E-2$
90.0000	$-.165E-3$	$-.232E-3$	$-.393E-3$	$-.481E-3$	$-.428E-3$	$.371E-3$
100.0000	$.176E-3$	$.293E-3$	$.617E-3$	$.961E-3$	$.136E-2$	$.261E-2$
110.0000	$.513E-3$	$.816E-3$	$.163E-2$	$.244E-2$	$.319E-2$	$.502E-2$
120.0000	$.832E-3$	$.130E-2$	$.262E-2$	$.384E-2$	$.507E-2$	$.752E-2$
130.0000	$.112E-2$	$.175E-2$	$.349E-2$	$.516E-2$	$.670E-2$	$.101E-1$
140.0000	$.136E-2$	$.214E-2$	$.424E-2$	$.628E-2$	$.811E-2$	$.120E-1$
150.0000	$.156E-2$	$.244E-2$	$.485E-2$	$.718E-2$	$.930E-2$	$.138E-1$
160.0000	$.170E-2$	$.268E-2$	$.531E-2$	$.785E-2$	$.102E-1$	$.151E-1$
170.0000	$.179E-2$	$.281E-2$	$.557E-2$	$.825E-2$	$.107E-1$	$.158E-1$
180.0000	$.182E-2$	$.285E-2$	$.565E-2$	$.838E-2$	$.108E-1$	$.159E-1$

Table E.5. Potential change $\widehat{\psi}^{(1)}(a, \theta)$ caused by a vertical strike-slip faulting

$\theta(o)$	$d_s = 0km$	$d_s = 2km$	$d_s = 5km$	$d_s = 10km$	$d_s = 20km$	$d_s = 32km$
.0000	$.000E+0$	$.000E+0$	$.000E+0$	$.000E+0$	$.000E+0$	$.000E+0$
.0001	$.625E-2$	$.348E-2$	$.224E-3$	$.213E-4$	$.518E-5$	$.122E-5$
.0010	$.675E-2$	$.346E+0$	$.224E-1$	$.213E-2$	$.518E-3$	$.122E-3$
.0100	$.567E-1$	$.222E+2$	$.207E+1$	$.208E+0$	$.516E-1$	$.122E-1$
.0200	$.204E+0$	$.357E+2$	$.665E+1$	$.777E+0$	$.203E+0$	$.484E-1$
.0300	$.437E+0$	$.323E+2$	$.110E+2$	$.156E+1$	$.445E+0$	$.108E+0$
.0400	$.737E+0$	$.259E+2$	$.135E+2$	$.240E+1$	$.763E+0$	$.189E+0$
.0600	$.145E+1$	$.165E+2$	$.144E+2$	$.369E+1$	$.155E+1$	$.409E+0$
.0800	$.217E+1$	$.114E+2$	$.127E+2$	$.420E+1$	$.242E+1$	$.689E+0$
.1000	$.276E+1$	$.865E+1$	$.106E+2$	$.411E+1$	$.321E+1$	$.101E+1$
.1600	$.331E+1$	$.497E+1$	$.586E+1$	$.277E+1$	$.462E+1$	$.197E+1$
.2000	$.296E+1$	$.373E+1$	$.408E+1$	$.203E+1$	$.482E+1$	$.248E+1$
.2500	$.229E+1$	$.265E+1$	$.273E+1$	$.144E+1$	$.462E+1$	$.286E+1$
.3000	$.168E+1$	$.190E+1$	$.191E+1$	$.107E+1$	$.421E+1$	$.305E+1$
.4000	$.877E+0$	$.998E+0$	$.102E+1$	$.658E+0$	$.334E+1$	$.301E+1$
.5000	$.466E+0$	$.550E+0$	$.590E+0$	$.435E+0$	$.263E+1$	$.272E+1$
.6000	$.255E+0$	$.318E+0$	$.361E+0$	$.302E+0$	$.208E+1$	$.237E+1$
.8000	$.797E-1$	$.119E+0$	$.157E+0$	$.165E+0$	$.136E+1$	$.176E+1$
1.0000	$.233E-1$	$.502E-1$	$.799E-1$	$.102E+0$	$.944E+0$	$.133E+1$
1.2000	$.407E-2$	$.235E-1$	$.467E-1$	$.695E-1$	$.693E+0$	$.102E+1$
1.6000	$-.299E-2$	$.853E-2$	$.232E-1$	$.411E-1$	$.429E+0$	$.663E+0$
2.0000	$.378E-3$	$.784E-2$	$.177E-1$	$.309E-1$	$.307E+0$	$.474E+0$
2.5000	$.637E-2$	$.111E-1$	$.176E-1$	$.267E-1$	$.234E+0$	$.348E+0$
3.0000	$.116E-1$	$.148E-1$	$.193E-1$	$.258E-1$	$.198E+0$	$.279E+0$
4.0000	$.183E-1$	$.200E-1$	$.224E-1$	$.260E-1$	$.167E+0$	$.210E+0$
5.0000	$.215E-1$	$.224E-1$	$.238E-1$	$.260E-1$	$.151E+0$	$.177E+0$
6.0000	$.224E-1$	$.230E-1$	$.239E-1$	$.252E-1$	$.139E+0$	$.155E+0$
7.0000	$.220E-1$	$.224E-1$	$.230E-1$	$.239E-1$	$.128E+0$	$.139E+0$
8.0000	$.210E-1$	$.213E-1$	$.217E-1$	$.224E-1$	$.118E+0$	$.125E+0$
9.0000	$.197E-1$	$.199E-1$	$.203E-1$	$.207E-1$	$.108E+0$	$.113E+0$
10.0000	$.183E-1$	$.185E-1$	$.187E-1$	$.191E-1$	$.983E-1$	$.102E+0$
12.0000	$.156E-1$	$.157E-1$	$.159E-1$	$.161E-1$	$.820E-1$	$.842E-1$
16.0000	$.112E-1$	$.113E-1$	$.113E-1$	$.115E-1$	$.579E-1$	$.589E-1$
20.0000	$.826E-2$	$.828E-2$	$.833E-2$	$.841E-2$	$.424E-1$	$.430E-1$
25.0000	$.590E-2$	$.591E-2$	$.594E-2$	$.600E-2$	$.302E-1$	$.306E-1$
30.0000	$.442E-2$	$.443E-2$	$.445E-2$	$.449E-2$	$.226E-1$	$.229E-1$
40.0000	$.286E-2$	$.287E-2$	$.288E-2$	$.291E-2$	$.147E-1$	$.149E-1$
50.0000	$.229E-2$	$.230E-2$	$.231E-2$	$.233E-2$	$.118E-1$	$.120E-1$
60.0000	$.219E-2$	$.219E-2$	$.220E-2$	$.222E-2$	$.111E-1$	$.113E-1$
70.0000	$.224E-2$	$.224E-2$	$.225E-2$	$.226E-2$	$.114E-1$	$.114E-1$
80.0000	$.229E-2$	$.228E-2$	$.229E-2$	$.230E-2$	$.115E-1$	$.116E-1$
90.0000	$.224E-2$	$.223E-2$	$.224E-2$	$.225E-2$	$.112E-1$	$.112E-1$
100.0000	$.207E-2$	$.207E-2$	$.207E-2$	$.207E-2$	$.103E-1$	$.103E-1$
110.0000	$.180E-2$	$.180E-2$	$.180E-2$	$.181E-2$	$.900E-2$	$.899E-2$
120.0000	$.147E-2$	$.147E-2$	$.147E-2$	$.147E-2$	$.732E-2$	$.731E-2$
130.0000	$.111E-2$	$.110E-2$	$.111E-2$	$.111E-2$	$.551E-2$	$.549E-2$
140.0000	$.757E-3$	$.753E-3$	$.754E-3$	$.757E-3$	$.375E-2$	$.374E-2$
150.0000	$.442E-3$	$.443E-3$	$.444E-3$	$.441E-3$	$.221E-2$	$.220E-2$
160.0000	$.198E-3$	$.203E-3$	$.203E-3$	$.197E-3$	$.101E-2$	$.101E-2$
170.0000	$.492E-4$	$.512E-4$	$.513E-4$	$.491E-4$	$.255E-3$	$.254E-3$
180.0000	$.000E+0$	$.000E+0$	$.000E+0$	$.000E+0$	$.000E+0$	$.000E+0$

(to be continued)

(continued)

$\theta(\circ)$	$d_s = 64km$	$d_s = 100km$	$d_s = 200km$	$d_s = 300km$	$d_s = 400km$	$d_s = 637km$
.0000	$.000E+0$	$.000E+0$	$.000E+0$	$.000E+0$	$.000E+0$	$.000E+0$
.0001	$.152E-6$	$.404E-7$	$.512E-8$	$.155E-8$	$.698E-9$	$.186E-9$
.0010	$.152E-4$	$.404E-5$	$.512E-6$	$.155E-6$	$.698E-7$	$.186E-7$
.0100	$.152E-2$	$.404E-3$	$.512E-4$	$.155E-4$	$.698E-5$	$.186E-5$
.0200	$.608E-2$	$.162E-2$	$.205E-3$	$.621E-4$	$.279E-4$	$.744E-5$
.0300	$.136E-1$	$.363E-2$	$.461E-3$	$.140E-3$	$.628E-4$	$.167E-4$
.0400	$.242E-1$	$.645E-2$	$.819E-3$	$.249E-3$	$.112E-3$	$.297E-4$
.0600	$.539E-1$	$.144E-1$	$.184E-2$	$.559E-3$	$.251E-3$	$.669E-4$
.0800	$.945E-1$	$.256E-1$	$.327E-2$	$.993E-3$	$.446E-3$	$.119E-3$
.1000	$.145E+0$	$.397E-1$	$.510E-2$	$.155E-2$	$.697E-3$	$.186E-3$
.1600	$.346E+0$	$.986E-1$	$.130E-1$	$.396E-2$	$.178E-2$	$.475E-3$
.2000	$.507E+0$	$.150E+0$	$.201E-1$	$.616E-2$	$.278E-2$	$.742E-3$
.2500	$.719E+0$	$.225E+0$	$.311E-1$	$.959E-2$	$.433E-2$	$.116E-2$
.3000	$.925E+0$	$.308E+0$	$.442E-1$	$.137E-1$	$.621E-2$	$.167E-2$
.4000	$.128E+1$	$.486E+0$	$.762E-1$	$.240E-1$	$.110E-1$	$.295E-2$
.5000	$.150E+1$	$.657E+0$	$.114E+0$	$.369E-1$	$.169E-1$	$.460E-2$
.6000	$.161E+1$	$.806E+0$	$.157E+0$	$.519E-1$	$.241E-1$	$.658E-2$
.8000	$.161E+1$	$.100E+1$	$.247E+0$	$.873E-1$	$.415E-1$	$.116E-1$
1.0000	$.146E+1$	$.108E+1$	$.335E+0$	$.127E+0$	$.622E-1$	$.178E-1$
1.2000	$.128E+1$	$.108E+1$	$.411E+0$	$.169E+0$	$.853E-1$	$.251E-1$
1.6000	$.960E+0$	$.958E+0$	$.511E+0$	$.246E+0$	$.135E+0$	$.424E-1$
2.0000	$.733E+0$	$.807E+0$	$.551E+0$	$.309E+0$	$.182E+0$	$.623E-1$
2.5000	$.548E+0$	$.645E+0$	$.543E+0$	$.353E+0$	$.232E+0$	$.885E-1$
3.0000	$.431E+0$	$.522E+0$	$.503E+0$	$.372E+0$	$.269E+0$	$.114E+0$
4.0000	$.299E+0$	$.364E+0$	$.405E+0$	$.356E+0$	$.296E+0$	$.158E+0$
5.0000	$.231E+0$	$.274E+0$	$.320E+0$	$.313E+0$	$.289E+0$	$.186E+0$
6.0000	$.189E+0$	$.218E+0$	$.258E+0$	$.267E+0$	$.266E+0$	$.199E+0$
7.0000	$.161E+0$	$.180E+0$	$.211E+0$	$.228E+0$	$.238E+0$	$.202E+0$
8.0000	$.140E+0$	$.153E+0$	$.177E+0$	$.195E+0$	$.211E+0$	$.198E+0$
9.0000	$.123E+0$	$.133E+0$	$.151E+0$	$.168E+0$	$.187E+0$	$.190E+0$
10.0000	$.110E+0$	$.116E+0$	$.131E+0$	$.147E+0$	$.167E+0$	$.181E+0$
12.0000	$.883E-1$	$.921E-1$	$.101E+0$	$.115E+0$	$.134E+0$	$.160E+0$
16.0000	$.605E-1$	$.620E-1$	$.670E-1$	$.769E-1$	$.923E-1$	$.125E+0$
20.0000	$.438E-1$	$.447E-1$	$.482E-1$	$.559E-1$	$.686E-1$	$.100E+0$
25.0000	$.311E-1$	$.317E-1$	$.344E-1$	$.406E-1$	$.509E-1$	$.797E-1$
30.0000	$.234E-1$	$.239E-1$	$.262E-1$	$.314E-1$	$.401E-1$	$.659E-1$
40.0000	$.153E-1$	$.157E-1$	$.177E-1$	$.218E-1$	$.286E-1$	$.503E-1$
50.0000	$.123E-1$	$.126E-1$	$.143E-1$	$.178E-1$	$.237E-1$	$.430E-1$
60.0000	$.115E-1$	$.118E-1$	$.131E-1$	$.163E-1$	$.217E-1$	$.393E-1$
70.0000	$.115E-1$	$.117E-1$	$.128E-1$	$.156E-1$	$.206E-1$	$.366E-1$
80.0000	$.116E-1$	$.116E-1$	$.124E-1$	$.150E-1$	$.195E-1$	$.339E-1$
90.0000	$.112E-1$	$.111E-1$	$.117E-1$	$.140E-1$	$.179E-1$	$.306E-1$
100.0000	$.102E-1$	$.102E-1$	$.106E-1$	$.125E-1$	$.158E-1$	$.265E-1$
110.0000	$.886E-2$	$.876E-2$	$.905E-2$	$.106E-1$	$.133E-1$	$.220E-1$
120.0000	$.718E-2$	$.709E-2$	$.728E-2$	$.844E-2$	$.106E-1$	$.173E-1$
130.0000	$.539E-2$	$.531E-2$	$.543E-2$	$.627E-2$	$.784E-2$	$.127E-1$
140.0000	$.367E-2$	$.361E-2$	$.367E-2$	$.422E-2$	$.527E-2$	$.846E-2$
150.0000	$.216E-2$	$.212E-2$	$.215E-2$	$.247E-2$	$.307E-2$	$.491E-2$
160.0000	$.987E-3$	$.970E-3$	$.983E-3$	$.113E-2$	$.140E-2$	$.223E-2$
170.0000	$.251E-3$	$.247E-3$	$.250E-3$	$.286E-3$	$.355E-3$	$.565E-3$
180.0000	$.000E+0$	$.000E+0$	$.000E+0$	$.000E+0$	$.000E+0$	$.000E+0$

Table E.6. Potential change $\widehat{\psi}^{(2)}(a, \theta)$ caused by a vertical dip-slip faulting

$\theta(\circ)$	$d_s = 0km$	$d_s = 2km$	$d_s = 5km$	$d_s = 10km$	$d_s = 20km$	$d_s = 32km$
.0000	$.000E+0$	$.000E+0$	$.000E+0$	$.000E+0$	$.000E+0$	$.000E+0$
.0001	$.000E+0$	$.166E+1$	$.255E+0$	$.684E-1$	$.240E-1$	$.916E-2$
.0010	$.000E+0$	$.166E+2$	$.255E+1$	$.684E+0$	$.240E+0$	$.916E-1$
.0100	$.000E+0$	$.111E+3$	$.237E+2$	$.672E+1$	$.239E+1$	$.914E+0$
.0200	$.000E+0$	$.986E+2$	$.385E+2$	$.128E+2$	$.471E+1$	$.182E+1$
.0300	$.000E+0$	$.662E+2$	$.429E+2$	$.176E+2$	$.689E+1$	$.270E+1$
.0400	$.000E+0$	$.436E+2$	$.406E+2$	$.210E+2$	$.888E+1$	$.356E+1$
.0600	$.000E+0$	$.206E+2$	$.297E+2$	$.239E+2$	$.121E+2$	$.514E+1$
.0800	$.000E+0$	$.108E+2$	$.202E+2$	$.232E+2$	$.143E+2$	$.653E+1$
.1000	$.000E+0$	$.627E+1$	$.140E+2$	$.208E+2$	$.154E+2$	$.767E+1$
.1600	$.000E+0$	$.226E+1$	$.634E+1$	$.131E+2$	$.147E+2$	$.965E+1$
.2000	$.000E+0$	$.170E+1$	$.465E+1$	$.967E+1$	$.129E+2$	$.100E+2$
.2500	$.000E+0$	$.134E+1$	$.347E+1$	$.695E+1$	$.106E+2$	$.955E+1$
.3000	$.000E+0$	$.107E+1$	$.268E+1$	$.521E+1$	$.863E+1$	$.882E+1$
.4000	$.000E+0$	$.668E+0$	$.165E+1$	$.318E+1$	$.588E+1$	$.709E+1$
.5000	$.000E+0$	$.436E+0$	$.108E+1$	$.208E+1$	$.417E+1$	$.557E+1$
.6000	$.000E+0$	$.301E+0$	$.745E+0$	$.144E+1$	$.306E+1$	$.438E+1$
.8000	$.000E+0$	$.163E+0$	$.406E+0$	$.795E+0$	$.180E+1$	$.281E+1$
1.0000	$.000E+0$	$.101E+0$	$.253E+0$	$.498E+0$	$.116E+1$	$.190E+1$
1.2000	$.000E+0$	$.687E-1$	$.171E+0$	$.339E+0$	$.805E+0$	$.135E+1$
1.6000	$.000E+0$	$.372E-1$	$.930E-1$	$.185E+0$	$.442E+0$	$.759E+0$
2.0000	$.000E+0$	$.231E-1$	$.577E-1$	$.115E+0$	$.273E+0$	$.473E+0$
2.5000	$.000E+0$	$.142E-1$	$.357E-1$	$.710E-1$	$.166E+0$	$.288E+0$
3.0000	$.000E+0$	$.958E-2$	$.240E-1$	$.479E-1$	$.110E+0$	$.190E+0$
4.0000	$.000E+0$	$.514E-2$	$.129E-1$	$.257E-1$	$.566E-1$	$.974E-1$
5.0000	$.000E+0$	$.320E-2$	$.801E-2$	$.160E-1$	$.344E-1$	$.587E-1$
6.0000	$.000E+0$	$.219E-2$	$.549E-2$	$.110E-1$	$.233E-1$	$.397E-1$
7.0000	$.000E+0$	$.161E-2$	$.402E-2$	$.803E-2$	$.172E-1$	$.292E-1$
8.0000	$.000E+0$	$.123E-2$	$.309E-2$	$.617E-2$	$.133E-1$	$.227E-1$
9.0000	$.000E+0$	$.981E-3$	$.246E-2$	$.490E-2$	$.108E-1$	$.185E-1$
10.0000	$.000E+0$	$.800E-3$	$.200E-2$	$.400E-2$	$.893E-2$	$.154E-1$
12.0000	$.000E+0$	$.563E-3$	$.141E-2$	$.281E-2$	$.651E-2$	$.114E-1$
16.0000	$.000E+0$	$.320E-3$	$.800E-3$	$.160E-2$	$.393E-2$	$.703E-2$
20.0000	$.000E+0$	$.201E-3$	$.504E-3$	$.101E-2$	$.261E-2$	$.474E-2$
25.0000	$.000E+0$	$.123E-3$	$.307E-3$	$.612E-3$	$.169E-2$	$.312E-2$
30.0000	$.000E+0$	$.784E-4$	$.196E-3$	$.391E-3$	$.114E-2$	$.215E-2$
40.0000	$.000E+0$	$.320E-4$	$.800E-4$	$.159E-3$	$.532E-3$	$.104E-2$
50.0000	$.000E+0$	$.908E-5$	$.227E-4$	$.454E-4$	$.195E-3$	$.401E-3$
60.0000	$.000E+0$	$-.352E-5$	$-.879E-5$	$-.175E-4$	$-.885E-5$	$.668E-5$
70.0000	$.000E+0$	$-.106E-4$	$-.265E-4$	$-.529E-4$	$-.131E-3$	$-.232E-3$
80.0000	$.000E+0$	$-.144E-4$	$-.360E-4$	$-.719E-4$	$-.198E-3$	$-.365E-3$
90.0000	$.000E+0$	$-.162E-4$	$-.405E-4$	$-.807E-4$	$-.229E-3$	$-.426E-3$
100.0000	$.000E+0$	$-.166E-4$	$-.416E-4$	$-.829E-4$	$-.236E-3$	$-.441E-3$
110.0000	$.000E+0$	$-.161E-4$	$-.404E-4$	$-.805E-4$	$-.228E-3$	$-.425E-3$
120.0000	$.000E+0$	$-.150E-4$	$-.374E-4$	$-.746E-4$	$-.209E-3$	$-.388E-3$
130.0000	$.000E+0$	$-.133E-4$	$-.332E-4$	$-.661E-4$	$-.183E-3$	$-.339E-3$
140.0000	$.000E+0$	$-.111E-4$	$-.278E-4$	$-.555E-4$	$-.152E-3$	$-.280E-3$
150.0000	$.000E+0$	$-.865E-5$	$-.216E-4$	$-.431E-4$	$-.117E-3$	$-.215E-3$
160.0000	$.000E+0$	$-.591E-5$	$-.148E-4$	$-.295E-4$	$-.793E-4$	$-.146E-3$
170.0000	$.000E+0$	$-.301E-5$	$-.753E-5$	$-.150E-4$	$-.403E-4$	$-.740E-4$
180.0000	$.000E+0$	$.000E+0$	$.000E+0$	$.000E+0$	$.000E+0$	$.000E+0$

(to be continued)

(continued)

$\theta(^\circ)$	$d_s = 64km$	$d_s = 100km$	$d_s = 200km$	$d_s = 300km$	$d_s = 400km$	$d_s = 637km$
.0000	$.000E+0$	$.000E+0$	$.000E+0$	$.000E+0$	$.000E+0$	$.000E+0$
.0001	$.232E-2$	$.956E-3$	$.243E-3$	$.111E-3$	$.668E-4$	$.301E-4$
.0010	$.232E-1$	$.956E-2$	$.243E-2$	$.111E-2$	$.668E-3$	$.301E-3$
.0100	$.232E+0$	$.956E-1$	$.243E-1$	$.111E-1$	$.668E-2$	$.301E-2$
.0200	$.463E+0$	$.191E+0$	$.485E-1$	$.223E-1$	$.134E-1$	$.601E-2$
.0300	$.693E+0$	$.286E+0$	$.728E-1$	$.334E-1$	$.200E-1$	$.902E-2$
.0400	$.922E+0$	$.381E+0$	$.970E-1$	$.445E-1$	$.267E-1$	$.120E-1$
.0600	$.137E+1$	$.570E+0$	$.145E+0$	$.667E-1$	$.401E-1$	$.180E-1$
.0800	$.180E+1$	$.756E+0$	$.194E+0$	$.889E-1$	$.534E-1$	$.240E-1$
.1000	$.222E+1$	$.939E+0$	$.242E+0$	$.111E+0$	$.668E-1$	$.300E-1$
.1600	$.333E+1$	$.146E+1$	$.384E+0$	$.177E+0$	$.107E+0$	$.480E-1$
.2000	$.392E+1$	$.178E+1$	$.477E+0$	$.221E+0$	$.133E+0$	$.600E-1$
.2500	$.449E+1$	$.214E+1$	$.590E+0$	$.275E+0$	$.166E+0$	$.750E-1$
.3000	$.488E+1$	$.246E+1$	$.699E+0$	$.328E+0$	$.198E+0$	$.898E-1$
.4000	$.523E+1$	$.294E+1$	$.904E+0$	$.431E+0$	$.263E+0$	$.119E+0$
.5000	$.503E+1$	$.323E+1$	$.109E+1$	$.530E+0$	$.325E+0$	$.149E+0$
.6000	$.467E+1$	$.336E+1$	$.125E+1$	$.622E+0$	$.385E+0$	$.178E+0$
.8000	$.374E+1$	$.322E+1$	$.149E+1$	$.787E+0$	$.498E+0$	$.234E+0$
1.0000	$.291E+1$	$.289E+1$	$.163E+1$	$.921E+0$	$.599E+0$	$.288E+0$
1.2000	$.226E+1$	$.249E+1$	$.169E+1$	$.102E+1$	$.687E+0$	$.340E+0$
1.6000	$.141E+1$	$.178E+1$	$.161E+1$	$.114E+1$	$.818E+0$	$.433E+0$
2.0000	$.924E+0$	$.127E+1$	$.142E+1$	$.115E+1$	$.896E+0$	$.511E+0$
2.5000	$.585E+0$	$.853E+0$	$.116E+1$	$.109E+1$	$.934E+0$	$.586E+0$
3.0000	$.393E+0$	$.597E+0$	$.931E+0$	$.983E+0$	$.901E+0$	$.637E+0$
4.0000	$.206E+0$	$.327E+0$	$.600E+0$	$.747E+0$	$.781E+0$	$.675E+0$
5.0000	$.125E+0$	$.202E+0$	$.405E+0$	$.558E+0$	$.640E+0$	$.654E+0$
6.0000	$.845E-1$	$.138E+0$	$.289E+0$	$.423E+0$	$.517E+0$	$.604E+0$
7.0000	$.621E-1$	$.102E+0$	$.217E+0$	$.329E+0$	$.420E+0$	$.543E+0$
8.0000	$.484E-1$	$.793E-1$	$.171E+0$	$.264E+0$	$.345E+0$	$.481E+0$
9.0000	$.393E-1$	$.643E-1$	$.139E+0$	$.216E+0$	$.289E+0$	$.424E+0$
10.0000	$.329E-1$	$.537E-1$	$.116E+0$	$.181E+0$	$.245E+0$	$.374E+0$
12.0000	$.244E-1$	$.398E-1$	$.850E-1$	$.134E+0$	$.183E+0$	$.294E+0$
16.0000	$.152E-1$	$.248E-1$	$.526E-1$	$.828E-1$	$.114E+0$	$.193E+0$
20.0000	$.104E-1$	$.169E-1$	$.358E-1$	$.564E-1$	$.781E-1$	$.136E+0$
25.0000	$.688E-2$	$.113E-1$	$.239E-1$	$.377E-1$	$.525E-1$	$.934E-1$
30.0000	$.479E-2$	$.786E-2$	$.167E-1$	$.265E-1$	$.370E-1$	$.671E-1$
40.0000	$.236E-2$	$.389E-2$	$.833E-2$	$.133E-1$	$.188E-1$	$.350E-1$
50.0000	$.942E-3$	$.157E-2$	$.343E-2$	$.556E-2$	$.798E-2$	$.155E-1$
60.0000	$.511E-4$	$.111E-3$	$.327E-3$	$.637E-3$	$.108E-2$	$.276E-2$
70.0000	$-.494E-3$	$-.788E-3$	$-.159E-2$	$-.241E-2$	$-.322E-2$	$-.523E-2$
80.0000	$-.797E-3$	$-.129E-2$	$-.267E-2$	$-.414E-2$	$-.568E-2$	$-.982E-2$
90.0000	$-.938E-3$	$-.153E-2$	$-.319E-2$	$-.498E-2$	$-.686E-2$	$-.121E-1$
100.0000	$-.974E-3$	$-.159E-2$	$-.333E-2$	$-.521E-2$	$-.722E-2$	$-.128E-1$
110.0000	$-.938E-3$	$-.153E-2$	$-.322E-2$	$-.505E-2$	$-.700E-2$	$-.124E-1$
120.0000	$-.856E-3$	$-.140E-2$	$-.295E-2$	$-.464E-2$	$-.642E-2$	$-.114E-1$
130.0000	$-.746E-3$	$-.122E-2$	$-.257E-2$	$-.405E-2$	$-.561E-2$	$-.994E-2$
140.0000	$-.616E-3$	$-.101E-2$	$-.213E-2$	$-.335E-2$	$-.464E-2$	$-.821E-2$
150.0000	$-.472E-3$	$-.769E-3$	$-.163E-2$	$-.257E-2$	$-.356E-2$	$-.628E-2$
160.0000	$-.319E-3$	$-.521E-3$	$-.110E-2$	$-.174E-2$	$-.241E-2$	$-.425E-2$
170.0000	$-.162E-3$	$-.264E-3$	$-.560E-3$	$-.877E-3$	$-.122E-2$	$-.216E-2$
180.0000	$.000E+0$	$.000E+0$	$.000E+0$	$.000E+0$	$.000E+0$	$.000E+0$

Table E.7. Potential change $\widehat{\psi}^{(30)}(a, \theta)$ caused by a 45° dip-slip faulting

$\theta(\circ)$	$d_s = 0km$	$d_s = 2km$	$d_s = 5km$	$d_s = 10km$	$d_s = 20km$	$d_s = 32km$
.0000	$.995E+1$	$.231E+3$	$.925E+2$	$.373E+2$	$.304E+2$	$.193E+2$
.0001	$.995E+1$	$.231E+3$	$.925E+2$	$.373E+2$	$.304E+2$	$.193E+2$
.0010	$.995E+1$	$.230E+3$	$.924E+2$	$.373E+2$	$.304E+2$	$.193E+2$
.0100	$.983E+1$	$.156E+3$	$.861E+2$	$.365E+2$	$.302E+2$	$.192E+2$
.0200	$.961E+1$	$.728E+2$	$.713E+2$	$.341E+2$	$.298E+2$	$.191E+2$
.0300	$.921E+1$	$.358E+2$	$.536E+2$	$.308E+2$	$.290E+2$	$.189E+2$
.0400	$.867E+1$	$.204E+2$	$.389E+2$	$.270E+2$	$.280E+2$	$.187E+2$
.0600	$.728E+1$	$.929E+1$	$.199E+2$	$.187E+2$	$.254E+2$	$.180E+2$
.0800	$.573E+1$	$.540E+1$	$.104E+2$	$.123E+2$	$.226E+2$	$.171E+2$
.1000	$.423E+1$	$.339E+1$	$.548E+1$	$.788E+1$	$.193E+2$	$.161E+2$
.1600	$.109E+1$	$.672E+0$	$.736E+0$	$.228E+1$	$.115E+2$	$.127E+2$
.2000	$.147E+0$	$.912E-3$	$.727E-1$	$.121E+1$	$.815E+1$	$.105E+2$
.2500	$-.307E+0$	$-.313E+0$	$-.163E+0$	$.666E+0$	$.539E+1$	$.813E+1$
.3000	$-.405E+0$	$-.376E+0$	$-.214E+0$	$.413E+0$	$.372E+1$	$.630E+1$
.4000	$-.325E+0$	$-.298E+0$	$-.187E+0$	$.180E+0$	$.192E+1$	$.384E+1$
.5000	$-.214E+0$	$-.198E+0$	$-.130E+0$	$.875E-1$	$.108E+1$	$.243E+1$
.6000	$-.136E+0$	$-.125E+0$	$-.841E-1$	$.493E-1$	$.663E+0$	$.160E+1$
.8000	$-.506E-1$	$-.467E-1$	$-.299E-1$	$.261E-1$	$.311E+0$	$.788E+0$
1.0000	$-.134E-1$	$-.120E-1$	$-.437E-2$	$.225E-1$	$.193E+0$	$.451E+0$
1.2000	$.453E-2$	$.487E-2$	$.851E-2$	$.226E-1$	$.146E+0$	$.294E+0$
1.6000	$.187E-1$	$.183E-1$	$.189E-1$	$.234E-1$	$.112E+0$	$.165E+0$
2.0000	$.219E-1$	$.213E-1$	$.211E-1$	$.224E-1$	$.958E-1$	$.115E+0$
2.5000	$.205E-1$	$.200E-1$	$.194E-1$	$.194E-1$	$.783E-1$	$.815E-1$
3.0000	$.170E-1$	$.165E-1$	$.160E-1$	$.155E-1$	$.608E-1$	$.584E-1$
4.0000	$.898E-2$	$.864E-2$	$.820E-2$	$.766E-2$	$.283E-1$	$.239E-1$
5.0000	$.219E-2$	$.196E-2$	$.165E-2$	$.122E-2$	$.216E-2$	$-.151E-2$
6.0000	$-.286E-2$	$-.302E-2$	$-.324E-2$	$-.354E-2$	$-.172E-1$	$-.199E-1$
7.0000	$-.642E-2$	$-.653E-2$	$-.669E-2$	$-.691E-2$	$-.309E-1$	$-.329E-1$
8.0000	$-.886E-2$	$-.894E-2$	$-.906E-2$	$-.922E-2$	$-.404E-1$	$-.418E-1$
9.0000	$-.105E-1$	$-.105E-1$	$-.106E-1$	$-.107E-1$	$-.466E-1$	$-.477E-1$
10.0000	$-.115E-1$	$-.115E-1$	$-.116E-1$	$-.117E-1$	$-.505E-1$	$-.513E-1$
12.0000	$-.124E-1$	$-.124E-1$	$-.124E-1$	$-.125E-1$	$-.538E-1$	$-.543E-1$
16.0000	$-.118E-1$	$-.118E-1$	$-.119E-1$	$-.119E-1$	$-.511E-1$	$-.514E-1$
20.0000	$-.102E-1$	$-.102E-1$	$-.102E-1$	$-.103E-1$	$-.440E-1$	$-.443E-1$
25.0000	$-.785E-2$	$-.787E-2$	$-.789E-2$	$-.792E-2$	$-.340E-1$	$-.342E-1$
30.0000	$-.554E-2$	$-.556E-2$	$-.558E-2$	$-.561E-2$	$-.241E-1$	$-.243E-1$
40.0000	$-.156E-2$	$-.158E-2$	$-.160E-2$	$-.164E-2$	$-.701E-2$	$-.723E-2$
50.0000	$.123E-2$	$.122E-2$	$.120E-2$	$.116E-2$	$.499E-2$	$.479E-2$
60.0000	$.283E-2$	$.282E-2$	$.280E-2$	$.276E-2$	$.119E-1$	$.117E-1$
70.0000	$.342E-2$	$.341E-2$	$.340E-2$	$.337E-2$	$.145E-1$	$.143E-1$
80.0000	$.328E-2$	$.327E-2$	$.326E-2$	$.323E-2$	$.139E-1$	$.138E-1$
90.0000	$.264E-2$	$.264E-2$	$.263E-2$	$.261E-2$	$.112E-1$	$.112E-1$
100.0000	$.173E-2$	$.173E-2$	$.172E-2$	$.172E-2$	$.738E-2$	$.735E-2$
110.0000	$.692E-3$	$.692E-3$	$.692E-3$	$.692E-3$	$.297E-2$	$.298E-2$
120.0000	$-.357E-3$	$-.354E-3$	$-.350E-3$	$-.343E-3$	$-.147E-2$	$-.144E-2$
130.0000	$-.134E-2$	$-.133E-2$	$-.132E-2$	$-.131E-2$	$-.564E-2$	$-.557E-2$
140.0000	$-.219E-2$	$-.219E-2$	$-.218E-2$	$-.216E-2$	$-.928E-2$	$-.919E-2$
150.0000	$-.289E-2$	$-.288E-2$	$-.287E-2$	$-.285E-2$	$-.122E-1$	$-.121E-1$
160.0000	$-.340E-2$	$-.339E-2$	$-.338E-2$	$-.335E-2$	$-.144E-1$	$-.143E-1$
170.0000	$-.371E-2$	$-.371E-2$	$-.369E-2$	$-.366E-2$	$-.157E-1$	$-.156E-1$
180.0000	$-.382E-2$	$-.381E-2$	$-.379E-2$	$-.376E-2$	$-.162E-1$	$-.161E-1$

(to be continued)

(continued)

$\theta(\circ)$	$d_s = 64km$	$d_s = 100km$	$d_s = 200km$	$d_s = 300km$	$d_s = 400km$	$d_s = 637km$
.0000	$.101E+2$	$.658E+1$	$.332E+1$	$.220E+1$	$.169E+1$	$.105E+1$
.0001	$.101E+2$	$.658E+1$	$.332E+1$	$.220E+1$	$.169E+1$	$.105E+1$
.0010	$.101E+2$	$.658E+1$	$.332E+1$	$.220E+1$	$.169E+1$	$.105E+1$
.0100	$.101E+2$	$.658E+1$	$.332E+1$	$.220E+1$	$.169E+1$	$.105E+1$
.0200	$.100E+2$	$.657E+1$	$.332E+1$	$.220E+1$	$.169E+1$	$.105E+1$
.0300	$.100E+2$	$.657E+1$	$.332E+1$	$.220E+1$	$.169E+1$	$.105E+1$
.0400	$.999E+1$	$.656E+1$	$.332E+1$	$.219E+1$	$.169E+1$	$.105E+1$
.0600	$.990E+1$	$.654E+1$	$.331E+1$	$.219E+1$	$.168E+1$	$.105E+1$
.0800	$.978E+1$	$.650E+1$	$.331E+1$	$.219E+1$	$.168E+1$	$.105E+1$
.1000	$.963E+1$	$.646E+1$	$.330E+1$	$.219E+1$	$.168E+1$	$.105E+1$
.1600	$.902E+1$	$.629E+1$	$.328E+1$	$.218E+1$	$.168E+1$	$.104E+1$
.2000	$.852E+1$	$.613E+1$	$.326E+1$	$.218E+1$	$.168E+1$	$.104E+1$
.2500	$.784E+1$	$.591E+1$	$.322E+1$	$.217E+1$	$.167E+1$	$.104E+1$
.3000	$.717E+1$	$.565E+1$	$.318E+1$	$.215E+1$	$.167E+1$	$.104E+1$
.4000	$.563E+1$	$.509E+1$	$.309E+1$	$.212E+1$	$.165E+1$	$.104E+1$
.5000	$.440E+1$	$.444E+1$	$.297E+1$	$.208E+1$	$.163E+1$	$.103E+1$
.6000	$.342E+1$	$.384E+1$	$.283E+1$	$.204E+1$	$.161E+1$	$.103E+1$
.8000	$.207E+1$	$.280E+1$	$.254E+1$	$.192E+1$	$.156E+1$	$.101E+1$
1.0000	$.131E+1$	$.201E+1$	$.220E+1$	$.180E+1$	$.149E+1$	$.991E+0$
1.2000	$.859E+0$	$.145E+1$	$.188E+1$	$.166E+1$	$.142E+1$	$.969E+0$
1.6000	$.423E+0$	$.785E+0$	$.134E+1$	$.135E+1$	$.126E+1$	$.914E+0$
2.0000	$.239E+0$	$.450E+0$	$.930E+0$	$.108E+1$	$.107E+1$	$.851E+0$
2.5000	$.132E+0$	$.241E+0$	$.582E+0$	$.783E+0$	$.856E+0$	$.766E+0$
3.0000	$.777E-1$	$.134E+0$	$.365E+0$	$.558E+0$	$.668E+0$	$.682E+0$
4.0000	$.228E-1$	$.378E-1$	$.138E+0$	$.270E+0$	$.385E+0$	$.490E+0$
5.0000	$-.615E-2$	$-.346E-2$	$.403E-1$	$.119E+0$	$.205E+0$	$.339E+0$
6.0000	$-.244E-1$	$-.254E-1$	$-.624E-2$	$.387E-1$	$.967E-1$	$.222E+0$
7.0000	$-.365E-1$	$-.384E-1$	$-.305E-1$	$-.535E-2$	$.316E-1$	$.134E+0$
8.0000	$-.446E-1$	$-.466E-1$	$-.439E-1$	$-.302E-1$	$-.765E-2$	$.710E-1$
9.0000	$-.499E-1$	$-.517E-1$	$-.516E-1$	$-.448E-1$	$-.319E-1$	$.260E-1$
10.0000	$-.531E-1$	$-.547E-1$	$-.559E-1$	$-.533E-1$	$-.468E-1$	$-.596E-2$
12.0000	$-.555E-1$	$-.568E-1$	$-.592E-1$	$-.609E-1$	$-.617E-1$	$-.451E-1$
16.0000	$-.522E-1$	$-.533E-1$	$-.562E-1$	$-.608E-1$	$-.670E-1$	$-.734E-1$
20.0000	$-.450E-1$	$-.460E-1$	$-.489E-1$	$-.541E-1$	$-.614E-1$	$-.758E-1$
25.0000	$-.348E-1$	$-.357E-1$	$-.385E-1$	$-.432E-1$	$-.502E-1$	$-.663E-1$
30.0000	$-.249E-1$	$-.257E-1$	$-.281E-1$	$-.321E-1$	$-.378E-1$	$-.521E-1$
40.0000	$-.778E-2$	$-.840E-2$	$-.101E-1$	$-.123E-1$	$-.152E-1$	$-.230E-1$
50.0000	$.430E-2$	$.384E-2$	$.285E-2$	$.214E-2$	$.153E-2$	$-.410E-3$
60.0000	$.113E-1$	$.110E-1$	$.105E-1$	$.108E-1$	$.117E-1$	$.137E-1$
70.0000	$.140E-1$	$.138E-1$	$.137E-1$	$.145E-1$	$.162E-1$	$.204E-1$
80.0000	$.136E-1$	$.135E-1$	$.135E-1$	$.146E-1$	$.165E-1$	$.213E-1$
90.0000	$.110E-1$	$.110E-1$	$.112E-1$	$.121E-1$	$.138E-1$	$.182E-1$
100.0000	$.729E-2$	$.731E-2$	$.753E-2$	$.826E-2$	$.950E-2$	$.127E-1$
110.0000	$.300E-2$	$.305E-2$	$.325E-2$	$.367E-2$	$.431E-2$	$.604E-2$
120.0000	$-.134E-2$	$-.127E-2$	$-.112E-2$	$-.106E-2$	$-.105E-2$	$-.978E-3$
130.0000	$-.543E-2$	$-.533E-2$	$-.524E-2$	$-.552E-2$	$-.614E-2$	$-.769E-2$
140.0000	$-.900E-2$	$-.889E-2$	$-.886E-2$	$-.945E-2$	$-.106E-1$	$-.137E-1$
150.0000	$-.119E-1$	$-.118E-1$	$-.118E-1$	$-.127E-1$	$-.143E-1$	$-.185E-1$
160.0000	$-.140E-1$	$-.139E-1$	$-.140E-1$	$-.150E-1$	$-.170E-1$	$-.221E-1$
170.0000	$-.153E-1$	$-.152E-1$	$-.153E-1$	$-.165E-1$	$-.187E-1$	$-.244E-1$
180.0000	$-.158E-1$	$-.156E-1$	$-.157E-1$	$-.169E-1$	$-.192E-1$	$-.251E-1$

Table E.8. Potential change $\widehat{\psi}^{(4)}(a, \theta)$ caused by a tensile faulting

$\theta(\circ)$	$d_s = 0km$	$d_s = 2km$	$d_s = 5km$	$d_s = 10km$	$d_s = 20km$	$d_s = 32km$
.0000	$.000E+0$	$.302E+3$	$.127E+3$	$.753E+2$	$.397E+2$	$.252E+2$
.0001	$.000E+0$	$.302E+3$	$.127E+3$	$.753E+2$	$.397E+2$	$.252E+2$
.0010	$.000E+0$	$.301E+3$	$.127E+3$	$.753E+2$	$.397E+2$	$.252E+2$
.0100	$.000E+0$	$.202E+3$	$.119E+3$	$.738E+2$	$.395E+2$	$.252E+2$
.0200	$.000E+0$	$.915E+2$	$.988E+2$	$.696E+2$	$.389E+2$	$.251E+2$
.0300	$.000E+0$	$.422E+2$	$.750E+2$	$.634E+2$	$.379E+2$	$.248E+2$
.0400	$.000E+0$	$.218E+2$	$.552E+2$	$.563E+2$	$.366E+2$	$.245E+2$
.0600	$.000E+0$	$.781E+1$	$.291E+2$	$.406E+2$	$.332E+2$	$.236E+2$
.0800	$.000E+0$	$.351E+1$	$.157E+2$	$.277E+2$	$.295E+2$	$.224E+2$
.1000	$.000E+0$	$.175E+1$	$.872E+1$	$.185E+2$	$.251E+2$	$.211E+2$
.1600	$.000E+0$	$.267E+0$	$.170E+1$	$.570E+1$	$.149E+2$	$.165E+2$
.2000	$.000E+0$	$.103E+0$	$.746E+0$	$.308E+1$	$.105E+2$	$.136E+2$
.2500	$.000E+0$	$.570E-1$	$.409E+0$	$.178E+1$	$.692E+1$	$.105E+2$
.3000	$.000E+0$	$.428E-1$	$.287E+0$	$.119E+1$	$.480E+1$	$.817E+1$
.4000	$.000E+0$	$.244E-1$	$.157E+0$	$.622E+0$	$.256E+1$	$.499E+1$
.5000	$.000E+0$	$.137E-1$	$.891E-1$	$.352E+0$	$.149E+1$	$.318E+1$
.6000	$.000E+0$	$.791E-2$	$.530E-1$	$.212E+0$	$.925E+0$	$.210E+1$
.8000	$.000E+0$	$.294E-2$	$.215E-1$	$.886E-1$	$.411E+0$	$.102E+1$
1.0000	$.000E+0$	$.117E-2$	$.101E-1$	$.433E-1$	$.211E+0$	$.554E+0$
1.2000	$.000E+0$	$.440E-3$	$.517E-2$	$.236E-1$	$.121E+0$	$.329E+0$
1.6000	$.000E+0$	$-.636E-4$	$.153E-2$	$.863E-2$	$.488E-1$	$.140E+0$
2.0000	$.000E+0$	$-.196E-3$	$.370E-3$	$.358E-2$	$.233E-1$	$.700E-1$
2.5000	$.000E+0$	$-.231E-3$	$-.141E-3$	$.116E-2$	$.104E-1$	$.336E-1$
3.0000	$.000E+0$	$-.225E-3$	$-.312E-3$	$.206E-3$	$.491E-2$	$.175E-1$
4.0000	$.000E+0$	$-.187E-3$	$-.365E-3$	$-.390E-3$	$.840E-3$	$.508E-2$
5.0000	$.000E+0$	$-.151E-3$	$-.328E-3$	$-.486E-3$	$-.362E-3$	$.106E-2$
6.0000	$.000E+0$	$-.123E-3$	$-.280E-3$	$-.465E-3$	$-.753E-3$	$-.442E-3$
7.0000	$.000E+0$	$-.103E-3$	$-.239E-3$	$-.419E-3$	$-.870E-3$	$-.105E-2$
8.0000	$.000E+0$	$-.868E-4$	$-.206E-3$	$-.372E-3$	$-.886E-3$	$-.129E-2$
9.0000	$.000E+0$	$-.750E-4$	$-.179E-3$	$-.332E-3$	$-.865E-3$	$-.138E-2$
10.0000	$.000E+0$	$-.660E-4$	$-.159E-3$	$-.298E-3$	$-.832E-3$	$-.140E-2$
12.0000	$.000E+0$	$-.537E-4$	$-.131E-3$	$-.250E-3$	$-.763E-3$	$-.135E-2$
16.0000	$.000E+0$	$-.420E-4$	$-.103E-3$	$-.202E-3$	$-.662E-3$	$-.123E-2$
20.0000	$.000E+0$	$-.378E-4$	$-.938E-4$	$-.185E-3$	$-.605E-3$	$-.113E-2$
25.0000	$.000E+0$	$-.369E-4$	$-.917E-4$	$-.182E-3$	$-.567E-3$	$-.105E-2$
30.0000	$.000E+0$	$-.378E-4$	$-.942E-4$	$-.187E-3$	$-.547E-3$	$-.100E-2$
40.0000	$.000E+0$	$-.405E-4$	$-.101E-3$	$-.202E-3$	$-.522E-3$	$-.924E-3$
50.0000	$.000E+0$	$-.414E-4$	$-.104E-3$	$-.207E-3$	$-.492E-3$	$-.846E-3$
60.0000	$.000E+0$	$-.395E-4$	$-.986E-4$	$-.197E-3$	$-.443E-3$	$-.747E-3$
70.0000	$.000E+0$	$-.347E-4$	$-.868E-4$	$-.173E-3$	$-.376E-3$	$-.624E-3$
80.0000	$.000E+0$	$-.278E-4$	$-.695E-4$	$-.139E-3$	$-.293E-3$	$-.481E-3$
90.0000	$.000E+0$	$-.195E-4$	$-.488E-4$	$-.974E-4$	$-.200E-3$	$-.325E-3$
100.0000	$.000E+0$	$-.105E-4$	$-.262E-4$	$-.524E-4$	$-.103E-3$	$-.164E-3$
110.0000	$.000E+0$	$-.134E-5$	$-.336E-5$	$-.676E-5$	$-.615E-5$	$-.467E-5$
120.0000	$.000E+0$	$.744E-5$	$.186E-4$	$.371E-4$	$.861E-4$	$.147E-3$
130.0000	$.000E+0$	$.155E-4$	$.386E-4$	$.771E-4$	$.170E-3$	$.284E-3$
140.0000	$.000E+0$	$.224E-4$	$.560E-4$	$.112E-3$	$.243E-3$	$.403E-3$
150.0000	$.000E+0$	$.280E-4$	$.701E-4$	$.140E-3$	$.301E-3$	$.499E-3$
160.0000	$.000E+0$	$.322E-4$	$.804E-4$	$.161E-3$	$.345E-3$	$.570E-3$
170.0000	$.000E+0$	$.347E-4$	$.867E-4$	$.173E-3$	$.371E-3$	$.613E-3$
180.0000	$.000E+0$	$.355E-4$	$.888E-4$	$.177E-3$	$.380E-3$	$.627E-3$

(to be continued)

(continued)

$\theta(^\circ)$	$d_s = 64km$	$d_s = 100km$	$d_s = 200km$	$d_s = 300km$	$d_s = 400km$	$d_s = 637km$
.0000	$.132E+2$	$.878E+1$	$.480E+1$	$.341E+1$	$.268E+1$	$.177E+1$
.0001	$.132E+2$	$.878E+1$	$.480E+1$	$.341E+1$	$.268E+1$	$.177E+1$
.0010	$.132E+2$	$.878E+1$	$.480E+1$	$.341E+1$	$.268E+1$	$.177E+1$
.0100	$.132E+2$	$.878E+1$	$.480E+1$	$.341E+1$	$.268E+1$	$.177E+1$
.0200	$.132E+2$	$.878E+1$	$.480E+1$	$.341E+1$	$.268E+1$	$.177E+1$
.0300	$.132E+2$	$.877E+1$	$.480E+1$	$.341E+1$	$.268E+1$	$.177E+1$
.0400	$.131E+2$	$.876E+1$	$.480E+1$	$.341E+1$	$.268E+1$	$.177E+1$
.0600	$.130E+2$	$.873E+1$	$.479E+1$	$.341E+1$	$.268E+1$	$.177E+1$
.0800	$.129E+2$	$.868E+1$	$.479E+1$	$.340E+1$	$.268E+1$	$.177E+1$
.1000	$.127E+2$	$.863E+1$	$.478E+1$	$.340E+1$	$.268E+1$	$.177E+1$
.1600	$.119E+2$	$.840E+1$	$.475E+1$	$.339E+1$	$.267E+1$	$.177E+1$
.2000	$.112E+2$	$.819E+1$	$.472E+1$	$.338E+1$	$.267E+1$	$.177E+1$
.2500	$.103E+2$	$.789E+1$	$.467E+1$	$.337E+1$	$.266E+1$	$.177E+1$
.3000	$.944E+1$	$.755E+1$	$.462E+1$	$.335E+1$	$.265E+1$	$.177E+1$
.4000	$.742E+1$	$.681E+1$	$.448E+1$	$.330E+1$	$.263E+1$	$.176E+1$
.5000	$.581E+1$	$.596E+1$	$.432E+1$	$.325E+1$	$.261E+1$	$.175E+1$
.6000	$.451E+1$	$.516E+1$	$.413E+1$	$.318E+1$	$.257E+1$	$.174E+1$
.8000	$.274E+1$	$.379E+1$	$.373E+1$	$.302E+1$	$.249E+1$	$.172E+1$
1.0000	$.173E+1$	$.275E+1$	$.326E+1$	$.283E+1$	$.240E+1$	$.169E+1$
1.2000	$.113E+1$	$.199E+1$	$.282E+1$	$.263E+1$	$.229E+1$	$.166E+1$
1.6000	$.542E+0$	$.110E+1$	$.206E+1$	$.219E+1$	$.205E+1$	$.158E+1$
2.0000	$.292E+0$	$.642E+0$	$.148E+1$	$.178E+1$	$.178E+1$	$.148E+1$
2.5000	$.151E+0$	$.354E+0$	$.972E+0$	$.135E+1$	$.146E+1$	$.135E+1$
3.0000	$.846E-1$	$.209E+0$	$.651E+0$	$.101E+1$	$.118E+1$	$.122E+1$
4.0000	$.305E-1$	$.822E-1$	$.307E+0$	$.558E+0$	$.750E+0$	$.930E+0$
5.0000	$.118E-1$	$.357E-1$	$.155E+0$	$.316E+0$	$.470E+0$	$.697E+0$
6.0000	$.413E-2$	$.160E-1$	$.821E-1$	$.185E+0$	$.297E+0$	$.513E+0$
7.0000	$.699E-3$	$.670E-2$	$.449E-1$	$.111E+0$	$.190E+0$	$.374E+0$
8.0000	$-.958E-3$	$.201E-2$	$.247E-1$	$.677E-1$	$.124E+0$	$.273E+0$
9.0000	$-.179E-2$	$-.507E-3$	$.131E-1$	$.417E-1$	$.811E-1$	$.200E+0$
10.0000	$-.222E-2$	$-.191E-2$	$.620E-2$	$.254E-1$	$.537E-1$	$.147E+0$
12.0000	$-.254E-2$	$-.318E-2$	$-.831E-3$	$.797E-2$	$.226E-1$	$.784E-1$
16.0000	$-.255E-2$	$-.376E-2$	$-.540E-2$	$-.440E-2$	$-.933E-3$	$.177E-1$
20.0000	$-.243E-2$	$-.377E-2$	$-.658E-2$	$-.818E-2$	$-.859E-2$	$-.496E-2$
25.0000	$-.229E-2$	$-.363E-2$	$-.689E-2$	$-.963E-2$	$-.119E-1$	$-.157E-1$
30.0000	$-.217E-2$	$-.346E-2$	$-.678E-2$	$-.985E-2$	$-.127E-1$	$-.189E-1$
40.0000	$-.197E-2$	$-.314E-2$	$-.623E-2$	$-.921E-2$	$-.120E-1$	$-.186E-1$
50.0000	$-.177E-2$	$-.281E-2$	$-.556E-2$	$-.821E-2$	$-.107E-1$	$-.162E-1$
60.0000	$-.154E-2$	$-.243E-2$	$-.481E-2$	$-.708E-2$	$-.917E-2$	$-.136E-1$
70.0000	$-.128E-2$	$-.201E-2$	$-.396E-2$	$-.583E-2$	$-.752E-2$	$-.110E-1$
80.0000	$-.976E-3$	$-.153E-2$	$-.303E-2$	$-.446E-2$	$-.575E-2$	$-.838E-2$
90.0000	$-.655E-3$	$-.103E-2$	$-.203E-2$	$-.300E-2$	$-.387E-2$	$-.562E-2$
100.0000	$-.326E-3$	$-.511E-3$	$-.101E-2$	$-.150E-2$	$-.194E-2$	$-.282E-2$
110.0000	$-.224E-5$	$-.173E-5$	$-.105E-4$	$-.272E-4$	$-.434E-4$	$-.603E-4$
120.0000	$.304E-3$	$.480E-3$	$.941E-3$	$.137E-2$	$.176E-2$	$.258E-2$
130.0000	$.583E-3$	$.917E-3$	$.180E-2$	$.265E-2$	$.341E-2$	$.499E-2$
140.0000	$.823E-3$	$.129E-2$	$.255E-2$	$.375E-2$	$.483E-2$	$.707E-2$
150.0000	$.102E-2$	$.160E-2$	$.316E-2$	$.465E-2$	$.599E-2$	$.878E-2$
160.0000	$.116E-2$	$.183E-2$	$.361E-2$	$.531E-2$	$.685E-2$	$.100E-1$
170.0000	$.125E-2$	$.196E-2$	$.388E-2$	$.571E-2$	$.737E-2$	$.108E-1$
180.0000	$.128E-2$	$.201E-2$	$.397E-2$	$.584E-2$	$.754E-2$	$.111E-1$

Table E.9. Gravity change $\Delta\hat{g}^{(1)}(a, \theta)$ caused by a vertical strike-slip faulting

$\theta(^\circ)$	$d_s = 0km$	$d_s = 2km$	$d_s = 5km$	$d_s = 10km$	$d_s = 20km$	$d_s = 32km$
.0000	$.000E+0$	$.000E+0$	$.000E+0$	$.000E+0$	$.000E+0$	$.000E+0$
.0001	$.715E+4$	$.440E+2$	$.114E+1$	$.591E-1$	$.678E-2$	$.979E-3$
.0010	$.716E+3$	$.437E+4$	$.114E+3$	$.591E+1$	$.678E+0$	$.979E-1$
.0100	$.147E+3$	$.227E+6$	$.101E+5$	$.572E+3$	$.673E+2$	$.976E+1$
.0200	$.331E+3$	$.238E+6$	$.291E+5$	$.208E+4$	$.263E+3$	$.387E+2$
.0300	$.658E+3$	$.144E+6$	$.414E+5$	$.401E+4$	$.571E+3$	$.859E+2$
.0400	$.108E+4$	$.831E+5$	$.427E+5$	$.579E+4$	$.964E+3$	$.150E+3$
.0600	$.201E+4$	$.323E+5$	$.324E+5$	$.769E+4$	$.188E+4$	$.318E+3$
.0800	$.282E+4$	$.160E+5$	$.213E+5$	$.717E+4$	$.276E+4$	$.524E+3$
.1000	$.332E+4$	$.950E+4$	$.138E+5$	$.579E+4$	$.340E+4$	$.742E+3$
.1600	$.299E+4$	$.361E+4$	$.435E+4$	$.223E+4$	$.372E+4$	$.128E+4$
.2000	$.216E+4$	$.223E+4$	$.229E+4$	$.120E+4$	$.323E+4$	$.145E+4$
.2500	$.127E+4$	$.125E+4$	$.116E+4$	$.636E+3$	$.249E+4$	$.144E+4$
.3000	$.705E+3$	$.704E+3$	$.646E+3$	$.387E+3$	$.186E+4$	$.133E+4$
.4000	$.219E+3$	$.235E+3$	$.233E+3$	$.175E+3$	$.107E+4$	$.102E+4$
.5000	$.696E+2$	$.828E+2$	$.931E+2$	$.883E+2$	$.654E+3$	$.726E+3$
.6000	$.201E+2$	$.294E+2$	$.399E+2$	$.483E+2$	$.421E+3$	$.522E+3$
.8000	$-.261E+1$	$.207E+1$	$.865E+1$	$.178E+2$	$.193E+3$	$.275E+3$
1.0000	$-.430E+1$	$-.165E+1$	$.220E+1$	$.815E+1$	$.101E+3$	$.158E+3$
1.2000	$-.335E+1$	$-.172E+1$	$.635E+0$	$.440E+1$	$.588E+2$	$.971E+2$
1.6000	$-.160E+1$	$-.824E+0$	$.206E+0$	$.189E+1$	$.257E+2$	$.444E+2$
2.0000	$-.586E+0$	$-.186E+0$	$.342E+0$	$.121E+1$	$.145E+2$	$.244E+2$
2.5000	$.820E-1$	$.262E+0$	$.525E+0$	$.962E+0$	$.900E+1$	$.141E+2$
3.0000	$.393E+0$	$.487E+0$	$.633E+0$	$.874E+0$	$.667E+1$	$.951E+1$
4.0000	$.589E+0$	$.627E+0$	$.680E+0$	$.769E+0$	$.466E+1$	$.571E+1$
5.0000	$.586E+0$	$.599E+0$	$.622E+0$	$.660E+0$	$.364E+1$	$.408E+1$
6.0000	$.517E+0$	$.524E+0$	$.535E+0$	$.553E+0$	$.292E+1$	$.312E+1$
7.0000	$.438E+0$	$.442E+0$	$.448E+0$	$.458E+0$	$.236E+1$	$.246E+1$
8.0000	$.366E+0$	$.368E+0$	$.372E+0$	$.377E+0$	$.192E+1$	$.197E+1$
9.0000	$.304E+0$	$.306E+0$	$.308E+0$	$.311E+0$	$.157E+1$	$.160E+1$
10.0000	$.253E+0$	$.254E+0$	$.255E+0$	$.257E+0$	$.130E+1$	$.131E+1$
12.0000	$.177E+0$	$.177E+0$	$.178E+0$	$.179E+0$	$.897E+0$	$.904E+0$
16.0000	$.919E-1$	$.921E-1$	$.924E-1$	$.929E-1$	$.465E+0$	$.467E+0$
20.0000	$.528E-1$	$.528E-1$	$.530E-1$	$.533E-1$	$.267E+0$	$.268E+0$
25.0000	$.296E-1$	$.296E-1$	$.297E-1$	$.299E-1$	$.150E+0$	$.151E+0$
30.0000	$.181E-1$	$.181E-1$	$.182E-1$	$.183E-1$	$.921E-1$	$.930E-1$
40.0000	$.845E-2$	$.848E-2$	$.853E-2$	$.863E-2$	$.436E-1$	$.444E-1$
50.0000	$.576E-2$	$.582E-2$	$.586E-2$	$.593E-2$	$.300E-1$	$.307E-1$
60.0000	$.565E-2$	$.565E-2$	$.568E-2$	$.573E-2$	$.289E-1$	$.293E-1$
70.0000	$.617E-2$	$.617E-2$	$.619E-2$	$.623E-2$	$.313E-1$	$.315E-1$
80.0000	$.655E-2$	$.655E-2$	$.657E-2$	$.660E-2$	$.330E-1$	$.330E-1$
90.0000	$.649E-2$	$.649E-2$	$.650E-2$	$.652E-2$	$.325E-1$	$.325E-1$
100.0000	$.600E-2$	$.600E-2$	$.601E-2$	$.602E-2$	$.300E-1$	$.299E-1$
110.0000	$.518E-2$	$.519E-2$	$.520E-2$	$.521E-2$	$.259E-1$	$.258E-1$
120.0000	$.418E-2$	$.418E-2$	$.418E-2$	$.419E-2$	$.208E-1$	$.207E-1$
130.0000	$.313E-2$	$.310E-2$	$.310E-2$	$.311E-2$	$.154E-1$	$.154E-1$
140.0000	$.211E-2$	$.210E-2$	$.210E-2$	$.210E-2$	$.104E-1$	$.104E-1$
150.0000	$.120E-2$	$.122E-2$	$.123E-2$	$.123E-2$	$.609E-2$	$.606E-2$
160.0000	$.505E-3$	$.549E-3$	$.547E-3$	$.550E-3$	$.273E-2$	$.272E-2$
170.0000	$.115E-3$	$.135E-3$	$.135E-3$	$.135E-3$	$.672E-3$	$.669E-3$
180.0000	$.000E+0$	$.000E+0$	$.000E+0$	$.000E+0$	$.000E+0$	$.000E+0$

(to be continued)

(continued)

$\theta(°)$	$d_s = 64km$	$d_s = 100km$	$d_s = 200km$	$d_s = 300km$	$d_s = 400km$	$d_s = 637km$
.0000	$.000E+0$	$.000E+0$	$.000E+0$	$.000E+0$	$.000E+0$	$.000E+0$
.0001	$.595E-4$	$.999E-5$	$.631E-6$	$.128E-6$	$.432E-7$	$.726E-8$
.0010	$.595E-2$	$.999E-3$	$.631E-4$	$.128E-4$	$.432E-5$	$.726E-6$
.0100	$.595E+0$	$.999E-1$	$.630E-2$	$.128E-2$	$.432E-3$	$.726E-4$
.0200	$.237E+1$	$.399E+0$	$.252E-1$	$.512E-2$	$.173E-2$	$.290E-3$
.0300	$.532E+1$	$.897E+0$	$.567E-1$	$.115E-1$	$.389E-2$	$.653E-3$
.0400	$.942E+1$	$.159E+1$	$.101E+0$	$.205E-1$	$.692E-2$	$.116E-2$
.0600	$.209E+2$	$.356E+1$	$.226E+0$	$.460E-1$	$.156E-1$	$.261E-2$
.0800	$.365E+2$	$.628E+1$	$.402E+0$	$.818E-1$	$.276E-1$	$.464E-2$
.1000	$.556E+2$	$.972E+1$	$.626E+0$	$.128E+0$	$.432E-1$	$.725E-2$
.1600	$.128E+3$	$.239E+2$	$.159E+1$	$.325E+0$	$.110E+0$	$.185E-1$
.2000	$.182E+3$	$.359E+2$	$.246E+1$	$.506E+0$	$.172E+0$	$.290E-1$
.2500	$.247E+3$	$.528E+2$	$.378E+1$	$.785E+0$	$.267E+0$	$.452E-1$
.3000	$.301E+3$	$.708E+2$	$.534E+1$	$.112E+1$	$.383E+0$	$.649E-1$
.4000	$.369E+3$	$.105E+3$	$.907E+1$	$.195E+1$	$.674E+0$	$.115E+0$
.5000	$.374E+3$	$.133E+3$	$.134E+2$	$.297E+1$	$.104E+1$	$.178E+0$
.6000	$.352E+3$	$.151E+3$	$.179E+2$	$.415E+1$	$.147E+1$	$.255E+0$
.8000	$.273E+3$	$.157E+3$	$.268E+2$	$.680E+1$	$.249E+1$	$.445E+0$
1.0000	$.196E+3$	$.143E+3$	$.340E+2$	$.960E+1$	$.367E+1$	$.680E+0$
1.2000	$.141E+3$	$.122E+3$	$.388E+2$	$.123E+2$	$.493E+1$	$.952E+0$
1.6000	$.745E+2$	$.802E+2$	$.405E+2$	$.164E+2$	$.737E+1$	$.157E+1$
2.0000	$.434E+2$	$.523E+2$	$.369E+2$	$.186E+2$	$.933E+1$	$.225E+1$
2.5000	$.250E+2$	$.321E+2$	$.298E+2$	$.183E+2$	$.109E+2$	$.306E+1$
3.0000	$.160E+2$	$.210E+2$	$.228E+2$	$.167E+2$	$.115E+2$	$.376E+1$
4.0000	$.819E+1$	$.105E+2$	$.132E+2$	$.122E+2$	$.101E+2$	$.465E+1$
5.0000	$.514E+1$	$.622E+1$	$.805E+1$	$.847E+1$	$.804E+1$	$.475E+1$
6.0000	$.361E+1$	$.412E+1$	$.525E+1$	$.586E+1$	$.609E+1$	$.446E+1$
7.0000	$.269E+1$	$.295E+1$	$.361E+1$	$.418E+1$	$.461E+1$	$.397E+1$
8.0000	$.209E+1$	$.222E+1$	$.261E+1$	$.305E+1$	$.349E+1$	$.344E+1$
9.0000	$.166E+1$	$.173E+1$	$.197E+1$	$.231E+1$	$.271E+1$	$.291E+1$
10.0000	$.134E+1$	$.138E+1$	$.153E+1$	$.179E+1$	$.212E+1$	$.247E+1$
12.0000	$.911E+0$	$.921E+0$	$.988E+0$	$.115E+1$	$.139E+1$	$.180E+1$
16.0000	$.467E+0$	$.469E+0$	$.494E+0$	$.572E+0$	$.706E+0$	$.103E+1$
20.0000	$.269E+0$	$.270E+0$	$.286E+0$	$.335E+0$	$.421E+0$	$.657E+0$
25.0000	$.152E+0$	$.153E+0$	$.165E+0$	$.197E+0$	$.252E+0$	$.418E+0$
30.0000	$.943E-1$	$.960E-1$	$.105E+0$	$.129E+0$	$.168E+0$	$.290E+0$
40.0000	$.459E-1$	$.476E-1$	$.548E-1$	$.694E-1$	$.937E-1$	$.174E+0$
50.0000	$.318E-1$	$.332E-1$	$.389E-1$	$.501E-1$	$.686E-1$	$.131E+0$
60.0000	$.301E-1$	$.310E-1$	$.353E-1$	$.447E-1$	$.604E-1$	$.113E+0$
70.0000	$.318E-1$	$.322E-1$	$.353E-1$	$.434E-1$	$.574E-1$	$.104E+0$
80.0000	$.329E-1$	$.329E-1$	$.350E-1$	$.420E-1$	$.545E-1$	$.947E-1$
90.0000	$.321E-1$	$.319E-1$	$.333E-1$	$.392E-1$	$.501E-1$	$.843E-1$
100.0000	$.295E-1$	$.291E-1$	$.299E-1$	$.349E-1$	$.440E-1$	$.723E-1$
110.0000	$.253E-1$	$.249E-1$	$.254E-1$	$.293E-1$	$.366E-1$	$.592E-1$
120.0000	$.203E-1$	$.199E-1$	$.202E-1$	$.232E-1$	$.288E-1$	$.460E-1$
130.0000	$.150E-1$	$.148E-1$	$.149E-1$	$.170E-1$	$.211E-1$	$.333E-1$
140.0000	$.101E-1$	$.991E-2$	$.997E-2$	$.113E-1$	$.140E-1$	$.220E-1$
150.0000	$.589E-2$	$.577E-2$	$.579E-2$	$.658E-2$	$.811E-2$	$.127E-1$
160.0000	$.268E-2$	$.262E-2$	$.263E-2$	$.298E-2$	$.367E-2$	$.573E-2$
170.0000	$.680E-3$	$.665E-3$	$.666E-3$	$.755E-3$	$.928E-3$	$.144E-2$
180.0000	$.000E+0$	$.000E+0$	$.000E+0$	$.000E+0$	$.000E+0$	$.000E+0$

Table E.10. Gravity change $\Delta\hat{g}^{(2)}(a, \theta)$ caused by a vertical dip-slip faulting

$\theta(^\circ)$	$d_s = 0km$	$d_s = 2km$	$d_s = 5km$	$d_s = 10km$	$d_s = 20km$	$d_s = 32km$
.0000	$.000E+0$	$.000E+0$	$.000E+0$	$.000E+0$	$.000E+0$	$.000E+0$
.0001	$.000E+0$	$.159E+5$	$.998E+3$	$.129E+3$	$.241E+2$	$.559E+1$
.0010	$.000E+0$	$.158E+6$	$.997E+4$	$.129E+4$	$.241E+3$	$.559E+2$
.0100	$.000E+0$	$.824E+6$	$.886E+5$	$.125E+5$	$.239E+4$	$.557E+3$
.0200	$.000E+0$	$.426E+6$	$.127E+6$	$.230E+5$	$.468E+4$	$.110E+4$
.0300	$.000E+0$	$.170E+6$	$.117E+6$	$.300E+5$	$.674E+4$	$.163E+4$
.0400	$.000E+0$	$.709E+5$	$.894E+5$	$.334E+5$	$.851E+4$	$.213E+4$
.0600	$.000E+0$	$.147E+5$	$.411E+5$	$.315E+5$	$.110E+5$	$.301E+4$
.0800	$.000E+0$	$.271E+4$	$.173E+5$	$.248E+5$	$.119E+5$	$.370E+4$
.1000	$.000E+0$	$-.299E+3$	$.729E+4$	$.179E+5$	$.118E+5$	$.417E+4$
.1600	$.000E+0$	$-.311E+3$	$.129E+4$	$.592E+4$	$.785E+4$	$.449E+4$
.2000	$.000E+0$	$.117E+3$	$.946E+3$	$.307E+4$	$.541E+4$	$.418E+4$
.2500	$.000E+0$	$.235E+3$	$.700E+3$	$.157E+4$	$.331E+4$	$.322E+4$
.3000	$.000E+0$	$.184E+3$	$.469E+3$	$.912E+3$	$.211E+4$	$.250E+4$
.4000	$.000E+0$	$.729E+2$	$.184E+3$	$.352E+3$	$.951E+3$	$.143E+4$
.5000	$.000E+0$	$.280E+2$	$.730E+2$	$.145E+3$	$.473E+3$	$.843E+3$
.6000	$.000E+0$	$.113E+2$	$.306E+2$	$.642E+2$	$.251E+3$	$.503E+3$
.8000	$.000E+0$	$.206E+1$	$.621E+1$	$.152E+2$	$.873E+2$	$.201E+3$
1.0000	$.000E+0$	$.390E+0$	$.149E+1$	$.451E+1$	$.350E+2$	$.906E+2$
1.2000	$.000E+0$	$.402E-1$	$.369E+0$	$.158E+1$	$.154E+2$	$.450E+2$
1.6000	$.000E+0$	$-.612E-1$	$-.624E-1$	$.170E+0$	$.390E+1$	$.135E+2$
2.0000	$.000E+0$	$-.597E-1$	$-.111E+0$	$-.936E-1$	$.970E+0$	$.432E+1$
2.5000	$.000E+0$	$-.462E-1$	$-.989E-1$	$-.142E+0$	$-.468E-1$	$.943E+0$
3.0000	$.000E+0$	$-.338E-1$	$-.763E-1$	$-.125E+0$	$-.276E+0$	$-.383E-1$
4.0000	$.000E+0$	$-.172E-1$	$-.404E-1$	$-.717E-1$	$-.243E+0$	$-.329E+0$
5.0000	$.000E+0$	$-.858E-2$	$-.204E-1$	$-.370E-1$	$-.142E+0$	$-.225E+0$
6.0000	$.000E+0$	$-.417E-2$	$-.993E-2$	$-.181E-1$	$-.733E-1$	$-.123E+0$
7.0000	$.000E+0$	$-.192E-2$	$-.455E-2$	$-.823E-2$	$-.346E-1$	$-.575E-1$
8.0000	$.000E+0$	$-.769E-3$	$-.178E-2$	$-.309E-2$	$-.133E-1$	$-.203E-1$
9.0000	$.000E+0$	$-.182E-3$	$-.374E-3$	$-.478E-3$	$-.201E-2$	$-.402E-4$
10.0000	$.000E+0$	$.110E-3$	$.325E-3$	$.811E-3$	$.377E-2$	$.102E-1$
12.0000	$.000E+0$	$.294E-3$	$.757E-3$	$.158E-2$	$.746E-2$	$.165E-1$
16.0000	$.000E+0$	$.228E-3$	$.578E-3$	$.117E-2$	$.591E-2$	$.127E-1$
20.0000	$.000E+0$	$.128E-3$	$.323E-3$	$.652E-3$	$.365E-2$	$.788E-2$
25.0000	$.000E+0$	$.580E-4$	$.146E-3$	$.294E-3$	$.208E-2$	$.461E-2$
30.0000	$.000E+0$	$.212E-4$	$.534E-4$	$.108E-3$	$.126E-2$	$.290E-2$
40.0000	$.000E+0$	$-.172E-4$	$-.430E-4$	$-.854E-4$	$.343E-3$	$.964E-3$
50.0000	$.000E+0$	$-.365E-4$	$-.914E-4$	$-.182E-3$	$-.206E-3$	$-.211E-3$
60.0000	$.000E+0$	$-.455E-4$	$-.114E-3$	$-.227E-3$	$-.516E-3$	$-.890E-3$
70.0000	$.000E+0$	$-.482E-4$	$-.121E-3$	$-.241E-3$	$-.658E-3$	$-.121E-2$
80.0000	$.000E+0$	$-.475E-4$	$-.119E-3$	$-.236E-3$	$-.689E-3$	$-.129E-2$
90.0000	$.000E+0$	$-.448E-4$	$-.112E-3$	$-.223E-3$	$-.661E-3$	$-.125E-2$
100.0000	$.000E+0$	$-.416E-4$	$-.104E-3$	$-.207E-3$	$-.609E-3$	$-.115E-2$
110.0000	$.000E+0$	$-.376E-4$	$-.944E-4$	$-.188E-3$	$-.541E-3$	$-.101E-2$
120.0000	$.000E+0$	$-.333E-4$	$-.836E-4$	$-.166E-3$	$-.467E-3$	$-.869E-3$
130.0000	$.000E+0$	$-.291E-4$	$-.720E-4$	$-.144E-3$	$-.394E-3$	$-.727E-3$
140.0000	$.000E+0$	$-.237E-4$	$-.596E-4$	$-.119E-3$	$-.318E-3$	$-.583E-3$
150.0000	$.000E+0$	$-.182E-4$	$-.455E-4$	$-.907E-4$	$-.238E-3$	$-.434E-3$
160.0000	$.000E+0$	$-.123E-4$	$-.310E-4$	$-.617E-4$	$-.160E-3$	$-.292E-3$
170.0000	$.000E+0$	$-.614E-5$	$-.158E-4$	$-.317E-4$	$-.831E-4$	$-.151E-3$
180.0000	$.000E+0$	$.000E+0$	$.000E+0$	$.000E+0$	$.000E+0$	$.000E+0$

(to be continued)

(continued)

$\theta(°)$	$d_s = 64km$	$d_s = 100km$	$d_s = 200km$	$d_s = 300km$	$d_s = 400km$	$d_s = 637km$
.0000	$.000E+0$	$.000E+0$	$.000E+0$	$.000E+0$	$.000E+0$	$.000E+0$
.0001	$.689E+0$	$.181E+0$	$.232E-1$	$.709E-2$	$.321E-2$	$.894E-3$
.0010	$.689E+1$	$.181E+1$	$.232E+0$	$.709E-1$	$.321E-1$	$.894E-2$
.0100	$.688E+2$	$.181E+2$	$.232E+1$	$.709E+0$	$.321E+0$	$.894E-1$
.0200	$.137E+3$	$.361E+2$	$.464E+1$	$.142E+1$	$.642E+0$	$.179E+0$
.0300	$.205E+3$	$.540E+2$	$.695E+1$	$.213E+1$	$.963E+0$	$.268E+0$
.0400	$.272E+3$	$.719E+2$	$.927E+1$	$.283E+1$	$.128E+1$	$.357E+0$
.0600	$.403E+3$	$.107E+3$	$.139E+2$	$.425E+1$	$.193E+1$	$.536E+0$
.0800	$.526E+3$	$.142E+3$	$.185E+2$	$.566E+1$	$.257E+1$	$.715E+0$
.1000	$.641E+3$	$.176E+3$	$.230E+2$	$.706E+1$	$.320E+1$	$.893E+0$
.1600	$.921E+3$	$.269E+3$	$.364E+2$	$.112E+2$	$.511E+1$	$.143E+1$
.2000	$.104E+4$	$.323E+3$	$.451E+2$	$.140E+2$	$.638E+1$	$.178E+1$
.2500	$.113E+4$	$.379E+3$	$.555E+2$	$.174E+2$	$.794E+1$	$.223E+1$
.3000	$.115E+4$	$.422E+3$	$.653E+2$	$.207E+2$	$.948E+1$	$.267E+1$
.4000	$.108E+4$	$.470E+3$	$.829E+2$	$.270E+2$	$.125E+2$	$.354E+1$
.5000	$.857E+3$	$.477E+3$	$.973E+2$	$.328E+2$	$.154E+2$	$.439E+1$
.6000	$.674E+3$	$.458E+3$	$.108E+3$	$.380E+2$	$.181E+2$	$.524E+1$
.8000	$.388E+3$	$.349E+3$	$.121E+3$	$.466E+2$	$.230E+2$	$.685E+1$
1.0000	$.223E+3$	$.253E+3$	$.122E+3$	$.524E+2$	$.270E+2$	$.836E+1$
1.2000	$.130E+3$	$.175E+3$	$.117E+3$	$.555E+2$	$.301E+2$	$.975E+1$
1.6000	$.486E+2$	$.840E+2$	$.882E+2$	$.558E+2$	$.335E+2$	$.121E+2$
2.0000	$.202E+2$	$.411E+2$	$.629E+2$	$.488E+2$	$.339E+2$	$.138E+2$
2.5000	$.744E+1$	$.179E+2$	$.389E+2$	$.387E+2$	$.319E+2$	$.150E+2$
3.0000	$.262E+1$	$.815E+1$	$.239E+2$	$.290E+2$	$.262E+2$	$.153E+2$
4.0000	$.205E+0$	$.199E+1$	$.927E+1$	$.152E+2$	$.172E+2$	$.140E+2$
5.0000	$-.124E+0$	$.529E+0$	$.396E+1$	$.802E+1$	$.106E+2$	$.115E+2$
6.0000	$-.102E+0$	$.165E+0$	$.191E+1$	$.439E+1$	$.658E+1$	$.897E+1$
7.0000	$-.428E-1$	$.991E-1$	$.105E+1$	$.257E+1$	$.422E+1$	$.681E+1$
8.0000	$.970E-3$	$.933E-1$	$.700E+0$	$.166E+1$	$.278E+1$	$.510E+1$
9.0000	$.268E-1$	$.963E-1$	$.498E+0$	$.112E+1$	$.194E+1$	$.383E+1$
10.0000	$.396E-1$	$.966E-1$	$.383E+0$	$.834E+0$	$.140E+1$	$.292E+1$
12.0000	$.450E-1$	$.867E-1$	$.252E+0$	$.507E+0$	$.815E+0$	$.176E+1$
16.0000	$.315E-1$	$.552E-1$	$.134E+0$	$.236E+0$	$.368E+0$	$.777E+0$
20.0000	$.194E-1$	$.333E-1$	$.772E-1$	$.132E+0$	$.200E+0$	$.420E+0$
25.0000	$.114E-1$	$.194E-1$	$.441E-1$	$.740E-1$	$.110E+0$	$.233E+0$
30.0000	$.723E-2$	$.124E-1$	$.278E-1$	$.463E-1$	$.690E-1$	$.147E+0$
40.0000	$.258E-2$	$.452E-2$	$.103E-1$	$.175E-1$	$.262E-1$	$.578E-1$
50.0000	$-.213E-3$	$-.187E-3$	$.802E-4$	$.801E-3$	$.232E-2$	$.975E-2$
60.0000	$-.185E-2$	$-.294E-2$	$-.588E-2$	$-.888E-2$	$-.117E-1$	$-.182E-1$
70.0000	$-.265E-2$	$-.428E-2$	$-.882E-2$	$-.136E-1$	$-.187E-1$	$-.322E-1$
80.0000	$-.286E-2$	$-.466E-2$	$-.972E-2$	$-.152E-1$	$-.210E-1$	$-.371E-1$
90.0000	$-.277E-2$	$-.453E-2$	$-.950E-2$	$-.149E-1$	$-.207E-1$	$-.369E-1$
100.0000	$-.255E-2$	$-.416E-2$	$-.878E-2$	$-.138E-1$	$-.192E-1$	$-.343E-1$
110.0000	$-.225E-2$	$-.367E-2$	$-.776E-2$	$-.122E-1$	$-.170E-1$	$-.303E-1$
120.0000	$-.191E-2$	$-.314E-2$	$-.662E-2$	$-.105E-1$	$-.145E-1$	$-.259E-1$
130.0000	$-.160E-2$	$-.261E-2$	$-.554E-2$	$-.873E-2$	$-.121E-1$	$-.215E-1$
140.0000	$-.128E-2$	$-.209E-2$	$-.443E-2$	$-.697E-2$	$-.972E-2$	$-.172E-1$
150.0000	$-.947E-3$	$-.155E-2$	$-.329E-2$	$-.523E-2$	$-.720E-2$	$-.127E-1$
160.0000	$-.636E-3$	$-.104E-2$	$-.220E-2$	$-.349E-2$	$-.483E-2$	$-.849E-2$
170.0000	$-.331E-3$	$-.539E-3$	$-.114E-2$	$-.174E-2$	$-.251E-2$	$-.441E-2$
180.0000	$.000E+0$	$.000E+0$	$.000E+0$	$.000E+0$	$.000E+0$	$.000E+0$

Table E.11. Gravity change $\Delta\hat{g}^{(30)}(a, \theta)$ caused by a 45° dip-slip faulting

$\theta(^\circ)$	$d_s = 0km$	$d_s = 2km$	$d_s = 5km$	$d_s = 10km$	$d_s = 20km$	$d_s = 32km$
.0000	$.949E+4$	$.144E+7$	$.235E+6$	$.537E+5$	$.206E+5$	$.782E+4$
.0001	$.949E+4$	$.144E+7$	$.235E+6$	$.537E+5$	$.206E+5$	$.782E+4$
.0010	$.949E+4$	$.143E+7$	$.234E+6$	$.536E+5$	$.206E+5$	$.782E+4$
.0100	$.935E+4$	$.625E+6$	$.203E+6$	$.515E+5$	$.204E+5$	$.779E+4$
.0200	$.907E+4$	$.787E+5$	$.140E+6$	$.456E+5$	$.198E+5$	$.771E+4$
.0300	$.849E+4$	$-.153E+5$	$.748E+5$	$.376E+5$	$.188E+5$	$.756E+4$
.0400	$.767E+4$	$-.201E+5$	$.352E+5$	$.296E+5$	$.176E+5$	$.737E+4$
.0600	$.579E+4$	$-.940E+4$	$.319E+4$	$.133E+5$	$.145E+5$	$.684E+4$
.0800	$.383E+4$	$-.433E+4$	$-.377E+4$	$.436E+4$	$.115E+5$	$.618E+4$
.1000	$.216E+4$	$-.248E+4$	$-.454E+4$	$.170E+3$	$.795E+4$	$.547E+4$
.1600	$-.368E+3$	$-.124E+4$	$-.236E+4$	$-.151E+4$	$.218E+4$	$.321E+4$
.2000	$-.655E+3$	$-.928E+3$	$-.134E+4$	$-.978E+3$	$.678E+3$	$.207E+4$
.2500	$-.535E+3$	$-.612E+3$	$-.703E+3$	$-.518E+3$	$-.861E+2$	$.111E+4$
.3000	$-.350E+3$	$-.388E+3$	$-.410E+3$	$-.307E+3$	$-.268E+3$	$.544E+3$
.4000	$-.134E+3$	$-.156E+3$	$-.171E+3$	$-.146E+3$	$-.289E+3$	$.338E+2$
.5000	$-.524E+2$	$-.666E+2$	$-.804E+2$	$-.836E+2$	$-.224E+3$	$-.972E+2$
.6000	$-.208E+2$	$-.301E+2$	$-.410E+2$	$-.507E+2$	$-.162E+3$	$-.125E+3$
.8000	$-.247E+1$	$-.693E+1$	$-.130E+2$	$-.215E+2$	$-.846E+2$	$-.952E+2$
1.0000	$.934E+0$	$-.149E+1$	$-.499E+1$	$-.104E+2$	$-.448E+2$	$-.610E+2$
1.2000	$.157E+1$	$.124E+0$	$-.201E+1$	$-.540E+1$	$-.250E+2$	$-.385E+2$
1.6000	$.151E+1$	$.880E+0$	$-.671E-1$	$-.161E+1$	$-.845E+1$	$-.167E+2$
2.0000	$.123E+1$	$.895E+0$	$.396E+0$	$-.424E+0$	$-.286E+1$	$-.771E+1$
2.5000	$.892E+0$	$.718E+0$	$.457E+0$	$.262E-1$	$-.509E+0$	$-.323E+1$
3.0000	$.623E+0$	$.523E+0$	$.371E+0$	$.119E+0$	$.133E+0$	$-.151E+1$
4.0000	$.271E+0$	$.230E+0$	$.167E+0$	$.630E-1$	$.128E+0$	$-.569E+0$
5.0000	$.848E-1$	$.646E-1$	$.341E-1$	$-.170E-1$	$-.125E+0$	$-.462E+0$
6.0000	$-.108E-1$	$-.219E-1$	$-.385E-1$	$-.663E-1$	$-.302E+0$	$-.481E+0$
7.0000	$-.581E-1$	$-.646E-1$	$-.745E-1$	$-.910E-1$	$-.393E+0$	$-.496E+0$
8.0000	$-.797E-1$	$-.839E-1$	$-.902E-1$	$-.101E+0$	$-.429E+0$	$-.492E+0$
9.0000	$-.877E-1$	$-.905E-1$	$-.947E-1$	$-.102E+0$	$-.432E+0$	$-.473E+0$
10.0000	$-.885E-1$	$-.904E-1$	$-.934E-1$	$-.983E-1$	$-.417E+0$	$-.445E+0$
12.0000	$-.808E-1$	$-.819E-1$	$-.836E-1$	$-.862E-1$	$-.366E+0$	$-.381E+0$
16.0000	$-.594E-1$	$-.599E-1$	$-.606E-1$	$-.617E-1$	$-.263E+0$	$-.269E+0$
20.0000	$-.428E-1$	$-.431E-1$	$-.434E-1$	$-.440E-1$	$-.188E+0$	$-.191E+0$
25.0000	$-.280E-1$	$-.282E-1$	$-.284E-1$	$-.287E-1$	$-.123E+0$	$-.124E+0$
30.0000	$-.170E-1$	$-.171E-1$	$-.172E-1$	$-.174E-1$	$-.745E-1$	$-.758E-1$
40.0000	$-.165E-2$	$-.171E-2$	$-.179E-2$	$-.193E-2$	$-.818E-2$	$-.896E-2$
50.0000	$.705E-2$	$.700E-2$	$.693E-2$	$.682E-2$	$.293E-1$	$.287E-1$
60.0000	$.108E-1$	$.107E-1$	$.107E-1$	$.106E-1$	$.455E-1$	$.450E-1$
70.0000	$.111E-1$	$.111E-1$	$.111E-1$	$.110E-1$	$.472E-1$	$.469E-1$
80.0000	$.952E-2$	$.950E-2$	$.948E-2$	$.942E-2$	$.405E-1$	$.403E-1$
90.0000	$.691E-2$	$.690E-2$	$.689E-2$	$.686E-2$	$.295E-1$	$.294E-1$
100.0000	$.393E-2$	$.393E-2$	$.392E-2$	$.391E-2$	$.168E-1$	$.168E-1$
110.0000	$.954E-3$	$.952E-3$	$.957E-3$	$.964E-3$	$.415E-2$	$.421E-2$
120.0000	$-.179E-2$	$-.178E-2$	$-.177E-2$	$-.175E-2$	$-.750E-2$	$-.738E-2$
130.0000	$-.419E-2$	$-.417E-2$	$-.415E-2$	$-.411E-2$	$-.177E-1$	$-.175E-1$
140.0000	$-.619E-2$	$-.617E-2$	$-.615E-2$	$-.609E-2$	$-.262E-1$	$-.260E-1$
150.0000	$-.775E-2$	$-.773E-2$	$-.770E-2$	$-.764E-2$	$-.328E-1$	$-.326E-1$
160.0000	$-.886E-2$	$-.883E-2$	$-.880E-2$	$-.873E-2$	$-.375E-1$	$-.373E-1$
170.0000	$-.953E-2$	$-.952E-2$	$-.948E-2$	$-.940E-2$	$-.405E-1$	$-.402E-1$
180.0000	$-.975E-2$	$-.975E-2$	$-.971E-2$	$-.964E-2$	$-.414E-1$	$-.412E-1$

(to be continued)

(continued)

$\theta(°)$	$d_s = 64km$	$d_s = 100km$	$d_s = 200km$	$d_s = 300km$	$d_s = 400km$	$d_s = 637km$
.0000	$.199E+4$	$.830E+3$	$.217E+3$	$.988E+2$	$.590E+2$	$.246E+2$
.0001	$.199E+4$	$.830E+3$	$.217E+3$	$.988E+2$	$.590E+2$	$.246E+2$
.0010	$.199E+4$	$.830E+3$	$.217E+3$	$.988E+2$	$.590E+2$	$.246E+2$
.0100	$.199E+4$	$.829E+3$	$.217E+3$	$.988E+2$	$.590E+2$	$.246E+2$
.0200	$.198E+4$	$.829E+3$	$.217E+3$	$.988E+2$	$.590E+2$	$.246E+2$
.0300	$.197E+4$	$.827E+3$	$.217E+3$	$.988E+2$	$.590E+2$	$.246E+2$
.0400	$.196E+4$	$.825E+3$	$.216E+3$	$.988E+2$	$.590E+2$	$.246E+2$
.0600	$.193E+4$	$.819E+3$	$.216E+3$	$.987E+2$	$.590E+2$	$.246E+2$
.0800	$.188E+4$	$.811E+3$	$.215E+3$	$.986E+2$	$.589E+2$	$.246E+2$
.1000	$.182E+4$	$.801E+3$	$.215E+3$	$.984E+2$	$.589E+2$	$.246E+2$
.1600	$.159E+4$	$.759E+3$	$.212E+3$	$.978E+2$	$.587E+2$	$.245E+2$
.2000	$.142E+4$	$.722E+3$	$.209E+3$	$.973E+2$	$.585E+2$	$.245E+2$
.2500	$.121E+4$	$.669E+3$	$.205E+3$	$.964E+2$	$.582E+2$	$.244E+2$
.3000	$.102E+4$	$.612E+3$	$.200E+3$	$.954E+2$	$.578E+2$	$.244E+2$
.4000	$.573E+3$	$.500E+3$	$.189E+3$	$.929E+2$	$.569E+2$	$.242E+2$
.5000	$.317E+3$	$.368E+3$	$.175E+3$	$.897E+2$	$.558E+2$	$.240E+2$
.6000	$.159E+3$	$.267E+3$	$.160E+3$	$.860E+2$	$.544E+2$	$.238E+2$
.8000	$.117E+2$	$.126E+3$	$.130E+3$	$.774E+2$	$.512E+2$	$.232E+2$
1.0000	$-.267E+2$	$.502E+2$	$.956E+2$	$.682E+2$	$.473E+2$	$.224E+2$
1.2000	$-.334E+2$	$.108E+2$	$.690E+2$	$.592E+2$	$.432E+2$	$.216E+2$
1.6000	$-.241E+2$	$-.118E+2$	$.317E+2$	$.389E+2$	$.349E+2$	$.195E+2$
2.0000	$-.149E+2$	$-.136E+2$	$.117E+2$	$.241E+2$	$.253E+2$	$.173E+2$
2.5000	$-.857E+1$	$-.103E+2$	$.676E-1$	$.117E+2$	$.163E+2$	$.145E+2$
3.0000	$-.498E+1$	$-.717E+1$	$-.362E+1$	$.450E+1$	$.963E+1$	$.121E+2$
4.0000	$-.223E+1$	$-.367E+1$	$-.427E+1$	$-.143E+1$	$.215E+1$	$.631E+1$
5.0000	$-.130E+1$	$-.213E+1$	$-.318E+1$	$-.251E+1$	$-.820E+0$	$.299E+1$
6.0000	$-.938E+0$	$-.142E+1$	$-.225E+1$	$-.228E+1$	$-.163E+1$	$.101E+1$
7.0000	$-.762E+0$	$-.105E+1$	$-.164E+1$	$-.188E+1$	$-.173E+1$	$-.125E+0$
8.0000	$-.655E+0$	$-.837E+0$	$-.125E+1$	$-.149E+1$	$-.154E+1$	$-.636E+0$
9.0000	$-.579E+0$	$-.698E+0$	$-.991E+0$	$-.121E+1$	$-.134E+1$	$-.855E+0$
10.0000	$-.517E+0$	$-.599E+0$	$-.805E+0$	$-.996E+0$	$-.112E+1$	$-.918E+0$
12.0000	$-.419E+0$	$-.462E+0$	$-.577E+0$	$-.702E+0$	$-.820E+0$	$-.873E+0$
16.0000	$-.284E+0$	$-.302E+0$	$-.351E+0$	$-.416E+0$	$-.499E+0$	$-.644E+0$
20.0000	$-.199E+0$	$-.209E+0$	$-.238E+0$	$-.280E+0$	$-.335E+0$	$-.470E+0$
25.0000	$-.129E+0$	$-.135E+0$	$-.153E+0$	$-.180E+0$	$-.219E+0$	$-.322E+0$
30.0000	$-.789E-1$	$-.830E-1$	$-.950E-1$	$-.113E+0$	$-.139E+0$	$-.210E+0$
40.0000	$-.109E-1$	$-.130E-1$	$-.186E-1$	$-.254E-1$	$-.342E-1$	$-.605E-1$
50.0000	$.273E-1$	$.261E-1$	$.238E-1$	$.232E-1$	$.237E-1$	$.226E-1$
60.0000	$.440E-1$	$.434E-1$	$.429E-1$	$.453E-1$	$.503E-1$	$.621E-1$
70.0000	$.462E-1$	$.460E-1$	$.464E-1$	$.500E-1$	$.565E-1$	$.729E-1$
80.0000	$.399E-1$	$.398E-1$	$.407E-1$	$.443E-1$	$.505E-1$	$.665E-1$
90.0000	$.292E-1$	$.292E-1$	$.302E-1$	$.331E-1$	$.381E-1$	$.512E-1$
100.0000	$.168E-1$	$.170E-1$	$.178E-1$	$.197E-1$	$.230E-1$	$.317E-1$
110.0000	$.436E-2$	$.456E-2$	$.516E-2$	$.611E-2$	$.742E-2$	$.112E-1$
120.0000	$-.709E-2$	$-.688E-2$	$-.650E-2$	$-.663E-2$	$-.709E-2$	$-.816E-2$
130.0000	$-.171E-1$	$-.169E-1$	$-.168E-1$	$-.178E-1$	$-.199E-1$	$-.252E-1$
140.0000	$-.255E-1$	$-.253E-1$	$-.253E-1$	$-.272E-1$	$-.307E-1$	$-.398E-1$
150.0000	$-.320E-1$	$-.318E-1$	$-.320E-1$	$-.345E-1$	$-.392E-1$	$-.512E-1$
160.0000	$-.367E-1$	$-.364E-1$	$-.368E-1$	$-.398E-1$	$-.451E-1$	$-.593E-1$
170.0000	$-.395E-1$	$-.393E-1$	$-.397E-1$	$-.429E-1$	$-.489E-1$	$-.643E-1$
180.0000	$-.405E-1$	$-.403E-1$	$-.407E-1$	$-.439E-1$	$-.501E-1$	$-.661E-1$

Table E.12. Gravity change $\Delta\hat{g}^{(4)}(a, \theta)$ caused by a tensile faulting

$\theta(\circ)$	$d_s = 0km$	$d_s = 2km$	$d_s = 5km$	$d_s = 10km$	$d_s = 20km$	$d_s = 32km$
.0000	$.000E+0$	$.191E+7$	$.316E+6$	$.102E+6$	$.271E+5$	$.103E+5$
.0001	$.000E+0$	$.191E+7$	$.316E+6$	$.102E+6$	$.271E+5$	$.103E+5$
.0010	$.000E+0$	$.190E+7$	$.316E+6$	$.102E+6$	$.271E+5$	$.103E+5$
.0100	$.000E+0$	$.828E+6$	$.275E+6$	$.980E+5$	$.268E+5$	$.103E+5$
.0200	$.000E+0$	$.104E+6$	$.191E+6$	$.879E+5$	$.260E+5$	$.102E+5$
.0300	$.000E+0$	$-.242E+5$	$.103E+6$	$.738E+5$	$.248E+5$	$.999E+4$
.0400	$.000E+0$	$-.310E+5$	$.499E+5$	$.594E+5$	$.231E+5$	$.973E+4$
.0600	$.000E+0$	$-.162E+5$	$.592E+4$	$.294E+5$	$.191E+5$	$.902E+4$
.0800	$.000E+0$	$-.850E+4$	$-.428E+4$	$.115E+5$	$.151E+5$	$.814E+4$
.1000	$.000E+0$	$-.501E+4$	$-.581E+4$	$.237E+4$	$.104E+5$	$.718E+4$
.1600	$.000E+0$	$-.150E+4$	$-.331E+4$	$-.299E+4$	$.273E+4$	$.417E+4$
.2000	$.000E+0$	$-.764E+3$	$-.182E+4$	$-.213E+4$	$.767E+3$	$.267E+4$
.2500	$.000E+0$	$-.363E+3$	$-.857E+3$	$-.115E+4$	$-.181E+3$	$.141E+4$
.3000	$.000E+0$	$-.198E+3$	$-.449E+3$	$-.653E+3$	$-.366E+3$	$.688E+3$
.4000	$.000E+0$	$-.819E+2$	$-.184E+3$	$-.292E+3$	$-.343E+3$	$.457E+2$
.5000	$.000E+0$	$-.427E+2$	$-.987E+2$	$-.171E+3$	$-.258E+3$	$-.115E+3$
.6000	$.000E+0$	$-.251E+2$	$-.594E+2$	$-.106E+3$	$-.189E+3$	$-.151E+3$
.8000	$.000E+0$	$-.108E+2$	$-.263E+2$	$-.499E+2$	$-.104E+3$	$-.119E+3$
1.0000	$.000E+0$	$-.556E+1$	$-.138E+2$	$-.267E+2$	$-.601E+2$	$-.789E+2$
1.2000	$.000E+0$	$-.323E+1$	$-.803E+1$	$-.158E+2$	$-.362E+2$	$-.522E+2$
1.6000	$.000E+0$	$-.137E+1$	$-.341E+1$	$-.676E+1$	$-.161E+2$	$-.255E+2$
2.0000	$.000E+0$	$-.700E+0$	$-.175E+1$	$-.348E+1$	$-.840E+1$	$-.138E+2$
2.5000	$.000E+0$	$-.359E+0$	$-.898E+0$	$-.179E+1$	$-.436E+1$	$-.736E+1$
3.0000	$.000E+0$	$-.208E+0$	$-.521E+0$	$-.104E+1$	$-.255E+1$	$-.436E+1$
4.0000	$.000E+0$	$-.879E-1$	$-.220E+0$	$-.440E+0$	$-.109E+1$	$-.189E+1$
5.0000	$.000E+0$	$-.449E-1$	$-.113E+0$	$-.225E+0$	$-.559E+0$	$-.980E+0$
6.0000	$.000E+0$	$-.259E-1$	$-.649E-1$	$-.130E+0$	$-.324E+0$	$-.570E+0$
7.0000	$.000E+0$	$-.162E-1$	$-.407E-1$	$-.813E-1$	$-.204E+0$	$-.359E+0$
8.0000	$.000E+0$	$-.108E-1$	$-.271E-1$	$-.542E-1$	$-.136E+0$	$-.240E+0$
9.0000	$.000E+0$	$-.755E-2$	$-.189E-1$	$-.378E-1$	$-.954E-1$	$-.169E+0$
10.0000	$.000E+0$	$-.547E-2$	$-.137E-1$	$-.274E-1$	$-.695E-1$	$-.123E+0$
12.0000	$.000E+0$	$-.313E-2$	$-.782E-2$	$-.156E-1$	$-.401E-1$	$-.711E-1$
16.0000	$.000E+0$	$-.130E-2$	$-.325E-2$	$-.650E-2$	$-.171E-1$	$-.304E-1$
20.0000	$.000E+0$	$-.670E-3$	$-.168E-2$	$-.335E-2$	$-.898E-2$	$-.161E-1$
25.0000	$.000E+0$	$-.362E-3$	$-.905E-3$	$-.181E-2$	$-.492E-2$	$-.887E-2$
30.0000	$.000E+0$	$-.236E-3$	$-.589E-3$	$-.118E-2$	$-.318E-2$	$-.572E-2$
40.0000	$.000E+0$	$-.149E-3$	$-.372E-3$	$-.743E-3$	$-.187E-2$	$-.328E-2$
50.0000	$.000E+0$	$-.121E-3$	$-.302E-3$	$-.604E-3$	$-.139E-2$	$-.235E-2$
60.0000	$.000E+0$	$-.103E-3$	$-.257E-3$	$-.512E-3$	$-.110E-2$	$-.182E-2$
70.0000	$.000E+0$	$-.834E-4$	$-.208E-3$	$-.416E-3$	$-.859E-3$	$-.140E-2$
80.0000	$.000E+0$	$-.618E-4$	$-.155E-3$	$-.309E-3$	$-.619E-3$	$-.993E-3$
90.0000	$.000E+0$	$-.392E-4$	$-.981E-4$	$-.196E-3$	$-.379E-3$	$-.598E-3$
100.0000	$.000E+0$	$-.164E-4$	$-.411E-4$	$-.822E-4$	$-.143E-3$	$-.214E-3$
110.0000	$.000E+0$	$.536E-5$	$.135E-4$	$.268E-4$	$.808E-4$	$.149E-3$
120.0000	$.000E+0$	$.254E-4$	$.638E-4$	$.127E-3$	$.286E-3$	$.482E-3$
130.0000	$.000E+0$	$.434E-4$	$.108E-3$	$.216E-3$	$.470E-3$	$.780E-3$
140.0000	$.000E+0$	$.582E-4$	$.146E-3$	$.291E-3$	$.625E-3$	$.103E-2$
150.0000	$.000E+0$	$.703E-4$	$.176E-3$	$.351E-3$	$.749E-3$	$.124E-2$
160.0000	$.000E+0$	$.790E-4$	$.198E-3$	$.395E-3$	$.840E-3$	$.138E-2$
170.0000	$.000E+0$	$.844E-4$	$.211E-3$	$.421E-3$	$.894E-3$	$.147E-2$
180.0000	$.000E+0$	$.861E-4$	$.215E-3$	$.430E-3$	$.913E-3$	$.150E-2$

(to be continued)

(continued)

$\theta(^\circ)$	$d_s = 64km$	$d_s = 100km$	$d_s = 200km$	$d_s = 300km$	$d_s = 400km$	$d_s = 637km$
.0000	$.261E+4$	$.110E+4$	$.302E+3$	$.145E+3$	$.877E+2$	$.380E+2$
.0001	$.261E+4$	$.110E+4$	$.302E+3$	$.145E+3$	$.877E+2$	$.380E+2$
.0010	$.261E+4$	$.110E+4$	$.302E+3$	$.145E+3$	$.877E+2$	$.380E+2$
.0100	$.261E+4$	$.110E+4$	$.302E+3$	$.145E+3$	$.877E+2$	$.380E+2$
.0200	$.260E+4$	$.110E+4$	$.302E+3$	$.145E+3$	$.877E+2$	$.380E+2$
.0300	$.259E+4$	$.109E+4$	$.302E+3$	$.145E+3$	$.877E+2$	$.380E+2$
.0400	$.258E+4$	$.109E+4$	$.301E+3$	$.145E+3$	$.877E+2$	$.380E+2$
.0600	$.253E+4$	$.108E+4$	$.301E+3$	$.145E+3$	$.876E+2$	$.379E+2$
.0800	$.247E+4$	$.107E+4$	$.300E+3$	$.145E+3$	$.876E+2$	$.379E+2$
.1000	$.239E+4$	$.106E+4$	$.299E+3$	$.144E+3$	$.875E+2$	$.379E+2$
.1600	$.209E+4$	$.100E+4$	$.295E+3$	$.144E+3$	$.872E+2$	$.379E+2$
.2000	$.187E+4$	$.955E+3$	$.292E+3$	$.143E+3$	$.870E+2$	$.378E+2$
.2500	$.159E+4$	$.886E+3$	$.286E+3$	$.142E+3$	$.865E+2$	$.377E+2$
.3000	$.134E+4$	$.811E+3$	$.280E+3$	$.140E+3$	$.860E+2$	$.377E+2$
.4000	$.753E+3$	$.663E+3$	$.264E+3$	$.137E+3$	$.847E+2$	$.374E+2$
.5000	$.419E+3$	$.489E+3$	$.245E+3$	$.132E+3$	$.831E+2$	$.371E+2$
.6000	$.212E+3$	$.356E+3$	$.224E+3$	$.127E+3$	$.812E+2$	$.368E+2$
.8000	$.182E+2$	$.170E+3$	$.184E+3$	$.115E+3$	$.765E+2$	$.359E+2$
1.0000	$-.334E+2$	$.693E+2$	$.137E+3$	$.101E+3$	$.710E+2$	$.348E+2$
1.2000	$-.436E+2$	$.166E+2$	$.100E+3$	$.887E+2$	$.650E+2$	$.335E+2$
1.6000	$-.329E+2$	$-.148E+2$	$.479E+2$	$.595E+2$	$.531E+2$	$.305E+2$
2.0000	$-.215E+2$	$-.181E+2$	$.193E+2$	$.380E+2$	$.391E+2$	$.271E+2$
2.5000	$-.132E+2$	$-.143E+2$	$.214E+1$	$.195E+2$	$.259E+2$	$.230E+2$
3.0000	$-.820E+1$	$-.104E+2$	$-.385E+1$	$.857E+1$	$.160E+2$	$.193E+2$
4.0000	$-.385E+1$	$-.553E+1$	$-.568E+1$	$-.986E+0$	$.451E+1$	$.106E+2$
5.0000	$-.206E+1$	$-.316E+1$	$-.440E+1$	$-.308E+1$	$-.275E+0$	$.543E+1$
6.0000	$-.122E+1$	$-.191E+1$	$-.311E+1$	$-.298E+1$	$-.174E+1$	$.231E+1$
7.0000	$-.774E+0$	$-.123E+1$	$-.219E+1$	$-.247E+1$	$-.204E+1$	$.518E+0$
8.0000	$-.520E+0$	$-.833E+0$	$-.156E+1$	$-.191E+1$	$-.183E+1$	$-.330E+0$
9.0000	$-.365E+0$	$-.587E+0$	$-.114E+1$	$-.148E+1$	$-.157E+1$	$-.708E+0$
10.0000	$-.266E+0$	$-.429E+0$	$-.848E+0$	$-.115E+1$	$-.127E+1$	$-.833E+0$
12.0000	$-.154E+0$	$-.248E+0$	$-.496E+0$	$-.707E+0$	$-.840E+0$	$-.802E+0$
16.0000	$-.657E-1$	$-.106E+0$	$-.214E+0$	$-.313E+0$	$-.404E+0$	$-.519E+0$
20.0000	$-.349E-1$	$-.563E-1$	$-.115E+0$	$-.173E+0$	$-.223E+0$	$-.335E+0$
25.0000	$-.193E-1$	$-.313E-1$	$-.643E-1$	$-.981E-1$	$-.132E+0$	$-.216E+0$
30.0000	$-.125E-1$	$-.202E-1$	$-.416E-1$	$-.638E-1$	$-.863E-1$	$-.145E+0$
40.0000	$-.700E-2$	$-.112E-1$	$-.228E-1$	$-.346E-1$	$-.464E-1$	$-.759E-1$
50.0000	$-.491E-2$	$-.778E-2$	$-.155E-1$	$-.232E-1$	$-.303E-1$	$-.470E-1$
60.0000	$-.372E-2$	$-.586E-2$	$-.116E-1$	$-.171E-1$	$-.221E-1$	$-.325E-1$
70.0000	$-.281E-2$	$-.441E-2$	$-.870E-2$	$-.128E-1$	$-.165E-1$	$-.237E-1$
80.0000	$-.198E-2$	$-.310E-2$	$-.612E-2$	$-.900E-2$	$-.116E-1$	$-.166E-1$
90.0000	$-.118E-2$	$-.184E-2$	$-.364E-2$	$-.539E-2$	$-.693E-2$	$-.989E-2$
100.0000	$-.407E-3$	$-.631E-3$	$-.126E-2$	$-.190E-2$	$-.245E-2$	$-.348E-2$
110.0000	$.323E-3$	$.513E-3$	$.988E-3$	$.142E-2$	$.179E-2$	$.259E-2$
120.0000	$.999E-3$	$.156E-2$	$.308E-2$	$.449E-2$	$.580E-2$	$.836E-2$
130.0000	$.160E-2$	$.251E-2$	$.494E-2$	$.725E-2$	$.935E-2$	$.137E-1$
140.0000	$.211E-2$	$.331E-2$	$.653E-2$	$.960E-2$	$.124E-1$	$.181E-1$
150.0000	$.251E-2$	$.395E-2$	$.780E-2$	$.115E-1$	$.148E-1$	$.217E-1$
160.0000	$.281E-2$	$.442E-2$	$.874E-2$	$.129E-1$	$.167E-1$	$.245E-1$
170.0000	$.299E-2$	$.471E-2$	$.930E-2$	$.137E-1$	$.177E-1$	$.260E-1$
180.0000	$.305E-2$	$.480E-2$	$.948E-2$	$.140E-1$	$.180E-1$	$.264E-1$

Table E.13. Gravity change $\delta\hat{g}^{(1)}(a, \theta)$ caused by a vertical strike-slip faulting

$\theta(\circ)$	$d_s = 0km$	$d_s = 2km$	$d_s = 5km$	$d_s = 10km$	$d_s = 20km$	$d_s = 32km$
.0000	—	$.000E+0$	$.000E+0$	$.000E+0$	$.000E+0$	$.000E+0$
.0001	$.452E$ 11	$-.881E+2$	$-.228E+1$	$-.121E+0$	$-.116E-1$	$-.162E-2$
.0010	$.452E+9$	$-.874E+4$	$-.228E+3$	$-.121E+2$	$-.116E+1$	$-.162E+0$
.0100	$.452E+7$	$-.436E+6$	$-.201E+5$	$-.117E+4$	$-.115E+3$	$-.162E+2$
.0200	$.113E+7$	$-.398E+6$	$-.569E+5$	$-.422E+4$	$-.449E+3$	$-.641E+2$
.0300	$.501E+6$	$-.193E+6$	$-.783E+5$	$-.805E+4$	$-.969E+3$	$-.142E+3$
.0400	$.282E+6$	$-.787E+5$	$-.769E+5$	$-.115E+5$	$-.163E+4$	$-.247E+3$
.0600	$.118E+6$	$-.408E+4$	$-.513E+5$	$-.146E+5$	$-.311E+4$	$-.520E+3$
.0800	$.650E+5$	$.919E+4$	$-.285E+5$	$-.127E+5$	$-.441E+4$	$-.845E+3$
.1000	$.343E+5$	$.980E+4$	$-.150E+5$	$-.927E+4$	$-.522E+4$	$-.118E+4$
.1600	$.965E+4$	$.455E+4$	$-.115E+4$	$-.176E+4$	$-.458E+4$	$-.187E+4$
.2000	$.474E+4$	$.277E+4$	$.662E+3$	$-.559E+2$	$-.315E+4$	$-.198E+4$
.2500	$.158E+4$	$.179E+4$	$.108E+4$	$.536E+3$	$-.159E+4$	$-.171E+4$
.3000	$.156E+4$	$.131E+4$	$.980E+3$	$.596E+3$	$-.511E+3$	$-.135E+4$
.4000	$.839E+3$	$.819E+3$	$.672E+3$	$.463E+3$	$.386E+3$	$-.666E+3$
.5000	$.611E+3$	$.546E+3$	$.466E+3$	$.343E+3$	$.598E+3$	$-.222E+3$
.6000	$.417E+3$	$.382E+3$	$.335E+3$	$.259E+3$	$.593E+3$	$.432E+0$
.8000	$.227E+3$	$.212E+3$	$.192E+3$	$.158E+3$	$.478E+3$	$.168E+3$
1.0000	$.139E+3$	$.133E+3$	$.123E+3$	$.105E+3$	$.364E+3$	$.186E+3$
1.2000	$.950E+2$	$.904E+2$	$.845E+2$	$.746E+2$	$.277E+3$	$.169E+3$
1.6000	$.508E+2$	$.490E+2$	$.465E+2$	$.424E+2$	$.171E+3$	$.123E+3$
2.0000	$.310E+2$	$.302E+2$	$.289E+2$	$.269E+2$	$.114E+3$	$.886E+2$
2.5000	$.187E+2$	$.183E+2$	$.177E+2$	$.167E+2$	$.730E+2$	$.604E+2$
3.0000	$.123E+2$	$.120E+2$	$.117E+2$	$.111E+2$	$.498E+2$	$.427E+2$
4.0000	$.611E+1$	$.602E+1$	$.589E+1$	$.569E+1$	$.261E+2$	$.234E+2$
5.0000	$.345E+1$	$.343E+1$	$.337E+1$	$.328E+1$	$.153E+2$	$.140E+2$
6.0000	$.215E+1$	$.213E+1$	$.210E+1$	$.206E+1$	$.973E+1$	$.907E+1$
7.0000	$.143E+1$	$.142E+1$	$.140E+1$	$.138E+1$	$.657E+1$	$.620E+1$
8.0000	$.101E+1$	$.997E+0$	$.988E+0$	$.973E+0$	$.467E+1$	$.444E+1$
9.0000	$.736E+0$	$.732E+0$	$.726E+0$	$.716E+0$	$.345E+1$	$.331E+1$
10.0000	$.560E+0$	$.557E+0$	$.553E+0$	$.547E+0$	$.265E+1$	$.255E+1$
12.0000	$.353E+0$	$.352E+0$	$.350E+0$	$.347E+0$	$.169E+1$	$.163E+1$
16.0000	$.177E+0$	$.176E+0$	$.176E+0$	$.174E+0$	$.852E+0$	$.831E+0$
20.0000	$.105E+0$	$.105E+0$	$.105E+0$	$.104E+0$	$.510E+0$	$.498E+0$
25.0000	$.630E-1$	$.626E-1$	$.625E-1$	$.622E-1$	$.305E+0$	$.299E+0$
30.0000	$.414E-1$	$.410E-1$	$.409E-1$	$.408E-1$	$.200E+0$	$.197E+0$
40.0000	$.207E-1$	$.206E-1$	$.205E-1$	$.204E-1$	$.100E+0$	$.986E-1$
50.0000	$.110E-1$	$.109E-1$	$.109E-1$	$.108E-1$	$.532E-1$	$.522E-1$
60.0000	$.552E-2$	$.536E-2$	$.534E-2$	$.532E-2$	$.261E-1$	$.256E-1$
70.0000	$.201E-2$	$.202E-2$	$.201E-2$	$.200E-2$	$.974E-2$	$.949E-2$
80.0000	$.218E-3$	$.116E-3$	$.110E-3$	$.107E-3$	$.450E-3$	$.351E-3$
90.0000	$-.755E-3$	$-.810E-3$	$-.812E-3$	$-.815E-3$	$-.407E-2$	$-.408E-2$
100.0000	$-.112E-2$	$-.115E-2$	$-.115E-2$	$-.115E-2$	$-.570E-2$	$-.567E-2$
110.0000	$-.110E-2$	$-.115E-2$	$-.115E-2$	$-.115E-2$	$-.571E-2$	$-.566E-2$
120.0000	$-.936E-3$	$-.970E-3$	$-.969E-3$	$-.969E-3$	$-.479E-2$	$-.475E-2$
130.0000	$-.713E-3$	$-.720E-3$	$-.720E-3$	$-.719E-3$	$-.356E-2$	$-.353E-2$
140.0000	$-.516E-3$	$-.489E-3$	$-.489E-3$	$-.488E-3$	$-.241E-2$	$-.239E-2$
150.0000	$-.236E-3$	$-.283E-3$	$-.283E-3$	$-.283E-3$	$-.140E-2$	$-.138E-2$
160.0000	$-.508E-4$	$-.116E-3$	$-.118E-3$	$-.116E-3$	$-.575E-3$	$-.570E-3$
170.0000	$-.659E-5$	$-.239E-4$	$-.239E-4$	$-.240E-4$	$-.119E-3$	$-.118E-3$
180.0000	$.000E+0$	$.000E+0$	$.000E+0$	$.000E+0$	$.000E+0$	$.000E+0$

(to be continued)

(continued)

$\theta(^\circ)$	$d_s = 64km$	$d_s = 100km$	$d_s = 200km$	$d_s = 300km$	$d_s = 400km$	$d_s = 637km$
.0000	$.000E+0$	$.000E+0$	$.000E+0$	$.000E+0$	$.000E+0$	$.000E+0$
.0001	$-.874E-4$	$-.135E-4$	$-.783E-6$	$-.155E-6$	$-.513E-7$	$-.826E-8$
.0010	$-.874E-2$	$-.135E-2$	$-.783E-4$	$-.155E-4$	$-.513E-5$	$-.826E-6$
.0100	$-.874E+0$	$-.135E+0$	$-.783E-2$	$-.155E-2$	$-.513E-3$	$-.826E-4$
.0200	$-.349E+1$	$-.538E+0$	$-.313E-1$	$-.620E-2$	$-.205E-2$	$-.330E-3$
.0300	$-.781E+1$	$-.121E+1$	$-.705E-1$	$-.140E-1$	$-.461E-2$	$-.743E-3$
.0400	$-.138E+2$	$-.214E+1$	$-.125E+0$	$-.248E-1$	$-.820E-2$	$-.132E-2$
.0600	$-.306E+2$	$-.479E+1$	$-.281E+0$	$-.558E-1$	$-.184E-1$	$-.297E-2$
.0800	$-.532E+2$	$-.844E+1$	$-.499E+0$	$-.991E-1$	$-.328E-1$	$-.528E-2$
.1000	$-.807E+2$	$-.130E+2$	$-.777E+0$	$-.155E+0$	$-.512E-1$	$-.825E-2$
.1600	$-.182E+3$	$-.318E+2$	$-.197E+1$	$-.394E+0$	$-.131E+0$	$-.211E-1$
.2000	$-.255E+3$	$-.474E+2$	$-.304E+1$	$-.612E+0$	$-.204E+0$	$-.329E-1$
.2500	$-.335E+3$	$-.691E+2$	$-.467E+1$	$-.950E+0$	$-.317E+0$	$-.514E-1$
.3000	$-.393E+3$	$-.913E+2$	$-.659E+1$	$-.136E+1$	$-.454E+0$	$-.738E-1$
.4000	$-.440E+3$	$-.131E+3$	$-.111E+2$	$-.235E+1$	$-.796E+0$	$-.131E+0$
.5000	$-.391E+3$	$-.158E+3$	$-.162E+2$	$-.357E+1$	$-.122E+1$	$-.203E+0$
.6000	$-.320E+3$	$-.171E+3$	$-.216E+2$	$-.496E+1$	$-.173E+1$	$-.289E+0$
.8000	$-.178E+3$	$-.155E+3$	$-.314E+2$	$-.805E+1$	$-.292E+1$	$-.504E+0$
1.0000	$-.765E+2$	$-.121E+3$	$-.384E+2$	$-.112E+2$	$-.427E+1$	$-.767E+0$
1.2000	$-.218E+2$	$-.864E+2$	$-.422E+2$	$-.141E+2$	$-.567E+1$	$-.107E+1$
1.6000	$.238E+2$	$-.351E+2$	$-.397E+2$	$-.180E+2$	$-.829E+1$	$-.175E+1$
2.0000	$.323E+2$	$-.918E+1$	$-.323E+2$	$-.195E+2$	$-.102E+2$	$-.247E+1$
2.5000	$.298E+2$	$.421E+1$	$-.220E+2$	$-.176E+2$	$-.113E+2$	$-.329E+1$
3.0000	$.247E+2$	$.832E+1$	$-.136E+2$	$-.146E+2$	$-.114E+2$	$-.393E+1$
4.0000	$.162E+2$	$.885E+1$	$-.414E+1$	$-.840E+1$	$-.853E+1$	$-.455E+1$
5.0000	$.106E+2$	$.708E+1$	$-.352E+0$	$-.419E+1$	$-.568E+1$	$-.423E+1$
6.0000	$.727E+1$	$.534E+1$	$.970E+0$	$-.174E+1$	$-.336E+1$	$-.356E+1$
7.0000	$.516E+1$	$.404E+1$	$.139E+1$	$-.490E+0$	$-.184E+1$	$-.277E+1$
8.0000	$.380E+1$	$.311E+1$	$.143E+1$	$.170E+0$	$-.851E+0$	$-.205E+1$
9.0000	$.289E+1$	$.243E+1$	$.134E+1$	$.468E+0$	$-.278E+0$	$-.141E+1$
10.0000	$.226E+1$	$.195E+1$	$.120E+1$	$.606E+0$	$.781E-1$	$-.954E+0$
12.0000	$.148E+1$	$.131E+1$	$.929E+0$	$.634E+0$	$.358E+0$	$-.363E+0$
16.0000	$.768E+0$	$.702E+0$	$.562E+0$	$.477E+0$	$.402E+0$	$.974E-1$
20.0000	$.465E+0$	$.431E+0$	$.363E+0$	$.332E+0$	$.313E+0$	$.182E+0$
25.0000	$.281E+0$	$.263E+0$	$.228E+0$	$.218E+0$	$.219E+0$	$.170E+0$
30.0000	$.185E+0$	$.174E+0$	$.153E+0$	$.150E+0$	$.155E+0$	$.138E+0$
40.0000	$.931E-1$	$.877E-1$	$.781E-1$	$.775E-1$	$.817E-1$	$.784E-1$
50.0000	$.493E-1$	$.463E-1$	$.410E-1$	$.404E-1$	$.421E-1$	$.381E-1$
60.0000	$.239E-1$	$.223E-1$	$.193E-1$	$.184E-1$	$.182E-1$	$.125E-1$
70.0000	$.873E-2$	$.797E-2$	$.634E-2$	$.523E-2$	$.400E-2$	$-.286E-2$
80.0000	$.146E-3$	$-.125E-3$	$-.923E-3$	$-.202E-2$	$-.371E-2$	$-.103E-1$
90.0000	$-.407E-2$	$-.408E-2$	$-.439E-2$	$-.538E-2$	$-.713E-2$	$-.131E-1$
100.0000	$-.556E-2$	$-.544E-2$	$-.550E-2$	$-.632E-2$	$-.790E-2$	$-.128E-1$
110.0000	$-.547E-2$	$-.532E-2$	$-.526E-2$	$-.590E-2$	$-.720E-2$	$-.110E-1$
120.0000	$-.459E-2$	$-.446E-2$	$-.434E-2$	$-.483E-2$	$-.580E-2$	$-.866E-2$
130.0000	$-.344E-2$	$-.332E-2$	$-.323E-2$	$-.356E-2$	$-.425E-2$	$-.617E-2$
140.0000	$-.229E-2$	$-.221E-2$	$-.214E-2$	$-.234E-2$	$-.279E-2$	$-.401E-2$
150.0000	$-.131E-2$	$-.127E-2$	$-.122E-2$	$-.134E-2$	$-.159E-2$	$-.226E-2$
160.0000	$-.589E-3$	$-.568E-3$	$-.547E-3$	$-.597E-3$	$-.708E-3$	$-.100E-2$
170.0000	$-.148E-3$	$-.143E-3$	$-.137E-3$	$-.149E-3$	$-.177E-3$	$-.247E-3$
180.0000	$.000E+0$	$.000E+0$	$.000E+0$	$.000E+0$	$.000E+0$	$.000E+0$

Table E.14. Gravity change $\delta\hat{g}^{(2)}(a, \theta)$ caused by a vertical dip-slip faulting

$\theta(\circ)$	$d_s = 0km$	$d_s = 2km$	$d_s = 5km$	$d_s = 10km$	$d_s = 20km$	$d_s = 32km$
.0000	$.000E+0$	$.000E+0$	$.000E+0$	$.000E+0$	$.000E+0$	$.000E+0$
.0001	$.000E+0$	$-.377E+5$	$-.236E+4$	$-.285E+3$	$-.513E+2$	$-.113E+2$
.0010	$.000E+0$	$-.374E+6$	$-.236E+5$	$-.285E+4$	$-.513E+3$	$-.113E+3$
.0100	$.000E+0$	$-.195E+7$	$-.209E+6$	$-.277E+5$	$-.509E+4$	$-.112E+4$
.0200	$.000E+0$	$-.101E+7$	$-.300E+6$	$-.506E+5$	$-.992E+4$	$-.222E+4$
.0300	$.000E+0$	$-.402E+6$	$-.276E+6$	$-.656E+5$	$-.143E+5$	$-.328E+4$
.0400	$.000E+0$	$-.167E+6$	$-.209E+6$	$-.723E+5$	$-.180E+5$	$-.428E+4$
.0600	$.000E+0$	$-.331E+5$	$-.937E+5$	$-.664E+5$	$-.229E+5$	$-.601E+4$
.0800	$.000E+0$	$-.447E+4$	$-.367E+5$	$-.501E+5$	$-.246E+5$	$-.734E+4$
.1000	$.000E+0$	$.267E+4$	$-.130E+5$	$-.341E+5$	$-.240E+5$	$-.819E+4$
.1600	$.000E+0$	$.216E+4$	$.116E+3$	$-.838E+4$	$-.145E+5$	$-.847E+4$
.2000	$.000E+0$	$.730E+3$	$.725E+2$	$-.317E+4$	$-.915E+4$	$-.764E+4$
.2500	$.000E+0$	$.681E+2$	$-.174E+3$	$-.107E+4$	$-.487E+4$	$-.546E+4$
.3000	$.000E+0$	$-.472E+2$	$-.168E+3$	$-.438E+3$	$-.271E+4$	$-.396E+4$
.4000	$.000E+0$	$-.173E+2$	$-.481E+2$	$-.103E+3$	$-.954E+3$	$-.197E+4$
.5000	$.000E+0$	$-.304E+0$	$-.467E+1$	$-.172E+2$	$-.393E+3$	$-.102E+4$
.6000	$.000E+0$	$.278E+1$	$.468E+1$	$.334E+1$	$-.178E+3$	$-.546E+3$
.8000	$.000E+0$	$.219E+1$	$.469E+1$	$.677E+1$	$-.547E+2$	$-.187E+3$
1.0000	$.000E+0$	$.125E+1$	$.280E+1$	$.447E+1$	$-.179E+2$	$-.752E+2$
1.2000	$.000E+0$	$.760E+0$	$.174E+1$	$.294E+1$	$-.460E+1$	$-.334E+2$
1.6000	$.000E+0$	$.371E+0$	$.877E+0$	$.158E+1$	$.947E+0$	$-.693E+1$
2.0000	$.000E+0$	$.228E+0$	$.549E+0$	$.102E+1$	$.184E+1$	$.313E+0$
2.5000	$.000E+0$	$.143E+0$	$.349E+0$	$.664E+0$	$.173E+1$	$.203E+1$
3.0000	$.000E+0$	$.968E-1$	$.237E+0$	$.457E+0$	$.140E+1$	$.209E+1$
4.0000	$.000E+0$	$.489E-1$	$.121E+0$	$.235E+0$	$.823E+0$	$.143E+1$
5.0000	$.000E+0$	$.267E-1$	$.663E-1$	$.130E+0$	$.478E+0$	$.876E+0$
6.0000	$.000E+0$	$.155E-1$	$.385E-1$	$.758E-1$	$.284E+0$	$.532E+0$
7.0000	$.000E+0$	$.942E-2$	$.235E-1$	$.464E-1$	$.173E+0$	$.329E+0$
8.0000	$.000E+0$	$.599E-2$	$.149E-1$	$.296E-1$	$.109E+0$	$.208E+0$
9.0000	$.000E+0$	$.397E-2$	$.991E-2$	$.197E-1$	$.704E-1$	$.135E+0$
10.0000	$.000E+0$	$.273E-2$	$.682E-2$	$.136E-1$	$.469E-1$	$.897E-1$
12.0000	$.000E+0$	$.144E-2$	$.360E-2$	$.717E-2$	$.227E-1$	$.429E-1$
16.0000	$.000E+0$	$.578E-3$	$.145E-2$	$.289E-2$	$.776E-2$	$.141E-1$
20.0000	$.000E+0$	$.319E-3$	$.800E-3$	$.160E-2$	$.390E-2$	$.689E-2$
25.0000	$.000E+0$	$.185E-3$	$.463E-3$	$.925E-3$	$.210E-2$	$.362E-2$
30.0000	$.000E+0$	$.120E-3$	$.301E-3$	$.600E-3$	$.130E-2$	$.220E-2$
40.0000	$.000E+0$	$.644E-4$	$.161E-3$	$.322E-3$	$.741E-3$	$.129E-2$
50.0000	$.000E+0$	$.415E-4$	$.104E-3$	$.207E-3$	$.589E-3$	$.110E-2$
60.0000	$.000E+0$	$.277E-4$	$.694E-4$	$.138E-3$	$.479E-3$	$.939E-3$
70.0000	$.000E+0$	$.182E-4$	$.452E-4$	$.902E-4$	$.364E-3$	$.737E-3$
80.0000	$.000E+0$	$.112E-4$	$.272E-4$	$.543E-4$	$.249E-3$	$.517E-3$
90.0000	$.000E+0$	$.597E-5$	$.149E-4$	$.298E-4$	$.153E-3$	$.324E-3$
100.0000	$.000E+0$	$.298E-5$	$.745E-5$	$.149E-4$	$.875E-4$	$.189E-3$
110.0000	$.000E+0$	$.975E-6$	$.276E-5$	$.593E-5$	$.404E-4$	$.892E-4$
120.0000	$.000E+0$	$-.226E-7$	$.228E-6$	$.450E-6$	$.108E-4$	$.264E-4$
130.0000	$.000E+0$	$-.578E-6$	$-.533E-6$	$-.124E-5$	$-.322E-5$	$-.552E-5$
140.0000	$.000E+0$	$-.435E-6$	$-.148E-5$	$-.173E-5$	$-.908E-5$	$-.175E-4$
150.0000	$.000E+0$	$-.438E-6$	$-.109E-5$	$-.217E-5$	$-.130E-4$	$-.277E-4$
160.0000	$.000E+0$	$-.512E-6$	$-.754E-6$	$-.142E-5$	$-.906E-5$	$-.195E-4$
170.0000	$.000E+0$	$-.769E-7$	$-.226E-6$	$-.173E-6$	$-.183E-5$	$-.387E-5$
180.0000	$.000E+0$	$.000E+0$	$.000E+0$	$.000E+0$	$.000E+0$	$.000E+0$

(to be continued)

(continued)

$\theta(^\circ)$	$d_s = 64km$	$d_s = 100km$	$d_s = 200km$	$d_s = 300km$	$d_s = 400km$	$d_s = 637km$
.0000	$.000E+0$	$.000E+0$	$.000E+0$	$.000E+0$	$.000E+0$	$.000E+0$
.0001	$-.121E+1$	$-.289E+0$	$-.334E-1$	$-.985E-2$	$-.437E-2$	$-.116E-2$
.0010	$-.121E+2$	$-.289E+1$	$-.334E+0$	$-.985E-1$	$-.437E-1$	$-.116E-1$
.0100	$-.121E+3$	$-.289E+2$	$-.334E+1$	$-.985E+0$	$-.437E+0$	$-.116E+0$
.0200	$-.242E+3$	$-.578E+2$	$-.668E+1$	$-.197E+1$	$-.873E+0$	$-.232E+0$
.0300	$-.361E+3$	$-.865E+2$	$-.100E+2$	$-.295E+1$	$-.131E+1$	$-.348E+0$
.0400	$-.479E+3$	$-.115E+3$	$-.134E+2$	$-.394E+1$	$-.175E+1$	$-.464E+0$
.0600	$-.707E+3$	$-.172E+3$	$-.200E+2$	$-.590E+1$	$-.262E+1$	$-.695E+0$
.0800	$-.922E+3$	$-.227E+3$	$-.266E+2$	$-.787E+1$	$-.349E+1$	$-.927E+0$
.1000	$-.112E+4$	$-.280E+3$	$-.332E+2$	$-.982E+1$	$-.436E+1$	$-.116E+1$
.1600	$-.159E+4$	$-.427E+3$	$-.524E+2$	$-.156E+2$	$-.695E+1$	$-.185E+1$
.2000	$-.178E+4$	$-.510E+3$	$-.648E+2$	$-.194E+2$	$-.867E+1$	$-.231E+1$
.2500	$-.189E+4$	$-.595E+3$	$-.796E+2$	$-.241E+2$	$-.108E+2$	$-.288E+1$
.3000	$-.189E+4$	$-.657E+3$	$-.936E+2$	$-.287E+2$	$-.129E+2$	$-.345E+1$
.4000	$-.171E+4$	$-.717E+3$	$-.118E+3$	$-.373E+2$	$-.169E+2$	$-.458E+1$
.5000	$-.126E+4$	$-.711E+3$	$-.138E+3$	$-.453E+2$	$-.208E+2$	$-.569E+1$
.6000	$-.938E+3$	$-.669E+3$	$-.153E+3$	$-.524E+2$	$-.245E+2$	$-.678E+1$
.8000	$-.487E+3$	$-.475E+3$	$-.167E+3$	$-.638E+2$	$-.310E+2$	$-.885E+1$
1.0000	$-.259E+3$	$-.325E+3$	$-.167E+3$	$-.710E+2$	$-.362E+2$	$-.108E+2$
1.2000	$-.138E+3$	$-.213E+3$	$-.157E+3$	$-.745E+2$	$-.401E+2$	$-.125E+2$
1.6000	$-.445E+2$	$-.923E+2$	$-.112E+3$	$-.732E+2$	$-.440E+2$	$-.155E+2$
2.0000	$-.149E+2$	$-.401E+2$	$-.754E+2$	$-.618E+2$	$-.437E+2$	$-.175E+2$
2.5000	$-.299E+1$	$-.140E+2$	$-.429E+2$	$-.468E+2$	$-.401E+2$	$-.188E+2$
3.0000	$.108E+1$	$-.408E+1$	$-.240E+2$	$-.333E+2$	$-.315E+2$	$-.188E+2$
4.0000	$.200E+1$	$.852E+0$	$-.692E+1$	$-.151E+2$	$-.189E+2$	$-.164E+2$
5.0000	$.149E+1$	$.141E+1$	$-.156E+1$	$-.656E+1$	$-.103E+2$	$-.127E+2$
6.0000	$.990E+0$	$.118E+1$	$.716E-1$	$-.263E+1$	$-.544E+1$	$-.922E+1$
7.0000	$.643E+0$	$.832E+0$	$.488E+0$	$-.928E+0$	$-.286E+1$	$-.643E+1$
8.0000	$.419E+0$	$.571E+0$	$.456E+0$	$-.273E+0$	$-.142E+1$	$-.433E+1$
9.0000	$.277E+0$	$.391E+0$	$.394E+0$	$.334E-1$	$-.720E+0$	$-.288E+1$
10.0000	$.187E+0$	$.270E+0$	$.315E+0$	$.106E+0$	$-.327E+0$	$-.191E+1$
12.0000	$.909E-1$	$.135E+0$	$.195E+0$	$.129E+0$	$-.274E-1$	$-.829E+0$
16.0000	$.298E-1$	$.462E-1$	$.787E-1$	$.880E-1$	$.592E-1$	$-.140E+0$
20.0000	$.144E-1$	$.226E-1$	$.416E-1$	$.538E-1$	$.518E-1$	$-.465E-2$
25.0000	$.752E-2$	$.118E-1$	$.226E-1$	$.314E-1$	$.363E-1$	$.260E-1$
30.0000	$.454E-2$	$.713E-2$	$.140E-1$	$.201E-1$	$.244E-1$	$.242E-1$
40.0000	$.275E-2$	$.436E-2$	$.878E-2$	$.132E-1$	$.176E-1$	$.263E-1$
50.0000	$.242E-2$	$.392E-2$	$.808E-2$	$.125E-1$	$.170E-1$	$.292E-1$
60.0000	$.213E-2$	$.348E-2$	$.725E-2$	$.114E-1$	$.158E-1$	$.288E-1$
70.0000	$.170E-2$	$.281E-2$	$.588E-2$	$.927E-2$	$.131E-1$	$.242E-1$
80.0000	$.121E-2$	$.199E-2$	$.423E-2$	$.670E-2$	$.949E-2$	$.179E-1$
90.0000	$.767E-3$	$.128E-2$	$.273E-2$	$.440E-2$	$.620E-2$	$.119E-1$
100.0000	$.450E-3$	$.753E-3$	$.163E-2$	$.260E-2$	$.376E-2$	$.733E-2$
110.0000	$.217E-3$	$.367E-3$	$.810E-3$	$.132E-2$	$.193E-2$	$.381E-2$
120.0000	$.535E-4$	$.122E-3$	$.236E-3$	$.515E-3$	$.637E-3$	$.145E-2$
130.0000	$-.937E-5$	$-.104E-4$	$.180E-5$	$.154E-4$	$.769E-4$	$.229E-3$
140.0000	$-.428E-4$	$-.678E-4$	$-.125E-3$	$-.209E-3$	$-.222E-3$	$-.357E-3$
150.0000	$-.648E-4$	$-.105E-3$	$-.206E-3$	$-.266E-3$	$-.426E-3$	$-.803E-3$
160.0000	$-.458E-4$	$-.761E-4$	$-.150E-3$	$-.224E-3$	$-.315E-3$	$-.573E-3$
170.0000	$-.932E-5$	$-.152E-4$	$-.327E-4$	$-.126E-3$	$-.615E-4$	$-.108E-3$
180.0000	$.000E+0$	$.000E+0$	$.000E+0$	$.000E+0$	$.000E+0$	$.000E+0$

Table E.15. Gravity change $\delta\hat{g}^{(30)}(a, \theta)$ caused by a 45° dip-slip faulting

$\theta(\circ)$	$d_s = 0km$	$d_s = 2km$	$d_s = 5km$	$d_s = 10km$	$d_s = 20km$	$d_s = 32km$
.0000	—	$-.377E+7$	$-.619E+6$	$-.156E+6$	$-.476E+5$	$-.169E+5$
.0001	$.351E+6$	$-.377E+7$	$-.619E+6$	$-.156E+6$	$-.476E+5$	$-.169E+5$
.0010	$.810E+5$	$-.374E+7$	$-.619E+6$	$-.156E+6$	$-.476E+5$	$-.169E+5$
.0100	$-.265E+4$	$-.172E+7$	$-.541E+6$	$-.150E+6$	$-.472E+5$	$-.168E+5$
.0200	$-.281E+5$	$-.297E+6$	$-.383E+6$	$-.135E+6$	$-.457E+5$	$-.166E+5$
.0300	$-.390E+5$	$-.174E+5$	$-.216E+6$	$-.114E+6$	$-.434E+5$	$-.163E+5$
.0400	$-.318E+5$	$.176E+5$	$-.113E+6$	$-.923E+5$	$-.404E+5$	$-.158E+5$
.0600	$-.157E+5$	$.844E+4$	$-.253E+5$	$-.484E+5$	$-.333E+5$	$-.146E+5$
.0800	$-.151E+5$	$.159E+4$	$-.251E+4$	$-.227E+5$	$-.263E+5$	$-.131E+5$
.1000	$-.999E+4$	$-.405E+3$	$.283E+4$	$-.932E+4$	$-.179E+5$	$-.116E+5$
.1600	$-.199E+4$	$-.220E+3$	$.214E+4$	$.809E+2$	$-.462E+4$	$-.654E+4$
.2000	$-.400E+3$	$.717E+2$	$.934E+3$	$.239E+3$	$-.135E+4$	$-.409E+4$
.2500	$.417E+2$	$.114E+3$	$.272E+3$	$.981E+1$	$.188E+3$	$-.210E+4$
.3000	$.561E+2$	$.624E+2$	$.668E+2$	$-.569E+2$	$.444E+3$	$-.100E+4$
.4000	$-.883E+1$	$-.527E+1$	$-.905E+1$	$-.414E+2$	$.370E+3$	$-.916E+2$
.5000	$-.237E+2$	$-.190E+2$	$-.169E+2$	$-.202E+2$	$.237E+3$	$.911E+2$
.6000	$-.201E+2$	$-.182E+2$	$-.158E+2$	$-.136E+2$	$.150E+3$	$.124E+3$
.8000	$-.130E+2$	$-.121E+2$	$-.107E+2$	$-.835E+1$	$.639E+2$	$.813E+2$
1.0000	$-.857E+1$	$-.820E+1$	$-.746E+1$	$-.612E+1$	$.291E+2$	$.449E+2$
1.2000	$-.640E+1$	$-.612E+1$	$-.568E+1$	$-.489E+1$	$.105E+2$	$.241E+2$
1.6000	$-.420E+1$	$-.406E+1$	$-.386E+1$	$-.351E+1$	$-.125E+1$	$.689E+1$
2.0000	$-.307E+1$	$-.299E+1$	$-.288E+1$	$-.268E+1$	$-.423E+1$	$.465E+0$
2.5000	$-.217E+1$	$-.213E+1$	$-.207E+1$	$-.197E+1$	$-.463E+1$	$-.203E+1$
3.0000	$-.157E+1$	$-.155E+1$	$-.152E+1$	$-.145E+1$	$-.404E+1$	$-.249E+1$
4.0000	$-.846E+0$	$-.838E+0$	$-.826E+0$	$-.805E+0$	$-.256E+1$	$-.193E+1$
5.0000	$-.459E+0$	$-.458E+0$	$-.455E+0$	$-.448E+0$	$-.150E+1$	$-.122E+1$
6.0000	$-.250E+0$	$-.250E+0$	$-.250E+0$	$-.249E+0$	$-.844E+0$	$-.710E+0$
7.0000	$-.132E+0$	$-.133E+0$	$-.134E+0$	$-.135E+0$	$-.452E+0$	$-.385E+0$
8.0000	$-.654E-1$	$-.662E-1$	$-.674E-1$	$-.693E-1$	$-.220E+0$	$-.185E+0$
9.0000	$-.272E-1$	$-.280E-1$	$-.293E-1$	$-.311E-1$	$-.838E-1$	$-.657E-1$
10.0000	$-.543E-2$	$-.621E-2$	$-.731E-2$	$-.908E-2$	$-.516E-2$	$.430E-2$
12.0000	$.130E-1$	$.124E-1$	$.116E-1$	$.102E-1$	$.617E-1$	$.641E-1$
16.0000	$.163E-1$	$.160E-1$	$.156E-1$	$.149E-1$	$.707E-1$	$.705E-1$
20.0000	$.115E-1$	$.114E-1$	$.112E-1$	$.108E-1$	$.497E-1$	$.493E-1$
25.0000	$.573E-2$	$.564E-2$	$.551E-2$	$.528E-2$	$.245E-1$	$.242E-1$
30.0000	$.102E-2$	$.958E-3$	$.879E-3$	$.748E-3$	$.429E-2$	$.412E-2$
40.0000	$-.499E-2$	$-.502E-2$	$-.505E-2$	$-.510E-2$	$-.214E-1$	$-.214E-1$
50.0000	$-.705E-2$	$-.705E-2$	$-.707E-2$	$-.709E-2$	$-.301E-1$	$-.301E-1$
60.0000	$-.656E-2$	$-.657E-2$	$-.658E-2$	$-.659E-2$	$-.281E-1$	$-.281E-1$
70.0000	$-.490E-2$	$-.492E-2$	$-.493E-2$	$-.492E-2$	$-.210E-1$	$-.211E-1$
80.0000	$-.299E-2$	$-.298E-2$	$-.298E-2$	$-.300E-2$	$-.128E-1$	$-.129E-1$
90.0000	$-.129E-2$	$-.129E-2$	$-.130E-2$	$-.131E-2$	$-.560E-2$	$-.566E-2$
100.0000	$.392E-4$	$.288E-4$	$.214E-4$	$.865E-5$	$.669E-4$	$.569E-5$
110.0000	$.980E-3$	$.102E-2$	$.973E-3$	$.962E-3$	$.415E-2$	$.410E-2$
120.0000	$.160E-2$	$.159E-2$	$.159E-2$	$.157E-2$	$.677E-2$	$.673E-2$
130.0000	$.197E-2$	$.196E-2$	$.195E-2$	$.193E-2$	$.835E-2$	$.830E-2$
140.0000	$.217E-2$	$.217E-2$	$.217E-2$	$.215E-2$	$.928E-2$	$.924E-2$
150.0000	$.227E-2$	$.228E-2$	$.227E-2$	$.226E-2$	$.970E-2$	$.966E-2$
160.0000	$.231E-2$	$.230E-2$	$.229E-2$	$.228E-2$	$.981E-2$	$.981E-2$
170.0000	$.232E-2$	$.234E-2$	$.231E-2$	$.232E-2$	$.993E-2$	$.990E-2$
180.0000	$.232E-2$	$.234E-2$	$.234E-2$	$.232E-2$	$.100E-1$	$.999E-2$

(to be continued)

(continued)

$\theta(\circ)$	$d_s = 64km$	$d_s = 100km$	$d_s = 200km$	$d_s = 300km$	$d_s = 400km$	$d_s = 637km$
.0000	$-.373E+4$	$-.142E+4$	$-.338E+3$	$-.150E+3$	$-.880E+2$	$-.355E+2$
.0001	$-.373E+4$	$-.142E+4$	$-.338E+3$	$-.150E+3$	$-.880E+2$	$-.355E+2$
.0010	$-.373E+4$	$-.142E+4$	$-.338E+3$	$-.150E+3$	$-.880E+2$	$-.355E+2$
.0100	$-.373E+4$	$-.142E+4$	$-.338E+3$	$-.150E+3$	$-.880E+2$	$-.355E+2$
.0200	$-.372E+4$	$-.142E+4$	$-.337E+3$	$-.150E+3$	$-.880E+2$	$-.355E+2$
.0300	$-.370E+4$	$-.142E+4$	$-.337E+3$	$-.150E+3$	$-.880E+2$	$-.355E+2$
.0400	$-.368E+4$	$-.142E+4$	$-.337E+3$	$-.150E+3$	$-.880E+2$	$-.355E+2$
.0600	$-.361E+4$	$-.140E+4$	$-.336E+3$	$-.150E+3$	$-.880E+2$	$-.354E+2$
.0800	$-.351E+4$	$-.139E+4$	$-.336E+3$	$-.149E+3$	$-.879E+2$	$-.354E+2$
.1000	$-.340E+4$	$-.137E+4$	$-.334E+3$	$-.149E+3$	$-.878E+2$	$-.354E+2$
.1600	$-.294E+4$	$-.130E+4$	$-.330E+3$	$-.148E+3$	$-.875E+2$	$-.354E+2$
.2000	$-.261E+4$	$-.123E+4$	$-.326E+3$	$-.147E+3$	$-.872E+2$	$-.353E+2$
.2500	$-.220E+4$	$-.113E+4$	$-.319E+3$	$-.146E+3$	$-.868E+2$	$-.352E+2$
.3000	$-.184E+4$	$-.103E+4$	$-.311E+3$	$-.145E+3$	$-.862E+2$	$-.352E+2$
.4000	$-.997E+3$	$-.839E+3$	$-.292E+3$	$-.141E+3$	$-.849E+2$	$-.349E+2$
.5000	$-.549E+3$	$-.607E+3$	$-.270E+3$	$-.136E+3$	$-.831E+2$	$-.346E+2$
.6000	$-.286E+3$	$-.438E+3$	$-.247E+3$	$-.130E+3$	$-.811E+2$	$-.343E+2$
.8000	$-.519E+2$	$-.211E+3$	$-.201E+3$	$-.117E+3$	$-.761E+2$	$-.334E+2$
1.0000	$.591E+1$	$-.934E+2$	$-.146E+3$	$-.103E+3$	$-.703E+2$	$-.323E+2$
1.2000	$.203E+2$	$-.330E+2$	$-.106E+3$	$-.892E+2$	$-.641E+2$	$-.310E+2$
1.6000	$.151E+2$	$.192E+1$	$-.504E+2$	$-.584E+2$	$-.518E+2$	$-.280E+2$
2.0000	$.805E+1$	$.765E+1$	$-.213E+2$	$-.366E+2$	$-.374E+2$	$-.247E+2$
2.5000	$.373E+1$	$.607E+1$	$-.430E+1$	$-.185E+2$	$-.242E+2$	$-.207E+2$
3.0000	$.104E+1$	$.387E+1$	$.123E+1$	$-.829E+1$	$-.146E+2$	$-.172E+2$
4.0000	$-.273E+0$	$.144E+1$	$.299E+1$	$.213E+0$	$-.402E+1$	$-.885E+1$
5.0000	$-.424E+0$	$.566E+0$	$.216E+1$	$.189E+1$	$.133E+0$	$-.424E+1$
6.0000	$-.311E+0$	$.194E+0$	$.138E+1$	$.175E+1$	$.124E+1$	$-.156E+1$
7.0000	$-.177E+0$	$.104E+0$	$.884E+0$	$.139E+1$	$.143E+1$	$-.806E-1$
8.0000	$-.730E-1$	$.878E-1$	$.597E+0$	$.998E+0$	$.121E+1$	$.528E+0$
9.0000	$-.383E-2$	$.908E-1$	$.429E+0$	$.744E+0$	$.101E+1$	$.759E+0$
10.0000	$.390E-1$	$.962E-1$	$.327E+0$	$.571E+0$	$.772E+0$	$.799E+0$
12.0000	$.754E-1$	$.979E-1$	$.197E+0$	$.336E+0$	$.483E+0$	$.697E+0$
16.0000	$.716E-1$	$.765E-1$	$.104E+0$	$.148E+0$	$.227E+0$	$.406E+0$
20.0000	$.491E-1$	$.507E-1$	$.622E-1$	$.854E-1$	$.116E+0$	$.235E+0$
25.0000	$.239E-1$	$.244E-1$	$.293E-1$	$.401E-1$	$.578E-1$	$.125E+0$
30.0000	$.386E-2$	$.397E-2$	$.607E-2$	$.108E-1$	$.187E-1$	$.531E-1$
40.0000	$-.215E-1$	$-.217E-1$	$-.221E-1$	$-.230E-1$	$-.245E-1$	$-.231E-1$
50.0000	$-.302E-1$	$-.305E-1$	$-.317E-1$	$-.347E-1$	$-.393E-1$	$-.488E-1$
60.0000	$-.282E-1$	$-.286E-1$	$-.299E-1$	$-.330E-1$	$-.380E-1$	$-.497E-1$
70.0000	$-.212E-1$	$-.215E-1$	$-.227E-1$	$-.253E-1$	$-.293E-1$	$-.392E-1$
80.0000	$-.130E-1$	$-.133E-1$	$-.142E-1$	$-.160E-1$	$-.187E-1$	$-.254E-1$
90.0000	$-.581E-2$	$-.602E-2$	$-.663E-2$	$-.761E-2$	$-.904E-2$	$-.126E-1$
100.0000	$-.139E-3$	$-.287E-3$	$-.613E-3$	$-.911E-3$	$-.128E-2$	$-.214E-2$
110.0000	$.397E-2$	$.387E-2$	$.378E-2$	$.395E-2$	$.446E-2$	$.580E-2$
120.0000	$.661E-2$	$.658E-2$	$.664E-2$	$.724E-2$	$.823E-2$	$.112E-1$
130.0000	$.822E-2$	$.820E-2$	$.842E-2$	$.926E-2$	$.106E-1$	$.145E-1$
140.0000	$.917E-2$	$.918E-2$	$.948E-2$	$.104E-1$	$.121E-1$	$.168E-1$
150.0000	$.960E-2$	$.965E-2$	$.999E-2$	$.111E-1$	$.129E-1$	$.179E-1$
160.0000	$.974E-2$	$.979E-2$	$.102E-1$	$.113E-1$	$.132E-1$	$.184E-1$
170.0000	$.986E-2$	$.991E-2$	$.103E-1$	$.115E-1$	$.134E-1$	$.189E-1$
180.0000	$.994E-2$	$.999E-2$	$.104E-1$	$.115E-1$	$.136E-1$	$.191E-1$

Table E.16. Gravity change $\delta\hat{g}^{(4)}(a,\ \theta)$ caused by a tensile faulting

$\theta(^{\circ})$	$d_s = 0km$	$d_s = 2km$	$d_s = 5km$	$d_s = 10km$	$d_s = 20km$	$d_s = 32km$
.0000	$.000E+0$	$-.777E+7$	$-.127E+7$	$-.388E+6$	$-.981E+5$	$-.354E+5$
.0001	$.000E+0$	$-.777E+7$	$-.127E+7$	$-.388E+6$	$-.981E+5$	$-.354E+5$
.0010	$.000E+0$	$-.771E+7$	$-.127E+7$	$-.387E+6$	$-.981E+5$	$-.354E+5$
.0100	$.000E+0$	$-.412E+7$	$-.114E+7$	$-.376E+6$	$-.973E+5$	$-.353E+5$
.0200	$.000E+0$	$-.122E+7$	$-.855E+6$	$-.345E+6$	$-.949E+5$	$-.350E+5$
.0300	$.000E+0$	$-.383E+6$	$-.546E+6$	$-.300E+6$	$-.911E+5$	$-.344E+5$
.0400	$.000E+0$	$-.150E+6$	$-.337E+6$	$-.253E+6$	$-.860E+5$	$-.336E+5$
.0600	$.000E+0$	$-.385E+5$	$-.128E+6$	$-.153E+6$	$-.737E+5$	$-.315E+5$
.0800	$.000E+0$	$-.143E+5$	$-.523E+5$	$-.867E+5$	$-.611E+5$	$-.289E+5$
.1000	$.000E+0$	$-.620E+4$	$-.228E+5$	$-.473E+5$	$-.462E+5$	$-.261E+5$
.1600	$.000E+0$	$-.927E+3$	$-.233E+4$	$-.786E+4$	$-.191E+5$	$-.168E+5$
.2000	$.000E+0$	$-.469E+3$	$-.945E+3$	$-.319E+4$	$-.106E+5$	$-.120E+5$
.2500	$.000E+0$	$-.299E+3$	$-.651E+3$	$-.164E+4$	$-.523E+4$	$-.774E+4$
.3000	$.000E+0$	$-.200E+3$	$-.492E+3$	$-.105E+4$	$-.297E+4$	$-.503E+4$
.4000	$.000E+0$	$-.896E+2$	$-.230E+3$	$-.466E+3$	$-.120E+4$	$-.223E+4$
.5000	$.000E+0$	$-.452E+2$	$-.114E+3$	$-.222E+3$	$-.589E+3$	$-.115E+4$
.6000	$.000E+0$	$-.259E+2$	$-.650E+2$	$-.129E+3$	$-.330E+3$	$-.636E+3$
.8000	$.000E+0$	$-.109E+2$	$-.269E+2$	$-.532E+2$	$-.132E+3$	$-.256E+3$
1.0000	$.000E+0$	$-.555E+1$	$-.138E+2$	$-.273E+2$	$-.654E+2$	$-.128E+3$
1.2000	$.000E+0$	$-.322E+1$	$-.801E+1$	$-.158E+2$	$-.392E+2$	$-.739E+2$
1.6000	$.000E+0$	$-.136E+1$	$-.338E+1$	$-.672E+1$	$-.167E+2$	$-.298E+2$
2.0000	$.000E+0$	$-.694E+0$	$-.174E+1$	$-.345E+1$	$-.856E+1$	$-.152E+2$
2.5000	$.000E+0$	$-.355E+0$	$-.886E+0$	$-.176E+1$	$-.438E+1$	$-.770E+1$
3.0000	$.000E+0$	$-.205E+0$	$-.512E+0$	$-.102E+1$	$-.253E+1$	$-.442E+1$
4.0000	$.000E+0$	$-.866E-1$	$-.216E+0$	$-.431E+0$	$-.107E+1$	$-.185E+1$
5.0000	$.000E+0$	$-.445E-1$	$-.111E+0$	$-.221E+0$	$-.548E+0$	$-.942E+0$
6.0000	$.000E+0$	$-.259E-1$	$-.647E-1$	$-.129E+0$	$-.318E+0$	$-.549E+0$
7.0000	$.000E+0$	$-.165E-1$	$-.411E-1$	$-.819E-1$	$-.203E+0$	$-.349E+0$
8.0000	$.000E+0$	$-.112E-1$	$-.279E-1$	$-.554E-1$	$-.138E+0$	$-.237E+0$
9.0000	$.000E+0$	$-.793E-2$	$-.198E-1$	$-.395E-1$	$-.977E-1$	$-.168E+0$
10.0000	$.000E+0$	$-.586E-2$	$-.146E-1$	$-.291E-1$	$-.719E-1$	$-.124E+0$
12.0000	$.000E+0$	$-.348E-2$	$-.869E-2$	$-.173E-1$	$-.426E-1$	$-.738E-1$
16.0000	$.000E+0$	$-.154E-2$	$-.386E-2$	$-.771E-2$	$-.188E-1$	$-.327E-1$
20.0000	$.000E+0$	$-.826E-3$	$-.207E-2$	$-.413E-2$	$-.100E-1$	$-.175E-1$
25.0000	$.000E+0$	$-.443E-3$	$-.111E-2$	$-.221E-2$	$-.540E-2$	$-.938E-2$
30.0000	$.000E+0$	$-.263E-3$	$-.658E-3$	$-.131E-2$	$-.324E-2$	$-.567E-2$
40.0000	$.000E+0$	$-.109E-3$	$-.272E-3$	$-.543E-3$	$-.142E-2$	$-.255E-2$
50.0000	$.000E+0$	$-.505E-4$	$-.126E-3$	$-.253E-3$	$-.738E-3$	$-.136E-2$
60.0000	$.000E+0$	$-.271E-4$	$-.678E-4$	$-.135E-3$	$-.439E-3$	$-.830E-3$
70.0000	$.000E+0$	$-.182E-4$	$-.458E-4$	$-.916E-4$	$-.303E-3$	$-.577E-3$
80.0000	$.000E+0$	$-.163E-4$	$-.396E-4$	$-.792E-4$	$-.242E-3$	$-.451E-3$
90.0000	$.000E+0$	$-.158E-4$	$-.395E-4$	$-.789E-4$	$-.216E-3$	$-.389E-3$
100.0000	$.000E+0$	$-.165E-4$	$-.412E-4$	$-.823E-4$	$-.204E-3$	$-.356E-3$
110.0000	$.000E+0$	$-.170E-4$	$-.429E-4$	$-.856E-4$	$-.197E-3$	$-.335E-3$
120.0000	$.000E+0$	$-.172E-4$	$-.438E-4$	$-.875E-4$	$-.191E-3$	$-.319E-3$
130.0000	$.000E+0$	$-.179E-4$	$-.442E-4$	$-.883E-4$	$-.188E-3$	$-.311E-3$
140.0000	$.000E+0$	$-.170E-4$	$-.439E-4$	$-.879E-4$	$-.184E-3$	$-.302E-3$
150.0000	$.000E+0$	$-.174E-4$	$-.436E-4$	$-.871E-4$	$-.181E-3$	$-.295E-3$
160.0000	$.000E+0$	$-.172E-4$	$-.431E-4$	$-.862E-4$	$-.178E-3$	$-.290E-3$
170.0000	$.000E+0$	$-.173E-4$	$-.428E-4$	$-.856E-4$	$-.176E-3$	$-.286E-3$
180.0000	$.000E+0$	$-.170E-4$	$-.427E-4$	$-.853E-4$	$-.176E-3$	$-.285E-3$

(to be continued)

(continued)

$\theta(^\circ)$	$d_s = 64km$	$d_s = 100km$	$d_s = 200km$	$d_s = 300km$	$d_s = 400km$	$d_s = 637km$
.0000	$-.799E+4$	$-.312E+4$	$-.788E+3$	$-.363E+3$	$-.214E+3$	$-.897E+2$
.0001	$-.799E+4$	$-.312E+4$	$-.788E+3$	$-.363E+3$	$-.214E+3$	$-.897E+2$
.0010	$-.799E+4$	$-.312E+4$	$-.788E+3$	$-.363E+3$	$-.214E+3$	$-.897E+2$
.0100	$-.799E+4$	$-.312E+4$	$-.788E+3$	$-.363E+3$	$-.214E+3$	$-.897E+2$
.0200	$-.797E+4$	$-.312E+4$	$-.787E+3$	$-.363E+3$	$-.214E+3$	$-.897E+2$
.0300	$-.794E+4$	$-.312E+4$	$-.787E+3$	$-.363E+3$	$-.214E+3$	$-.897E+2$
.0400	$-.790E+4$	$-.311E+4$	$-.787E+3$	$-.363E+3$	$-.214E+3$	$-.897E+2$
.0600	$-.777E+4$	$-.309E+4$	$-.786E+3$	$-.363E+3$	$-.214E+3$	$-.897E+2$
.0800	$-.761E+4$	$-.306E+4$	$-.784E+3$	$-.362E+3$	$-.214E+3$	$-.897E+2$
.1000	$-.740E+4$	$-.303E+4$	$-.782E+3$	$-.362E+3$	$-.214E+3$	$-.897E+2$
.1600	$-.660E+4$	$-.289E+4$	$-.773E+3$	$-.360E+3$	$-.213E+3$	$-.896E+2$
.2000	$-.598E+4$	$-.278E+4$	$-.765E+3$	$-.359E+3$	$-.213E+3$	$-.895E+2$
.2500	$-.523E+4$	$-.260E+4$	$-.753E+3$	$-.356E+3$	$-.212E+3$	$-.893E+2$
.3000	$-.454E+4$	$-.242E+4$	$-.739E+3$	$-.353E+3$	$-.211E+3$	$-.891E+2$
.4000	$-.292E+4$	$-.205E+4$	$-.703E+3$	$-.345E+3$	$-.208E+3$	$-.887E+2$
.5000	$-.194E+4$	$-.161E+4$	$-.662E+3$	$-.336E+3$	$-.205E+3$	$-.881E+2$
.6000	$-.130E+4$	$-.127E+4$	$-.616E+3$	$-.325E+3$	$-.201E+3$	$-.874E+2$
.8000	$-.603E+3$	$-.771E+3$	$-.525E+3$	$-.299E+3$	$-.192E+3$	$-.857E+2$
1.0000	$-.316E+3$	$-.472E+3$	$-.418E+3$	$-.271E+3$	$-.180E+3$	$-.835E+2$
1.2000	$-.178E+3$	$-.290E+3$	$-.332E+3$	$-.243E+3$	$-.168E+3$	$-.809E+2$
1.6000	$-.722E+2$	$-.127E+3$	$-.204E+3$	$-.180E+3$	$-.143E+3$	$-.749E+2$
2.0000	$-.358E+2$	$-.629E+2$	$-.125E+3$	$-.131E+3$	$-.113E+3$	$-.683E+2$
2.5000	$-.169E+2$	$-.305E+2$	$-.678E+2$	$-.860E+2$	$-.841E+2$	$-.599E+2$
3.0000	$-.989E+1$	$-.167E+2$	$-.393E+2$	$-.564E+2$	$-.612E+2$	$-.521E+2$
4.0000	$-.390E+1$	$-.637E+1$	$-.151E+2$	$-.246E+2$	$-.318E+2$	$-.340E+2$
5.0000	$-.196E+1$	$-.304E+1$	$-.695E+1$	$-.117E+2$	$-.165E+2$	$-.224E+2$
6.0000	$-.113E+1$	$-.176E+1$	$-.373E+1$	$-.630E+1$	$-.920E+1$	$-.146E+2$
7.0000	$-.716E+0$	$-.111E+1$	$-.225E+1$	$-.366E+1$	$-.536E+1$	$-.948E+1$
8.0000	$-.486E+0$	$-.753E+0$	$-.147E+1$	$-.238E+1$	$-.343E+1$	$-.639E+1$
9.0000	$-.347E+0$	$-.539E+0$	$-.103E+1$	$-.163E+1$	$-.227E+1$	$-.443E+1$
10.0000	$-.258E+0$	$-.401E+0$	$-.763E+0$	$-.116E+1$	$-.166E+1$	$-.319E+1$
12.0000	$-.154E+0$	$-.242E+0$	$-.474E+0$	$-.705E+0$	$-.971E+0$	$-.178E+1$
16.0000	$-.690E-1$	$-.110E+0$	$-.220E+0$	$-.337E+0$	$-.438E+0$	$-.767E+0$
20.0000	$-.371E-1$	$-.593E-1$	$-.120E+0$	$-.182E+0$	$-.252E+0$	$-.414E+0$
25.0000	$-.200E-1$	$-.320E-1$	$-.655E-1$	$-.997E-1$	$-.134E+0$	$-.219E+0$
30.0000	$-.121E-1$	$-.195E-1$	$-.401E-1$	$-.616E-1$	$-.835E-1$	$-.139E+0$
40.0000	$-.553E-2$	$-.903E-2$	$-.190E-1$	$-.297E-1$	$-.411E-1$	$-.729E-1$
50.0000	$-.303E-2$	$-.498E-2$	$-.106E-1$	$-.169E-1$	$-.237E-1$	$-.444E-1$
60.0000	$-.188E-2$	$-.311E-2$	$-.667E-2$	$-.107E-1$	$-.151E-1$	$-.287E-1$
70.0000	$-.131E-2$	$-.215E-2$	$-.463E-2$	$-.732E-2$	$-.103E-1$	$-.196E-1$
80.0000	$-.101E-2$	$-.166E-2$	$-.347E-2$	$-.546E-2$	$-.756E-2$	$-.138E-1$
90.0000	$-.850E-3$	$-.138E-2$	$-.286E-2$	$-.442E-2$	$-.607E-2$	$-.106E-1$
100.0000	$-.759E-3$	$-.122E-2$	$-.250E-2$	$-.382E-2$	$-.517E-2$	$-.871E-2$
110.0000	$-.702E-3$	$-.112E-2$	$-.227E-2$	$-.345E-2$	$-.459E-2$	$-.744E-2$
120.0000	$-.666E-3$	$-.104E-2$	$-.216E-2$	$-.320E-2$	$-.433E-2$	$-.668E-2$
130.0000	$-.638E-3$	$-.989E-3$	$-.203E-2$	$-.307E-2$	$-.406E-2$	$-.642E-2$
140.0000	$-.613E-3$	$-.972E-3$	$-.196E-2$	$-.296E-2$	$-.387E-2$	$-.597E-2$
150.0000	$-.597E-3$	$-.922E-3$	$-.190E-2$	$-.287E-2$	$-.377E-2$	$-.580E-2$
160.0000	$-.586E-3$	$-.929E-3$	$-.188E-2$	$-.281E-2$	$-.373E-2$	$-.578E-2$
170.0000	$-.581E-3$	$-.914E-3$	$-.184E-2$	$-.278E-2$	$-.364E-2$	$-.558E-2$
180.0000	$-.576E-3$	$-.908E-3$	$-.182E-2$	$-.277E-2$	$-.358E-2$	$-.541E-2$

References

AKI, K. and P.G. RICHARDS, 1980, *Quantitative seismology,* Freeman, 557pp.

ALTERMAN, Z., H. JAROSCH and C.L. PEKERIS, 1959, Oscillation of the earth, *Proc. Roy. Soc., London, Ser. A.,* **252:** 80–95.

BACKUS, G.E., 1967, Converting vector and tensor equations to scaler equations in spherical co-ordinates, *Geophys. J. R. astr. Soc.,* **13:** 71–101.

BARNES, D.F., 1966, Gravity changes during the Alaska Earthquake, *J. Geophys. Res.,* **71:** 451–456.

BEN-MENAHEM, A. and D. HARKRIDER, 1964, Radiation pattern of seismic surface waves from buried bipolar sources in a flat stratified earth, *J. Geophys. Res.,* **69:** 2605–2620.

BEN-MENAHEM, A. and S.J. SINGH, 1968, Eigenvector expansions of Green's dyads with applications to geophysical theory, *Geophys. J. R. astr. Soc.,* **16**: 417–452.

BEN-MENAHEM, A., S.J. SINGH and *F. Solomon*, 1969, Static deformation of a spherical earth model by internal dislocations, *Bull. Seism. Soc. Am.*, **59:** 813–853.

BEN-MENAHEM, A. and M. ISRAEL, 1970, Effects of major seismic events on the rotation of the earth, *Geophys. J. R. astr. Soc.,* **19:** 367–393.

BERRY, D.T. and T.W. SALES, 1962, An elastic treatment of ground movement due to mining. 3. Tree dimensional problem, transversely isotropic ground, *Geophys. J. Mesh. Phys. Solids,* **10:** 73–83.

BURRIDGE, R. and L. KNOPOFF, 1964, Body force equivalents for seismic dislocations, *Bull. Seism. Soc. Am.*, **54:** 1875–1888.

CHINNERY, M.A., 1961, The deformation of ground around surface faults, *Bull. Seism. Soc. Am.*, **51:** 355–372.

CHINNERY, M.A., 1963, The stress changes that accompany strike-slip faulting, *Bull. Seism. Soc. Am.*, **53:** 921–932.

DAHLEN, F.A., 1971, The excitation of the Chandler wobble by earthquakes, *Geophys. J. R. astr. Soc.*, **25:** 157–206.

DAHLEN, F.A., 1972, Elastic dislocation theory for a self-gravitating elastic configuration with an initial static stress field, *Geophys. J. R. astr. Soc.*, **28:** 357–383.

DAHLEN, F.A., 1973, A correction to the excitation of the Chandler wobble by earthquakes, *Geophys. J. R. astr. Soc.*, **32:** 203–217.

DAVIS, P.M., 1983, Surface deformation associated with a dipping hydrofracture, *J. Geophys. Res.*, **88**: 5826–5834.

FARRELL, W.E., 1972, Deformation of the earth by surface loads, *Rev. Geophys. Space Phys.*, **10:** 761–797.

GILBERT, F. and G. BACKUS, 1966, Propagator matrices in elastic wave and vibration problems, *Geophysics*, **2:** 326–332.

GILBERT, F. and A.M. DZIEWONSKI, 1975, An application of normal mode theory to the retrieval of structural parameters and source mechanisms from seismic spectra, *Phil. Trans. Roy. Soc. London, Ser. A*, **278:** 187–269.

HAGIWARA, Y., 1977, The Mogi model as a possible cause of the crustal uplift in the eastern part of Izu Peninsula and the related gravity change, *Bull. Earthq. Res. Inst., Univ. Tokyo*, **52:** 301–309.

HAGIWARA, Y., H. TAJIMA, S. IZUTSUYA, K. NAGASAWA, I. MURATA, S. OKUBO and T. ENDO, 1985, Gravity change in the Izu Peninsula in the last decade, *J. Geod. Soc. Jpn.*, **31:** 220–235.

ISRAEL, M., A. BEN-MENAHEM and S.J. SINGH, 1973, Residual deformation of real earth models with application to the Chandler wobble, *Geophys. J. R. astr. Soc.*, **32:** 219–247.

IWASAKI, T. and R. SATO, 1979, Strain field in a semi-infinite medium due to an inclined rectangular fault, *J. Phys. Earth*, **27:** 285–314.

JEFFERYS, H. and R.O. VINCENTE, 1966, Comparison of forms of the elastic equations for the earth, *Mem. Acad. R. Belgique*, **37:** 5–31.

KAGAN, Y.Y., 1987a, Point sources of elastic deformation: elementary sources, static displacements, *Geophys. J. R. astr. Soc.*, **90:** 1–34.

KAGAN, Y.Y., 1987b, Point sources of elastic deformation: elementary sources, dynamic displacements, *Geophys. J. R. astr. Soc.*, **91:** 891–912.

KANAMORI, H., 1970, The Alaska earthquake of 1964: radiation of long period surface waves and source mechanism, *J. Geophys. Res.*, **75:** 5029–5040.

KANAMORI, H., 1977, The energy released in great earthquakes, *J. Geophys. Res.*, **82:** 2981–2987.

KASAHARA, K., 1981, *Earthquake Mechanics*, Cambridge University Press, 248pp.

LONGMAN, I.M., 1962, A Green's function for determining the deformation of the earth under surface mass loads, 1. Theory, *J. Geophys. Res.*, **67:** 845–850.

LONGMAN, I.M., 1963, A Green's function for determining the deformation of the earth under surface mass loads, 2. Computations and numerical results, *J. Geophys. Res.*, **68:** 485–496.

LOVE, A.E.H., 1911, *Some Problems of Geodynamics*, Cambridge University Press.

MANSINHA, L. and D.E. SMYLIE, 1967, Effect of earthquakes on the Chandler wobble and the secular polar shift, *J. Geophys. Res.*, **72:** 4731–4743.

MARUYAMA, T., 1964, Statical elastic dislocations in an infinite and semi-infinite medium, *Bull. Earthq. Res. Inst., Univ. Tokyo*, **42:** 289–368.

MCGINLEY, J.R., 1969, A comparison of observed permanent tilts and strains due to earthquakes with those calculated from displacement dislocations in elastic earth model, *Bull. Ph.D. Thesis*,, California Institute of Technology, Pasadena, California.

MELCHIOR, P., 1983, *The tide of the planet earth*, Pergamon Press, 641pp.

MERRIAM, J.B., 1985, Toroidal Love numbers and transverse stress at the earth's surface, *J. Geophys. Res.*, **90:** 7795–7802.

OKADA, Y., 1976, Surface force equivalents for point sources coming up to the surface of a half space (in Japanese), *Zisin Ser. 2*, **29:** 83–86.

OKADA, Y., 1985, Surface deformation due to shear and tensile faults in a half-space, *Bull. Seism. Soc. Am.*, **75:** 1135–1154.

OKUBO, S. and T. ENDO, 1986, Static spheroidal deformation of degree 1 – consistency relation, stress solution and partials, *Geophys. J. R. astr. Soc.*, **86:** 91–102.

OKUBO, S., 1988, Asymptotic solutions to the static deformation of the earth – 1. Spheroidal mode, *Geophys. J. Int.*, **92:** 39–51.

OKUBO, S., H. WATANABE, H. TAJIMA, M. SAWADA, S. SAKASHITA, I. YOKOYAMA and T. MAEKAWA, 1988, Gravity change caused by the 1986 eruption of Izu-Oshima volcano, *Bull. Earthq. Res. Inst., Univ. Tokyo*, **63:** 131–144.

OKUBO, S. and H. WATANABE, 1989, Gravity change caused by a fissure eruption, *Geophys. Res. Lett.*, **16:** 445–448.

OKUBO, S., 1989, Gravity change caused by fault motion on a finite rectangular plane, *J. Geod. Soc. Jpn.*, **35:** 159–164.

OKUBO, S., 1991a, Potential and gravity changes raised by point dislocations, *Geophys. J. Int.*, **105:** 573–586.

OKUBO, S., 1991b, A technique to compute the coseismic crustal movement for a spherical earth model using the reciprocity theorem, in preparation.

OKUBO, S., Y. HIRATA, M. SAWADA and K. NAGASAWA, 1991, Gravity change caused by the 1989 earthquake swarm and submarine eruption off Ito, Japan, –Test on the magma intrusion hypothesis–, *J. Phys. Earth*, **39:** 219–230.

OKUBO, S., 1992, Gravity and potential changes due to shear and tensile faults in a half-space, *J. Geophys. Res.*, **97:** 7137–7144.

PHINNEY, R.A. and R. BURRIDGE, 1973, Representation of the elastic-gravitational excitation of a spherical earth model by generalized spherical harmonics, *Geophys. J. R. astr. Soc.*, **34:** 451–487.

PLAFKER, G., 1965, Tectonics of the March 27, 1964 Alaska earthquake, *Science*, **148:** 1675–1687.

PRESS, F., 1965, Displacements, strains and tilts at teleseismic distances, *J. Geophys. Res.*, **70:** 2395–2412.

RUNDLE, J.B., 1978, Gravity changes and the Palmdale uplift, *Geophys. Res. Lett.*, **5:** 41–44.

SAITO, M., 1967, Excitation of free oscillations and surface waves by a point source in a vertically heterogeneous earth, *J. Geophys. Res.*, **72:** 3689–3699.

SAITO, M., 1974, Some problems of static deformation of the earth, *J. Phys. Earth*, **22:** 123–140.

SAITO, M., 1978, Relationship between tidal and load Love numbers, *J. Phys. Earth*, **26:** 13–16.

SASAI, Y., 1986, Multiple tension crack model for dilatancy: surface displacement, gravity and magnetic change, *Bull. Earthq. Res. Inst., Univ. Tokyo*, **61:** 429–473.

SASAI, Y., 1988, Correction to the paper 'Multiple tension crack model for dilatancy: surface

displacement, gravity and magnetic change', *Bull. Earthq. Res. Inst., Univ. Tokyo*, **62:** 323−326.
SAVAGE, J.C. and L.M. HASTIE, 1966, Surface deformation associated with dip-slip faulting, *J. Geophys. Res.*, **71:** 4897−4904.
SCHOLZ, C.H., M. WYSS and S. SMITH, 1969, Seismic and aseismic slip on the San Andreas Fault, *J. Geophys. Res.*, **74:** 2049−2069.
SINGH, S.J. and A. BEN-MENAHEM, 1969, Deformation of a homogeneous gravitating sphere by internal dislocation, *Pure Appl. Geophys.*, **76:** 17−39.
SMYLIE, D.S. and L. MANSINHA, 1971, The elasticity theory of dislocation in real earth models and changes in the rotation of the earth, *Geophys. J. R. astr. Soc.*, **23:** 329−354.
STAUDER, W. and G.A. BOLLINGER, 1966, The focal mechanism of the Alaska earthquake of March 28, 1964, and of its aftershock sequence, *J. Geophys. Res.*, **71:** 5283−5296.
STEKETEE, J.A., 1958, On Volterra's dislocations in a semi-infinite elastic medium, *Can. J. Phys.*, **36:** 192−205.
TAKEUCHI, H., 1950, On the earth tide of the compressible earth of variable density and elasticity, *Trans. Amer. Geophys. Union*, **31:** 651−689.
TAKEUCHI, H. and M. SAITO, 1972, Seismic surface waves, *Meth. Comp. Phys.*, **11:** 217−295.
VANIČEK, P. and J. KRAKISKY, 1982, *Geodesy*, North-Holland, 691pp.
WALSH, J.B. and J.R. RICE, 1979, Local changes in gravity resulting from deformation, *J. Geophys. Res.*, **16:** 445−448.
WIDEMAN, C.J. and M.W. MAJOR, 1967, Strain steps associated with earthquakes, *Bull. Seism. Soc. Am.*, **57:** 1429−1444.
YAMAZAKI, K., 1978, Theory of crustal deformation due to dilatancy and quantitative evaluation of earthquake precursors, *Sci. Rep. Tohoku Univ., Ser. 5, Geophys.*, **25:** 115−167.

球対称地球モデルの中におかれた Point Dislocation によって生じるポテンシャルと重力変化

孫　　文科

東京大学地震研究所

この研究では，球対称地球モデルの中に発生したディスロケーションによってひきおこされるポテンシャルおよび重力の変化をとりあつかった．この変化の数式化をおこなった．ディスロケーション Love 数（h_n^d, l_n^d, k_n^d）を定義する．これを利用して，点源関数により地球に生じる弾性変形を記述する．

典型的な 3 種のタイプを検討する．すなわち，ずり型ディスロケーション，開口型ディスロケーション，それに膨張型ディスロケーションである．これらは 4 個の独立成分：鉛直面横ずれ，鉛直面縦ずれ，45°面縦ずれ，鉛直面開口タイプの重ね合わせにより表現することができる．

本研究における問題の表式化は簡単のようにみえるが，数値的な困難のために，今まで誰も無限級数による数値解を得ることはできなかった．われわれは以下に示すような対応をして式の評価に成功した．1. 計算の都合上，すべての等式，境界条件，点源関数を無次元化すること；2. 級数解を $N= 10\, a/d_s$ の点で打ち切っても，本研究の目的のためには十分の精度をもっているということを確認すること（d_s は震源深度，a は地球半径）；3. 級数展開の収束を加速するため，級数の各項に disk factor 係数を乗ずること；4. 交代級数の和を作るのに，Euler 変換が有効であることが知られているので，元表現を（部分和の）交代級数の形に変換すること；5. ディスロケーション Love 関数は Legendre 関数の高次の項まで分かっている必要がある．しかし，内挿処理を行なっても差し支えないものならば，各次数の各項を 1 項ずつ積分する必要はなく，ディスロケーション Love 数はところどころ分かっていればよい；6. d_s が 1km 以下のように非常に浅い場合には，級数解の必要な打ち切り次数が極端に大きくなり，事実上の困難にゆきあたる．この困難をのりきるため，大

久保の漸近解を利用した.

計算は均質地球と半径方向に異方性のある地球との両方について行った. 均質地球については1066A 地球モデルの各パラメータの地表値を採用した. 数値積分には, Runge-Kutta 法を使用した. 深さ 0, 2, 5, 10, 20, 32, 64, 100, 200, 300, 400, 637km の各深度についてディスロケーション Love 数を算出した. 得られたディスロケーション Love 数を用いて各場合の変位分布を計算した. 計算で得られた重力変化は, 点源の近傍の 1°(111km) 以近の領域においては, 大久保の平面モデルの場合 (1991) によく一致した. 両者が一致することは今回の研究に誤りがないことを示している. 両者の食い違いは点源距離10°以内では, 10%より小さいが, 10°を過ぎると差は大きくなる. 地球の曲率の影響が現れていることが明かである.

ついで, 半径方向に異方性のある場合のモデルについて計算を行った. 大まかに言えば, 計算結果は均質地球の場合に類似している. しかしながら, 場合により差が非常に大きくなることがある. 例えば, 重力変化の節線は両者で大きく離れる. 深さ方向の層構造があるために大きく異なることを示している.

本研究で最も重要な結果であるディスロケーション Love 数, 鉛直変位, ポテンシャル変化, 重力変化の表を Appendix にしておいた. この表を使用することにより, SNREI 地球モデルについて, どのタイプのディスロケーションの場合でも, 地表の任意の地点のポテンシャル, 重力変化が計算できる.

点ディスロケーションの結果を有限の面積について積分すれば, 現実の地震による重力変化をより正確に推定できる. 地震断層面を細分化し, 各要素面に対応する変形を Appendix E の表から内挿して使用しながら計算しそれを合算することにより実行できる. この方法で 1964 年 Alaska 地震 (m_W=9.2) に伴って発生した重力変化を推算した. 断層面の周辺において計算結果と実測結果とはよい一致を示した. この地震に伴う far field の重力変化も計算した. 結果は驚くべきもので, 震央距離 6°以内の領域では, 重力変化は 10μgal 以上に達し, 震央距離 16°以内の領域で 1μgal 以上, 震央距離 40°以内の領域で 0.1μgal 以上, そして全地球上で 0.01μgal を超える変化を示す.

本研究の成果は次の 6 点である:

1. 初めて球対称地球モデルについて dislocation によって生じる重力変化を計算することができた.
2. 地震断層の種類によって, 結果はいろいろ特徴的なパターンを示すことが分かった. 例えば, 水平横ずれ断層の場合には, 4 象限型になった.
3. Flat-Earth の結果と均質球の結果は, 震源に近い範囲 (θ<10°) では, よく一致した (定式化と計算手法が正しいことの確認).
4. 均質球の結果と成層構造球体の結果は大局的に一致するが, 震央距離によっては両者が符号を含めて大きく異なることもありうる.
5. Alaska 地震の観測例を理論がほぼ説明することを確認した.
6. Alaska 地震についての Case Study の結果から, 震央距離が 4000km 以内であれば大地震にともなう重力変化が検出可能であることを示した.